Rich Passage Passenger Only Ferry Study – Phase 1

Agreement FTA-WA-26-7007-005

Wave Energy Evaluation of Passenger Only Ferries in Rich Passage – April 2005

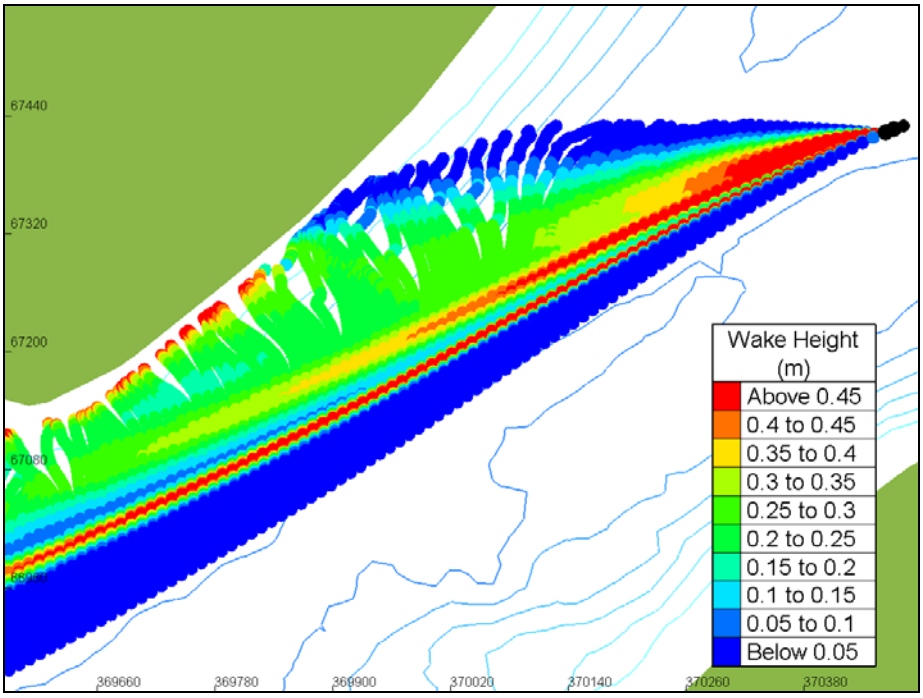

Federal Transit Administration

DISCLAIMER NOTICE

This document is disseminated under the sponsorship of the U.S. Department of Transportation in the interest of information exchange. The United States Government assumes no liability for its contents or use thereof.

The United States Government does not endorse products of manufacturers. Trade or manufacturers' names appear herein solely because they are considered essential to the objective of this report.

REPORT DOCUMENTATION PAGE

Form Approved
OMB No. 0704-0188

Public reporting burden for this collection of information is estimated to average 1 hour per response, including the time for reviewing instructions, searching existing data sources, gathering and maintaining the data needed, and completing and reviewing the collection of information. Send comments regarding this burden estimate or any other aspect of this collection of information, including suggestions for reducing this burden, to Washington Headquarters Services, Directorate for Information Operations and Reports, 1215 Jefferson Davis Highway, Suite 1204, Arlington, VA 22202-4302, and to the Office of Management and Budget, Paperwork Reduction Project (0704-0188), Washington, DC 20503.

1. AGENCY USE ONLY (Leave blank)	2. REPORT DATE April 2005	3. REPORT TYPE AND DATES COVERED

4. TITLE AND SUBTITLE Wave Energy Evaluation of Passenger Only Ferries in Rich Passage	5. FUNDING NUMBERS
6. AUTHOR(S) Philip D. Osborne, Ms.C, Ph.D., Neil J. MacDonald, Ph.D.	
7. PERFORMING ORGANIZATION NAME(S) AND ADDRESS(ES) Pacific International Engineering, PLLC 123 Second Avenue South Edmonds, Washington 98020	8. PERFORMING ORGANIZATION REPORT NUMBER Y-8977
9. SPONSORING/MONITORING AGENCY NAME(S) AND ADDRESS(ES) Federal Transit Administration U.S. Department of Transportation Washington, DC 20590 Website URL [www.fta.dot.gov]	10. SPONSORING/MONITORING AGENCY REPORT NUMBER FTA-WA-26-7007-2005

11. Supplementary Notes.

12a. DISTRIBUTION/AVAILABILITY STATEMENT	12b. DISTRIBUTION CODE
Available From: National Technical Information Service/NTIS, 5285 Port Royal Road, Springfield, Virginia 22161. Phone 703.605.6000, Fax 703.605.6900, Email [orders@ntis.fedworld.gov]	

13. ABSTRACT (Maximum 200 words)

The Rich Passage Passenger Only Fast Ferry Study is investigating the feasibility of restoring passenger only fast ferry (POFF) service between Seattle and Bremerton. This report documents the first phase of the Study, conducted between June 2004 and February 2005. Rich Passage shorelines are compartmentalized into several discrete littoral cells of varying dimension and sediment characteristics. Beach response to POFF operation is a result of POFF and non-POFF wakes, large water level variations and currents, and wind waves. The complexity of the problem and sensitivity of the community and environment, require a multi-disciplinary effort with tasks that include outreach to waterfront property owners and the general public, numerical model development and application, physical and biological monitoring, data analysis, coastal engineering, and research testing of candidate vessels. In the first phase of study, new physical and biological monitoring data were collected as a baseline for the current studies and for comparison against previous POFF operations. Model applications include: tidal circulation, wave climatology, beach profile evolution, and a new wake prediction model for high speed vessels. The wake model predicts the generation of wakes and transformation by tidal currents and bathymetry between vessel and shore. Wake data from trials of various POFFs were acquired to assist in model development and for successful validation. The wake model will be used to study the spatial variation in shore impacts from alternative candidate hull forms. In-situ testing of a foil-assisted catamaran was initiated to provide data for model validation and enhancement.

14. SUBJECT TERMS	15. NUMBER OF PAGES
High Speed Vessels, Wake Wash, Wakes, Beach Dynamics, Wake Propagation Model, Mixed Beach, Super-critical, Sub-critical, Energy Density, Passenger Only Fast Ferry	16. PRICE CODE

17. SECURITY CLASSIFICATION OF REPORT	18. SECURITY CLASSIFICATION OF THIS PAGE	19. SECURITY CLASSIFICATION OF ABSTRACT	20. LIMITATION OF ABSTRACT
Unclassified	Unclassified	Unclassified	

Rich Passage Passenger Only Ferry Study – Phase 1

Agreement FTA-WA-26-7007-2005 - Wave Energy Evaluation of Passenger Only Ferries in Rich Passage

Prepared by:

Pacific International Engineering, PLLC

April 2005

Table of Contents

Foreword xiii
Executive Summary xv
1.0 Introduction 1
1.1 Background 1
1.2 Purpose and Objectives of Study 2
1.3 Scope of Study 3
1.4 Organization of this Report 4
1.5 History of POFF Service on Seattle-Bremerton Route 5
2.0 Study Approach 7
2.1 Shoreline-focused versus Vessel-focused Approach to POFF Selection 7
2.1.1 Outreach to Property Owners and Public 8
2.2 Criteria and Performance Indicators 9
2.3 Tool Development and Application 12
2.3.1 Existing/Historical Conditions 13
2.3.2 Evaluation of Alternatives 13
3.0 Review of Data and Data Requirements 15
3.1 Existing Aerial Photographs 15
3.2 Properties and Structures 16
3.2.1 Geographical Information Systems (GIS) and Computer Aided Design (CAD) Drawings 16
3.2.2 Ground-based photographs 19
3.3 Bathymetry and Topography 20
3.4 Beaches, Shorelines, and Sediments 21
3.4.1 Beach Profile Data 21
3.4.2 Sediment Characterization 23
3.5 Tides, Currents, and Water Levels 24
3.5.1 Water Levels 26
3.5.2 Currents 30
3.6 Wind 35
3.7 Waves and Wakes 40
3.7.1 Wind Waves 41
3.7.2 Wake Data 42
3.8 Habitat 57

3.8.1 Site 1 58
3.8.2 Site 3 58
3.8.3 Site 5 59
3.8.4 Site 9 59
3.8.5 Site 10 59
3.8.6 Site 12 59
4.0 Shoreline Conditions and Change in Response to POFFs 61
4.1 Beach Characteristics in the Study Area 61
4.2 Beach Profile Response to POFFs 62
4.2.1 Bainbridge Island (Sites 3 to 7) 62
4.2.2 Point Glover (Sites 8 to 10) 64
4.2.3 Existing Conditions (June 2004 to January 2005)67
4.3 Dynamics and processes on low-energy mixed beaches67
4.3.1 Hydraulic conductivity 68
4.3.2 Reflection and long waves 70
4.3.3 Threshold of motion, selective entrainment, overpassing and inverse grading 70
4.3.4 Interactions with coastal structures 71
4.3.5 Tidal range 71
4.3.6 Proximity to deep water and surf zone-swash zone processes 71
5.0 Wake Impact Model Development 73
5.1 Modeling Domain and Grid Development 73
5.1.1 Data Sources 73
5.1.2 Finite Element Mesh Generation 73
5.2 Tidal Circulation Model 76
5.2.1 ADCIRC Model 76
5.2.2 Boundary Conditions 76
5.2.3 Model Validation 77
5.3 Wind Wave Modeling 86
5.3.1 Wave Hindcasting 86
5.3.2 Wave Modeling 89
5.4 Wake Generation and Propagation Model 94
5.4.1 Background 94
5.4.2 Existing Models 103
5.4.3 Proposed Approach 104
5.4.4 Governing Equations 105

5.3.5 Initial Kinematic Boundary Conditions 109
5.4.5 Breaking Boundary Conditions 114
5.4.6 Initial Dynamic Boundary Conditions 114
5.4.7 Wake Model Operation 117
5.4.8 Wake Model Validation 119
5.4.9 Practical Application in Rich Passage and Surrounding Shorelines 127
5.4.10 Additional Developments Required 127
5.5 Wave Impact Assessment Modeling 128
5.5.1 Relative Impact Assessment - Model Application 128
5.5.2 Absolute Impact Assessment - Descriptive Model 140
5.5.3 Absolute Impact Assessment - Proposed Approach 141
6.0 Wake and Wake Impact Studies with a Foil-assisted Catamaran 143
7.0 Summary and Recommendations 151
7.1 Recommendations 157
8.0 References 159

Appendices

Appendix A - Samples of Sub-Surface Beach Sediment in Rich Passage, Grain Size Analysis – AMTEST Laboratories
Appendix B - Analysis of Photographics Grain Size Beach Surface Sediment in Rich Passage
Appendix C - Wake Trial Time Series
Appendix D - Wake Measurements
Appendix E - Naval Architecture
Appendix F - Nearshore Habitat Assessment Data Report
Appendix G - Beach Profiles
Appendix H - LSV Simulations of the Spatial Distributions of Wake Power on Point White, Bainbridge Island

List of Figures

Figure 1-1. Seattle-Bremerton ferry route and Rich Passage study area 2
Figure 2-1. Schematic of study methodology 8

Figure 3-1. Recent aerial photographs obtained from the Washington Department of Natural Resources (WDNR 2002) 16

Figure 3-2. GIS layers from the Bainbridge Island Shoreline Inventory showing the distribution of shore drift cells and coastal structures in the study area 17

Figure 3-3. Bulkhead classification for class-action properties in Rich Passage 19

Figure 3-4. DEM for the study area compiled from CRM dataset; the location of water level monitoring and prediction stations in the study area is also shown 21

Figure 3-5. Beach Monitoring Sites 23

Figure 3-6. Example photographic sample of beach surface sediments 24

Figure 3-7. Locations of 1999-2002 water level and current monitoring stations 25

Figure 3-8. Distribution of daily maximum tides based on 1986-1998 NOAA tide gauge observations at Seattle Harbor 26

Figure 3-9. Measured surface water elevation at four stations in different deployment periods (water level data is not available at Station A-1) 27

Figure 3-10. Daily maximum tides observed at Seattle 29

Figure 3-11. Time series of annual maximum water levels and the ONI 29

Figure 3-12. Measured current speed and direction at Station A, September 16 through October 23, 1999 32

Figure 3-13. Measured current speed and direction at Station A, March 3 through March 24, 2000 32

Figure 3-14. Measured current speed and direction at Station B, October 23 through December 7, 1999 33

Figure 3-15. Measured current speed and direction at Station C, March 24 through May 11, 2000 33

Figure 3-16. Measured current speed and direction at Station D, May 12 through June 27, 2000 34

Figure 3-17. Vertical variations of mean and maximum current speeds at flood and ebb tides 35

Figure 3-18. Wind data recording sites in proximity to the study area 36

Figure 3-19. Wind rose for measured winds at West Point between 1984 and 2005 37

Figure 3-20. Wind rose for measured winds at Bremerton Airport between 1984 and 2005 38

Figure 3-21. Rich Passage Total Wind Speed Hours, Greater Than 10 Knots, SE Direction (Data from West Point Station) 39

Figure 3-22. Rich Passage Mean Wind Speed, Greater Than 10 Knots, SE Direction (Data from West Point Station) 40

Figure 3-23. Wind speed and direction recorded at Bremerton Airport on February 4, 2005 42
Figure 3-24. Surface wind waves recorded at buoy station IT-01 at 1:00PM, February 4, 2004 (Significant wave height 0.51 m, Peak period = 2.32 sec).....42
Figure 3-25. Average H_{max} as a function of vessel speed between 10 and 25 knots based on measurements of *Tyee* wakes 45
Figure 3-26. H_{max} measured during the *Tyee* trials as a function of distance from the sailing line for a range of speeds; the solid lines indicate the best fit for $r^{-1/3}$ and the dashed lines indicate the best fit for $r^{-1/2}$ 46
Figure 3-27. Tyee positions in Rich Passage, August 2002 47
Figure 3-28. Wake height normalized to 300 m as a function of vessel speed for a selection of vessels (reproduced from Fox and Associates 2002) 51
Figure 3-29. Wake Energy normalized to 300 m as a function of vessel speed for a selection of vessels (reproduced from Fox and Associates 2002) 52
Figure 3-30. Example of wake statistical parameters for Chinook class ferries measured nearshore in Rich Passage at a range of speeds 54
Figure 3-31. Time series of Chinook class wakes: water surface elevation and height (top), period (middle), and energy density (bottom) at slow speed (left) and at high speed (right) 55
Figure 3-32. Time series of a car ferry wake: water surface elevation and wave height (top), period (middle), and energy density (bottom).....56
Figure 4-1. Beach evolution after 180 days at SEPA Site 5 on Point White 65
Figure 4-2. Progression of beach morphological development at Site 5 66
Figure 4-3. Progression of beach morphological development at Site 3 66
Figure 5-1. Coverage of the finite element tidal model 74
Figure 5-2. Finite element mesh developed for the ADCIRC tidal model. Inserts show the density of the mesh in various locations 75
Figure 5-3. Depths in the finite element mesh 75
Figure 5-4. Locations of Stations A, B and D during the 1999-2000 Rich Passage field campaign 78
Figure 5-5. Comparison of field data and computed data for spring tide at Station A 80
Figure 5-6. Comparison of field data and computed data for spring tide at Station B 81
Figure 5-7. Comparison of field data and computed data for spring tide at Station D 82

Figure 5-8. Comparison of field data and computed data for neap tide at Station A 83
Figure 5-9. Comparison of field data and computed data for neap tide at Station B 84
Figure 5-10. Comparison of field data and computed data for neap tide at Station D 85
Figure 5-11. Comparison of measured and computed wind wave heights for February 4, 2005 89
Figure 5-12. Typical four-point application of STWAVE in a tidal cycle 90
Figure 5-13. Predicted wave heights at the entrance to Rich Passage as predicted by STWAVE (Hs=0.68m, T=2.87s, Dir=245deg)..... 92
Figure 5-14. Predicted wave heights at the entrance to Rich Passage as predicted by STWAVE (Hs=0.68m, T=2.87s, Dir=245deg, Wind=210deg) 92
Figure 5-15. Predicted wave heights at the entrance to Rich Passage as predicted by CoastL (Hs=0.68m, T=2.87s, Dir=245deg). Also shows detail for location of Figure 5-6 93
Figure 5-16. Detail of computed wave conditions at the shore near survey site 4 as predicted by CoastL..... 94
Figure 5-17. Typical results for high-speed vessel at super-critical speed (Top: surface elevation and wake height; Middle: wake period; Bottom: energy spectra)..... 96
Figure 5-18. Typical results for a high-speed vessel at sub-critical speed (Top: surface elevation and wake height; Middle: wake period; Bottom: energy spectra)..... 97
Figure 5-19. Typical results for displacement vessel (Top: surface elevation and wake height; Middle: wake period; Bottom: energy spectra)..... 98
Figure 5-20. Wake pattern generated by a sub-critical vessel..... 99
Figure 5-21. Wake pattern produced by: a) sub-critical vessel; b) super-critical vessel 100
Figure 5-22. Illustration of the *hump*, the speed at which a vessel's wake is twice as long as the vessel itself 101
Figure 5-23. Evolution of the wake pattern of a vessel with depth Froude number 109
Figure 5-24. Theoretical wake pattern predicted by a sub-critical vessel (F_d =0.6)..... 111
Figure 5-25. Theoretical wake pattern predicted by a super-critical vessel (F_d =1.2)..... 111
Figure 5-26. Theoretical wake pattern predicted by a super-critical vessel (F_d =1.8)..... 112
Figure 5-27. Wake crest pattern with Mach cone restriction imposed 113
Figure 5-28. Illustration showing phase and wavelength isolines for a typical super-critical wake pattern 114

Figure 5-29. Measured wake energy spectra from Snohomish trials 115
Figure 5-30. Measured wake energy spectra from trials of the *Snohomish* and frequency harmonic frequencies 115
Figure 5-31. Example of a wake spectra composed using a series of Gaussian distributions 117
Figure 5-32. Example of wake model parcel output.....118
Figure 5-33. LSV model simulation of wake pattern from Chinook: (a) full domain – shows detail window, b) detail around vessel) 119
Figure 5-34. *Snohomish* Test 18 (F_d =1.01, F_L =0.88 – surface elevation, wake height and period computed from field measurements.....121
Figure 5-35. *Snohomish* Test 6 (F_d =1.28, F_L =0.79) – surface elevation, wake height and period computed from field measurements.....121
Figure 5-36. *Snohomish* Test 7 (F_d =1.44, F_L =0.89) – surface elevation, wake height and period computed from field measurements.....121
Figure 5-37. *Snohomish* Test 28 (F_d =1.58, F_L =0.89) – surface elevation, wake height and period computed from field measurements – Synchronization 1 122
Figure 5-38. *Snohomish* Test 28 (F_d =1.58, F_L =0.89) – surface elevation, wake height and period computed from field measurements – Synchronization 2 122
Figure 5-39. Measured wave heights from the Condor Express trials – 39 knot tests (Note: Time axis has been shifted to line up data) 123
Figure 5-40. Comparison of the decay characteristics of the LSV model with other rates used in the literature.....124
Figure 5-41. Comparison of measured and computed wake heights for *Condor Express* at 39 knots. The measured results for the 90 m offset are dissimilar to any other measurements and may be somewhat suspect. (Note: time axis has been shifted to align start of wake event) ... .124
Figure 5-42. Comparison of measured and computed wake heights for *Condor Express* at 34 knots. (Note: time axis has been shifted to align start of wake even 125
Figure 5-43. Comparison of measured and computed wake height for *Bravest* (Note: time axis has been shifted to align start of wake event) 126
Figure 5-44. Comparison of measured and computed wake period for *Bravest* (Note: time axis has been shifted to align start of wake event) 126
Figure 5-45. Predicted wake height along the Bainbridge Island shore at three times.....127
Figure 5-46. Alongshore wave power from the wake of three POFFs (Bremerton to Seattle, high water slack).....129

Figure 5-47. Cumulative alongshore wave power from the wake of three POFFs (Bremerton to Seattle, high water slack)..... 130
Figure 5-48. Cumulative alongshore wave power from the wake of three POFFs (Seattle to Bremerton, high water slack)..... 130
Figure 5-49. Cumulative alongshore wave power from the wake of three POFFs (Bremerton to Seattle, low water slack) 131
Figure 5-50. Cumulative alongshore wave power from the wake of three POFFs (Seattle to Bremerton, low water slack) 131
Figure 5-51. Map of port side wake height pattern for *M/V Snohomish* (Bremerton – Seattle, low water slack).....132
Figure 5-52. Map of port side wake height pattern for *M/V Bravest* (Bremerton – Seattle, low water slack).....132
Figure 5-53. Map of port side wake height pattern for *M/V Condor Express* (Bremerton – Seattle, low water slack).....133
Figure 5-51. Spatial distribution of wake power from *M/V Snohomish* (Seattle-Bremerton, high water slack) 134
Figure 5-52. Spatial distribution of wake power from *M/V Bravest* (Seattle-Bremerton, high water slack) 134
Figure 5-52. Spatial distribution of wake power from *M/V Condor Express* (Seattle-Bremerton, high water slack) 135
Figure 5-54. Spatial distribution of wake power from *M/V Snohomish* (Bremerton-Seattle, high water slack) 135
Figure 5-55. Spatial distribution of wake power from *M/V Bravest* (Bremerton-Seattle, high water slack) 136
Figure 5-56. Spatial distribution of wake power from *M/V Condor Express* (Bremerton-Seattle, high water slack) 136
Figure 5-57. Spatial distribution of wake power from *M/V Snohomish* (Seattle-Bremerton, low water slack).....137
Figure 5-58. Spatial distribution of wake power from *M/V Bravest* (Seattle-Bremerton, low water slack).....137
Figure 5-59. Spatial distribution of wake power from *M/V Condor Express* (Seattle-Bremerton, low water slack).....138
Figure 5-60. Spatial distribution of wake power from *M/V Snohomish* (Bremerton-Seattle, low water slack).....138
Figure 5-61. Spatial distribution of wake power from *M/V Bravest* (Bremerton-Seattle, low water slack).....139
Figure 5-62. Spatial distribution of wake power from *M/V Condor Express* (Bremerton-Seattle, low water slack).....139
Figure 6-1. The research test vessel *M/V Spirit* in Rich Passage.145
Figure 6-2. Location of the 5-point instrument array for intensive trials of *M/V Spirit* in Port Orchard Reach.....145
Figure 6-3. Cross-shore profile seaward of mllw showing the location of the 4 stations in the instrument array.....146
Figure 6-4. Deployment of a wave gauge on a taut-line mooring at the instrument array in Port Orchard Reach.....146
Figure 6-5. Aerial photograph of Spirit Wake (30-35 knots) at the

instrument array 147
Figure 6-6. Dynamic motion sensor installed on M/V Spirit. The sensor signal was multi-plexed with signals from Real-Time Kinematic GPS, and compass 147

Figure 6-7. Time series of vessel speed and heading (top panel), vessel pitch and roll (middle panel), and vessel track relative to instrument position (lower panel) through time during an intensive trial run on February 4, 2005 148
Figure 6-8. Water tanks used for ballast on board the research test vessel *M/V Spirit* 149

List of Tables

Table 2-1 Potential project impacts, criteria and performance indicators 11
Table 3-1. Summary of beach profile monitoring surveys at SEPA sites in Rich Passage 22
Table 3-2. 1999-2000 Rich Passage current monitoring stations and deployment time 26
Table 3-3. Summary of correlations between Kitsap Ferry Company operation schedule and water levels at Seattle based in 2004 30
Table 3-4. Characteristics of flood and ebb currents at monitoring stations 31
Table 3-5. Rich Passage Wind Data 36
Table 3-6. Summary of wake parameters normalized to a distance of 300 m based on trial measurements for the vessel *Bravest* 48
Table 3-7. Macroalgae and invertebrates observed within intertidal quadrats in Rich Passage, January 2005 57
Table 4-1. Beach slopes at baseline survey (4-19-2000 to 5-8-2000) 63
Table 4-2. Beach slopes at monitoring survey # 6 (9-4-2001) 64
Table 5-1. Test periods selected for validation of the ADCIRC tidal model 77
Table 5-2. ADCIRC model validation for tides and currents at 3 gauge stations 79
Table 5-3 Measured winds at Bremerton Airport 88
Table 5-4. *Chinook/Snohomish* Test Cases for LSV Validation .. 120

Foreword

This report documents the first phase of the Rich Passage Passenger Only Fast Ferry Study, which was conducted between June 2004 and February 2005. The Study is investigating the feasibility of restoring passenger only fast ferry (POFF) service between Seattle and Bremerton. The Study was initiated in June 2004 and is funded under a federal grant program administered by the Federal Transportation Administration (FTA), designed to support research and investigations of emerging transportation systems.

The report includes a brief historical background to POFF operation on the Seattle-Bremerton ferry route, an outline of the approach and methodology of the study, review of existing data and data requirements for the present study, followed by an analysis of historical and new shoreline conditions and changes in response to POFF operations in Rich Passage. The report describes the development of numerical models for predicting waves, wakes, tidal processes, and shoreline response. The development of model grids and boundary conditions is outlined and the process of model calibration and verification is discussed. A preliminary screening level application of the new integrated wake propagation and tidal current modeling is discussed. The model provides estimates of indicator parameters useful for assessing shore impact. The report describes research conducted with a state-of-the art foil-assisted to provide data for numerical model development and wake impact studies. Finally, a summary of findings from the first phase of work and recommendations for further study are included. Appendices provide technical memoranda and reports supplementary to the first phase of work including: review of state of the art hulls, biological studies, wake trial results, and field data. A data CD is also provided with an electronic version of the report and raw data collected during the initial testing of a research vessel.

The report will be of interest to organizations interested in providing fast ferry service through Rich Passage, to property owners along the Seattle-Bremerton ferry route, and to other organizations in the state and country interested in providing environmentally benign fast ferry service.

This report is an interim report summarizing the first phase of the Study. Further reports will document subsequent phases of the Study pending available funds.

DISCLAIMER NOTICE

This document is disseminated under the sponsorship of the U.S. Department of Transportation in the interest of information exchange. The United States Government assumes no liability for its contents or use thereof.

The United States Government does not endorse products of manufacturers. Trade or manufacturers' names appear herein solely because they are considered essential to the objective of this report.

Executive Summary

The Rich Passage Passenger Only Fast Ferry Study is designed to investigate the feasibility of restoring passenger only fast ferry (POFF) service between Seattle and Bremerton. The Study was initiated in June 2004 and is funded under a federal grant program administered by the Federal Transportation Administration (FTA), designed to support research and investigations of emerging transportation systems. This report documents the first phase of the Study, which was conducted between June 2004 and February 2005.

The shorelines of Rich Passage are very complicated and are comprised of several discrete littoral cells ranging from a few tens of meters in length up to a kilometer or more. The sediment distribution is also relatively complex, with beaches that may consist of a hard bottom, sand, gravel, or some combination of these. The response of these beaches to POFF operation is a result of many factors, including POFF and non-POFF wakes, large tidal water level variations and currents, and wind waves. Because of the complexity of the problem and sensitivity of the community and environment, the Rich Passage Passenger Only Fast Ferry Study was initiated as a multi-disciplinary effort with specific tasks that include outreach to waterfront property owners and the general public, numerical model development and application, physical and biological monitoring and data analysis, coastal engineering, and research testing of a state-of-the-art foil-assisted catamaran.

Public outreach efforts include meetings with property owners and the general public, posting of information on a project website, and distribution of a series of monthly newsletters. New physical and biological monitoring data were collected from the Rich Passage environment in the first phase of the Study to provide a baseline for the current studies and a comparison against conditions during previous POFF operations. Data collected include information on waterfront properties, shoreline protection schemes, shore types, sediment characteristics, bathymetry and topography, tidal currents and water levels, and wind wave and wake climates in Rich Passage.

Computer model application in the Study includes a tidal circulation model, a wave climatology model, a beach profile evolution model and a new wake prediction model for high speed vessels. The wake model can be used to predict both the generation and transformation of the wake by tidal currents and bathymetry from a vessel to the shore. Wake data from trials of various POFF vessels were acquired to assist in the development of the model, which has been successfully validated against measurements of a number of high speed vessels. The wake model will be used to study the spatial variation in shore impacts from alternative candidate hull forms. Additional review of compiled wake wash data published in the scientific and engineering literature as part of the Study identified three candidate hull forms considered worthy of further consideration in the Study: air cavity hull catamarans, air-lubricated hull catamarans and foil-assisted catamarans.

Research testing was conducted with the foil-assisted catamaran *M/V Spirit* built by All American Marine, Inc of Bellingham, WA and designed by Technikraft Inc., NZ to acquire data from a candidate low-wake vessel both in terms of the spatial and temporal patterns of wake height and energy and also the potential shoreline impacts from the wakes. The research testing will provide valuable data for direct validation of the numerical wake and shoreline response models being developed in the Study. The models and data will enable a

detailed assessment of potential shore impacts and provide a tool to evaluate possible shore protection solutions for areas where impacts cannot be minimized. In the first year of Study, the research vessel was acquired, mobilized, and outfitted for the trials, instrumentation was prepared and deployed for measurement of the wakes and a preliminary series of intensive tests were executed in Port Orchard Reach. Raw data from these initial intensive tests are provided on CD with the report. The vessel trials will continue into the second year of the Study and to examine shoreline impacts in Rich Passage. Analysis and reporting of the datasets collected as part of both tests will be conducted in later phases of the Study.

Work undertaken in the first phase of the Study has led to the identification of a number of additional tasks for subsequent phases of the work. The recommended tasks include:

- application and enhancement of the predictive models to evaluate alternative POFF low-wake vessels and operational plans to assess shoreline impacts;
- in-situ and model testing of low-wake candidate hulls;
- compilation of a project GIS to integrate geospatial data and guide analysis;
- wake monitoring and additional physical and biological monitoring to gather data for model verification;
- development and evaluation of alternative plans for mitigating any unavoidable effects on shorelines, and;
- an economic analysis to assess existing and new rider demand, vessel operating costs for the POFF service and to evaluate potential cost recovery plans and alternatives.

The Rich Passage Passenger Only Fast Ferry Study is presently in its second phase, which will extend from March 2005 to February 2006.

1.0 Introduction

For over two decades, there has been considerable interest in providing passenger only fast ferry (POFF) service on central Puget Sound between the cities of Seattle and Bremerton. POFF service may offer considerable savings in commuting time over the conventional car ferry service offered by Washington State Ferries (WSF). The one-way distance between Seattle and Bremerton along the ferry route is approximately 14 nautical miles (Figure 1-1). A one-way trip at a speed of 35 knots would take approximately half an hour, whereas the conventional car ferry service offered by WSF operates at half that speed and takes approximately one hour to make the trip (WSDOT, 2005). This report documents the results of the Rich Passage Passenger Only Fast Ferry Study, designed to investigate the feasibility of restoring POFF service between Seattle and Bremerton.

1.1 Background

Despite the interest in POFF service and its potential benefits to commuters, a major difficulty arises owing to the need for waterborne traffic between the cities to pass through Rich Passage, a narrow body of water separating the south end of Bainbridge Island from the mainland portion of Kitsap Peninsula at Port Orchard. Rich Passage is no more than 800 m wide at its narrowest point between Point White and Point Glover. In the past, Rich Passage property owners have filed complaints and a lawsuit alleging bulkhead damage, beach erosion, and biological degradation caused by high-speed ferry wakes. In October 2001, the State Attorney General reached a settlement with Rich Passage property owners concerning damage to property associated with POFF operation through Rich Passage and agreed to maintain speeds of passenger ferries at less than 16 knots through Rich Passage. In February 2003, WSF suspended POFF service on the Seattle-Bremerton route due to budget shortfalls. The history of POFF service is examined further in Section 1.5.

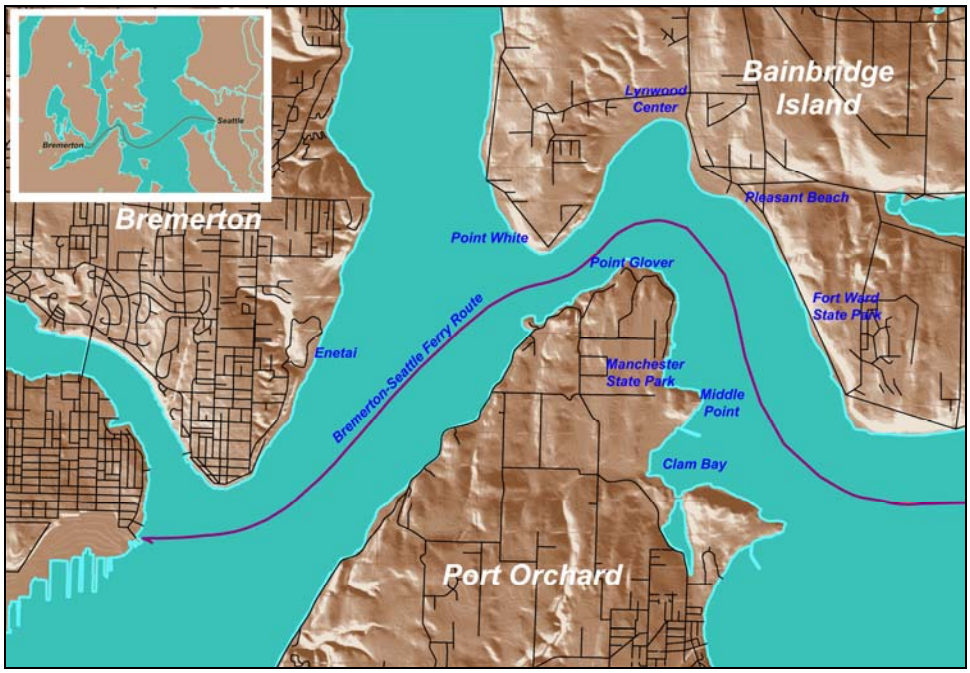

Figure 1-1. Seattle-Bremerton ferry route and Rich Passage study area

1.2 Purpose and Objectives of Study

The Rich Passage Passenger Only Fast Ferry Study is designed to investigate the feasibility of restoring POFF service between Seattle and Bremerton. The study was initiated in June 2004 and is funded under a federal grant program administered by the Federal Transportation Administration (FTA), designed to support research and investigations of emerging transportation systems. The study is being conducted under the direction of Pacific International Engineering, PLLC (PI Engineering) of Edmonds, WA.

The primary objective of the first phase of the Study is to develop the means to identify and minimize the impact of alternative POFF operation plans. Later phases of the study will apply the information and tools developed to identify POFF vessels which will have the least impact on Rich Passage shorelines.

It is anticipated that a successful POFF operation will contribute to sustainable growth in the region by:

- Improving commuter mobility
  - Reducing average travel time to approximately 30 to 35 minutes for Bremerton - Seattle commuters
  - Offering more sailings/day to increase commuter flexibility
- Minimizing negative impacts to the environment
  - avoiding significant impact to existing habitat and wildlife
  - avoiding or addressing impacts to shorelines or property along the route

- Offering a cost-competitive alternative to conventional car ferry service

Another fundamental objective of the project is to preclude legal action against a fast ferry operation that might follow from recommendations or findings of the study. This may require balancing of tradeoffs between an exclusive vessel-based solution and addressing shoreline effects. The results of the project will be relevant to organizations interested in providing fast ferry service through Rich Passage, to property owners along the Seattle-Bremerton ferry route, and to other organizations in the state and country interested in providing environmentally benign fast ferry service.

1.3 Scope of Study

A first and critical step in the study process is to accurately assess potential shore and marine impacts associated with POFF watercraft that may be chosen to operate in Rich Passage. Therefore, the first phase of the study focuses on developing shoreline impact prediction and assessment models. The models are being developed on the basis of a scientific understanding of vessel wake-generation, propagation, and impacts to shorelines in Rich Passage. The first generation of models has been developed after a review of relevant existing data on shorelines and their response to wakes and other processes in Rich Passage, and available wake trial data from a range of low-wake vessels that could provide a POFF design. New physical and biological monitoring data were collected from the Rich Passage environment in this first phase of the study to provide a baseline for the current studies and a comparison against conditions during previous POFF operations. In-situ tests of a state-of-the art foil-assisted catamaran were conducted to provide data for numerical model development and wake impact studies. Later phases of the study may involve:

- application and enhancement of the predictive models to evaluate alternative POFF plans (including potential candidate low-wake vessel and hull design variants, vessel operating speeds and vessel routings, and vessel testing against various shoreline configurations and compositions at various tide and current levels to assess shoreline impacts);
- in-situ and model testing of low-wake candidate hulls;
- wake monitoring and additional physical and biological monitoring to gather data for model verification;
- analysis and interpretation of wake and wake impact data from research testing;
- development and evaluation of concepts for addressing declining sediment supply to beaches and erosion resulting from wakes and natural processes and impacts associated with high energy wakes and elevated water levels; and

- assessment of POFF alternatives in terms of operating and maintenance costs and cost recovery potential.

As will be described in Section 2.1, the study will involve an iterative model application and alternative evaluation process to develop the means for selecting a technically, economically, and environmentally acceptable plan for POFF operation through Rich Passage.

1.4 Organization of this Report

This report documents the first phase of the Rich Passage Passenger Only Fast Ferry Study conducted between June 2004 and February 2005. Historical background to POFF operation on the Seattle-Bremerton ferry route is provided in the following sub-section.

Section 2 outlines the approach and methodology of the study. The study is a multi-disciplinary effort with specific tasks including outreach to waterfront property owners and the general public, numerical model development and application, physical and biological monitoring and data analysis, and coastal engineering.

Section 3 provides a review of existing data and outlines the data requirements for the present study. Data required for the study include information on waterfront properties, shoreline protection schemes, shore types, sediment characteristics, bathymetry and topography, tidal currents and water levels, and wave and wake climates in Rich Passage. Wake data from trials of various POFF vessels are also required for development of the wake prediction models.

Section 4 presents an analysis of historical and new shoreline conditions and changes in response to POFF operation.

Section 5 describes the development of numerical models for predicting waves, wakes, tidal processes, and shoreline response. The development of model grids and boundary conditions is outlined and the process of model calibration and verification is discussed. A preliminary screening level application of the integrated wake propagation and tidal current modeling is discussed. The model provides estimates of indicator parameters useful for assessing shore impact.

Section 6 describes research conducted with a state-of-the art foil-assisted to provide data for numerical model development and wake impact studies.

Section 7 summarizes findings from the first phase of work and recommendations for further study. Appendices provide technical memoranda and reports supplementary to the first phase of work including: review of state of the art hulls, biological studies, wake trial results, and field data.

1.5 History of POFF Service on Seattle-Bremerton Route

POFF service was first implemented on Seattle-Bremerton route by WSF in 1985 with the vessel *M/V Tyee*. Shortly after service began, waterfront property owners along Rich Passage reported changes to the shoreline from ferry wakes including erosion of sand and gravel beaches, damage to bulkheads and property, and loss of clam beds, kelp beds, and crabs. WSF responded by restricting passenger-only ferry speeds in Rich Passage to 12 knots.

In 1988, WSF purchased *M/V Skagit* and *M/V Kalama* which were placed in service on April 23, 1990. Shortly thereafter, property owners expressed concern about the impacts caused by these vessels and WSF slowed their operation through Rich Passage to less than 12 knots starting June 18, 1990.

WSF conducted a study between July and November 1990 (Hartman et al., 1990) to evaluate Rich Passage shoreline impacts from operation of the Seattle-Bremerton POFFs. Impacts at four sites (Enetai Beach, Point White, Point Glover, and Manette Beach) were evaluated on the basis of ferry wake measurements, site assessments, and physical and biological processes. Based on the conclusions of the study, WSF continued to limit speed of POFFs in Rich Passage to 12 knots. Following the reduction to speeds of 12 knots, property owners discontinued their complaints and indicated that beaches were returning to pre-POFF conditions.

Over the next several years, WSF studied wake parameters from its existing vessels and a broad range of other vessel types. This led to the development of a wake criterion for selection of POFF vessels. The wake criterion was to keep the largest wave in a wake to less than or equal to a wave height of 0.28 m with an energy density of not more than 2450 J/m as measured in deep water at a distance of 300 m from the vessel sailing line (RPWAST, 2001).

In 1998, WSF introduced the Chinook-class POFF on the Seattle–Bremerton route. The water-jet propelled catamaran *M/V Chinook* began operation through Rich Passage on May 28, 1998 at nominal operating speeds between 34 and 37 knots. Following the introduction of *M/V Chinook*, several waterfront property owners in Rich Passage complained about POFF wakes and damage caused by the wakes.

In March 1999, Rich Passage property owners filed a lawsuit alleging that damage to bulkheads, beach erosion, and damage to habitat were caused by the POFFs. In August 1999, WSF was directed by Kitsap County Superior Court to reduce POFF speed between the east entrance to Rich Passage and Bremerton to 12 knots pending either full compliance with the State Environmental Policy Act (SEPA) or further order from court. WSF complied with the court order and reduced operating speed of the POFFs to 12 knots beginning August 24, 1999. By October 1999, property owners reported that beaches in Rich Passage were recovering to pre-POFF conditions (e.g., Friedrich, 1999).

The Rich Passage Wave Action Study Team (RPWAST) was formed by WSF to address the Court's order and to perform environmental review and documentation under SEPA. In March 2000, the Washington Supreme Court reversed the preliminary injunction; the Supreme Court ruled that the Kitsap Superior Court's order did not contain all the findings required under the circumstances to support the preliminary injunction. WSF decided to resume high-speed operation of *M/V Chinook* through Rich Passage in May 2000. WSF acquired *M/V Snohomish*, a POFF vessel with similar design to *M/V Chinook*, in early 2000. *M/V Snohomish* was put into service at high speed on the Seattle-Bremerton route in June 2000.

The RPWAST implemented a monitoring program in April 2000 to determine the impact of POFF service to the physical and biological environments in Rich Passage. The results of the study are documented in RPWAST 2001 and 2002. A comprehensive list of studies conducted by RPWAST may be found in RPWAST (2002).

Following the study, RPWAST recommended that WSF slow the POFFs to speeds less than 16 knots from Point White to Middle Point with the expectation that beaches would recover following slowdown of the POFF. Additional monitoring data were collected in February 2002 following the POFF slow-down in October 2001. Beach monitoring data indicated that beaches began to recover in the months following the slowdown of the POFFs. A detailed review and analysis of these data is included in Section 4.2 of this report. The State Attorney General reached a settlement with Rich Passage property owners concerning damage to property associated with POFF operation through Rich Passage.

WSF suspended POFF service on the Seattle-Bremerton route in February 2003 due to budget shortfalls. Private operation of a POFF vessel, *M/V Spirit of Adventure*, began in August 2004. That ferry travels at speeds up to 25 knots between Bremerton terminal and Point White (Buoy #10) depending on traffic and other conditions, a maximum speed of 12 knots over the ground between Point White and Point Glover, at 16 knots between Point Glover and Buoy #6, and up to 25 knots between Seattle and Bremerton; the ferry achieves a crossing time of approximately 40 minutes (pers. comm. Greg Donkert , Kitsap Ferry Company, 2005). Car ferries and naval vessels have continued to operate at normal speeds in Rich Passage throughout this period.

2.0 Study Approach

2.1 Shoreline-focused versus Vessel-focused Approach to POFF Selection

The basic goal of the study is to develop the means to identify and minimize the impacts of alternative POFF operation plans. POFF alternatives are to be evaluated in terms of a range of impact assessment criteria relating to the physical and biological environments. At the most fundamental level, this requires defining performance indicators and metrics for each impact criterion and conducting comparative evaluations of alternative POFF operation plans.

Previous attempts at establishing a wake criterion for POFF service on the Seattle-Bremerton route have been based on wave height and energy density levels as measured in deep water. This approach does not adequately account for the transformations in wake properties that occur between the sailing line and shoreline, nor does it account for the variability in shoreline conditions that influence the degree of impact that may occur at a given location. Selection of POFF vessels for operation through Rich Passage must begin with a consideration of the character of wakes reaching the shoreline and with their potential to cause shoreline erosion, structural damage, or impact to habitat at a given location. This section outlines the approach and methodology of a multi-disciplinary study to evaluate shoreline impacts from alternative POFF operations. The basic elements of the study include: outreach to waterfront property owners and the general public, numerical model development and application, physical and biological monitoring and data analysis, and coastal engineering.

The most effective description of impacts of a POFF operation through Rich Passage would come from comprehensive empirical data collected throughout Rich Passage concurrent with POFF operations. Rich Passage is a complex and highly variable system with multiple natural and human components operating over a wide range of space and time scales. Typically, the more complex the system, the more important the need for high quality measured data. Wake generation by moving vessels, wake propagation, sediment transport, and shoreline dynamics in response to wave and current forcing are complex processes that are not fully understood. At the time of the study, many of these processes can not be completely described with predictive models. On the other hand, collection of high quality measured data on processes and associated impacts is time consuming, expensive, and complicated by the fact that multiple processes may operate simultaneously to cause an observed response. Furthermore, it is not possible to test all potential candidate POFF vessels and operations in-situ in Rich Passage. Because information on wakes and shore processes in Rich Passage is limited, a combination of measured data and modeling to describe these processes was adopted for this study.

The general approach to the evaluation of impacts associated with alternative POFF operations involves an iterative process outlined in Figure 2-1. Data from previous POFFs for which open water wake trial data, nearshore wake measurements in Rich Passage, and associated observations of shore impact, are limited. The most comprehensive data available are from the monitoring program conducted by the RPWAST during the operation of *M/V Chinook* and *M/V Snohomish*. The data from previous studies provide a benchmark against which to compare potential alternatives. Wake trial data and in-situ measurements from previous POFF operations are also used to develop and verify a wake propagation predictive model. The wake propagation model is coupled with a tidal circulation model and wind wave model to predict nearshore wave, current, and sediment transport conditions throughout the study reach for the base case and POFF operation alternatives. Impacts are assessed on the basis of physical and biological criteria and metrics for a set of representative indicator sites. Relationships generated for indicator sites are applied to generate data for system-wide impact assessments. The POFF operation is optimized by improvements to vessel design, operating speed, or routing. In cases where potential impacts following optimization may be unavoidable, mitigation alternatives may need to be developed and analyzed. The individual elements of this iterative approach are described in more detail in the sub-sections that follow.

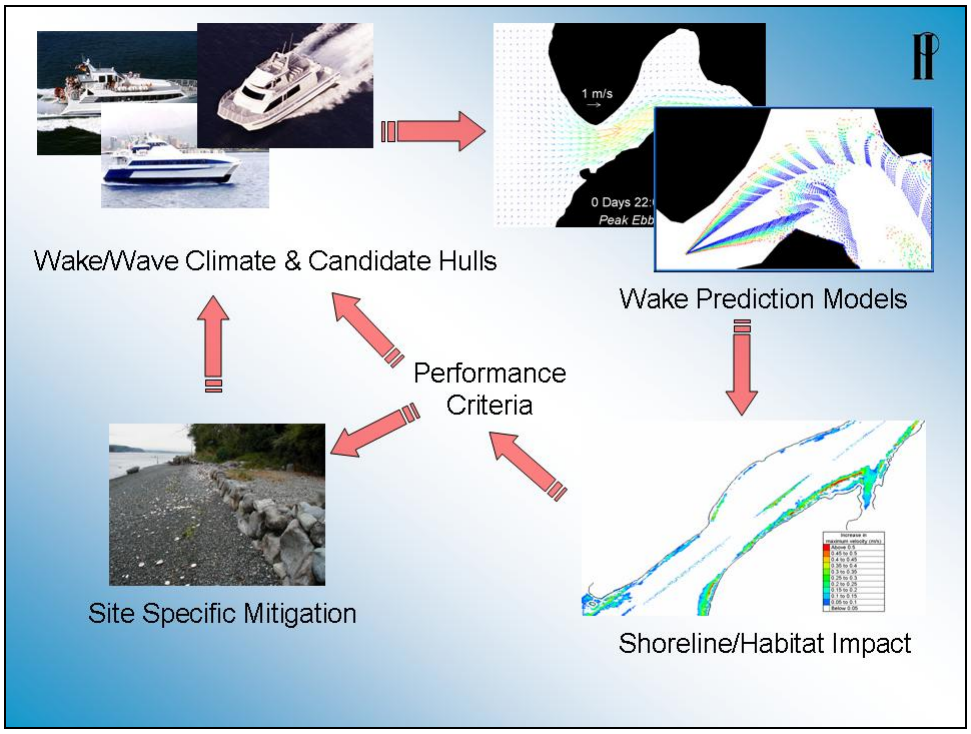

Figure 2-1. Schematic of study methodology

2.1.1 Outreach to Property Owners and Public

Input, observations, and perspectives from waterfront property owners, some of whom have been residents on Rich Passage for many years, is

of significant value to the study. Outreach efforts include meetings with property owners and the general public, posting of information on a project website, and distribution of a series of newsletters.

Meetings were held with Rich Passage property owners in October 2004 on Bainbridge Island and at Port Orchard. Letters of invitation to the meetings were sent to approximately 400 residents and the meetings were advertised on the project website. Attendance included 25 residents at the Bainbridge Island meeting and 15 residents at the Port Orchard meeting. The purpose of the meetings was to share information on the project and to get feedback from property owners.

In addition to the meetings with property owners, three general community meetings were held in October 2004 in Port Orchard, Bainbridge, and Bremerton. These meetings were advertised in local newspapers and on the project website. Although not as well attended, the community meetings provided an opportunity to brief several waterfront property owners who had not been able to attend the earlier meetings.

Project team members have established contact with residents who own properties on which long-term monitoring and data collection sites are located. Owners of these properties are notified each time monitoring teams need access for beach profile surveys, sediment and beach substrate characterization, and biological surveys.

Information on the project and its status is posted on the project website at www.pugetsoundfastferry.com. The website will be updated as information is collected during later phases of the study. The website includes a comments and feedback page that summarizes input from area residents. Response to the website has been positive; particularly with respect to the publication of comments received from property owners and other interested parties.

Monthly newsletters have been sent to waterfront property owners to introduce the study and its objectives, and to explain the study plan and schedule. Newsletters will continue to be prepared and sent to property owners to share information and solicit input during later study phases.

2.2 Criteria and Performance Indicators

The ultimate aim of the study is to determine whether an efficient and environmentally acceptable POFF operation can be introduced to the Seattle-Bremerton route. This objective requires tools for assessment of impacts associated with alternative POFF operations. In this Section, the criteria and metrics for assessing impacts to the physical and biological environment are outlined.

As described in Section 2.1, the most effective description of impacts to the environment would come from having either comprehensive empirical data or complete models describing all of the relevant processes operating in the environment for a range of alternatives and the existing condition throughout the study area. Because there are significant gaps in understanding of nearshore processes under wakes, waves, and tidal processes and the data available to describe nearshore processes and associated response are incomplete, an absolute description of impacts may not be realistic for the present study. It is necessary to resort to an approach that involves relative comparisons among a number of indicator parameters for a representative set of indicator sites. Furthermore, the most effective and direct way of achieving the goal of an environmentally acceptable POFF service is to use low-wake vessels. If this can be achieved, then there may be no need for fully developed deterministic impact assessment models. Wake modeling tools can be used to ensure there are no "hot spots" along the route where a concentration of wake energy might cause problems. Once these hot spots are identified, route changes can be made to eliminate them or alternative concepts developed to address them. This may be the most likely outcome of the study. In other words, if beach modeling is required, then the impacts are too great. In this respect, the aim of the wake impact assessment modeling should be the determination of thresholds, below which the evolution of the beach is unaffected. This task is more achievable than the prediction of the morphology development of mixed sand-gravel beaches from just a few waves every few hours over several months.

Table 2-1 summarizes a number of potential impacts, criteria, and performance indicators or metrics that are relevant to the study. Table 2-1 includes both primary (or direct) metrics for each criterion as well as secondary (or in-direct) metrics for several criteria where the definition of primary indicators may be limited by the present state of knowledge, available data, measurement or modeling capability.

As an example, criteria related to shoreline impacts include minimizing erosion, changes to the beach profile, and changes to the recreational or aesthetic quality of the beach. Direct or primary metrics for beach erosion include: beach area, shoreline position, and beach volume. Monitoring and modeling the combined effects of water levels, currents, wind waves and vessel traffic, the changes in beach area, shoreline position, or beach volume throughout the domain is a major challenge and probably quite unrealistic as a goal for the present study. However, a comparative evaluation of alternative POFF operations in terms of sediment transport indicators (at a number of representative indicator sites) as surrogates for changes in beach area, shoreline position, or beach volume, would permit an assessment of the relative effects of the alternatives. Indirect or secondary indicators of sediment transport include: sediment mobility, wave energy flux, maximum current velocity.

Modeling of biological processes in response to physical processes is perhaps even more primitive. Assessment of biological impacts will depend on monitoring potential impacts including loss of habitat through changes in slope, grain size, and algal cover, and loss of species diversity. The criteria are the same as those listed above. Direct metrics include absolute and/or relative abundance of benthic alga and invertebrate species. Subsurface grain size/habitat will also play a role in the species distribution, though currents and substrate within Rich Passage provide limiting factors to both abundance and distribution for algal and invertebrate populations.

Table 2-1 Potential project impacts, criteria and performance indicators

Impact	Criterion	Primary Performance Indicator	Secondary Performance Indicator
Shoreline	Minimize erosion	Beach area Shoreline position Beach volume	Sediment mobility Wave energy flux Maximum current velocity
	Minimize change in beach profile	Beach slope	As above
	Recreational or aesthetic quality of beach	Change in shore type (gravel → sand; sediment → bare rock)	
Habitat	Minimize loss of eelgrass	Area of eelgrass coverage	
Biological	Endangered species	Effects on species or designated critical habitats	
Structural	Minimize toe scour	Downcutting at structure	Sediment mobility Wave energy flux Maximum current velocity Wave reflection coefficient
	Minimize structural damage	Depends on structure characteristics	Wave loading
	Minimize overtopping	Overtopping rate Freeboard	
Navigation Safety Rider Safety	Minimize risk of injury, personal or property loss		
Pollution	Water quality	Pollutant types and concentrations	
	Noise	dB	
Commuter Transit System	Efficiency	Travel time Load and offload time	
	Capacity of transportation system	Frequency of service Number of passengers/hour	

Impact	Criterion	Primary Performance Indicator	Secondary Performance Indicator
	Reliability of service	Percent level of reliability	
	Quality of service	Available seating	
	Economy	Cost and Fares	

2.3 Tool Development and Application

As discussed in Section 2.1, there are two general study approaches that can be used; first, minimize the wake produced by the vessel, and second, investigate concepts to address potential shore impacts.

The impacts of new vessels could be investigated by treating Rich Passage as a full-scale laboratory; selected vessels could be operated in Rich Passage and the shore response indicators to that vessel monitored. This would provide valuable data, but just for that particular vessel. The study of a large number of vessels would likely prove to be both impractical and financially prohibitive. To do this requires a different approach: numerical modeling.

Numerical modeling has a number of advantages over other types of analysis. In this specific case, they include the following:

- Numerous vessels can be investigated with very limited cost
- Vessels that are unavailable, or still in the design stage, can be investigated
- The numerical shoreline can be exposed to extensive testing, saving the real shoreline from potential damage
- Many simulations can be performed in a limited amount of time
- The effects of an operating schedule over an extended period of time can be assessed

Numerical modeling requires validation to ensure that the model accurately describes the behavior seen in nature and, in certain cases, calibration must be performed to provide additional values or data for the model. In the present case, there is an extensive set of field data to meet these needs.

This section outlines the numerical modeling plan for the present study and identifies the numerical models that will be developed and/or used. Specific details of the numerical models can be found in Section 5 of this report.

The ultimate aim of the modeling program is to predict the response of the shoreline of Rich Passage and the immediate vicinity to the introduction of POFFs. Several different types of numerical models are required. These include:

- Tidal model to predict the water levels and currents
- Wind-wave generation and propagation model to predict nearshore waves generated by wind

- Wake generation and propagation model to predict the wake produced by the vessel and its transformation from the vessel to the shore
- Shore response model to predict the response of the shore over time

Tidal models are well-developed, widely-available, and routinely applied to coastal areas. The ADCIRC model (Luettich et al, 1992) developed by the University of North Carolina and Notre Dame University, through funding from the U.S. Army Corps of Engineers, will be used in the present study. Wind-wave prediction and transformation models are also relatively well established. A simple parametric wave hindcast model will be used to predict wind wave growth and decay (e.g. EM1110-2-1100 (Part II); Dupuis et al, 1996), the STWAVE model (McKee-Smith et al, 2001), and the CoastL model (MacDonald, 1998) will be used to transform waves in the presence of currents to the nearshore. The remaining two models will need to be developed within the present study, because such models are either not presently available (high-speed wake models) or will have to be modified to suit the special conditions of Rich Passage and the surrounding shores (shore response model for gravel coastlines). These models will be discussed in detail in Section 5.

2.3.1 Existing/Historical Conditions

A number of data sets on the wake generation characteristics of high-speed vessels are available. These include data sets for vessels that have been operated between Seattle and Bremerton. Both offshore data (i.e., excluding the transforming effects of bathymetry) and nearshore data exist. These data will be used to design and validate the wake generation and transformation model. From this work, a number of vessel profiles can be developed that can be applied to Rich Passage.

Large amounts of data (e.g., measurements of wakes, shore profile response at a number of time intervals, etc.) exist from POFFs that have operated in Rich Passage in the past. These data will be used to design, test, and validate the beach profile response model. The data from previous POFF operations in Rich Passage and from trials of other high speed vessels are reviewed in Section 3.

The end product of the examination of the historical data will be a set of models that can be used to predict the response or potential response of the existing shorelines to new conditions (e.g., vessels, routes, service frequency, beach nourishment).

2.3.2 Evaluation of Alternatives

There are a number of free variables that may need to be investigated in order to determine the feasibility of a viable POFF service for the Seattle to Bremerton route. These may include, among others:

- Vessel type and vessel size

- Vessel speed, route, and service frequency
- Implications and conceptual design of hard and soft shore protection

The initial modeling exercises will be used to evaluate each of the above variables, to develop feasible ferry service conceptual alternatives. These alternatives would need to be evaluated using other criteria (e.g., economics) in addition to those used in the preliminary assessment for any practical applications.

3.0 Review of Data and Data Requirements

This section describes the information and data obtained and reviewed specifically for this study and the relevance of that information. The effort to gather the information required extensive research among agencies and PI Engineering archives, and the collection of additional field data. Data from previous POFF operations include open water wake trial data, nearshore wake measurements in Rich Passage, and associated shoreline and environment data. The most comprehensive data available are from the monitoring program conducted by the RPWAST during the operation of *M/V Chinook* and *M/V Snohomish*. The data from previous studies provide a benchmark against which to compare potential alternatives. High quality data are required to develop and verify the models described in Section 2.3. A monitoring program was developed as part of the present study to continue the collection of beach profiles at monitoring sites in the study area, and the collection of biological and habitat data.

3.1 Existing Aerial Photographs

As part of previous work for WSF and the Attorney General's office, PI Engineering conducted a search for aerial photographs covering the study area for the period 1961 to 1998 (PI Engineering, 1999). The purpose of collecting historical aerial photographs was to establish trends in beaches and shorelines prior to and following the operation of POFFs in Rich Passage. A subset of the photo archive was used to evaluate beach sediment characteristics and dynamics for the interval 1982 to 1992.

Not all aerial photographs located were used in the study because many contained various deficiencies such as inappropriate scale, insufficient coverage, or poor image quality. Many of the earlier photos were at too small a scale for identifying relevant shore features. Also, because of the presence of vegetation, buildings, and structures overhanging the shoreline or casting shadows across the shore, it was not always possible to delineate or identify shore features from the photos.

The study included analysis of the sand beach footprints derived from the aerial photographs for two sand beaches on the Port Orchard side of Rich Passage between 1961 and 1992. Beaches on the Bainbridge Island side of Rich Passage were not included in the analysis because the areas of gravel and cobble sediments were not distinguishable from areas of exposed hardpan (bedrock) in the photographs. The results of the analysis indicate that the sand beach areas decreased between 1962 and 1985, and increased between 1985 and 1992. The changes in area associated with each of these trends was determined to be greater than the potential errors in the accuracy of the photo derived sand bar footprints. The results indicate that significant cyclic variations in beach area may occur in response to climatic factors (PI Engineering, 1999).

Oblique aerial photographs from the Washington Department of Ecology (2000) were also downloaded and reviewed for the present study. These

provided useful qualitative information for classifying shore types and identifying coastal structures.

Recent aerial photographs obtained from the Washington Department of Natural Resources (WDNR 2000) included black and white digital orthophoto (E,N, .shp). A color orthophoto of the study area dated 2002 is shown in Figure 3-1.

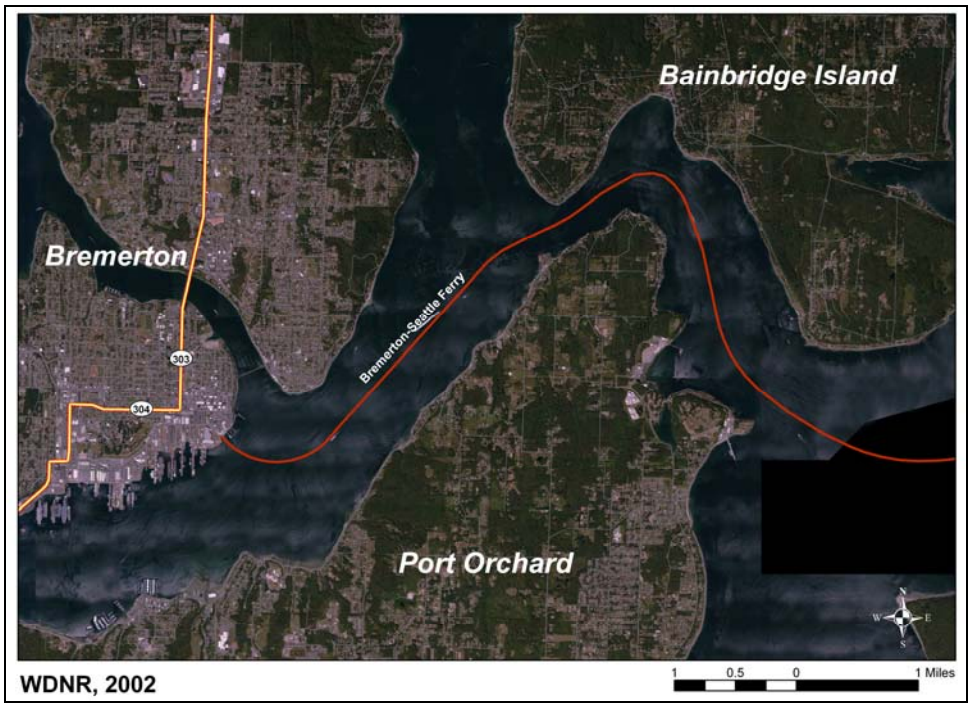

Figure 3-1. Recent aerial photographs obtained from the Washington Department of Natural Resources (WDNR 2002)

3.2 Properties and Structures

3.2.1 Geographical Information Systems (GIS) and Computer Aided Design (CAD) Drawings

Extensive GIS and CAD data exist for the study area including those databases residing with Washington State Departments of Natural Resources (WDNR), Ecology (WDOE), and Transportation (WSDOT), Kitsap County, and the City of Bainbridge Island.

The City of Bainbridge Island conducted a detailed inventory of nearshore structural modifications (e.g., bulkheads, groins, docks) and selected natural shoreline features during the summer of 2001 (Best, 2004). Using GPS technology, existing GIS data, and recent Department of Ecology aerial photography, the City inventoried 53 miles of shoreline, including approximately 4 miles within the study area. The inventory supports the Bainbridge Island Nearshore Assessment and the City's Shoreline Management Master Program by developing a baseline inventory of existing structural modifications,

mapping a detailed regulatory shoreline (ordinary high water mark), and ground-truthing aspects of the Washington State ShoreZone Inventory (WDNR, 2001). Figure 3-2 shows the distribution of shore drift cells and coastal structures (stairs, groins or drift sills, and shore armour) on the Bainbridge Island shoreline within the study area.

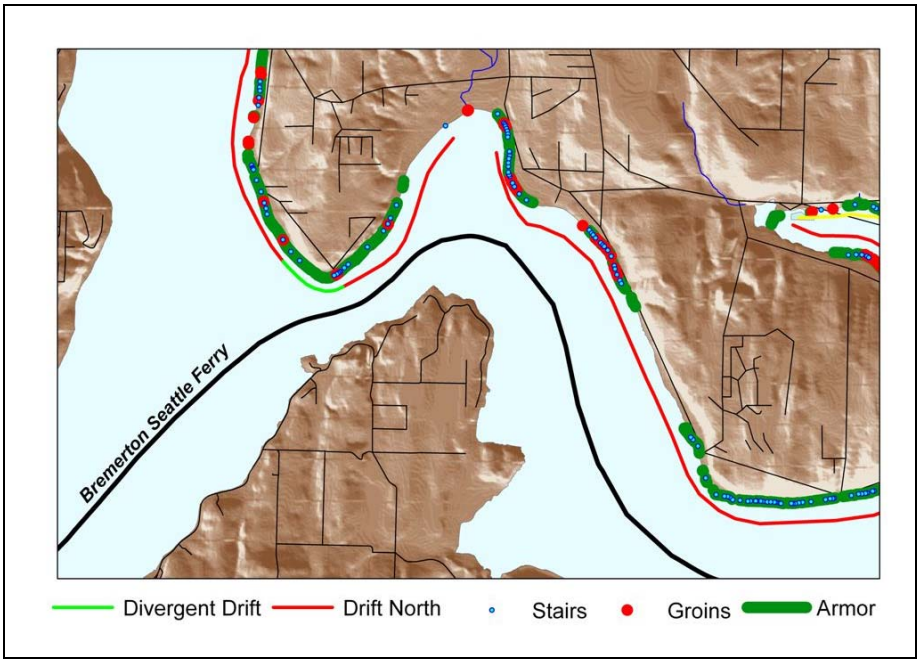

Figure 3-2. GIS layers from the Bainbridge Island Shoreline Inventory showing the distribution of shore drift cells and coastal structures in the study area

As part of previous work for WSF, PI Engineering reviewed existing bulkhead and seawall design along the Rich Passage shoreline and assessed the potential for impact from *Chinook* wake wash on bulkheads and seawalls (PI Engineering, 1999). The assessment identified that the majority of bulkhead construction began in the late 1950s and has continued up to the present time so that now the majority of the Rich Passage shoreline is bordered by some form of shore protection structure. The assessment noted that structures built prior to the mid 1980s would have been built to protect properties from beach and bluff erosion that would have been occurring as a result of coastal processes prior to the introduction of POFF. Many of the structures have been repaired or replaced a number of times since original construction. The assessment also noted that a number of factors related to the design of a large number of the bulkheads and seawalls present in Rich Passage may have lead to an exacerbation of the erosion that occurred during the previous POFF operations. These factors include:

- Reduction, or in most cases total elimination, of the primary sediment supply to the upper foreshore

- Construction of the bulkhead or structure seaward of Mean Higher High Water (MHHW)
- Presence of a vertical impermeable face which enhances wave reflection with the potential to increase scour of sediment from in front of the structure and to intercept alongshore transport of sediment
- Absence of adequate toe protection to prevent erosion of the structure foundation, loss of back fill material from behind the structure and potential failure or collapses of the structure.

The assessment concludes that the combination of the above factors together with a trend of increasing water levels and wind speeds (wind induced waves) (Section 3.5) during the decade preceding the introduction of Chinook class vessels likely contributed to the erosion that was observed during the 1998-1999 interval.

PI Engineering developed a classification of bulkhead types in Rich Passage to assist WSF with the assessment of the relative effects of POFF wakes and natural processes on shoreline erosion (PI Engineering, 2002). The bulkhead classification (Figure 3-3) is as follows:

- Beach without bulkhead
- Upper-beach bulkhead; Mid-beach bulkhead; Lower-beach bulkhead
- Bulkhead without beach (hardpan), temporary or intermittent beach veneer
- Unprotected bluff

Additional work is needed to integrate GIS information from various sources and to incorporate project specific data, including but not limited to photographs, property information, digital elevation models, nearshore structures, and habitat and physical environment process data. A project specific GIS would provide a valuable decision support tool to guide further analysis.

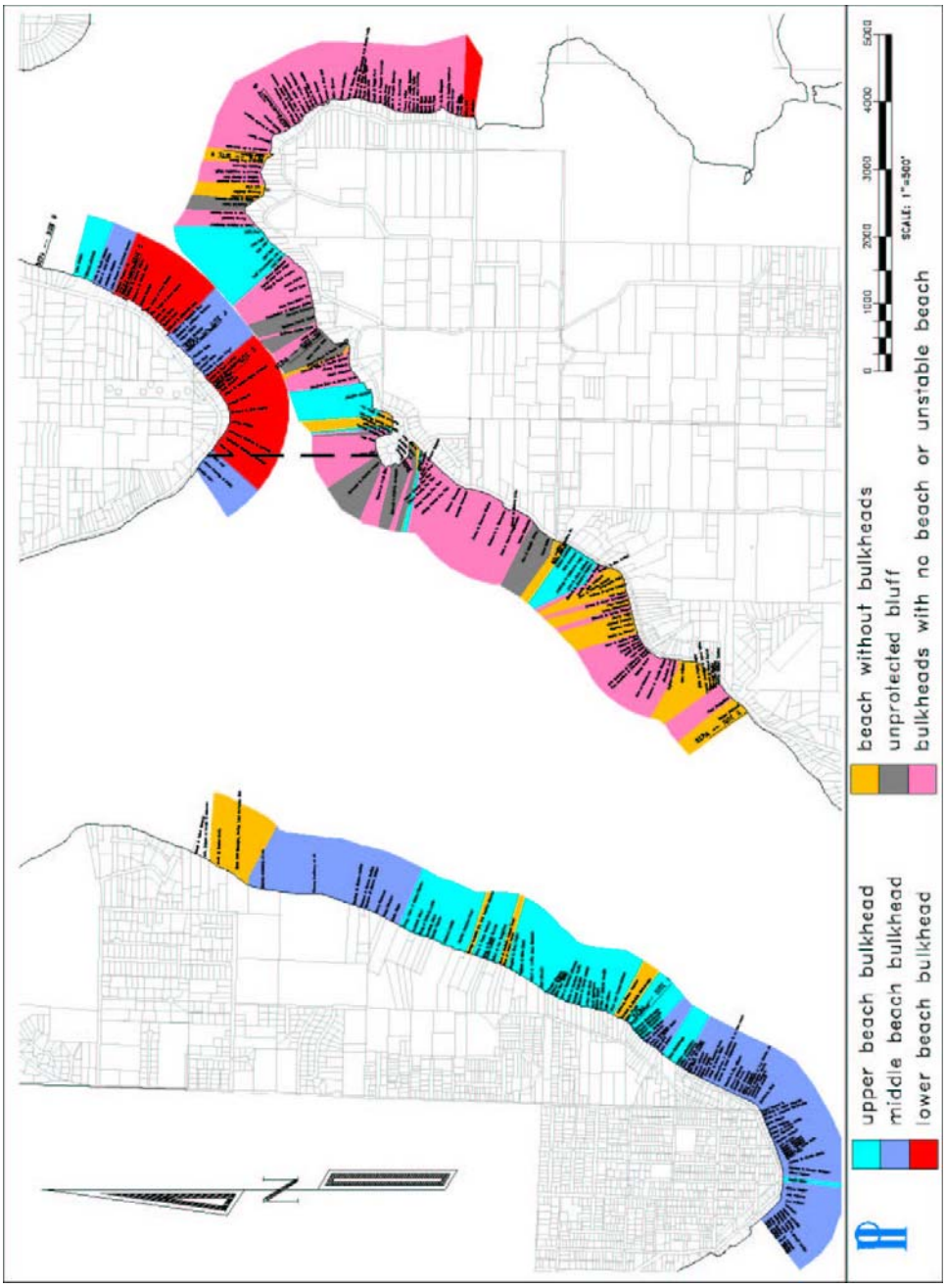

Figure 3-3. Bulkhead classification for class-action properties in Rich Passage

3.2.2 Ground-based photographs

As part of previous work for WSF and the Attorney General's Office, PI Engineering conducted an extensive ground-based photography monitoring program. This program has been continued, expanded, and improved for the present study through the integration of photos with GPS, GIS, and aerial photography.

3.3 Bathymetry and Topography

Bathymetric data, primarily required for development of numerical model grids, were gathered from three sources:

- NOAA - National Ocean Service Hydrographic Survey Data
- NOAA - National Geodetic Data Center Coastal Relief Model
- PI Engineering – Bathymetric Surveys of Rich Passage 1999-2000

The most comprehensive data available are those collected by NOAA-National Ocean Service (NOS) for navigation chart development. NOAA makes these hydrographic survey data publicly available via online and CD formats through their Geophysical Data System for Hydrographic Survey Data (GEODAS) software. The NOS data are the actual soundings, corrected for tide and elevation datum, that are used in the preparation of published charts. The high quality and reliability of these data, the large area of coverage, and recent surveys in the vicinity of Rich Passage lead this data set to be used as the primary source of bathymetric data for this study. The primary shortcoming of using the NOS data for the current study is that the data do not extend above mean low water elevations, thus excluding the areas of the shoreline most prone to vessel wake effects.

The NOAA Coastal Relief Model (CRM) is a digitally merged compilation of bathymetric and topographic data for coastal areas of the Unites States. The CRM data are available in digital format and include bathymetric data collected by NOS, U.S. Geological Survey (USGS), Monterey Bay Aquarium Research Institute (MBARI), U.S. Army Corps of Engineers LIDAR (SHOALS), and various other academic institutions. Topographic data are from the USGS digital elevation models (DEMs) and Shuttle Radar Topography data (SRTM). The CRM data have become available to the public in the past 2 years and are not particularly well documented. Our initial hope was that the data would help to fill in the areas above mean low water that are not covered by the NOS data, as discussed above. As the CRM data are not truly measured data, but a derivation of multiple data sets, comparisons of CRM data with NOS and other local measurements was conducted. The results of the comparison showed that the CRM elevations differed significantly from elevations in the NOS data and the PI Engineering survey data. It is presumed that these differences are a result of the procedures of used to combine, grid, and generate the CRM data. Although these data may be useful for large-scale analysis and graphics (e.g., Figure 3-4), the accuracy, quality, and reliability of the data are not acceptable for the use of model grid development.

PI Engineering conducted bathymetric monitoring surveys in 1999-2000 as litigation support for the Attorney General's Office. These surveys covered a wide area, with sparsely located transects to evaluate temporal changes in the beach profile. Although the data from these surveys at elevations above mean low water are somewhat helpful in extending the NOS data for the

model grid, additional measured data are necessary to characterize the beaches of Rich Passage.

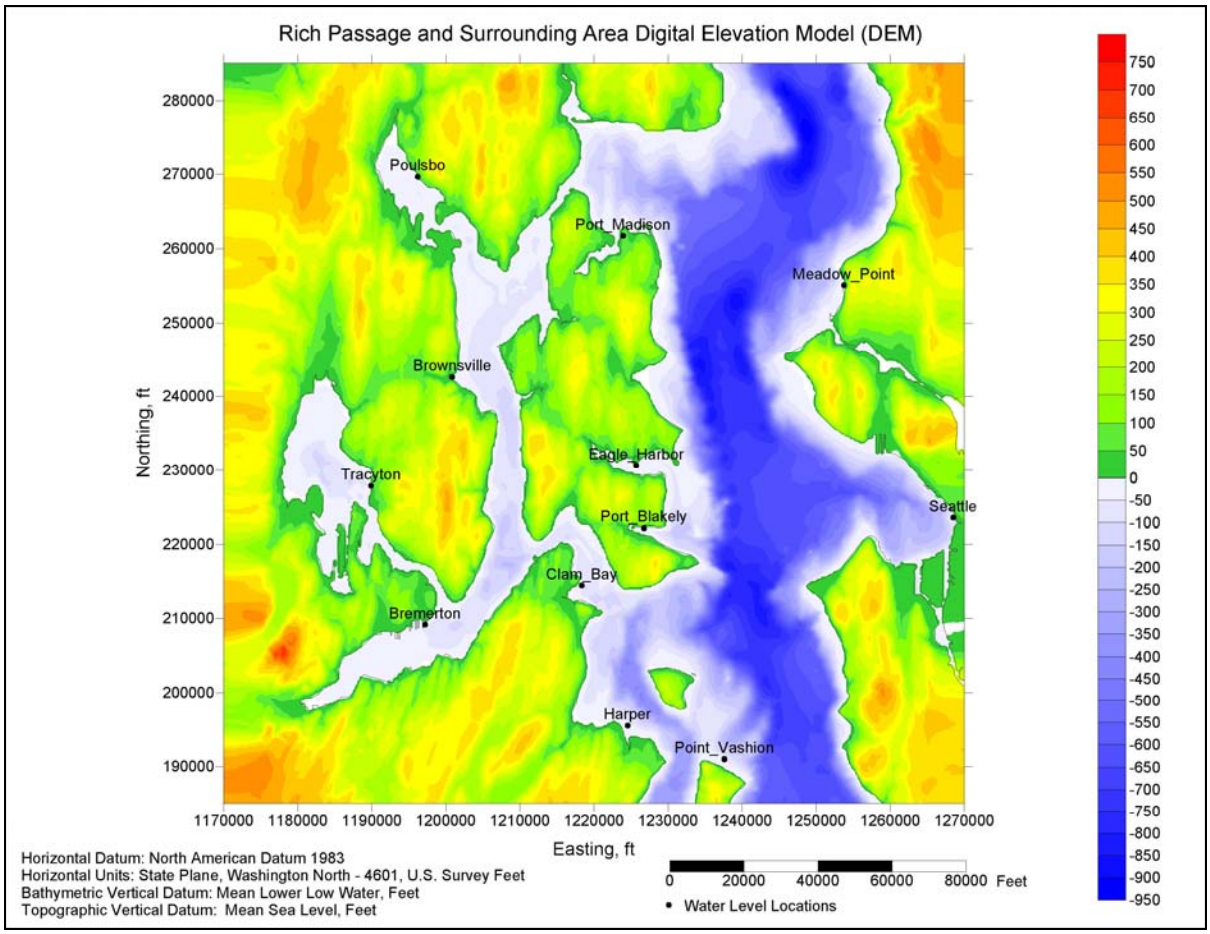

Figure 3-4. DEM for the study area compiled from CRM dataset; the location of water level monitoring and prediction stations in the study area is also shown

3.4 Beaches, Shorelines, and Sediments

3.4.1 Beach Profile Data

As part of the work for the SEPA review, the RPWAST selected ten shoreline sites along the POFF route and three shoreline reference sites in a nearby area outside the influence of POFFs, to monitor the impact of POFFs on physical and biological processes. Figure 3-5 shows the location of the RPWAST monitoring sites. After establishing baseline conditions in April and May 2000 (prior to resumption of normal POFF operations), the study team periodically monitored the sites from May 2000 until June 2001. The monitoring data included beach profile surveys, chronological photos of the upper beach and shoreline protection structures, sediment samples, biological samples, and observations of wave run-up. The study team compared the monitoring data at the sites against baseline conditions and reference

sites to help define the impact of POFF-generated waves on shorelines (RPWAST, 2001; 2002).

As part of this study, beach profiles were surveyed at 14 monitoring sites as shown in Figure 3-5. Monitoring surveys were conducted with a Trimble Real Time Kinematic Global Positioning System (RTK GPS). Profiles were surveyed from the top of bulkheads to low water. Profiles were extended to subtidal elevations by hydrographic surveying with a boat equipped with RTK GPS and echosounder. Total profile length was established at 400 ft. The RTK-GPS enabled horizontal accuracy of approximately +/-10 cm and vertical accuracy of +/-5 cm. A field calibration of the RTK GPS was conducted to reduce discrepancies between local control and GPS-derived coordinates. This was accomplished by centering the GPS antenna over at least four known monuments in the area and recording data for a period of time. The surveyed positions are then spatially adjusted to convert the GPS-derived coordinates to local coordinates.

Beach profile monitoring including plots of profiles are summarized in Appendix D.

Table 3-1. Summary of beach profile monitoring surveys at SEPA sites in Rich Passage

Survey	Date	Collected by
Baseline	April 19-26, May 1-3, May 6-8, 2000	Lin & Associates
1	May 30-31, June 1-2, 2000	Lin & Associates
2	July 17-20,2000	Lin & Associates
3	October 24-27, 2000	Lin & Associates
4	February 12-15, 2001	Lin & Associates
5	June 3, 2001	Lin & Associates
6	September 4, 2001	Lin & Associates
7	January - February 2002	Lin & Associates
8	August 4, 2004	PI Engineering
9	November 8-9, 2004	PI Engineering
10	January 17-18, 2004	PI Engineering
11	March 3-4, 2005	PI Engineering

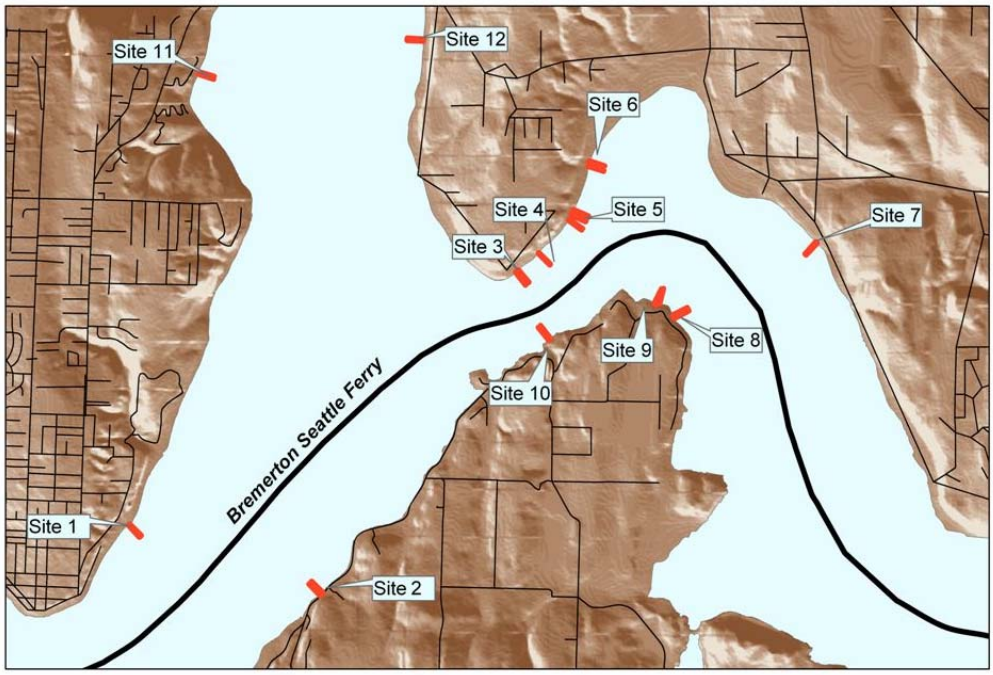

Figure 3-5. Beach Monitoring Sites

3.4.2 Sediment Characterization

As part of this study, PI Engineering collected data on the surface and subsurface sediments on beaches in the study area. Two methods were used to collect these data: sediment cores and photographic sampling. These methods are discussed in more detail below.

3.4.2.1 Sediment cores

Sampling transects were established from MHHW to -5 ft MLLW (Mean Lower Low Water) at each of 6 study sites. Four sediment cores were taken at three locations along each transect, within the uppermost, lowermost, and midpoint quadrats of the transect. The core sampler was 4 inches in diameter and 6 inches deep. Where the substrate was composed of 100 percent bedrock within the quadrat, cores were not taken. One core from each location was set aside for grain size analysis. This core was taken after removing the uppermost armoring layer of substrate, approximately 1-2 inches deep. Grain size analysis was performed following standard ASTM D-422 protocols. The remaining three cores from each site were sieved using a 0.5 mm mesh sieve.

3.4.2.2 Photographic sampling and analysis

Because photographs can provide a quick assessment of sizes and an accurate representative measure, photographic sampling was used as

one of the tools to determine the particle size distribution (PSD) of the surface layer of beach sediments. Photographic samples of the surface layer of exposed beach surface sediments were acquired from areas accessible above the low water line. One photograph of the sediment surface was taken at 3 locations along each transect, within the uppermost, lowermost, and midpoint quadrats of the transect. Photographic sampling consisted of photographing surface sediments using either an Olympus D460 digital camera or a Canon G6 digital camera. For accurate analysis of the PSD and to reduce sampling errors, all photographs were taken as close as possible to perpendicular to the plane of the bed material. A 0.5 m square sampling frame covering the entire plane of the image was employed to scale images and quantify particle sizes (Figure 3-6). The techniques for determination of PSD from photographic images is described in Appendix A (Grain Size Analysis of Beach Sediment in Rich Passage, Washington, August 3, 2004).

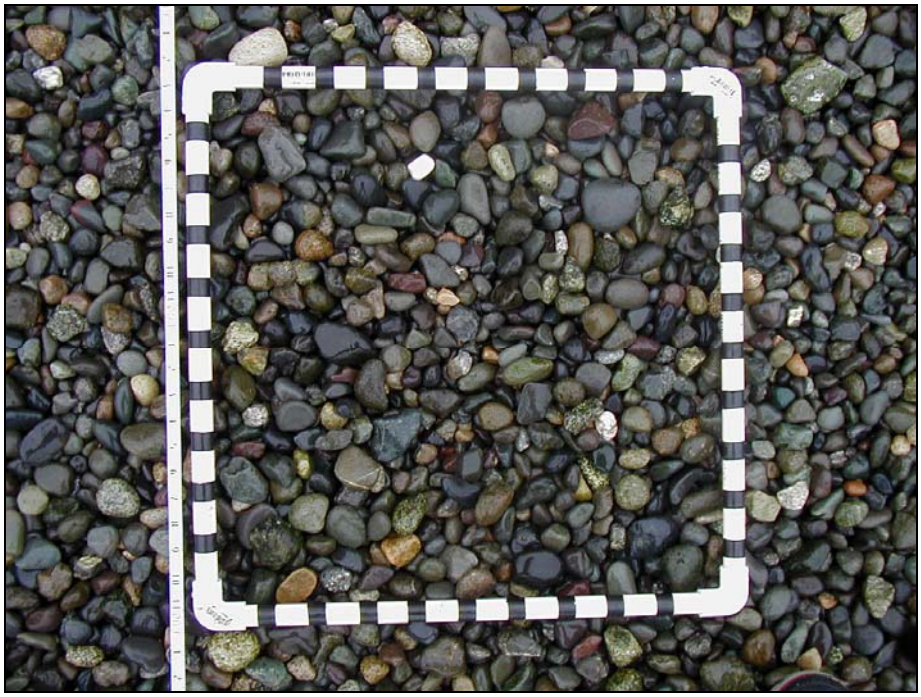

Figure 3-6. Example photographic sample of beach surface sediments

Beach sediment characteristics and their relationship to beach morphology and coastal processes are discussed in Section 4.

3.5 Tides, Currents, and Water Levels

As part of previous work for WSF and the Attorney General's office, PI Engineering conducted extensive water level and current monitoring in the study area during 1999 and 2000 to characterize current speeds and directions in response to water levels variations and bathymetry.

Figure 3-7 shows the locations of four monitoring stations in the study area. Three stations were located in Rich Passage at depths of about 8 to10 m near the shore and another was located in the shallow water in the Port Orchard reach offshore from downtown Bremerton. Five deployments were carried out independently in separate intervals. A SonTek Acoustic Doppler Profiler (ADP) with an imbedded pressure sensor was deployed on the seafloor at all stations to measure both currents at different depths (speed and direction) and surface elevation at 10-second intervals. Table 3-2 shows the data recording intervals, station coordinates (WASP, N), and the depth for each deployment. The pressure sensor failed to record surface elevation in the first deployment for Station A, so an additional deployment (Deployment 3) was carried out later as a replacement.

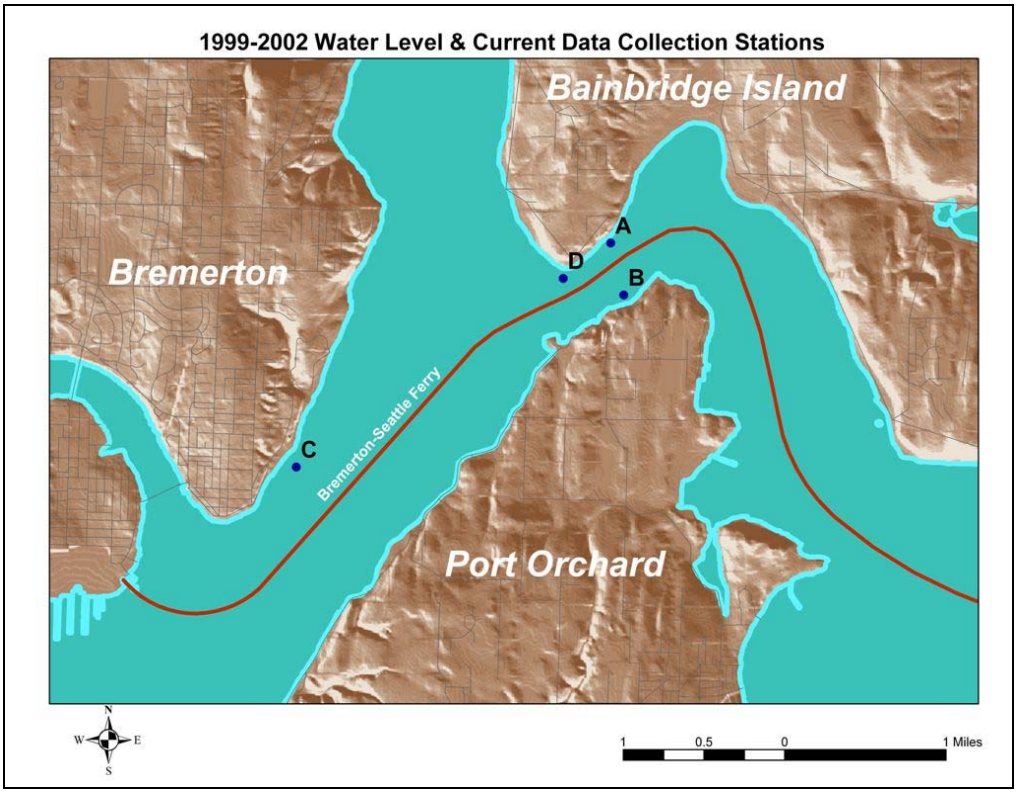

Figure 3-7. Locations of 1999-2002 water level and current monitoring stations

Table 3-2. 1999-2000 Rich Passage current monitoring stations and deployment time

Deployment	Station	Start Time (UTC)	End Time (UTC)	Easting (m)	Northing (m)	Depth (m, mllw)
1	A	9/16/1999 0:59	10/23/1999 0:09	370024.70	67411.13	7.00
2	B	10/23/1999 0:59	12/7/1999 9:39	370153.80	66886.71	8.47
3	C	3/3/2000 16:59	3/24/2000 21:29	370024.23	67403.95	8.01
4	D	3/24/2000 21:59	5/11/2000 20:29	366887.76	65177.82	8.66
5	E	5/12/2000 17:59	6/27/2000 1:19	369549.88	67052.65	10.13

3.5.1 Water Levels

The rise and fall of water level in the area is fairly uniform, dominated by astronomical tides in Puget Sound propagating into the bay area through Rich Passage in the southeast and Agate Passage at the north end of Bainbridge Island. Tides in the area are characterized as mixed semi-diurnal with two high and low tides per lunar day. Statistics for a 12-year-long tidal elevation records from the NOAA long-term monitoring station at Seattle (shown in Figure 3-8) indicates that the average high tide in the area is at about 3.5 m MLLW, and the highest daily high tide may reach 4.4 m above MLLW. The highest tides and greatest tidal ranges in the annual cycle usually occur in winter months.

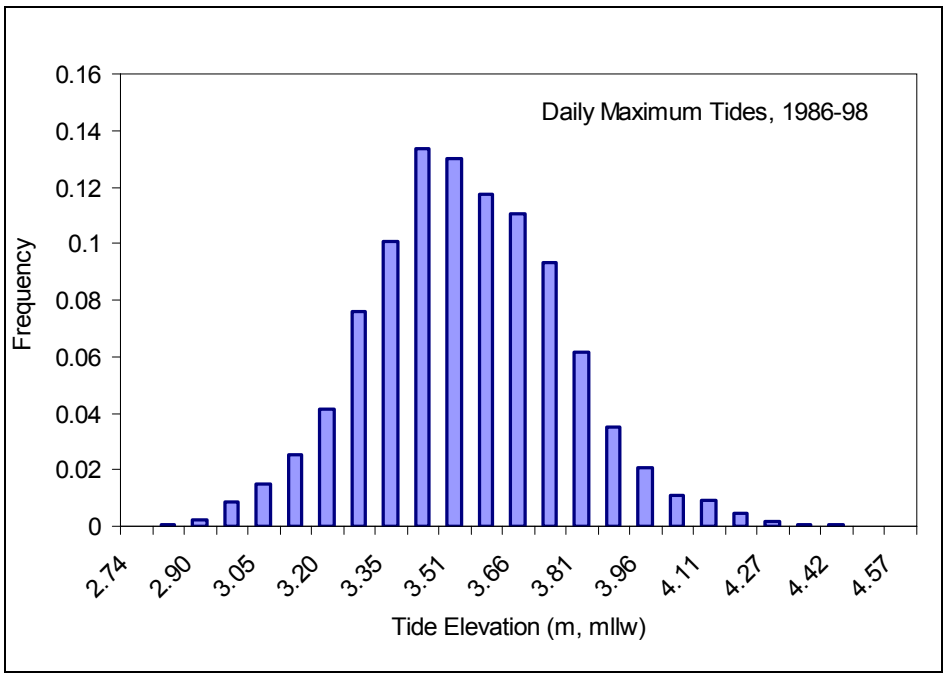

Figure 3-8. Distribution of daily maximum tides based on 1986-1998 NOAA tide gauge observations at Seattle Harbor

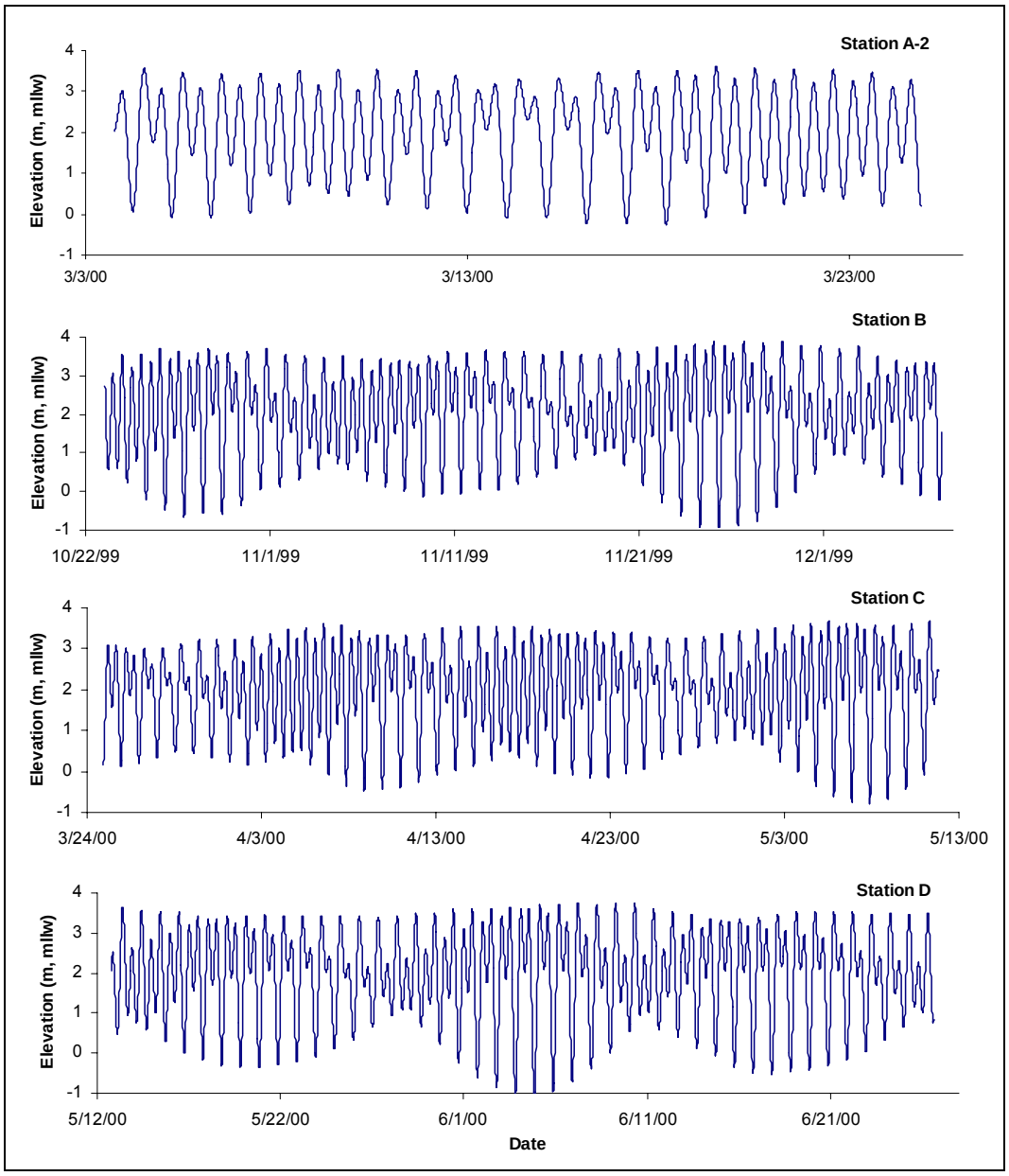

Figure 3-9. Measured surface water elevation at four stations in different deployment periods (water level data is not available at Station A-1)

Figure 3-9 is a plot of the measured water surface elevation at four stations for different deployment periods. Figure 3-9 indicates that tidal ranges in November and June are greater than March, April, or September. These variations reflect the semi-annual and annual cycles of the astronomical tides in the region. A two-week-period spring and neap cycle is clearly seen in all time series plots, and a diurnal tide is dominant most days, especially in the spring cycle.

Other factors that may affect water level in the study area besides astronomical forcing include storm surges, seasonal effects of water temperatures, El Niño, and climate change. For example, sea-levels

more than 0.3 m above normal levels in the eastern Pacific have been correlated with the occurrence of El Niño (e.g. Komar, 1998). So far no detailed studies of sea-level variations in response to El Niño have been documented for the Puget Sound region (Miller, 2003).

Figure 3-10 shows a time series of maximum daily water levels measured at Seattle between 1980 and April 2005. The time series of daily maximum elevations indicates that there are long-term sea level variations super-imposed on the diurnal, spring-neap, annual, and semi-annual cycles. Such variations may be caused by storms and large-scale climatic processes such as El Niño.

Figure 3-11 shows time series of the annual maximum high water level based on the measurements from Seattle together with the Oceanic Niño Index (ONI). The ONI is calculated as a three-month running mean of Sea surface Temperature (SST) anomalies in the Niño 3.4 region (5ºN-5ºS, 120º-170ºW) as described by Smith and Reynolds (2003). ONI data shown in Figure 3-11 are from the NOAA Climate Prediction Center (http://www.cpc.ncep.noaa.gov/). An ONI of more than +0.5^{o}C for 5 or more consecutive over-lapping seasons indicates El Niño while ONI of less than -0.5^{o}C for 5 or more consecutive over-lapping seasons indicates La Niña. With the exception of 1996 and 1997, there is a strong correlation between the annual maximum high water levels and the ONI. The annual maximum water levels in 1996 and 1997 also correlate with high wind speed events in those years. The observed correlation between the annual maximum high water level and ONI series suggests that water level variations in Puget Sound may respond to El Niño cycles.

In general, higher water surface elevations make beach properties along the Rich Passage shorelines more vulnerable to wave/wake actions because more wave energy is able to reach backshore beach areas, directly act on bulkheads and seawalls, and waves may overtop bulkheads and seawalls during high water levels.

The correlation between a typical passenger ferry operation and occurrences of high water levels in the study area was analyzed to illustrate the potential vulnerability of properties to wakes generated by a POFF operation at high tides. The Kitsap Ferry Company currently runs a passenger only ferry between Seattle and Bremerton on four return trips five days per week. Transit time for each leg of the journey is about 40 minutes. Ferry transits based on the 2004 timetable for the Kitsap Ferry were correlated with concurrent water surface elevations measured at the NOAA tide gauge, Seattle. The total number of hours of operation was then estimated for various tide elevations. The results of this analysis are summarized in Table 3-3. The results indicate that there are 327 hrs (or equivalently 490 crossing times) in a year that the ferry will be operating during water levels above 10 ft (3.048 m), MLLW. This accounts for approximately 24%

of the total ferry operation time. Analysis correlating high water level occurrence associated with tides and wave overtopping with bulkhead and seawall elevations is required to fully assess the implications of wake impacts associated with high water levels.

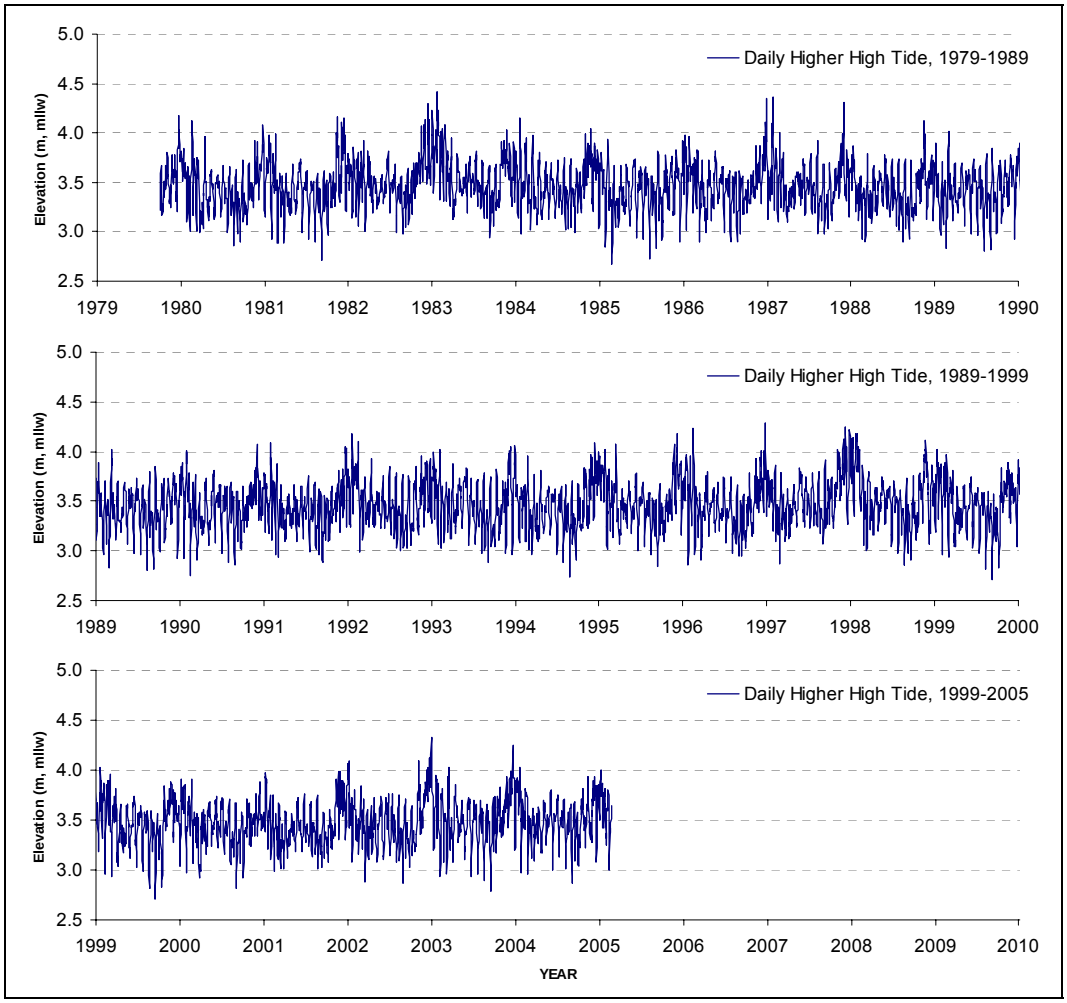

Figure 3-10. Daily maximum tides observed at Seattle

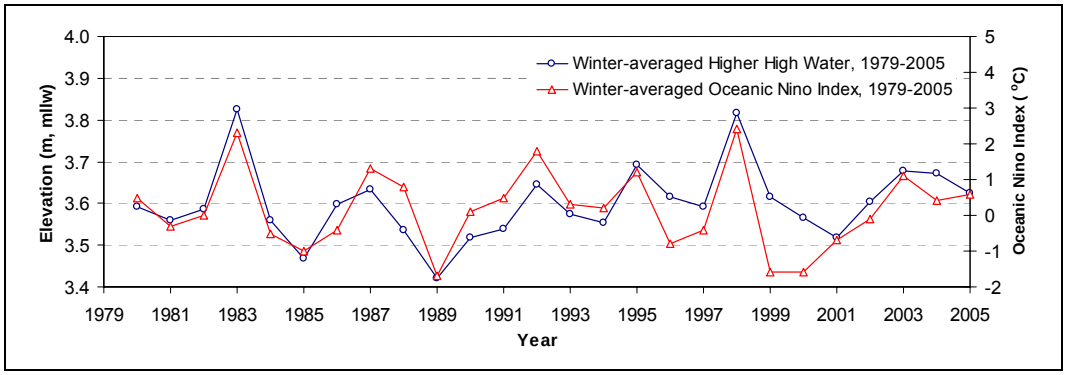

Figure 3-11. Time series of annual maximum water levels and the ONI

Table 3-3. Summary of correlations between Kitsap Ferry Company operation schedule and water levels at Seattle based in 2004

Water level exceedance		Total ferry transits	
(ft, MLLW)	(m, MLLW)	Hours	Percent
12	3.66	29	2
10	3.05	327	24
8	2.44	684	50
6	1.83	959	69
4	1.22	1123	81

3.5.2 Currents

Currents in the study area are generated by a number of forcing mechanisms including tides, wave breaking, wind, and pressure and density gradients that may arise from salinity, temperature, and atmospheric pressure variations (e.g. Mofjeld and Larsen, 1984). Tidal variations (rising and falling water levels) produce predictable current patterns that may be significantly influenced by topographic variations and wind forcing in space and time, respectively. The predictive modeling of tidal currents for the study area is described in more detail in Section 5.

Figures 3-12 through 3-16 show time series of the depth-averaged current speeds and directions measured at stations shown in Figure 3-7. Current speeds vary rapidly with changes in tidal phase and time series exhibit strong diurnal cycles in the peak ebb and peak flood currents. Time series of the depth-averaged current speeds and directions were separated into approximate ebb and flood phases on the basis of current direction at each measurement location. It is important to note that tidal phase defined in this manner is location-specific and may not reflect the phase of tidal currents observed at larger scales. Table 3-4 shows a summary of the current characteristics for location-specific ebb and flood phases for each monitoring station. The data suggest that currents at Station A are strongly flood-dominated (in both speed and duration) while ebb dominance prevails elsewhere (Stations B, C, and D). The data in Table 3-4 also indicates that the flood current at Station D near the tip of Point White is toward the southwest, whereas the ebb current is toward the southeast. These patterns are consistent with the observation that the ebb current entering Rich Passage from Port Orchard Reach and Sinclair Inlet is forced to flow around the tip of Point White resulting in the main body of the ebb flow being deflected to the southeast away from the central axis of the channel toward the Point Glover side of Rich Passage on ebb. This results in stronger and longer ebb currents at Station B than at Station A. The much longer apparent duration of flooding at Station A also reflects the presence of

a re-circulation eddy or gyre that develops along the east shore of Point White during the ebb as a result of flow separation at the tip of Point White. Nearshore flow in the eddy (e.g. at Station A) is to the southwest (flood direction) while the main body of flow is to the north-east (ebb direction). These patterns are explored further in Section 5.

The Acoustic Doppler Profilers (ADP) used to measure tidal currents recorded vertical profiles at 0.5 m intervals. The current profiles were also analyzed to examine vertical variations of tidal current speeds and directions. Figure 3-17 shows an example of the vertical profiles of peak and average flood and ebb currents at Stations A and B. The vertical variation of the currents is not significant, indicating that the circulation of the entire region is predominantly controlled by tidal dynamics. These observations provide justification for the use of a depth-averaged hydrodynamic model such as ADCIRC-2DDI. Circulation modeling is further discussed in Section 5; the data presented in this section is applied to calibration and validation of the circulation model.

Table 3-4. Characteristics of flood and ebb currents at monitoring stations

Station	Phase*	Percentage in Time	Maximum Current		Mean Current	
			Speed (m/s)	Dir (deg-T)	Speed (m/s)	Dir (deg-T)
A-1	flood	82%	1.43	231	0.47	234
	ebb	18%	0.51	43	0.19	60
A-2	flood	83%	1.43	225	0.52	227
	ebb	17%	0.48	44	0.21	41
B	flood	44%	0.86	230	0.31	232
	ebb	56%	1.26	62	0.45	65
C	flood	43%	0.35	204	0.14	216
	ebb	57%	0.87	28	0.18	27
D	flood	46%	1.11	234	0.37	236
	ebb	54%	1.98	105	0.7	102

* Phase is defined on the basis of current direction at location of measurement and may not reflect the tidal phase at larger scales.

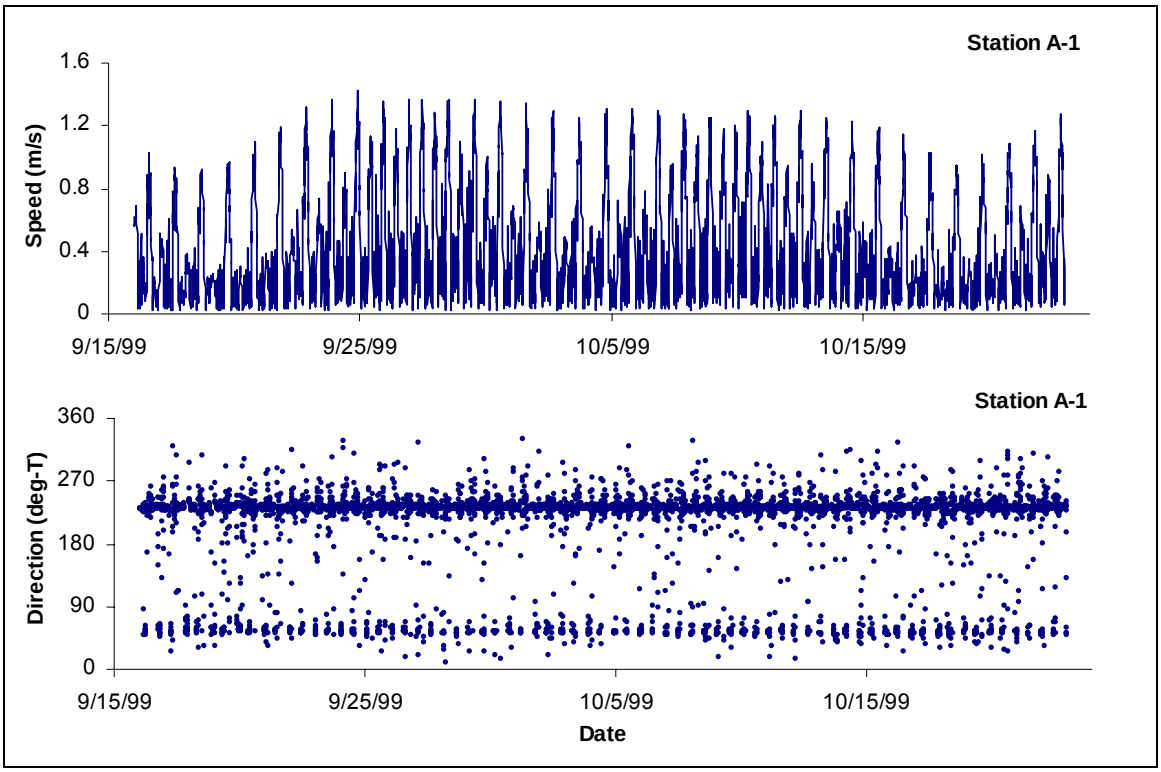

Figure 3-12. Measured current speed and direction at Station A, September 16 through October 23, 1999

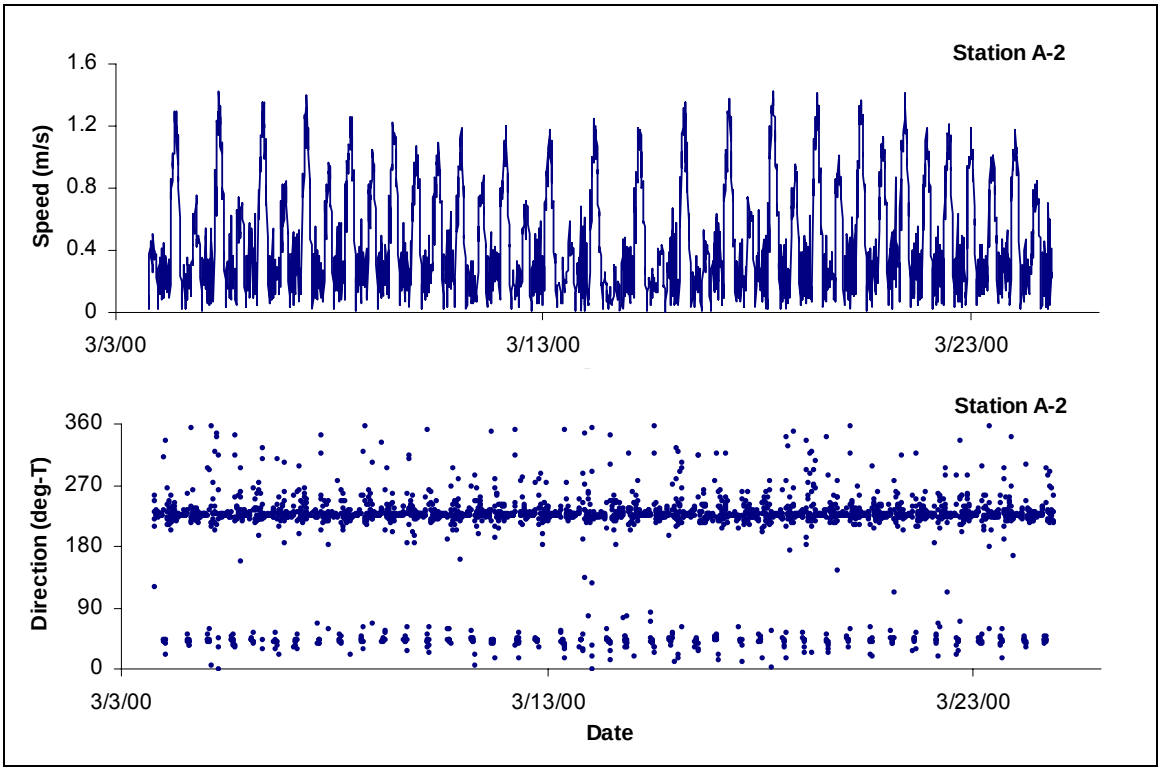

Figure 3-13. Measured current speed and direction at Station A, March 3 through March 24, 2000

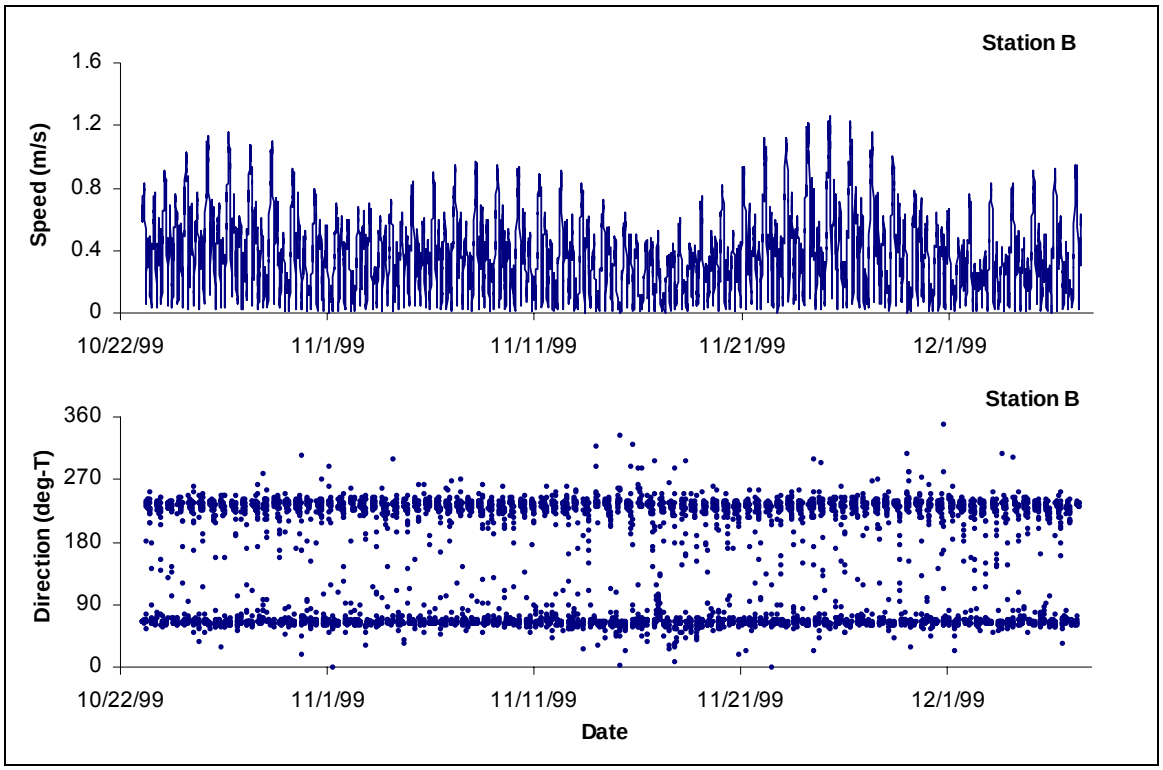

Figure 3-14. Measured current speed and direction at Station B, October 23 through December 7, 1999

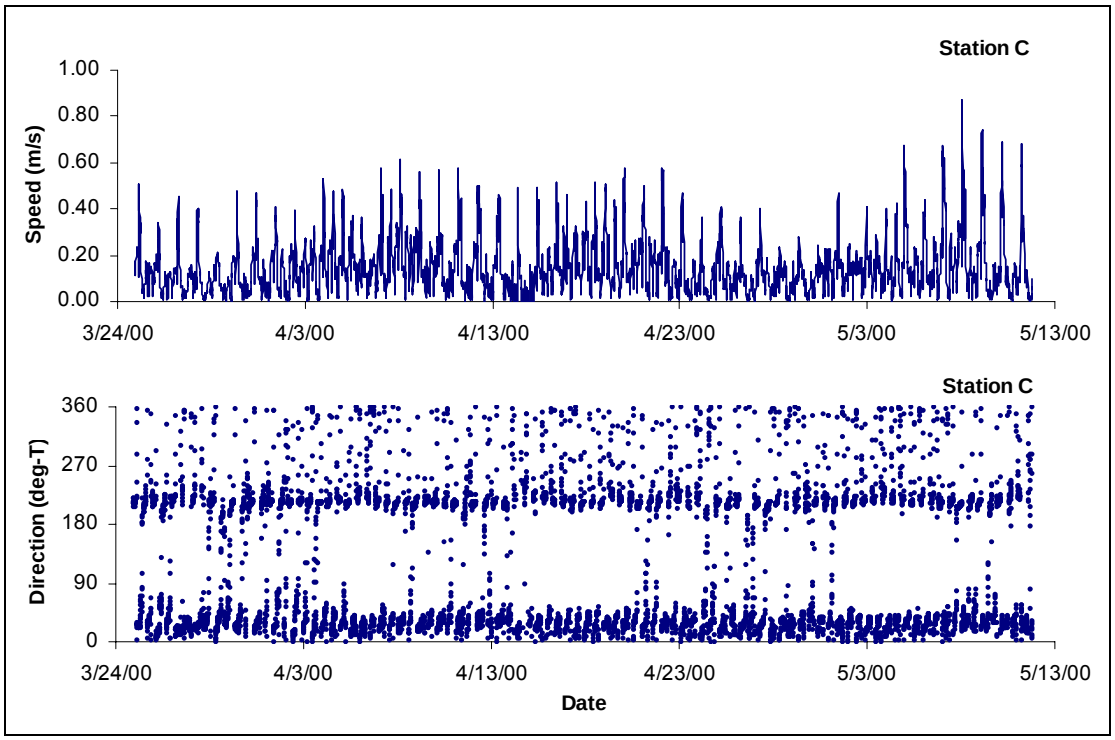

Figure 3-15. Measured current speed and direction at Station C, March 24 through May 11, 2000

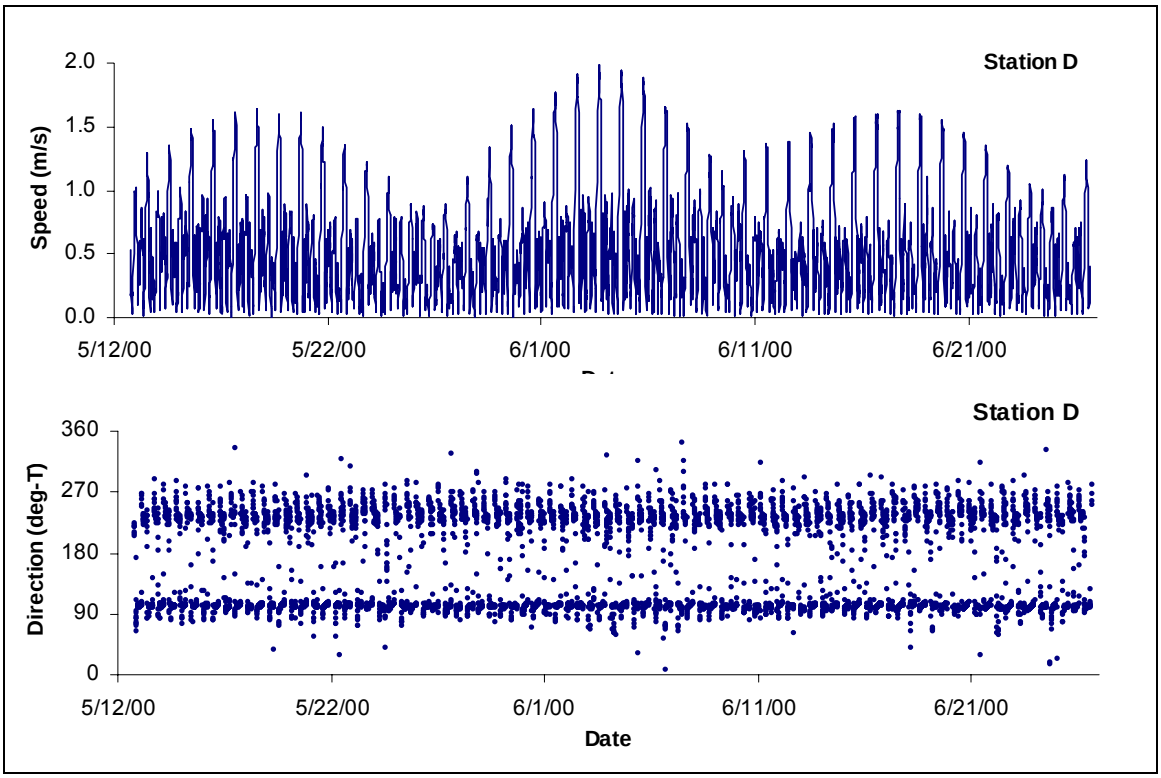

Figure 3-16. Measured current speed and direction at Station D, May 12 through June 27, 2000

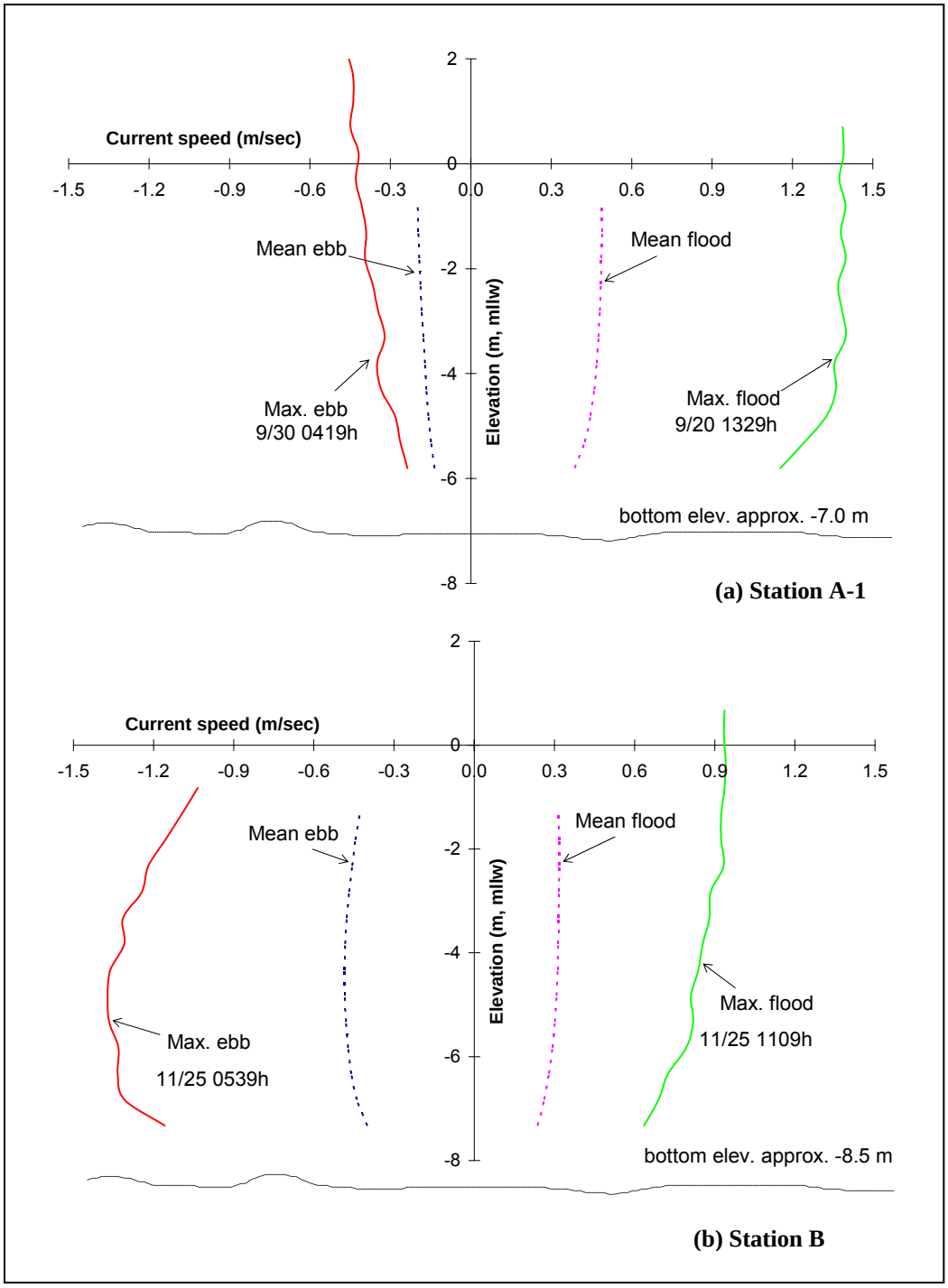

Figure 3-17. Vertical variations of mean and maximum current speeds at flood and ebb tides

3.6 Wind

Wind data are required for predicting and hindcasting locally generated wind waves in the study area. Winds in Puget Sound and western Washington are strongly influenced by the local topography (e.g. Harris, 1954), and therefore

wind data from sites distant from Rich Passage must be applied with caution. Direct measurements of winds inside Rich Passage have not been found. Wind data have been recorded at a number of sites around Puget Sound (Figure 3-18). Included are Washington Department of Transportation stations, used to collect information on road conditions, WSF terminal stations, airports, and NOAA weather stations. Readily available data that are the most relevant to Rich Passage are listed in Table 3-5.

Table 3-5. Rich Passage Wind Data

Monitoring Location	Period of Record	Format
West Point NOAA gage	1984-present	Digital, directional, hourly and every 10 minutes
SEA-TAC Airport	1944-present	Digital, directional
Boeing Field, Seattle	1930-present	
Bremerton Airport	1973 to present	Digitized from paper records, directional, hourly, with gaps
Southworth Ferry Terminal		
Alki Point, WSDOT station		

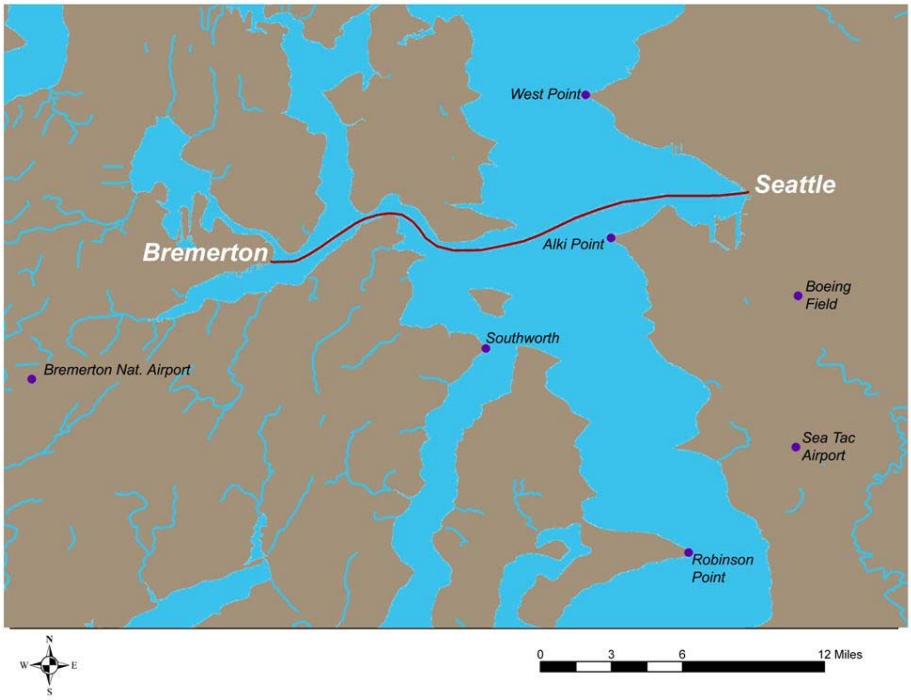

Figure 3-18. Wind data recording sites in proximity to the study area

The West Point station (NOAA, 2004) has the longest record of wind measurements that may be applicable to Rich Passage. The station is located

on a point extending into Puget Sound, thereby minimizing the influence of overland measurements and topographic effects. West Point data are the most similar to "overwater" data and the station is reasonably close to Rich Passage. Figure 3-19 shows a wind rose for West Point station measurements between 1984 and 2005. The measurements indicate two dominant wind directions: north-northeast and south-southeast, indicating an alignment of local winds along the axis of Puget Sound. Southeasterly winds have potential to generate wind waves in the eastern half of Rich Passage.

The Bremerton Airport data were collected inland and are influenced by local topography. However, Rich Passage can also be considered "inland" and therefore the Bremerton Airport data may be applicable. Figure 3-20 shows a wind rose for Bremerton Airport wind measurements between 1996 and 2005. The measurements indicate two dominant directions: north-northeast and south-southwest to southwest. Wind speeds at Bremerton are also generally less than at West Point. Bremerton is to the southwest of Rich Passage and winter storms typically enter Puget Sound from the southwest. Therefore, a wind location southwest of Rich Passage may be a good source for wind data when modeling winds from the southwest. The relationship is further examined in Sections 3.7.1 and 5.3.

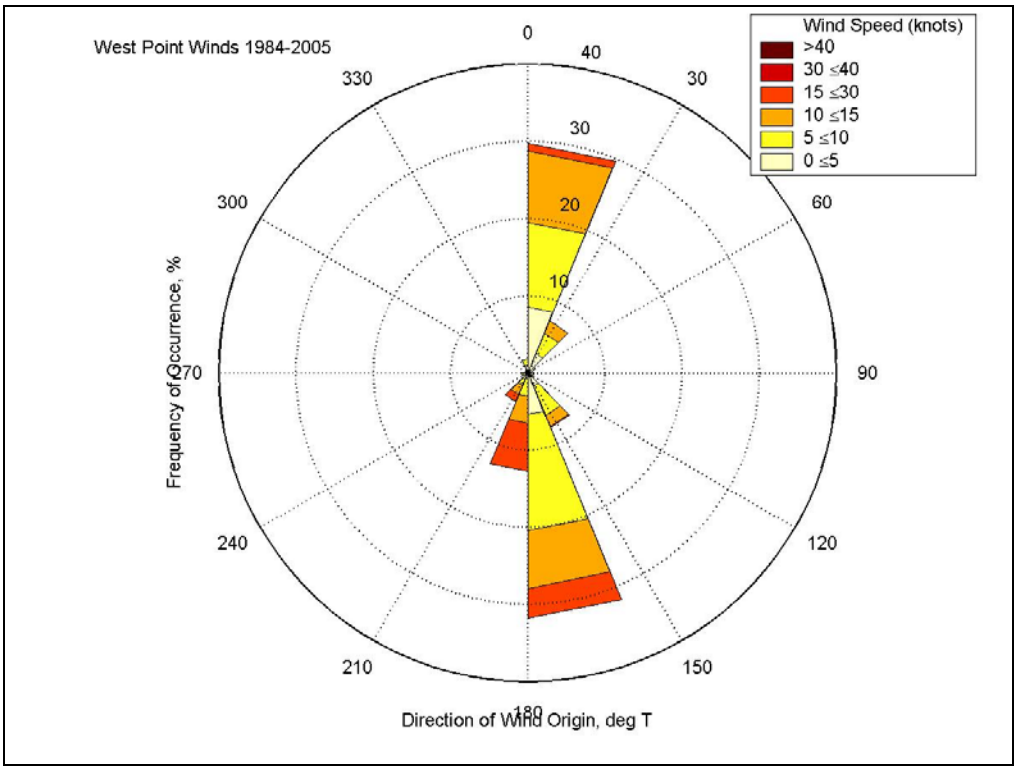

Figure 3-19. Wind rose for measured winds at West Point between 1984 and 2005

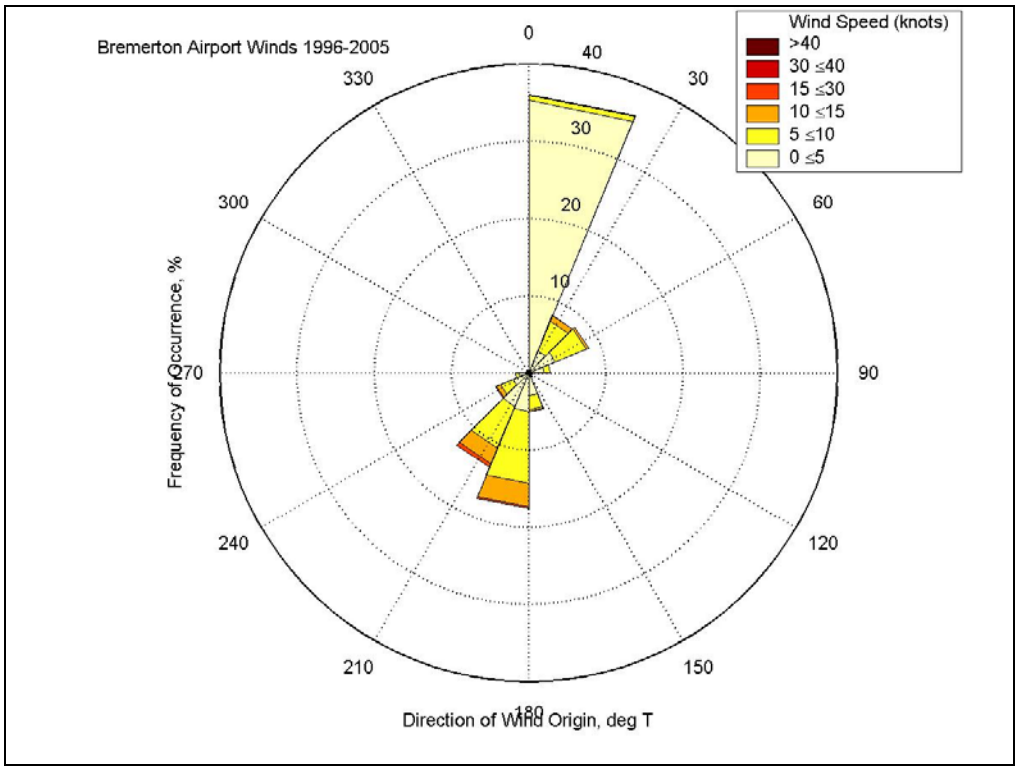

Figure 3-20. Wind rose for measured winds at Bremerton Airport between 1984 and 2005

SEA-TAC airport and Boeing Field have the longest period of record, which is valuable for constructing a wind-wave hindcast. These airports are not on the shoreline or particularly near to the study area. Therefore, the wind data are less applicable to Rich Passage.

The Southworth ferry terminal and Alki Point stations are maintained by the Washington State Department of Transportation. Wind data from these stations are used to inform travelers of weather and road conditions. Further investigation is needed to determine what data are available and in what format. The Southworth terminal is southeast of Rich Passage, and may be valuable for modeling wind waves from the southeast.

Statistical analysis of wind data obtained from the National Weather Service wind monitoring station at the West Point Lighthouse was conducted as part of a previous study (PI Engineering, 1999) to identify long-term trends in mean wind speeds from the southeast direction. The mean hourly wind speeds for winds higher than 10 knots from the south-southeast (090 to 180 degrees azimuth) are calculated for every summer, winter, and yearly time period. Figures 3-19a and 3-19b, respectively, show the change in the number of hours per year (annual) and winter wind speed exceeding 10 knots during the period 1984-1998. Figures 3-20a and 3-20b show the change in the wind speed per year (annual) and winter months during the period 1984-1998.

In the last several years, specifically after winter 1997, there was an increase in the number of hours of a strong wind from the southeast. This direction has

the largest fetch for Rich Passage and can generate significant wave activity. An increase in wind speed and duration is linked to processes causing beach erosion and impact on shore protection structures. Stronger winds generate larger waves. A longer duration of strong winds increases the amount of time that shoreline is affected by a storm, and consequently, the amount of wave energy delivered to the shoreline. It has been estimated that a southeast wind speed from 10 knots to 20 knots can generate wind waves at heights of 0.3 to 0.6 m at the north side of Rich Passage (PI Engineering, 1999).

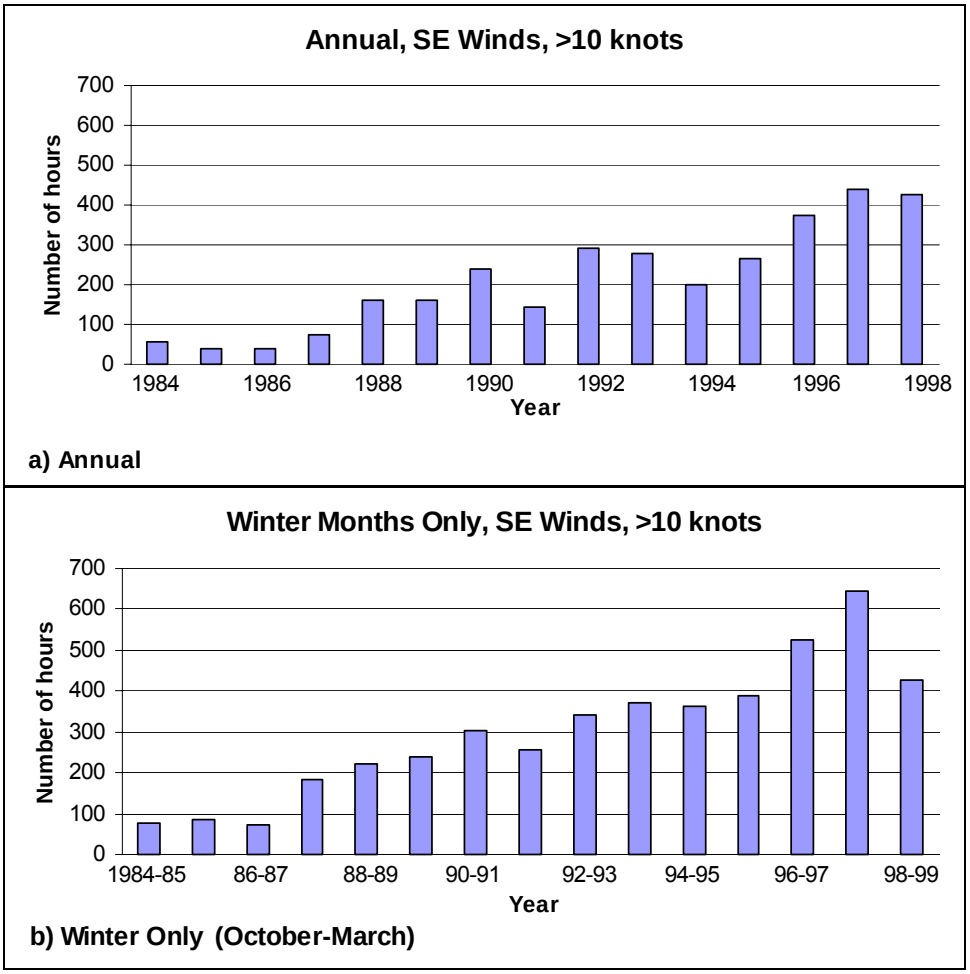

Figure 3-21. Rich Passage Total Wind Speed Hours, Greater Than 10 Knots, SE Direction (Data from West Point Station)

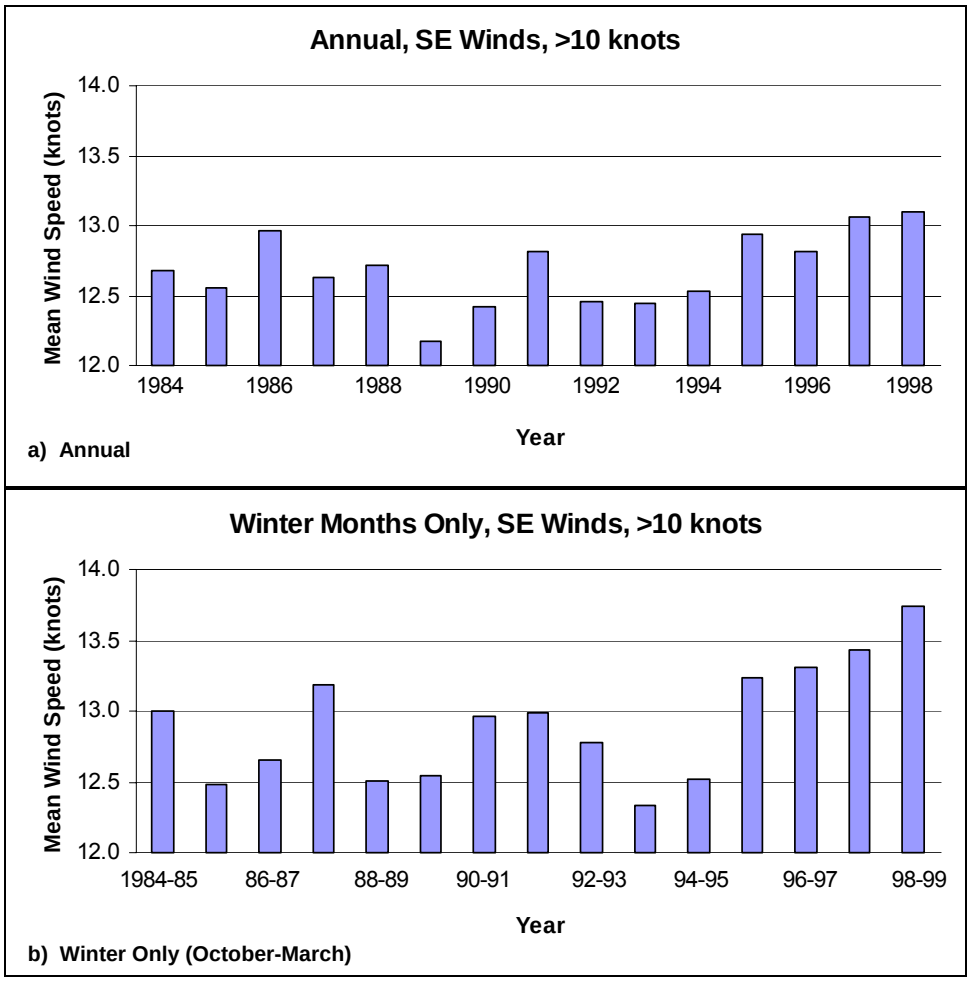

Figure 3-22. Rich Passage Mean Wind Speed, Greater Than 10 Knots, SE Direction (Data from West Point Station)

3.7 Waves and Wakes

As part of previous work for WSF and the Attorney General's office, PI Engineering conducted extensive wave and wake monitoring in Rich Passage to characterize wind wave climate and wakes associated with POFFs and other vessels transiting Rich Passage. PI Engineering also compiled an extensive archive of vessel position data recorded with GPS from a number of vessels transiting Rich Passage, including POFFs. A portion of these data were reviewed and further analyzed for this study to provide verification data for wake prediction models.

Wake data collected as part of sea trials of a number of vessels were also contributed by Fox and Associates for analysis to provide calibration data for wake prediction models.

3.7.1 Wind Waves

Wave and water surface elevation measurements were collected as part of previous work for WSF and the Attorney General's office at several sites in Rich Passage. The wave measurement program is described in Appendix D (Figure D-1) (e.g. PI Engineering, 1999).

The generation of waves by wind depends mainly on the following factors: the fetch (distance of open water over which the wind blows), the wind speed, the length of time the wind blows at a given speed and fetch, and the water depth along the fetch. Wind waves will also be influenced by bathymetry (water depth) and the speed and direction of currents (tidal, wind) as they propagate.

PI Engineering (1999) made preliminary calculations of wave parameters at wave monitoring site 1 which is located on Point White. The longest and most direct fetch at Site 1 is to the southeast and therefore southeasterly winds were only considered in the calculations. Wave parameters including significant wave height, period and energy density were calculated and summarized in a Table in the original report. The calculations of nearshore waves were made with the relatively simple open water wave hindcasting equations as described in the Coastal Engineering Manual (USACE, 2001).

A more comprehensive analysis of wind waves at a number of representative locations in the study area is required to determine the relative importance of wind waves to other forcing mechanisms in causing beach changes.

Figure 3-23 shows time series of wind speed and direction measured at Bremerton Airport on February 4, 2005. The figure below shows a time series of water surface elevations measured in relatively open water at a depth of 95 ft in Port Orchard Reach during a southwesterly wind on February 4, 2005. Winds at the time of measurement were varying between 15 and 20 knots from the southwest as measured at the Bremerton Airport wind station (Figure 3-24). A hand held wind gauge confirmed wind speeds and direction at the time and location of measurement in Port Orchard are consistent with those measured at Bremerton Airport.

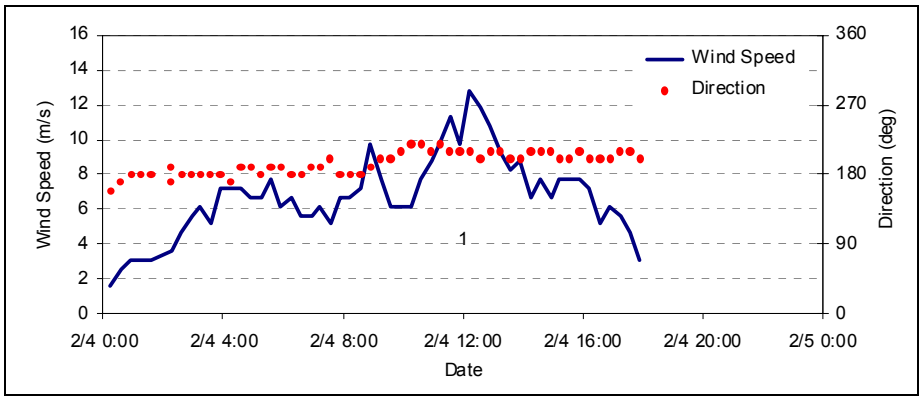

Figure 3-23. Wind speed and direction recorded at Bremerton Airport on February 4, 2005

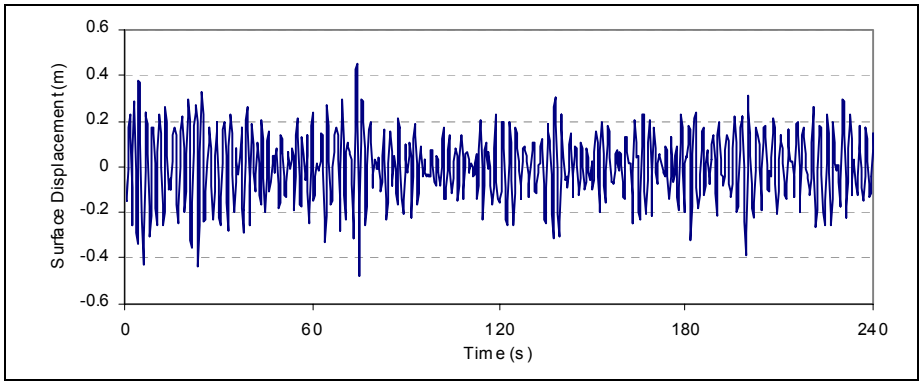

Figure 3-24. Surface wind waves recorded at buoy station IT-01 at 1:00PM, February 4, 2004 (Significant wave height 0.51 m, Peak period = 2.32 sec)

The wind wave measurements obtained at wave monitoring sites in the study area provide the basis for the development and verification of a wave prediction model for the Seattle-Bremerton ferry route. Wind wave prediction models will be applied to the development of a wind wave climate for representative sections of the ferry route. Wave modeling is needed to predict and hindcast wind wave conditions for offshore locations in Rich Passage. Combined wave and current modeling is needed to transform the offshore waves to the nearshore areas so that the comparisons can be made between wind wave parameters and vessel-generated wake parameters. The application of a wind wave model is discussed in Section 5.3.

3.7.2 Wake Data

Wake time series from several WSF POFFs: *M/V Chinook*, *M/V Snohomish, M/V Tyee*, and several WSF car ferries were extracted from water surface elevation time series from in-situ nearshore measurements collected by PI Engineering. Associated positions of vessels transiting Rich Passage including POFFs were recorded with

GPS. The GPS positions were used to correlate vessel transits with wake time series in the wave and water level measurements and to determine vessel position and speed relative to the instruments.

Wake time series measurements from trials of a number of candidate vessels were obtained from Fox and Associates. These vessel trial data include: *M/V Chinook/Snohomish, M/V Bravest, M/V St. Nicholas, M/V Tyee, M/V Condor Express,* and *M/V Red Jet 4*.

3.7.2.1 Wake measurements from trials

Wake trial measurements were also obtained from other vessels considered as candidates for use in Rich Passage. The wake trial data include times series of wakes generated by *M/V Chinook*, *M/V Snohomish, M/V Bravest,* and *M/V St Nicholas* obtained from trials conducted by WSF, and wake trial measurements from *M/V Tyee* obtained by PI Engineering under contract to WSF. Wake trial measurements were also provided by Fox and Associates for *M/V Condor Express* and *M/V Red Jet 4.*

Wake time series during deep water trials conducted by WSF and Fox and Associates are measured using a submerged pressure sensing wave gauge on a taut line mooring. The wave gauge assembly is described in Appendix D. Processing of the pressure time series involves conversion to surface elevation time series to correct for pressure attenuation as a function of depth. Fox and Associates also implement frequency domain filters depending on the presence of wind waves in the record.

During trials, the test vessel passes the deployed instruments at a convenient distance at various specified speeds. Fox and Associates and WSF employed a navigational sextant or a laser range finder to measure distances between the wave gauge and the vessel sailing line. The test vessel is ballasted to simulate the fully loaded condition in both displacement and trim. A series of runs may also have been conducted with all ballast pumped (no passengers) to determine the sensitivity of the vessel's wash to varying displacement due to passenger load. Typically, a series of six runs at each speed increment were conducted to ensure consistent and repeatable results. WSF and Fox and Associates adjusted their estimates of wake height and energy to a distance off centerline of travel of 300 meters by applying a –1/3 wave height decay and averaged the multiple run results at each speed to develop plots of wake height, period, and energy density as a function of vessel speed.

PI Engineering re-analyzed the original wake trial time series collected by WSF and Fox and Associates to provide data for input to wake propagation modeling for several candidate vessels. The re-analysis involved computation of zero-upcrossing and zero-down-crossing

wave heights, wave period, and wave energy density time series as well as spectral analysis to determine the distribution of energy as a function of wave frequency. Time series and results of the analysis are included in Appendix C. The wave propogation modeling for the candidate vessels is described in Section 5.

In addition, a review of wake trial measurements published in the scientific and engineering literature was conducted as part of this study by Art Anderson and Associates of Bremerton. This review is included as part of Appendix E.

M/V Chinook and M/V Snohomish

The AMD 385 *Chinook,* and sister ship *Snohomish,* are 196 tonne, 350-passenger ferries designed by Advanced Multihull Designs of Sydney, Australia and built by Dakota Creek Industries of Anacortes, WA. As discussed in Section 1.4, *Chinook* and *Snohomish* were purchased in 1998 and 2000, respectively, for service as POFFs on the Seattle-Bremerton ferry route.

WSF tested *Chinook* and *Snohomish* by conducting various wake trials at a number of different locations on Puget Sound. Only limited trial data for these vessels were made available to this study. Trial data for *Snohomish* acquired on February 27, 2000 are available to the present study. Trial data for *Chinook* acquired on April 1, 2000 are available to the present study. The *Chinook* trials were conducted to test the effects of interceptors on the wake height and energy density (Stumbo, pers comm., 2004). The results have been published in several related papers (Stumbo et al., 1998; Stumbo et al., 1999; Stumbo et al., 2000). Stumbo et al. (2000) report that a significant reduction of wake energy was achieved in deep water by optimizing trim with interceptors.

Time series from the February and April 2000 trials were analyzed by Pacific International Engineering as part of this study. The time series analysis was conducted to provide input to calibrations of the LSV model as described in Section 5. The time series analysis is provided in Appendix C.

M/V Tyee

M/V Tyee is a 94 ft twin engine displacement catamaran with beam of 31 ft built in 1985 by Nichols Brothers of Whidbey Island. The vessel has a capacity of 270 passengers and a cruising speed of 23 knots. *Tyee* was used by WSF on the Seattle to Bremerton route and later from Vashon to Seattle. At first the vessel was run at cruising speeds, but WSF reduced speeds following complaints from property owners. Beginning in January 2005, *Tyee* has been operated by Aqua Express between Kingston and Seattle.

PI Engineering conducted a study, at the request of WSF, to determine optimal speeds for operating *Tyee* on the Seattle to Bremerton ferry

route (PI Engineering, 2003). The study included compiling, reviewing, and analyzing existing wake data, new field trials in Rich Passage using *Tyee* during June 17 to 20, 2002, and field measurements during *Tyee* ferry operations from August 1 to September 1, 2002. Details of the measurements are summarized in PI Engineering 2003. The results document the relationships between vessel wake parameters (wake height, *H*; period, *T*; and energy, *E*) as a function of distance from the Rich Passage shoreline and vessel speed and compared measured wake parameters with several empirical predictors (e.g. Sorensen, 1997; Verhey and Bogaerts, 1989). In summary, a speed of 16 knots in Rich Passage between Clam Bay and Waterman Point, and a speed of 20 knots in Rich Passage between Waterman Point and Bremerton were recommended as optimal speeds for *Tyee* while operating on the Seattle to Bremerton ferry route. However, further analysis of the relationship between the average H_{max} and vessel speed based on measurements of *Tyee* wakes reveals that H_{max} reaches a maximum at vessel speeds between 16 and 20 knots (Figure 3-25). Also shown are the average heights of the 3 largest and 6 largest waves in the wake train for comparison with H_{max}.

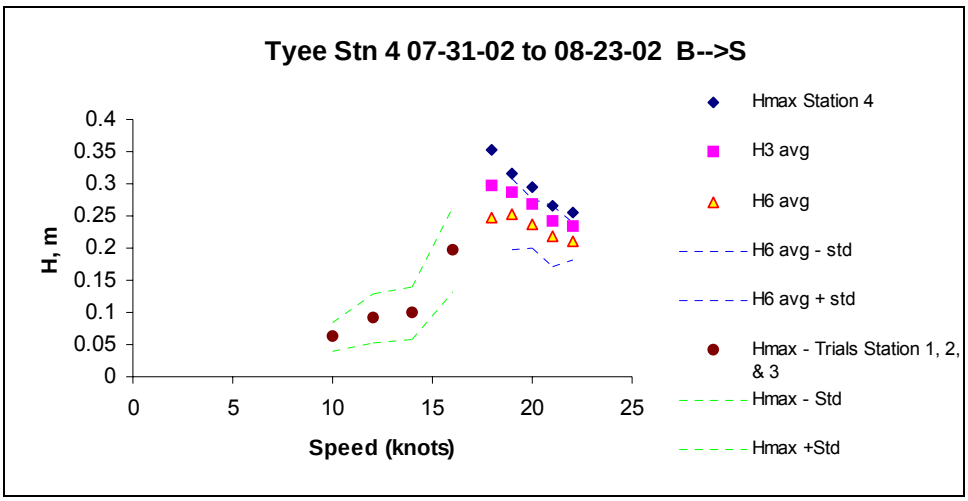

Figure 3-25. Average H_{max} as a function of vessel speed between 10 and 25 knots based on measurements of *Tyee* wakes

According to theory (Kelvin, 1887; Havelock, 1908) the rate of wave height decay in deep water is expected to follow an exponential decay rate of $r^{-1/2}$, where *r* is the distance from the sailing line, in the interior of the disturbance region (transverse waves). At the boundary of the wake (diverging waves) the theoretical decay rate is $r^{-1/3}$ (Stoker, 1957; Crapper, 1984). Thus, the diverging waves decay more slowly than the transverse waves. H_{max} measured during the *Tyee* trials is plotted in Figure 3-26 as a function of distance from the sailing line for a range of speeds; the best fit curves based on non-linear regressions for the theoretical decay rates of $r^{-1/2}$ and $r^{-1/3}$ are also shown. The R^2

values for the non-linear regressions indicate that there is no significant difference in the explanation of variance between the two sets of curves within the range of the data.

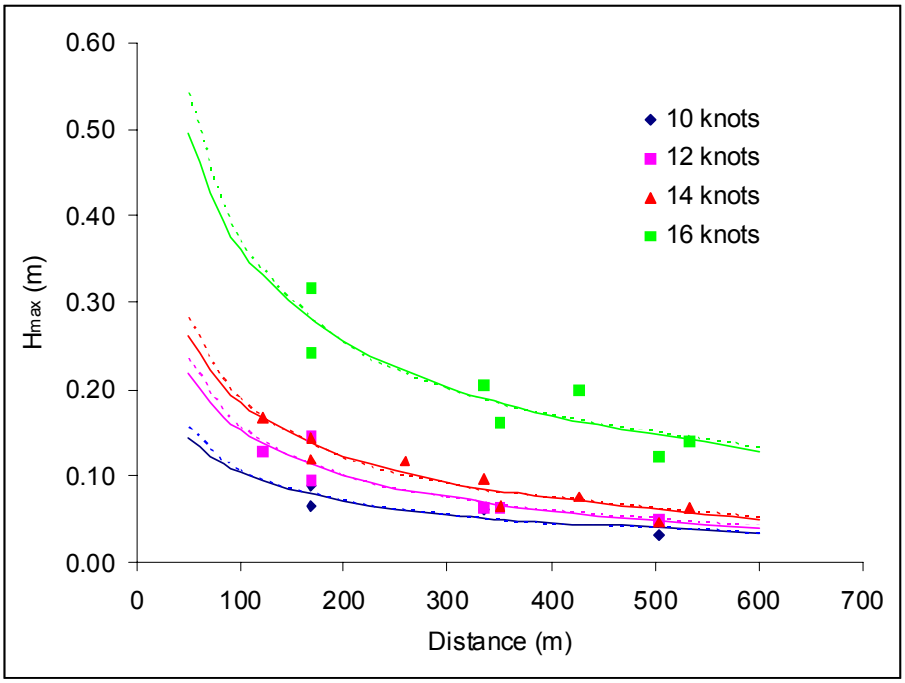

Figure 3-26. ***H_{max}* measured during the *Tyee* trials as a function of distance from the sailing line for a range of speeds; the solid lines indicate the best fit for $r^{-1/3}$ and the dashed lines indicate the best fit for $r^{-1/2}$**

GPS positions of the *Tyee* tracks were obtained from MCI, then processed and plotted on Figure 3-27. The figure shows a variable band of ferry positions during 360 transits through Rich Passage from Clam Bay to Waterman Point. The deviation of ferry position from the centerline of Rich Passage changes from 700 ft at the widest portion to 250 ft at the narrowest portion of the pass. A clear differentiation between eastbound and westbound traffic is evident in the widest portion but not in the narrow portion of the route. The data confirm that with certain reasonable limits, the ferry can be positioned along the centerline of Rich Passage to maximize the distance between sailing line and shoreline.

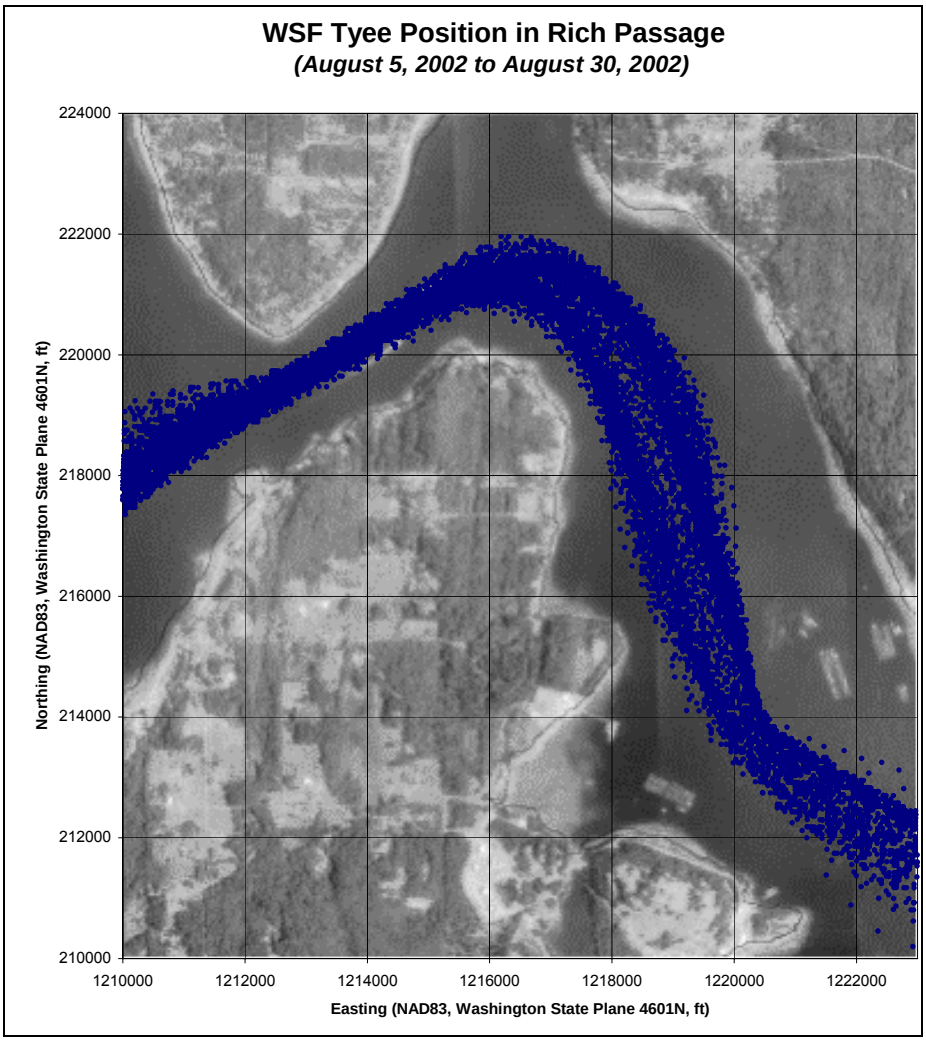

Figure 3-27. Tyee positions in Rich Passage, August 2002

M/V Bravest

WSF tested the suitability of *M/V Bravest* for service on Puget Sound in sensitive locations, by conducting wake trials on February 23, 1998 on Long Island Sound, New York, to determine the wake signature of the vessel (Stumbo, 1998). *Bravest* is a 38-meter, 140 tonne, 350-passenger aluminum catamaran, with a 10 meter beam, designed by Nigel Gee Associates of Southampton England. *Bravest* was built by Derecktor Shipyards in their Mamaroneck NY yard, and placed in service in 1997 with NY Fast Ferries.

Wake measurements during the trials were conducted at three speeds: 22, 27, and 31.5 (maximum) knots with the vessel ballasted to simulate the fully loaded condition. A summary of wake parameters (H, E) based on the trial measurements is provided in Table 3-6. Time series from the *Bravest* trials are included in Appendix C. In comparison

with other vessels tested by WSF at that time, the height and energy density of *Bravest* wash is lower than other vessels with a service speed of 25 knots or more and a passenger capacity of 250 or more (Stumbo, 1998).

Time series from the *Bravest* trials were analyzed by PI Engineering as part of this study. The time series analysis was conducted to provide input to calibrations of the LSV model as described in Section 5. The time series analysis is provided in Appendix C.

Table 3-6. Summary of wake parameters normalized to a distance of 300 m based on trial measurements for the vessel *Bravest*

	Wash Height (cm)	Energy Density (joules/meter)
WSF Standard	28	2450
22 Knots	36.7	8725
27 Knots	24.2	2333
31.4 Knots	20.6	1677
32 Knots (No Psngrs.)	11.5	524

M/V St. Nicholas

Fox (2000) measured the wakes of *St Nicholas* on March 16, 2000 in Port Madison, Puget Sound. *St. Nicholas* is a 25-meter, 57-tonne catamaran that was designed and built by Allen Marine of Sitka, Alaska. She is one of a series of several sister ship catamarans built for New York Waterways between 1996 and 2002. *St. Nicholas* has operated as a whale watch tour ship, as well as a ferry, in Alaska and Puget Sound.

During the trials, six runs at each nominal speed were recorded at 12, 16, 20, 24 and 28 knots with the vessel in the fully loaded condition. Fox and Associates conducted a second set of trials of *St. Nicholas* on November 16, 2001 in Port Madison, Puget Sound to test the sensitivity of the wakes to displacement and trim. Fox et al (2000) normalized the wake measurements to a nominal distance from sailing line of approximately 300 m to facilitate comparison with other vessels. The measurements suggest that *St Nicholas* generates a maximum wake height of 0.16 m and a maximum wash energy density of 1603 J/m at a service speed of 27.7 knots.

Time series from the two *St. Nicholas* trials were analyzed by PI Engineering as part of this study. The time series analysis was conducted to provide input to calibrations of the LSV model as described in Section 5. The time series analysis is provided in Appendix C.

M/V Condor Express

Fox and Associates measured the wakes of *M/V Condor Express*, a 149-passenger foil-assisted catamaran designed by Teknicraft, New Zealand, and built by All American Marine, Inc. of Bellingham, WA.

The wake trials were conducted in Bellingham Bay on 22 February 2002, in water depths that are similar to those found in several west coast waterways such as Rich Passage in Puget Sound and the high speed vessel lanes in San Francisco Bay. Wind conditions were minimal. Water depth along the navigation track used for the trials varied between 6 m and 33 m with an average depth of approximately 17 m at the location of measurement. Fox and Associates (2002) applied spectral filtering to remove variance at the wind wave frequencies (periods less than 2 sec) from the time series. The vessel was loaded to approximate the weight and weight distribution of an average passenger load for a vessel with a capacity for 149 passengers.

Fox and Associates (2002) concluded that *Condor Express* has exceptionally low wash characteristics, both in height and in energy. Specifically:

- At full speed, 39 knots, *Condor Express* has a lower wash energy (776 joules/meter) than any vessel with a capacity of 149 passengers or more tested to date by the investigators at any service speed.
- At full speed, 39 knots, the wash height is less than 20 cm. and well below the deep water threshold established by WSF for Rich Passage.
- At speeds below 12 knots and above 23 knots, *Condor Express* meets the standard for operation in Rich Passage.

Time series from *Condor Express* trials were analyzed by PI Engineering as part of this study. The time series analysis was conducted to provide input to calibrations of the LSV model as described in Section 5. The time series analysis is provided in Appendix C.

M/V Red Jet 4

Red Jet 4 is a 39.8 m catamaran, with beam of 10.8 m, draught (loaded) of 1.3 m, and passenger capacity of 275. *Red Jet 4* was built in 2003 by North West Bay Ships Pty Ltd, Tasmania for Red Funnel Line, UK. *Red Jet 4* currently provides ferry service between Southampton, England and Cowes, on the Isle of Wight. Anecdotal evidence from several independent naval architects (Fox and Associates, pers. comm., 2005) suggests the wakes generated by *Red Jet 4* might make it a low-wake candidate vessel for consideration for use on the Seattle-Bremerton route.

Wakes were measured by an independent company during a trial of *Red Jet 4* in Norfolk Bay, Tasmania in March 2003 and the data were made available to this study by North West Bay Ships for the purpose of evaluating the suitability of the design for use in the study. Unfortunately, ambient conditions during the trials were not favorable for measurement of wake time series; ambient winds of 10-15 knots produced wind waves in the order of 1.0 to 1.5 m during the wake measurement trials. The wake trial measurements were analyzed as part of this study to determine if the wind waves could be filtered from the wake time series however this proved to be entirely unsuccessful and the data were deemed unsuitable for further analysis.

3.7.2.2 Comparison of candidate hulls

Figures 3-28 and 3-29 (reproduced by permission from Fox and Associates, 2002) compare the maximum wake height and maximum energy density of several of the vessels that have been measured by Fox and Associates. The comparison includes vessels that commonly transit Rich Passage as well as *Condor Express* and *St Nicholas*, both 149-passenger vessels for which the wake wash data has been made available to this study. The wake measurements of all vessels included in the figures have been adjusted to a distance of 300 meters applying a –1/3 wave height decay. The analysis of Fox and Associates reveals that a number of conventional displacement catamarans as well as the foil-assisted catamaran, *Condor Express*, achieved normalized wake heights and energy densities that were lower than the *Chinook* trial results at speeds of 25 knots or higher.

Art Anderson and Associates also compiled wake wash data published in the scientific and engineering literature as part of this study. The compilation included several of the Fox and Associates data sets as well as a number of others. The data were adjusted to a distance of 300 m from vessel sailing line. The data were also non-dimensionalized and plotted with respect to vessel Froude number in an attempt to remove bias due to the different physical size and weight of the candidate hull forms. The results of the analysis are included as Appendix E of this report. The analysis identified three candidate hull forms considered worthy of further consideration in this study:

- Air cavity hull catamaran
- Air-lubricated hull catamaran
- Foil-assisted catamaran

Wake trial time series from full-scale measurements of the air cavity and air-lubricated type hulls are not publicly or readily available at the time of this report. *Condor Express* provides an example of the potential for a foil-assisted catamaran to produce low wake heights and energy density.

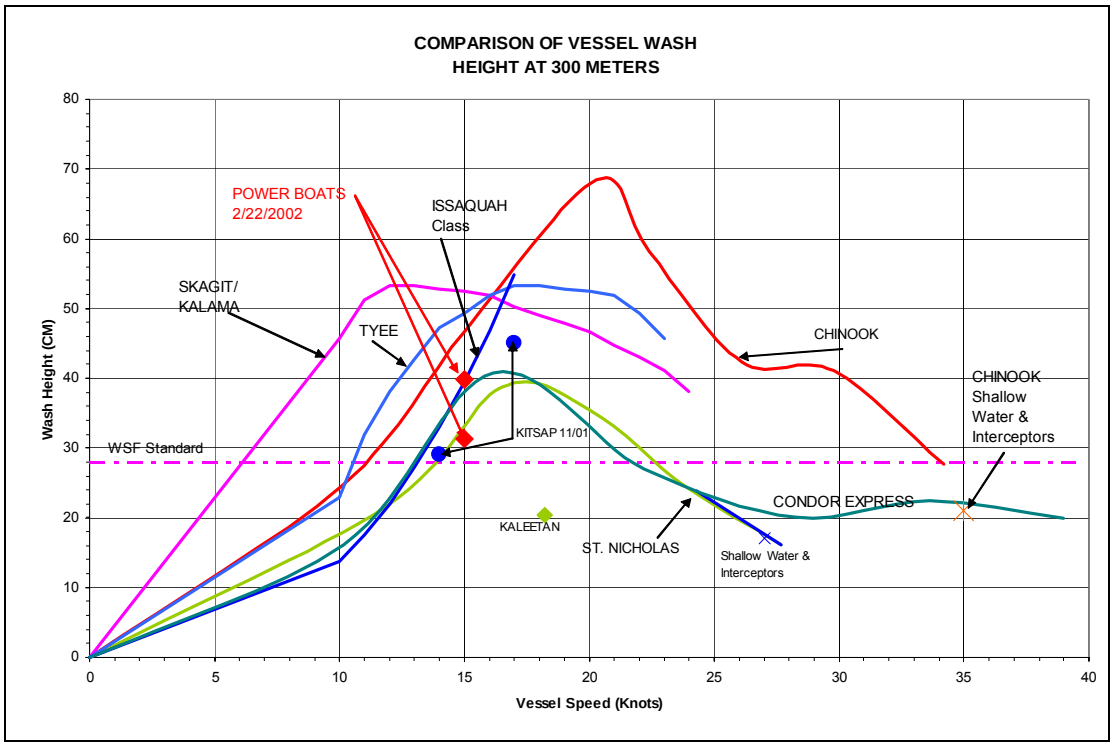

Figure 3-28. Wake height normalized to 300 m as a function of vessel speed for a selection of vessels (reproduced from Fox and Associates 2002)

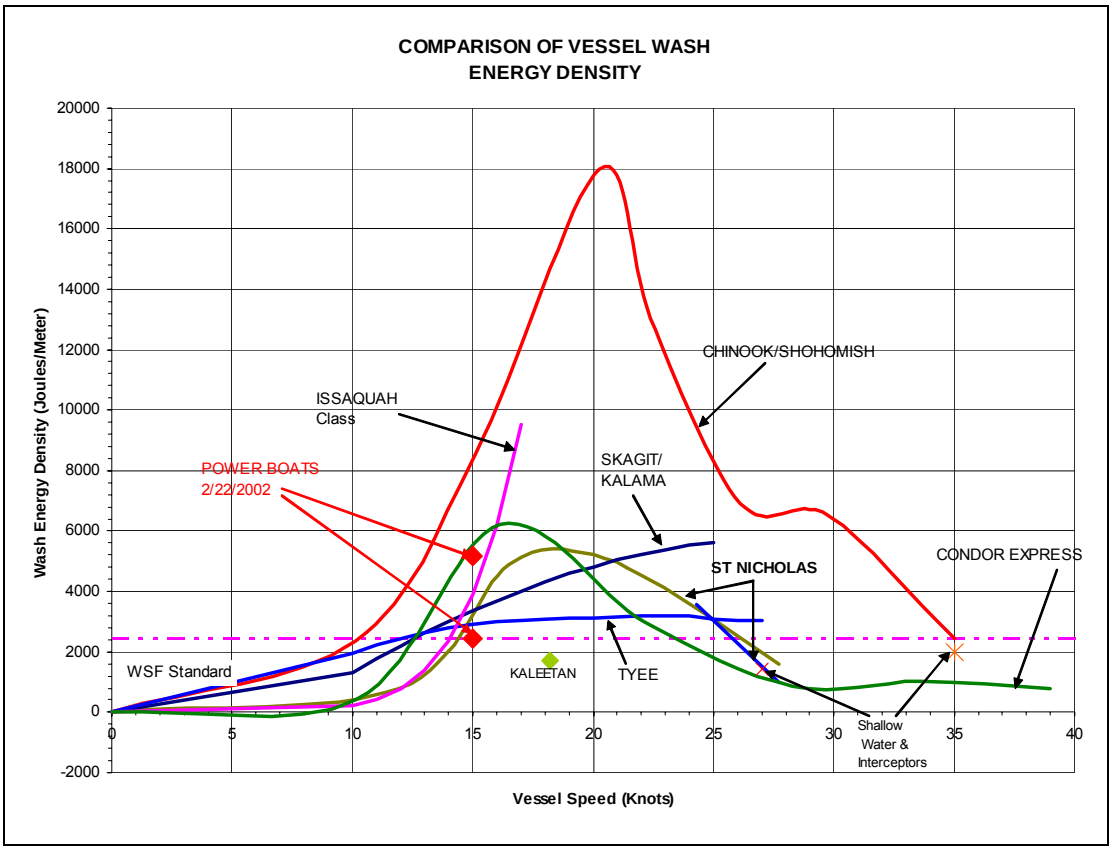

Figure 3-29. Wake Energy normalized to 300 m as a function of vessel speed for a selection of vessels (reproduced from Fox and Associates 2002)

3.7.2.3 Wakes measured in Rich Passage

As part of previous work for WSF and the Attorney General's office, PI Engineering conducted extensive monitoring of water surface elevation in the study area during 1999 and 2000 to characterize wake heights, periods and energy for a number of vessels on the Seattle-Bremerton ferry route (e.g. PI Engineering, 1999, 2002, 2003). The data provide nearshore characterization of the wake parameters for a wide range of water level variations, tidal currents and bathymetry.

PI Engineering conducted a study to statistically describe vessel wake characteristics generated by *Chinook*-class ferries in Rich Passage following a change in POFF operating speed from 12 knots to 16 knots (PI Engineering, 2002). The results are based on collection of field measurements of waves at several stations located along Rich Passage shorelines (Figure D-1 Appendix D), data processing, analysis, and comparison with the previous results (e.g. PI Engineering, 1999).

Data collection methods and data processing procedures are described and additional examples are provided in Appendix D.

Examples of nearshore wake parameter plots for *Chinook* class ferries transiting Rich Passsage between September 1999 and August 2000

are shown in Figure 3-30. Additional examples are provided in Appendix D. The variation in wake parameters for Chinook class POFF shown in Figure 3-30 occur over a range of nominal vessel speeds between 8 and 17 knots (slow speeds) and between 30 and 39 knots (high speeds). Variability in speeds in each of the two groups may be attributed to a number of factors that include differences in vessel loading (fuel and passengers), and direction of travel relative to ambient tidal currents. Although wave heights are approximately similar for the two speed regimes there is a significant increase in wave period at high speeds. The increase in wave period at high speed translates to a significant increase in wave energy density at high speed.

PI Engineering re-analyzed the original wake trial time series for *Chinook* class ferries and several car ferries collected in Rich Passage to provide data for preliminary verification of wake propagation models as discussed in Section 5. The re-analysis involved computation of zero-upcrossing and zero-down-crossing wave heights, wave period, and wave energy density time series as well as spectral analysis to determine the distribution of energy as a function of wave frequency. Examples are shown in Figure 3-31. Additional time series and results of the analysis are included in Appendix D. The time series reveal that the wakes are of similar height at both slow speeds and high speeds. However, the wave period varies continuously in the high speed wake train from a maximum of more than 12 sec to approximately 3 sec, whereas, the wave period is relatively constant throughout the wake train at slow speeds. The energy density of the longer period waves is several times larger than that associated with the shorter period waves. These patterns and plots are discussed in more detail in Section 5.

A time series for a car ferry wake measured nearshore in Rich Passage is shown in Figure 3-32. The time series are characteristics of a slow speed displacement vessel with relatively low wake heights and the wave period and wave energy are relatively constant throughout the wake train. Energy density associated with car ferry wakes is typically several times lower than the wakes for Chinook class POFFs at high speeds.

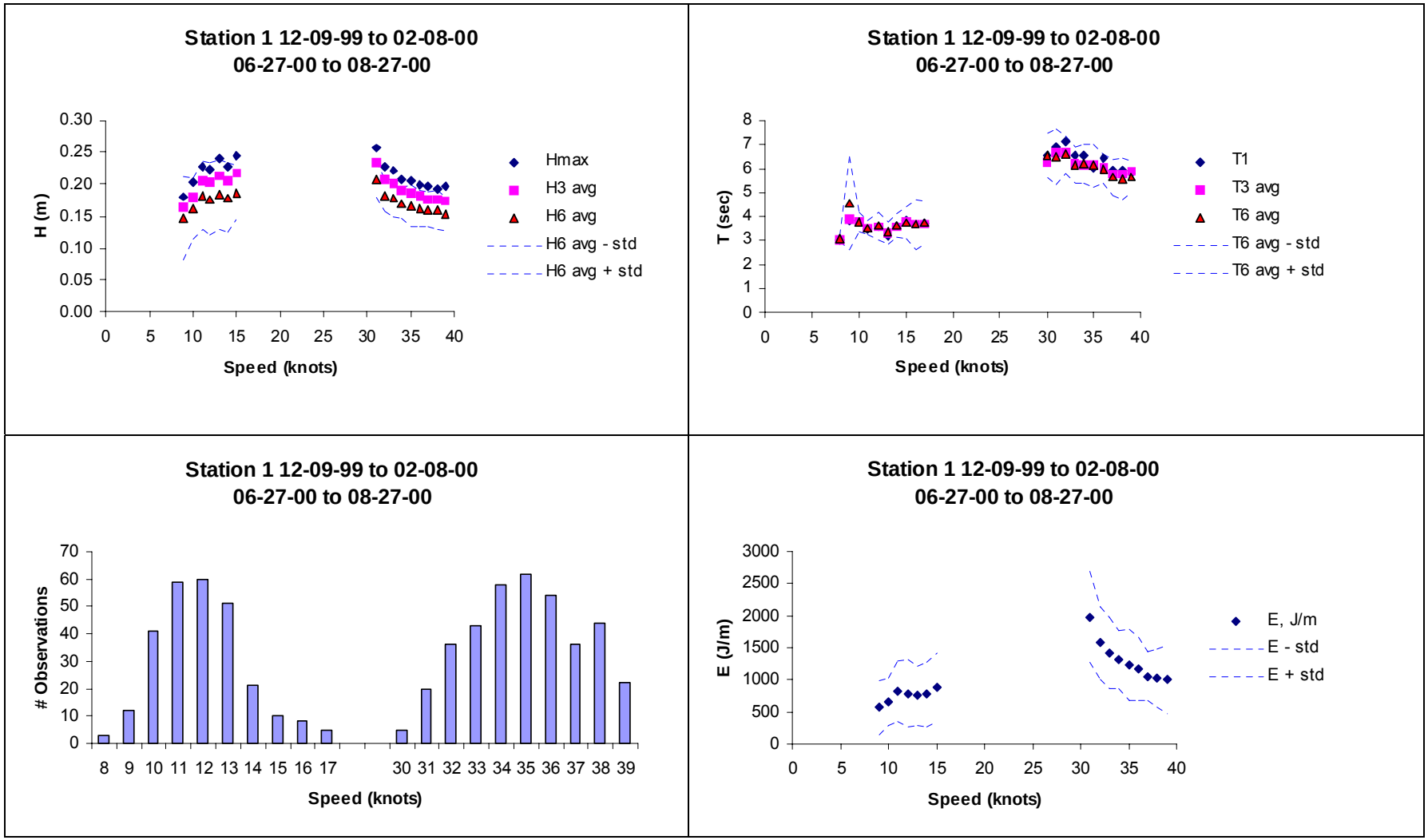

Figure 3-30. Example of wake statistical parameters for Chinook class ferries measured nearshore in Rich Passage at a range of speeds

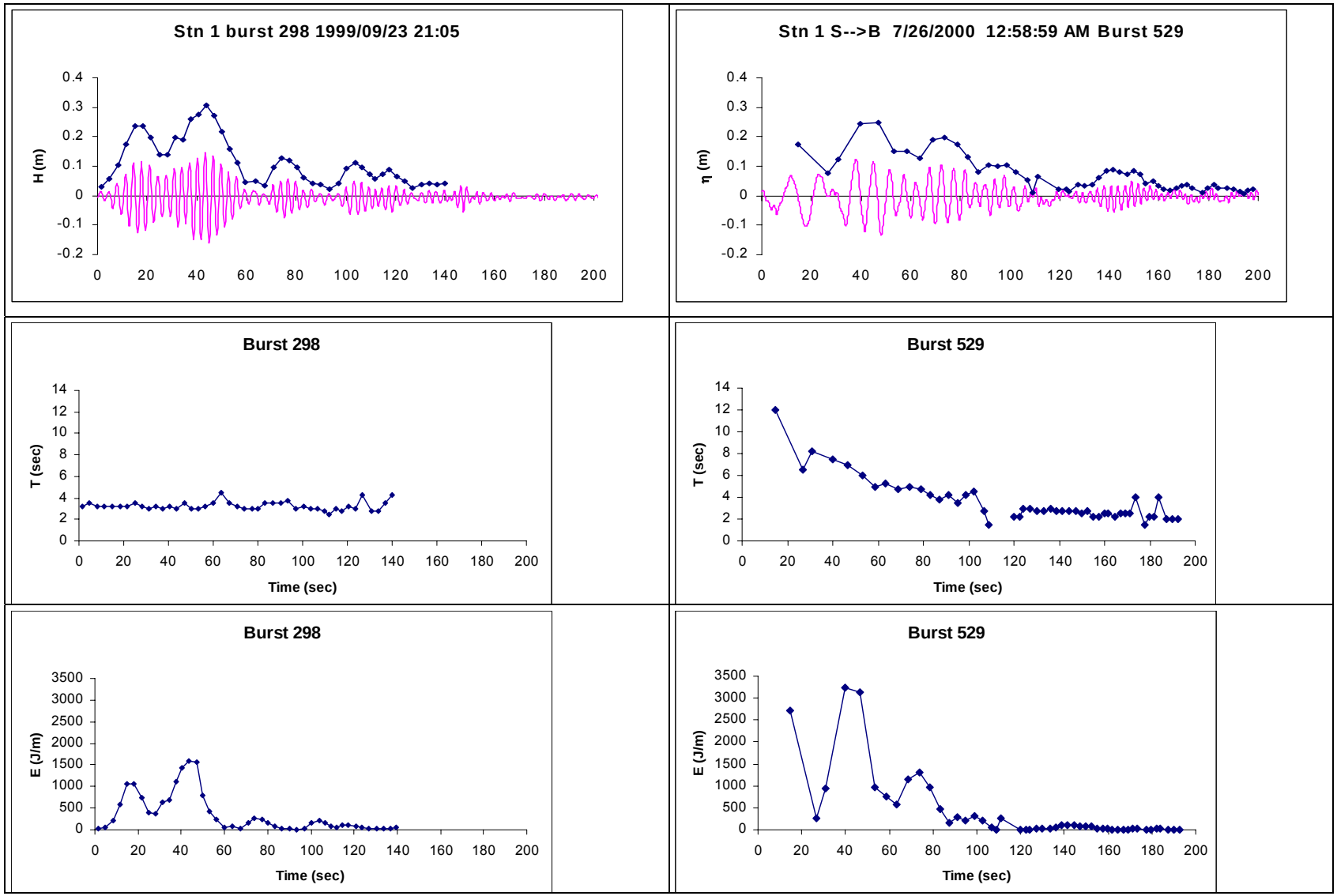

Figure 3-31. Time series of Chinook class wakes: water surface elevation and height (top), period (middle), and energy density (bottom) at slow speed (left) and at high speed (right)

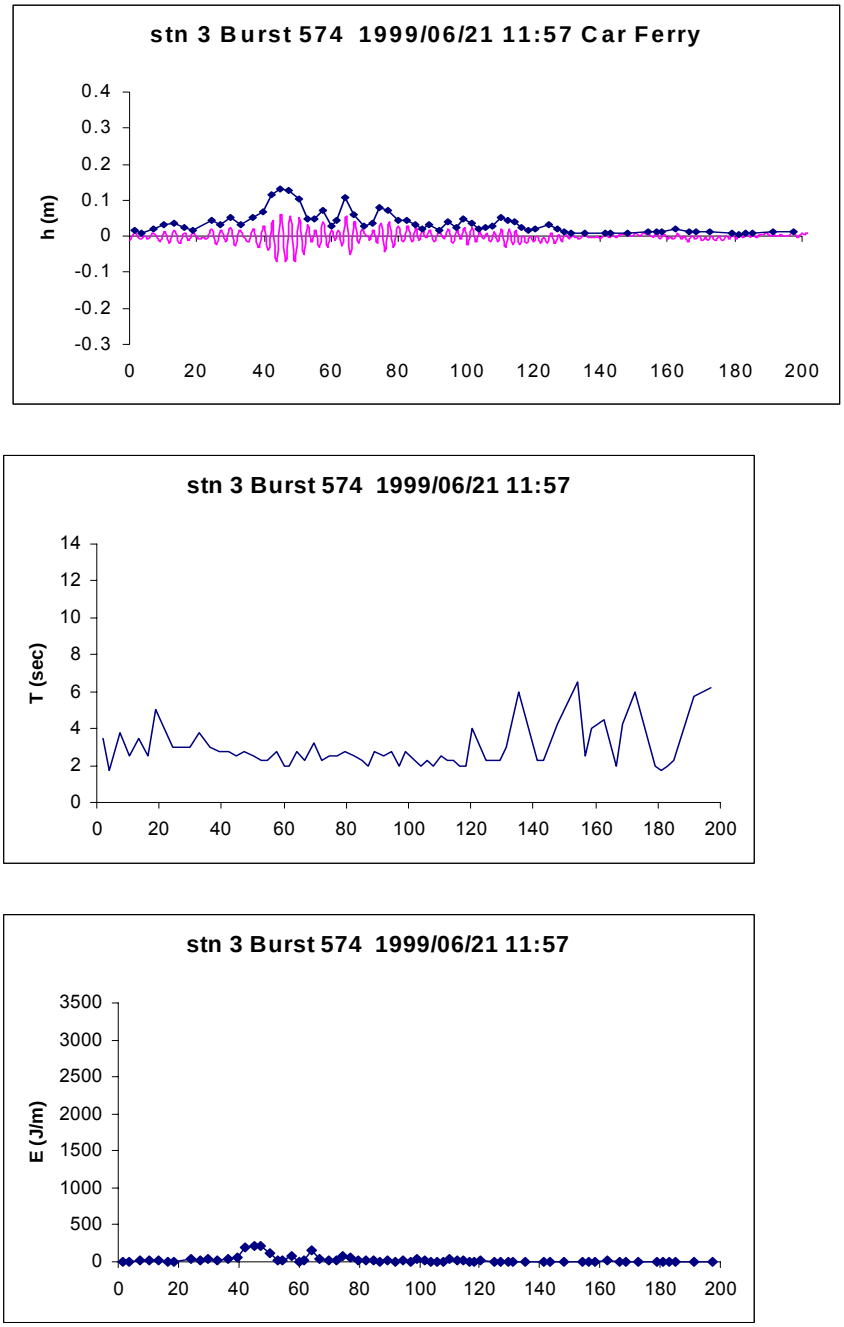

Figure 3-32. Time series of a car ferry wake: water surface elevation and wave height (top), period (middle), and energy density (bottom)

3.8 Habitat

Effects of vessel wake and run-up on the biological community in the intertidal and shallow subtidal zone (from MHHW to MLLW) were last investigated in 2001 (WSDOT, 2001). The 2001 studies included surveys of intertidal habitat, benthic infauna, and aquatic vegetation (kelp, macro-algae, and eelgrass). A biological survey of sites within Rich Passage was conducted in January, 2005 prior to the start of the high-speed vessel trials. The purpose of this survey was to obtain winter baseline information on the existing biological community and nearshore habitat in Rich Passage for comparison with data to be collected during and after the vessel trials. A detailed report on this survey prepared by Grette Associates (2005) is contained in Appendix F.

Biological parameters were surveyed at six study sites. The biological community composition was evaluated in terms of macroalgae and macroinvertebrate presence and percent cover. Samples for analysis of benthic infauna were collected and have been archived for later analysis. Due to seasonal die-back, eelgrass and kelp beds were not delineated during the January survey, but will be investigated during later surveys.

The surveys sites were Manette Beach (#1), Point White (#3) and (#5), Point Glover (#9) and (#10), along with a reference site, Crystal Springs (#12) (Figure 3-5). Site numbers are consistent with beach monitoring sites established by RPWAST during previous studies conducted in Rich Passage (RPWAST, 2001). Site 1 is an east-facing beach north of Bremerton on the Kitsap Peninsula. Sites 3 and 5 are located on the south shore of Bainbridge Island, facing southeast. Sites 9 and 10 are located on the south shore across Rich Passage from Sites 3 and 5, and face north and northwest. Site 12 is located on the west shore of Bainbridge Island, facing west. This site is not subjected to frequent wakes from ferries but is subject to tidal and wind driven forcing mechanisms and was therefore used as the reference site.

At each study site, a transect line was established from MHHW to -5 ft MLLW. A 0.25 m^2 quadrat was placed every 15 feet along the transect tape from the onshore edge to -5 ft MLLW. Within these quadrats, algae were identified to genus and percent cover was estimated. Surface invertebrates were identified and enumerated and barnacle abundance was estimated as percent cover.

Table 3-7 lists the macroalgae and invertebrates observed at the survey sites.

Table 3-7. Macroalgae and invertebrates observed within intertidal quadrats in Rich Passage, January 2005

Common Name	Scientific Name
Ulvaria	*Ulvaria fusca*
Ulva	*Ulva fenestrata*
Bleached brunette	*Cryptosiphonia woodii*

Iridea	*Mazzaella splendens*
Turkish towel	*Gigartina exasperata*
Sargassum	*Sargassum sp.*
Colander kelp	*Agarum fimbriatum*
Prionitis	*Prionitis spp.*
Rockweed	*Fucus distichus*
Nudibranch	*Nudibranchia*
Limpet	*Lottidae*
Chiton	*Mopalia sp.*
Snail	*Trochidae*
Moon snail	*Polinices lewisii*
Scallop	*Pectinidae* *Limidae*
Lyre crab	*Hyas lyratus*
Dungeness crab	*Cancer magister*
Hermit crab	*Pagurus sp.*
Decorator crab	*Oregonia gracilis*
Anemone	*Metridium senile*
Sea star	*Pisaster ochraceus*
Barnacle	*Chthamalus sp.* *Balanus sp.*
Tube worm	*Sabellidae* *Serpulidae*

3.8.1 Site 1

At Site 1, the upper beach was devoid of aquatic vegetation. Few species were observed along the transect in general, but those present included *Ulvaria*, bleached brunette (*Cryptosiphonia woodii*), *Mazzaella*, and *Sargassum*. Vegetation cover did not exceed 10 percent in any quadrat. Few macroinvertebrates were observed at Site 1. All invertebrates were seen beyond 75 ft on the transect tape. Anemones were sparsely present in the middle of the transect, covering less than 5 percent of the quadrat area. Barnacles were present at 90 and 135 ft, covering 1-2 percent of the area at the lower station. Mobile invertebrates were observed at the lower extent of the transect, and included lyre crabs (*Hyas lyratus*), limpets, sea stars, and a Dungeness crab (*Cancer magister*).

3.8.2 Site 3

Vegetation was lacking in the upper intertidal zone at Site 3. Beyond 75 ft on the transect, *Ulva*, bleached brunette, *Mazzaella*, *Sargassum*, Turkish towel (*Gigartina exasperata*), and an unidentified red alga were observed. The percent cover increased with depth; at 75 ft, vegetation cover was no more than 1 percent, increasing to 25 percent at 90 ft, and finally reaching 45 percent at the end of the transect.

Few macroinvertebrates were observed at this site; all those observed were seen beyond 45 ft. Barnacles were seen in the middle of the transect, covering approximately 5 percent of the quadrat area. Hermit crabs, snails, and a chiton were also noted.

3.8.3 Site 5

At Site 5, no vegetation was seen above 60 ft on the transect, but beyond this distance vegetation included *Ulva*, *Mazzaella*, *Prionitis*, Turkish towel, an unidentified red filamentous alga. A kelp identified as *Agarum fimbriatum* was also noted. Vegetation cover was minimal, however, until the lowest quadrat, which had roughly 30 percent cover.

Macroinvertebrates observed in the lower reaches of the transect included barnacles, a chiton, snails, hermit crabs, decorator crabs, sea stars, tube worms, scallops, nudibranchs, and a limpet. The highest invertebrate density along the transect was observed beyond 90 ft.

3.8.4 Site 9

No vegetation was observed in the upper reaches of the transect at Site 9. At 90 ft, *Ulva* was encountered. Bleached brunette, Turkish towel, and *Agarum* were present in the lower quadrats, although cover was dominated by eelgrass, with eelgrass covering as much as 80 percent of the quadrat area.

Snails were the most commonly observed invertebrate along the transect. Chitons, anemones, and a nudibranch were also observed near the middle of the transect.

3.8.5 Site 10

There was no vegetation on the upper beach at Site 10. In the middle of the transect, vegetation included *Fucus*, *Ulva*, *Prionitis*, *Mazzaella*, an unidentified red filamentous alga, *Sargassum*, Turkish towel, and *Agarum*. Generally, vegetation cover was sparse except for *Sargassum*, which covered 35 percent of the quadrat at 120 ft, Turkish towel, which covered 40 percent of the quadrat at 135 ft, and *Agarum*, which covered 35 percent of the quadrat at 150 ft.

The only invertebrates observed at this site were barnacles on bedrock at 60 and 75 ft. The barnacles were not abundant, covering approximately 5 percent of the quadrat.

3.8.6 Site 12

At Site 12, no vegetation was observed landward of 90 ft on the transect. Below this, macroalgae species included *Ulva*, *Mazzaella*,

and bleached brunette. The maximum cover provided by these species combined was 20 percent of the quadrat area.

Barnacles were observed in the middle reaches of the transect, covering as much as 40 percent of the quadrat. Hermit crabs, limpets, snails, and chitons were found beyond 90 ft; tube worms were the only invertebrates seen at 165 and 180 ft.

4.0 Shoreline Conditions and Change in Response to POFFs

4.1 Beach Characteristics in the Study Area

Beaches in the Rich Passage study area are composed of varying mixtures of shell hash, silt, sand, gravel and cobble overlying bedrock. In addition to vessel-generated waves, the beaches are exposed to fetch-limited wind waves, macro-tidal water level shifts and in some instances strong tidal currents. Beach profiles vary in shape depending on the underlying geology, exposure, and shoreline planform. The irregular planform shape of the Rich Passage shoreline results in compartmentalization of the coast into several discrete littoral cells ranging from a few tens of meters in length up to a kilometer or more (Youngmann, 1977; Keuler, 1988; Wallace, 1988). Variations in wave and tidal energy, longshore sediment flux, and sediment supply lead to variations in morphological and sediment character. Pocket beaches or embayed beaches, such as those found in Lynwood Bay, Clam Bay, and adjacent to Waterman Point, Middle Point, and around Point Glover, feature a relatively steep foreshore transitioning to a low tide terrace or bedrock platform. More exposed beaches, such as those extending along Enetai Beach, Watermans, and Point White, may lack a low tide terrace in which case the steep foreshore transitions more directly to deep water. Quality and quantity of sediment on the foreshore also varies considerably depending on location, degree of compartmentalization, and availability of supply.

A description of the typical features of gravel and mixed beaches in Puget Sound may be found in Shipman (1996, 1997) and Downing (1983). The natural elevation of the primary berm and backshore varies with the local tidal range, but is generally about 0.5 meters above Mean Higher High Water (MHHW). The upper foreshore on natural Puget Sound beaches generally slopes between 1:5 and 1:11. In the study area, beach slopes above MLLW range from 1:5 to 1:7.

The source of most beach sediment in Puget Sound outside of major river deltas is bluff erosion (Shipman, 2001). In the Rich Passage study area a number of small streams also contribute sediment although no estimates of the quantity derived from small streams are available.

The intertidal foreshore of most exposed beaches in the study area is composed of a mixture of sand, pebble, gravel, and cobble. Distinctive layering of the sediment is typically present at most locations with a higher percentage of gravel, pebble, and cobble occurring in the upper layer on the foreshore and the percentage of sand increasing with depth beneath the surface layer. A layer of well-sorted gravel may be present beneath the surface layer and above a less well-sorted lower layer. Beaches also tend to exhibit progressive fining of the upper sediment layer with increasing elevation on the beach.

Less exposed beaches, in particular the pocket beaches found on Point Glover, are typically composed of finer grained sediment including shell hash, sand, and silt underlain by mudstones or backed by highly erodable soft shale.

Shore perpendicular rock groins are present in the study area on Point Glover at the Duff property and several locations on Point White. These low rock groins, locally referred to as drift sills (Shipman, 1997), have been used to control longshore drift of sediment. The groins typically exhibit larger accumulations of sediment on the southwest side than on the northeast side, indicating prevailing northeastward drift consistent with descriptions of the net longshore drift patterns published in the literature (e.g. Jacobsen and Schwartz, 1981; Schwartz and Wallace, 1989; WDNR, 2001).

Most beaches in the study area are backed by engineered structures such as concrete walls and rock revetments designed to protect the properties behind the structures from erosion. Only a small percentage of the shoreline in the study area remains unprotected. The engineered structures vary widely in terms of their construction and in particular their intersection with local tidal datum planes. This has implications for their interactions with waves incident on the structure during periods of elevated water levels. Construction of bulkheads along most of the Rich Passage shoreline has significantly reduced the primary supply of sediment in the study area.

4.2 Beach Profile Response to POFFs

The observations of beach response summarized below are from a review of RPWAST (2001; 2002) and personal communication with William Reynolds, a coastal geomorphologist appointed to RPWAST (Reynolds, pers. comm. 2004). Beach profile survey data are included in Appendix D.

The baseline survey (Table 4-1) was acquired during a period when the WSF ferries *Chinook* and *Snohomish* were operating at slow speed (12-16 knots). Monitoring surveys 1 through 6 were obtained during a period when the ferries were operating at high speed (34-37 knots) through Rich Passage. Monitoring survey 7 was acquired after the fast ferries had reduced speed to 12-16 knots. Unfortunately, no profile monitoring data are available prior to April 2000.

4.2.1 Bainbridge Island (Sites 3 to 7)

The intertidal foreshore between Sites 3 and 5 at Point White on Bainbridge Island experienced the greatest change during the RPWAST monitoring in 2000-2001. Figures 4-1 through 4-3 show the changes that occurred during the RPWAST monitoring surveys on Point White between the baseline survey and the sixth monitoring survey.

Beach changes were first detected in July between survey Sites 3 and 4, near Point White, and progressed to the north past Sites 4 and then 5. By December 2000, the erosional zone had progressed to between

Sites 5 and 6. The eroded gravel and cobble material was transported across the beach, offshore, near MLLW. No significant beach changes were noted north of Site 6 (Lynwood Bay) or at Site 7 (Pleasant Beach) during the one-year survey period.

Change was detected on Bainbridge Island beaches (Sites 3, 4, and 5) within one month of the ferry speed increase in May 2000. These beaches consisted largely of a layer of flattened, well-sorted gravel and pebble sized material overlying a layer of coarse to medium sand. When fast ferry operation began, the gravel was eroded from the upper beach and transported down the profile (compare slopes above and below MLLW at Sites 4 and 5 in Tables 4-1 and 4-2 and profile surveys in Figures 4-1, 4-2, and 4-3). The removal of the gravel exposed the underlying sand layer with depth varying from 6 inches to 2 feet. Once the gravel was removed, the sand layer also experienced some erosion but at a very reduced rate. The sand layer was thought to be more cohesive and generally more difficult to move than the gravel (Reynolds, pers. com.,2004). Eventually the beach reached equilibrium, with the remaining sand layer reduced to a maximum depth of about 9 inches between Sites 3 and 5. Note that the observations reported above are contrary to what might be expected for transport of sand and gravel. Usually larger waves result in gravel moving up the profile, with sand being lost downslope as suspended load. Also, larger sized sediment is typically more difficult to mobilize and erode than sand. Also note that it may not be true that the sand is more cohesive than gravel, or if different cohesiveness accounts for the observed sediment distribution and redistribution under POFF waves. These processes are examined in more detail in the sections that follow.

The magnitude of the material loss at the base of bulkheads varied from approximately 6 inches to over 3 feet at Site 5 (the former DeBoer property). The entire stretch of beach from Point White to north of Site 5 suffered erosion, whereas no change in beach slope or texture was detected from midway between Sites 5 and 6 to Site 7.

After the ferry speed was reduced from 32 to 14 knots through Rich Passage in October 2001, the Bainbridge Island beaches returned to their approximate original slope and sediment composition within six months (see monitoring survey 7 in Appendix D).

Table 4-1. Beach slopes at baseline survey (4-19-2000 to 5-8-2000)

Site	Above MLLW	Below MLLW
3	1:7	1:6.4
4	1:5.4	1:5.4
5	1:6.2	1:5.9

6	1:6.9	1:18.2

Table 4-2. Beach slopes at monitoring survey # 6 (9-4-2001)

Site	Above MLLW	Below MLLW
3	1:7.2	N/A
4	1:6.1	1:5.8
5	1:6.9	1:7.2
6	1:6.9	1:18.7

Bill Reynolds, an independent geomorphologist, has provided anecdotal evidence about the erosion along the east shore of Point White during the last period when fast ferries were operating in Rich Passage. The first evidence of erosion appeared near the tip of Point White. It manifested as downcutting at the base of the bulkhead and a general decrease in the beach profile. There was a slow, steady northeastward movement of the line of this erosion; according to Bill Reynolds, "the line of erosion moved like a wave along the shore." Little change in the beach profile at points along the beach were observed until the line of erosion reached that point, after which there was a rapid decrease in beach volume.

Animations of the beach evolution at a number of monitoring sites have been prepared using the measured profiles. These animations are not large enough in plan to show spatial variability in the evolution (i.e. temporal lags), except at Site 5. The pattern of development at Site 5 shown in the animation confirms the observations of Bill Reynolds; the beach erodes first at the southern end of the domain (see Figure 4-2).

It is suspected that change in beach morphology in this area was caused by both longshore and cross-shore sediment transport. It is not clear which, if either, process dominates.

4.2.2 Point Glover (Sites 8 to 10)

Small quantities of loose material were present on the Point Glover beaches when monitoring was initiated in April 2000; a thin veneer of loose sediment, approximately 1-2 inches thick, covered the underlying mudstone bedrock. This sediment, mostly broken shell and sand, was quickly eroded when POFF operation began. There was evidence, reinforced by residents' comments, that the beaches had a history of erosion, possibly due to earlier (before 2000) fast ferry wakes. In some locations, bulkhead toes were exposed when monitoring began in May 2000.

Some damage to bulkheads was noted during the monitoring surveys by RPWAST (Reynolds, pers. comm., 2004). The most notable was the Manees property bulkhead between survey Sites 9 and 10. Some beaches between Sites 9 and 10 experienced erratic effects, with alternating periods of relatively minor erosion and accretion.

There are sections of exposed (unprotected) bluffs between Sites 8 and 10. However, there was no apparent erosion of these bluffs during Chinook class POFF operation. There were also several "pocket beaches" on the Point Glover shore that showed no noticeable change during the operation of the fast ferries.

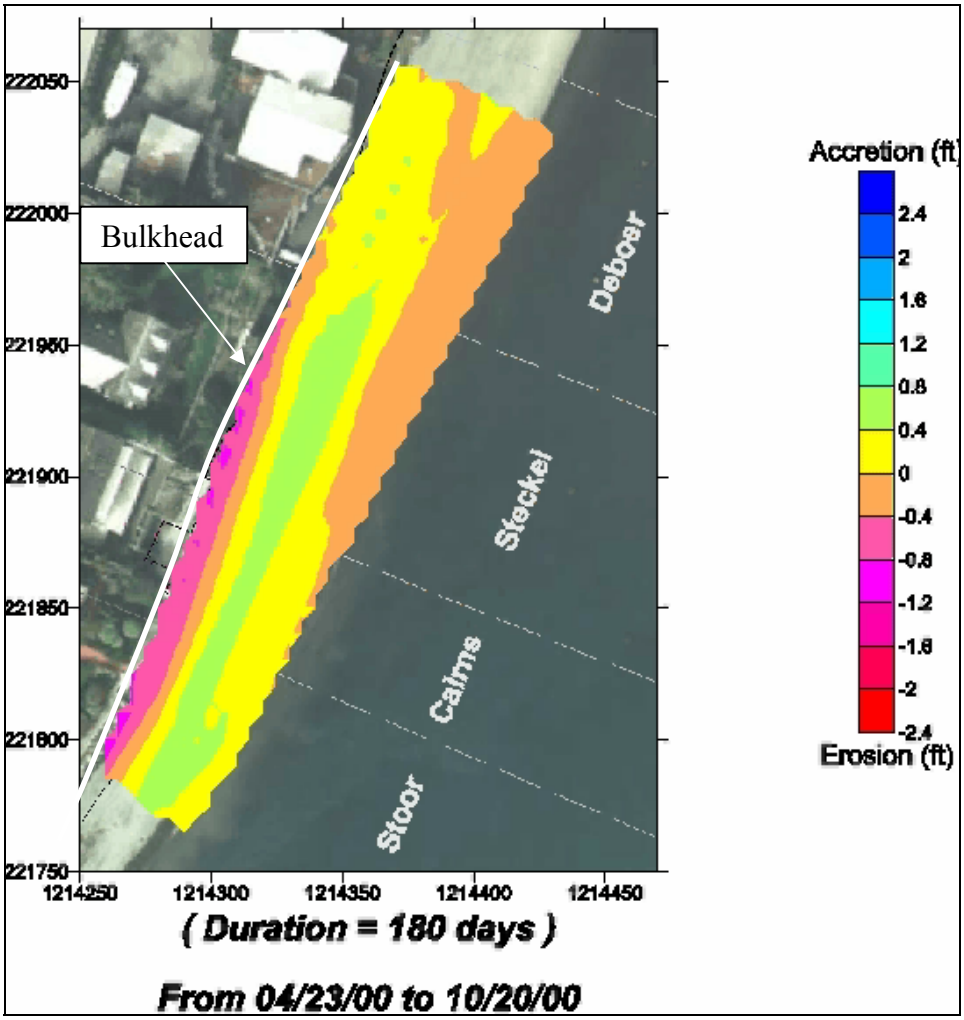

Figure 4-1. Beach evolution after 180 days at SEPA Site 5 on Point White

The observed patterns of the progression of beach response is illustrated in Figure 4-2. and 4-3. Erosion begins at the northeast end of Site 3 and progresses northeastward to between Site 5 and Site 6. Profiles on the southwest end of Site 3 only show minor change

because these transects have only a thin veneer of cobble overlying bedrock.

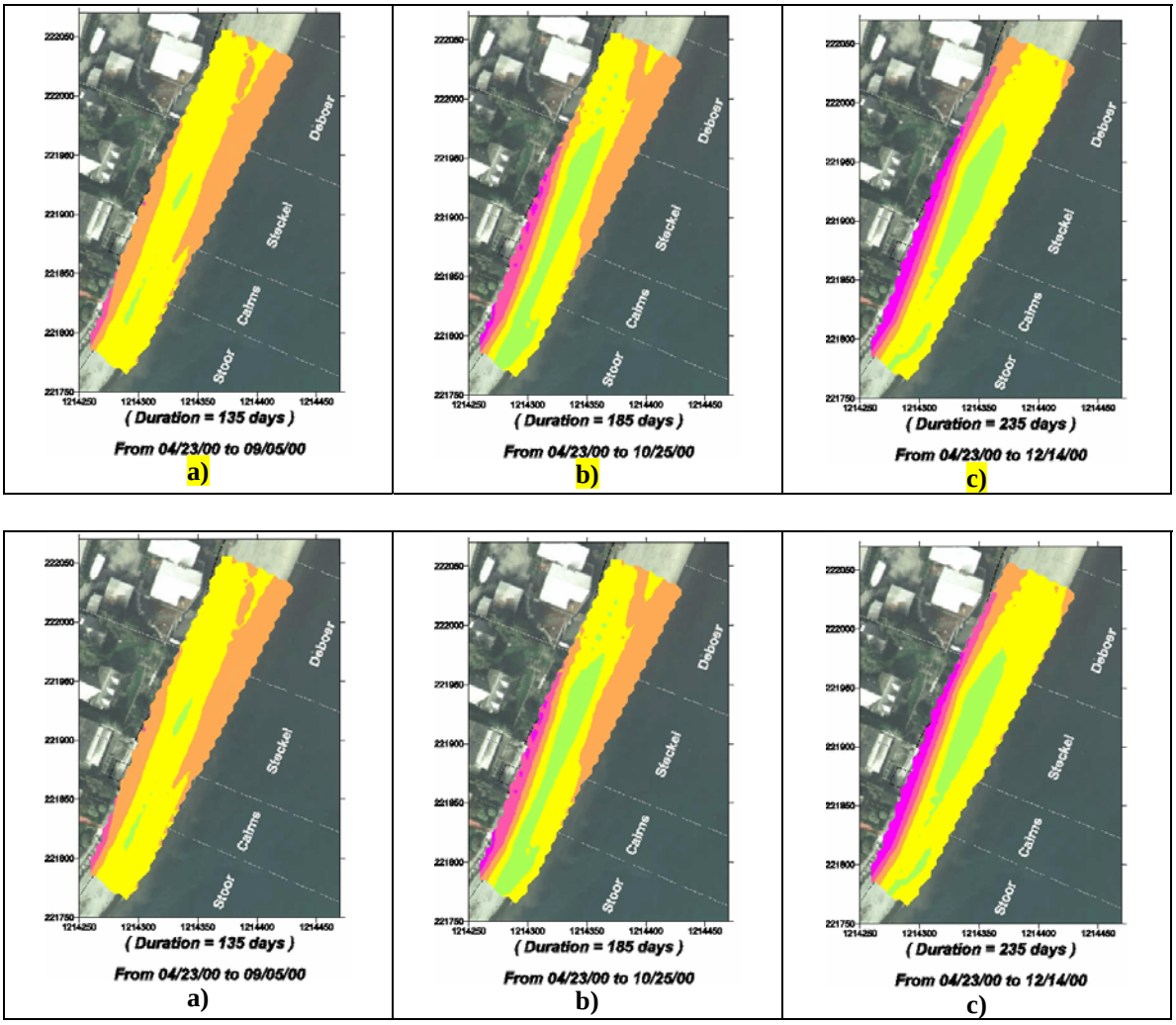

Figure 4-2. Progression of beach morphological development at Site 5

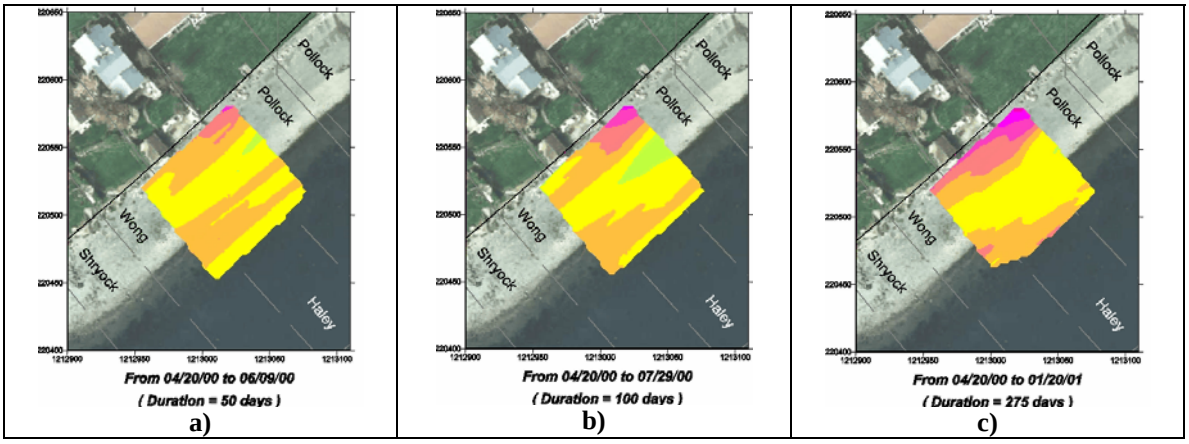

Figure 4-3. Progression of beach morphological development at Site 3

4.2.3 Existing Conditions (June 2004 to January 2005)

A site visit on June 3, 2004 allowed preliminary observation of the general beach and structure conditions of Rich Passage properties. The observations and photographs acquired during the site visit are summarized in a separate trip report (PI Engineering, 2004). There has been no attempt to compare the June 3, 2004 photos with those taken in 2001-2002.

Beach profiles were surveyed at the monitoring sites in August and November 2004, and January 2005. In general, no significant changes were observed between each of these surveys.

As of June 2004, the Bainbridge Island beach profiles appear to have maintained their configuration relative to the most recent survey in September 2002. The profiles also exhibit similarity with the baseline survey of April 2000. Bill Reynolds noted an accumulation of sediment at a property near Site 6 on Point White during the site visit, but it could not be determined if this was due to natural processes or artificial nourishment.

The condition of the Point Glover shoreline was less clear. Several locations near Site 10 may have experienced change (Reynolds, pers. comm., 2004). Sediment accumulation is still absent on most of the shoreline except for the pocket beaches and those protected by drift sills.

4.3 Dynamics and processes on low-energy mixed beaches

The response of the beaches in the study area to POFF operation is a result of many factors that include the following:

- the differences between POFF wakes and non-POFF wakes
- beaches composed of mixed sediments
- high relative tidal range
- low relative ambient wave height to water depth ratio

This section provides a review of mixed beaches with particular focus on low wave energy high tide range environments.

Mason and Coates (2001) conducted an extensive review and summary of mixed sand and gravel beaches. Instrumented field studies with direct process measurements on mixed sand and gravel beaches are rare (e.g. Walker, et al., 1991; Miller, 1997). Mason and Coates (2001) note only three reports of laboratory studies on mixed sediment beaches: Quick and Dyksterhuis (1994) examined profile development on mixed sand and gravel beaches in a 2d wave flume, Holmes et al. (1996) investigated profile development for mixed sands only, and Petrov (1989) studied the sorting of mixed sand and gravel. Recent physical model studies, at 1:1 scale, are reported in de San Roman-Blanco and Holmes (2002) and Bradbury and McCabe (2003).

A major difficulty with physical models of mixed sand and gravel beaches is the scaling of the different sized sediments. Mason and Coates (2001) conclude that large-scale, prototype models are necessary for modeling the vertical structure of mixed sediments on natural beaches. Smaller wave flumes are restricted to investigating a limited sub-set of beach processes, such as infiltration, run-up, and berm formation.

Bradbury and McCabe (2003) investigate scale effects, based on prototype scale model tests, and conclude that there are inadequate data to develop robust empirical profile response models for mixed sand and gravel beaches. However, small-scale testing of gravel-only beaches is adequate for determining the cross-shore profile response under normally incident wave conditions.

In addition to modeling the beach profile change of mixed sand and gravel beaches, the layering, sorting, and mixing processes are of interest in Rich Passage. The Rich Passage sediment distribution is relatively complex. The beach may consist of a hard bottom, a sand beach, a gravel beach, a mixed sand and gravel beach, a cobble "lag" layer overlying and "armoring" a sand layer, or some combination of these. The beach profile can include a flat, sandy terrace exposed at low tide and a gravel and cobble berm near the high tide line, with a distinct demarcation between the two. Isla (1993) reports the results of field data analysis on armoring and differential transport on gravel beaches.

Longshore transport of gravel and cobble is reviewed in van Wellen, et al. (2000) and Damgaard and Soulsby (1996). Existing formulae for calculating longshore transport are compared to field data and numerical model results. It is concluded that energetics-based equations provide the most accurate predictions. Energetics-based formulae similar to the CERC equation (USACE, 1986) are calibrated in both papers.

Several factors have been noted to influence the unique behavioral response of mixed beaches, these include:

- Hydraulic conductivity
- Reflection and long waves
- Threshold of motion and entrainment processes
- Interactions with Coastal Structures
- Tidal range
- Proximity to deep water

4.3.1 Hydraulic conductivity

Quick and Dyksterhuis (1994) suggest that waves breaking on a permeable beach produce net onshore shear stress over the swash and backwash cycle, leading to net onshore transport and profile steepening until beach equilibrium is reached. In contrast, less permeable beaches (including mixed sand and gravel beaches) are

subject to net offshore stress causing the profile to flatten; thus, hydraulic conductivity is directly responsible for equilibrium profile steepness. Field observations of the contrasting behavior of cobble berms and sand berms in summer and winter by Everts et al. (2002) are consistent with this idea. Permeable cobble berms accrete (and steepen) in winter and lose volume in summer. In contrast, less permeable sand berms lose volume (flatten) in winter and gain volume in summer. This observation is also consistent with theories that describe cobble beach profile development being controlled by threshold of motion differences between cobble and sand beaches.

The infiltration losses on a beach are proportional to the size of voids and the volume of fluid captured in each swash cycle. The hydraulic conductivity of the beach controls the velocity at which fluid enters the beach face and moves within it. The quantity of fluid that can be absorbed by a porous beach layer, accommodation volume, is a function of the thickness of the porous layer above a layer with lower hydraulic conductivity.

The potential for gravel accretion and erosion on open coast beaches fluctuates depending on the wave climate and availability (transportability) of sand in the gravel. Storms present optimum conditions for coarse grain berm accretion and build-up on the upper foreshore. High tides and setup accentuate the run-up phase of the swash cycle, maximizing the upward movement of larger particles. The active berm expels sand in the outer layer of the berm which gets transported preferentially offshore by return flows and gravity. The removal of sand further increases porosity of the upper layer reducing the potential for gravel and cobble scour during backwash. During lower energy waves, the sand fraction is likely to be transported preferentially onshore, resulting in a decrease in permeability of the gravel layer and thereby reducing the potential for build-up of coarse particles.

The response of the beaches in Rich Passage does not follow the high-energy gravel-cobble dominated beach model; rather, it is more consistent with the response expected for a low-energy mixed beach (e.g., Quick and Dyksterhuis, 1994; Nordstrom and Jackson, 1993; Nordstrom, 1992).

The larger waves caused by POFFs result in erosion and removal of coarse and fine sediment particles from the upper beach; the smaller waves at slower POFF speeds result in accretion of gravel on the upper beach.

The Rich Passage situation is further complicated by the apparent differential rates of erosion for sand as opposed to gravel, the presence of structures, and the differences in the characteristics of fast and slow

ferry wakes in contrast with storm and swell conditions for open coast beaches.

Rich Passage is also very complex in planform. The different wave angles at the shoreline, and different longshore transport rates and directions are likely significant factors affecting shoreline changes.

4.3.2 Reflection and long waves

Powell (1988) showed that energy of long low waves (Hs/L < 0.02) is not dissipated as effectively as for short waves on gravel beaches. Neither increasing D50 nor doubling effective depth of the beach had a noticeable effect on wave reflection. Powell concluded from this that the main processes dissipating energy on a gravel beach are wave breaking and frictional losses at the water-sediment interface, rather than infiltration. (Note, however, that Powell's data were not from mixed beaches). Mason et al. (1997) conclude that a mixed beach will reflect more energy than either a sand beach (due to steeper gradient) or a gravel beach (due to less energy dissipation through infiltration).

The frequency dependence of the reflection coefficient noted above may be relevant to the beach response in Rich Passage owing to the presence of a significant long wave component in fast ferry wakes and the abundance of vertical reflecting surfaces that intersect the waterline on beaches in the area.

4.3.3 Threshold of motion, selective entrainment, overpassing and inverse grading

Entrainment threshold is generally related to sediment size. Threshold is complicated for mixed sediments by "hiding," pivoting angle, and angle of repose. The literature suggests some contradiction in relative role. Some research suggests larger clasts are more easily entrained due to higher exposure to flow (Fenton and Abott, 1977; Naden, 1987); whereas Komar and Li (1986) report granules in mixed sediment are removed first owing to lower critical threshold.

Flatter gravel and cobble particles, with a large surface area, may also be "selectively" entrained as a result of grain exposure to flow and moved downslope more easily by backwash and gravity. Classic overpassing process (Everts, 1973) during backwash may help to explain the observed inverse grading observed after the POFFs were introduced on the Seattle-Bremerton route. Sand granules and fine gravels are more easily trapped than larger particles that have greater inertia, so finer particles deposit more readily, while larger particles continue to roll downslope.

4.3.4 Interactions with coastal structures

Coastal structures such as bulkheads may interfere with the uprush-infiltration phase of a more permeable gravel layer, especially at higher tides, resulting in a localized loss of sediment and beach lowering at the toe of the bulkhead.

The presence of the structure may limit the effectiveness of uprush-infiltration process to transport coarse grains landward under energetic waves and limited infiltration may lead to enhanced backwash. The enhanced uprush of larger ferry waves meets an impermeable structure and rushes up the impermeable face of the structure rather than infiltrating a porous layer on the upper beach face. The enhanced backwash readily carries both fine and coarse material that has accumulated at the toe of the bulkhead seaward to the lower foreshore (+/- MLLW) where the gravel is more likely to be mixed with finer particles (sand and silt) and thereby become less mobile.

4.3.5 Tidal range

Relative time of occurrence of swash, breaking, and shoaling conditions on the profile may be fundamental to causing change in the beach morphology observed under different wake wave climates.

Nordstrom and Jackson (1993) observed that rapid migration of the swash zone on a sandy macro-tidal beach during the ebb reduced the time during which pebbles could be deposited at any particular elevation on the profile. Nordstrom and Jackson (1993) developed a conceptual model for distribution of surface gravel particles on a sand beach. Offshore transport of both sand and gravel occurs during high-energy conditions, with subsequent burial of pebbles just above the low tide terrace. Fines are then removed from the coarse matrix by exfiltration at low tide. In the low-energy recovery phase, sand and finer material is preferentially transported landward, leaving a lag of coarsest material near the low tide terrace. This is probably the conceptual model most relevant to Puget Sound beaches (with their prevalence of coarse cobble lag at or near low water). This is in direct contrast to patterns observed on open coast mixed profiles where the cobbles accumulate at the top of the profile. This is consistent with the results of Isla (1993).

4.3.6 Proximity to deep water and surf zone-swash zone processes

Deep water in proximity to the shoreline in Rich Passage owing to the steep foreshore slope means that larger waves can reach closer to shore before shoaling and breaking. This results in a narrow zone of breaker turbulence where hydrodynamics are dominated by the shore-break, usually of the plunging type, and swash uprush and backwash hydrodynamics.

The transient nature of POFF wakes means that no steady longshore currents develop and no undertow or rips develop during a vessel wake. However, oblique swash in a narrow breaker zone may be highly effective in transporting sediment alongshore (e.g., Coates and Lowe, 1993). Also, larger waves reach closer to shore at more oblique angles on a steeper foreshore.

Despite a relatively small difference in height, the POFF waves are significantly more energetic because their periods are longer than the slow ferry wakes. The longer waves result in more energetic and greater horizontal excursion in the swash and backwash. The beach profile response to changes in POFF operating speed was rapid. The waves observed during high-speed POFF operation have a longer uprush and backwash compared with the regular waves observed under slow POFF and car ferry operations. The long period waves associated with high-speed POFF operation behave at times like a surf bore.

Energetic backwash assisted by gravity may be more conducive to downslope removal of gravel and cobble as well as sand, particularly on the ebb phase of the tide, whereas the effectiveness of the swash uprush in energetic longwaves may be limited by reflection and structure interaction near high tide (e.g. Nordstrom, 1992; Nordstrom and Jacobsen, 1993).

In this relatively low-energy environment, the shorter and somewhat steeper waves under the slow-speed ferries may be more conducive to net onshore transport of sand, pebble, and gravel, leaving a large cobble lag at the base of the intertidal zone.

5.0 Wake Impact Model Development

Several different numerical models are required to investigate the impacts of fast ferry wakes relative to other mechanisms on the shorelines of Rich Passage. As identified in Section 2, these include:

- a tidal model to predict the water levels and currents;
- a wind wave prediction model to predict the growth, propagation, and transformation of wind generated waves;
- a wake generation and propagation model to predict the wake produced by the vessel and its transformation from the vessel to the shore, and;
- a shore response model to predict the response of the shore over time.

This section describes the selection/development of each of these models and their validation/calibration for use in the Rich Passage area.

5.1 Modeling Domain and Grid Development

All of the models that will be applied to the Rich Passage area will require bathymetric and elevation data. The tidal, wake, and wave models all require large scale, two-dimensional data. This may be fairly coarse in resolution for the tidal model and the deepwater region of the wake model. The resolution of the bathymetry in the nearshore zone, where wave shoaling, refraction and breaking are important, will have to be increased in the wake model in order to resolve these processes. The shore evolution model will likely require even higher resolution, so that beach ridges and other morphodynamic features can be resolved.

To ensure that output data from one model can be used as input data in another model, there should be agreement in the bathymetric and elevation data used for the models. The best way to ensure this is to develop a common bathymetric data set or digital elevation model (DEM) of the study area. Different types or formats of bathymetry or elevation data can be extracted from this DEM as required.

5.1.1 Data Sources

The bathymetry in the area was compiled using data from the National Ocean Service GEODAS (GEOphysical Data System) database and most recent beach and channel cross section survey data collected by PI Engineering during 2000 to 2004 as described in Section 3.

5.1.2 Finite Element Mesh Generation

The ADCIRC tidal model and the wake generation-transformation model both use a finite element mesh. Using the bathymetry described in the preceding section, a mesh was generated that covered the region shown in Figure 5-1. The mesh includes Rich Passage, Dyes Inlet and

Sinclair Inlet. The mesh has two open boundaries, one located near Brownsville and the other at Clam Bay, near Manchester. These two limits were selected because tidal stations are located nearby.

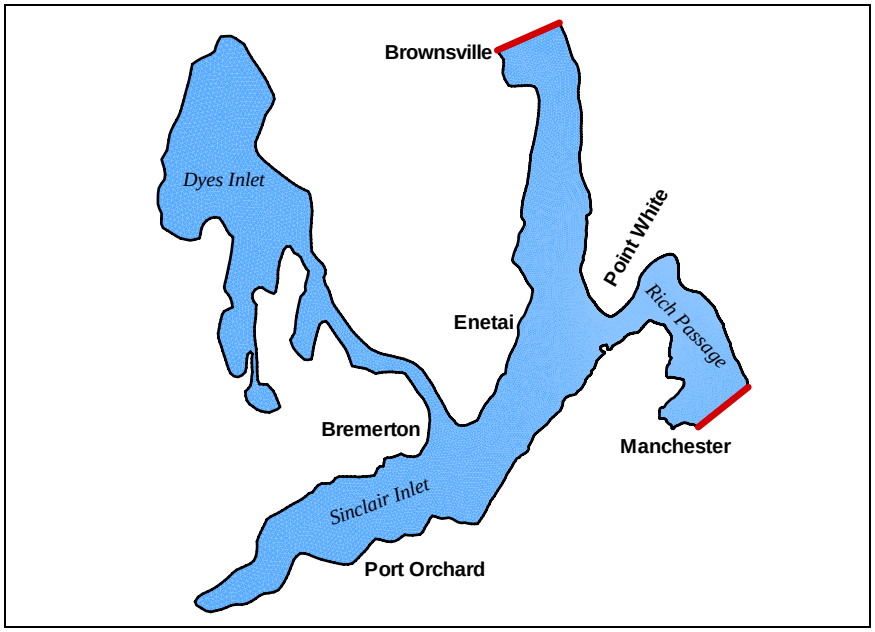

Figure 5-1. Coverage of the finite element tidal model

Figure 5-2 shows the actual finite element mesh, which has 23366 nodes and 44651 elements. The inserts in the figure illustrate the density of the mesh. The mesh in the vicinity of Bremerton has an average dimension of 70 m. The mesh in the center of Rich Passage has an average dimension of 20 m, whereas the mesh near the shore in Rich Passage has an average dimension of 7 m. The density of the mesh in other areas of the domain where wake impacts at the shore are important (e.g., the shore near Enetai) will likely be increased once new survey data becomes available in the next project year. The depths corresponding with the coverage of the finite model and mesh are shown in Figure 5-3.

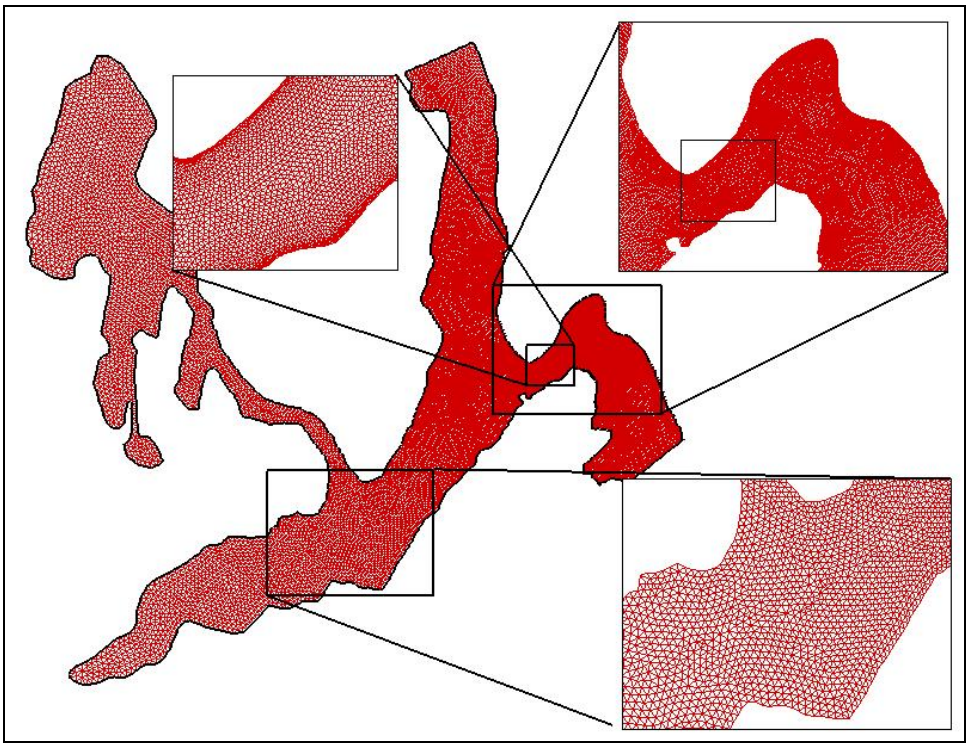

Figure 5-2. Finite element mesh developed for the ADCIRC tidal model. Inserts show the density of the mesh in various locations

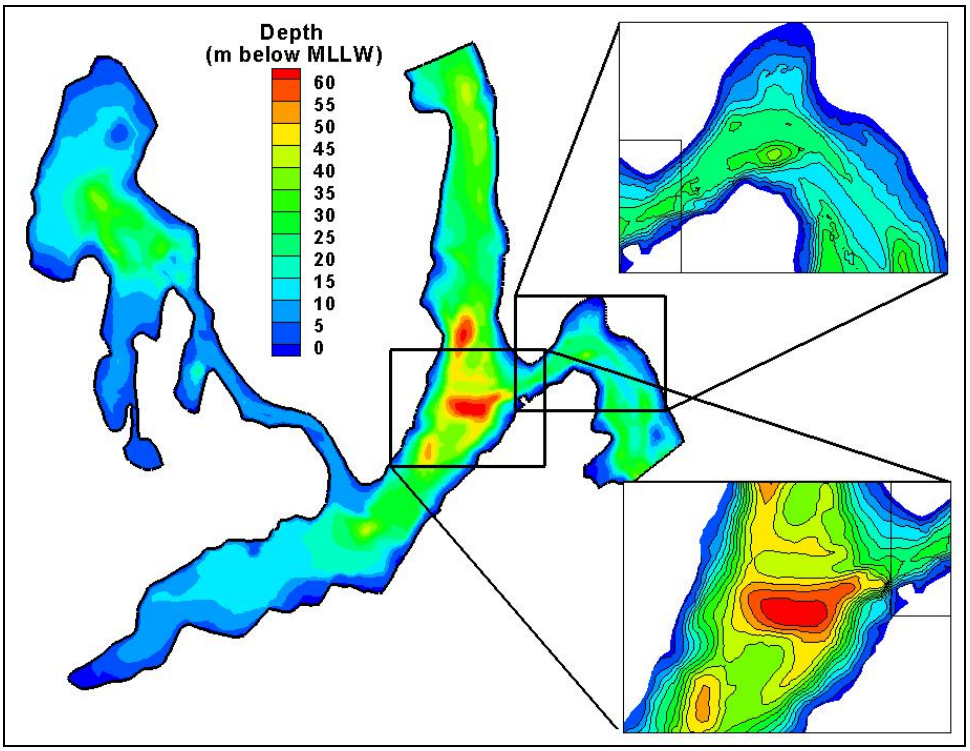

Figure 5-3. Depths in the finite element mesh

5.2 Tidal Circulation Model

Tidal circulation modeling is essential for studies in the Rich Passage area because of the large tidal range and strong tidal currents. The propagation and transformation of a wake is dependent upon the movement of the water in which it is traveling. As well, the wake patterns and wake heights produced by a vessel vary with the depth of water in which the vessel is sailing. At the shore, the part of the beach profile exposed to wake action is controlled by the tidal elevation at the time.

5.2.1 ADCIRC Model

The ADCIRC model (Luettich et al., 1992), developed by the University of North Carolina and the University of Notre Dame, was selected for the tidal simulations. The two-dimensional version of the model, ADCIRC-2DDI, was selected for the present study.

The ADCIRC model calculates the time dependent, free-surface elevation and depth-averaged flow velocities using a finite element formulation. The model is one of the most numerically-advanced and highly-validated tidal models available. Because of problems associated with finite element solution of the classical momentum and continuity equations in their primitive form, the ADCIRC model has been formulated to solve the depth-integrated continuity equation in Generalized Wave-Continuity Equation (GWCE) form. This approach produces a smooth and stable, yet highly accurate, solution. The velocity field is obtained from the solution of the depth-averaged momentum equations. All non-linear terms have been retained in both of these equations.

The ADCIRC model was applied using Cartesian coordinates, because of the small area of the domain. A time step of 1 sec, which is quite short for tidal modeling, was required, because of the fineness of the mesh in the nearshore areas of Rich Passage. The wetting and drying option in the model was turned on.

5.2.2 Boundary Conditions

The ADCIRC model was applied to the finite element mesh shown in Figure 5-2. This mesh has two open boundaries, one near Brownsville and the other at Clam Bay, near Manchester, at which information about the tidal conditions must be specified. The model is operated using surface elevation data at both boundaries.

Tidal information for the two boundaries was obtained from the Puget Sound Tide Channel Model (PSTCM) (Lavelle et al., 1988). This is a large, coarse resolution tidal prediction model of Puget Sound developed at NOAA's Pacific Marine Environmental Laboratory (PMEL). PSTCM output is available online through the

Oceanography Department of the University of Washington[1]. Tidal elevation time series data were extracted from the PSTCM at a 10-minute interval at nodes 243 (Clam Bay) and 284 (Brownsville) for each period that was modeled.

5.2.3 Model Validation

The ADCIRC model application to Rich Passage and Sinclair Inlet was validated by comparison to measured data collected by PI Engineering in 1999 and 2000. The test periods are shown in Table 5-1.

Table 5-1. Test periods selected for validation of the ADCIRC tidal model

Test Name	Test Period (UTC)
Station_A_spring	2000/03/12_24:00 → 2000/03/18_24:00
Station_B_spring	1999/11/22_07:00 → 1999/11/28_07:00
Station_D_spring	2000/05/31_18:00 → 2000/06/06_18:00
Station_A_neap	2000/03/07_08:00 → 2000/03/13_08:00
Station_B_neap	1999/11/13_10:00 → 1999/11/19_10:00
Station_D_neap	2000/05/24_23:00 → 2000/05/30_23:00

The first part of each test name refers to the location of the deployed instrument. The last part of the name refers to the spring-neap tidal cycle. The locations of the instruments are shown in Figure 5-4.

[1] http://students.washington.edu/dfinlays/tides/

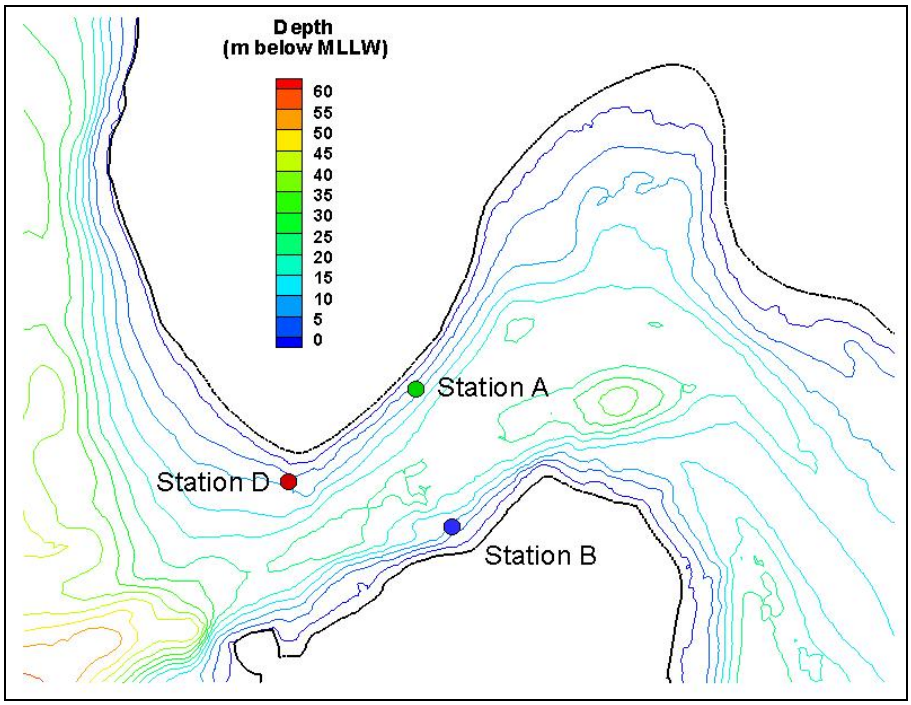

Figure 5-4. Locations of Stations A, B and D during the 1999-2000 Rich Passage field campaign

Comparisons of the results of the ADCIRC model simulations and the measured data are presented in Figures 5-5 through 5-10. Three plots are shown in each case; the upper plot shows the comparison of surface elevation, the middle plot shows a comparison of current speed and the lower plot shows a comparison of current direction. In each case, the computed surface elevation is quite similar to the measured. The amplitude and phase are well-matched at all stations.

The current speeds are reasonably well predicted, especially at Station A. An examination of the results in Figure 5-5 suggests that some components of the tide are accurately modeled each day, while the solution for others is repeatedly in error. This suggests that the harmonic input boundary conditions may be the source of some of the inaccuracies. It should be noted that the wind-stress was not modeled in these simulations. There are high-frequency oscillations in each case that may be attributable to wind-driven flows or to sub-grid scale turbulence not represented in the model.

Table 5-2 presents an estimate of the error in the model simulations. The percentage errors in the water surface elevations at all three sites are all in the range of 0.5 percent. The errors in the velocities are larger, especially at Station D. The errors in the velocities at Stations A and B are less than 5 percent and the errors in velocities at Station D are less than 10 percent.

Table 5-2. ADCIRC model validation for tides and currents at 3 gauge stations

Station		Max Range		Mean Error		RMS Error		Percent Error	
		El, m	V, m/sec	El, m	V, m/sec	El, m	V, m/sec	El, %	V, %
A	Spring	3.76	1.34	0.04	0.00	0.01	0.05	0.3	3.9
	Neap	3.50	1.30	0.07	0.00	0.01	0.06	0.3	4.6
B	Spring	4.78	1.18	0.04	-0.02	0.02	0.04	0.4	3.0
	Neap	3.48	0.74	-0.02	0.07	0.02	0.03	0.6	4.0
D	Spring	4.81	1.95	-0.01	0.19	0.02	0.15	0.4	7.9
	Neap	3.39	1.48	-0.01	0.24	0.01	0.14	0.2	9.5

The accuracy of the computed current directions is more difficult to assess, since there can be large errors in direction when the current speed is low. With the exception of Station D, the direction of the peak flood and ebb currents is well predicted. Station D is a particularly difficult location to model, since the flow separates between Port Orchard and Rich Passage near this point, whereas the other two stations are located on straighter parts of the shoreline. The accuracy of the comparison of model predictions with point measurements in areas where the flow is complex, may also be reduced by uncertainty in the horizontal position of the measurement point and limited resolution of bathymetry features in the model grid. With respect to the overall aims of the study, it is more important that the model predicts tidal flows in these latter areas, which are more subject to wake-induced damage.

The ADCIRC model of Rich Passage will be used as a platform upon which the wake model will be run and, in that respect, the accuracy of the tidal current predictions is secondary, compared to that of the wake model. The results presented in this section show that the tidal model is sufficiently accurate for that purpose.

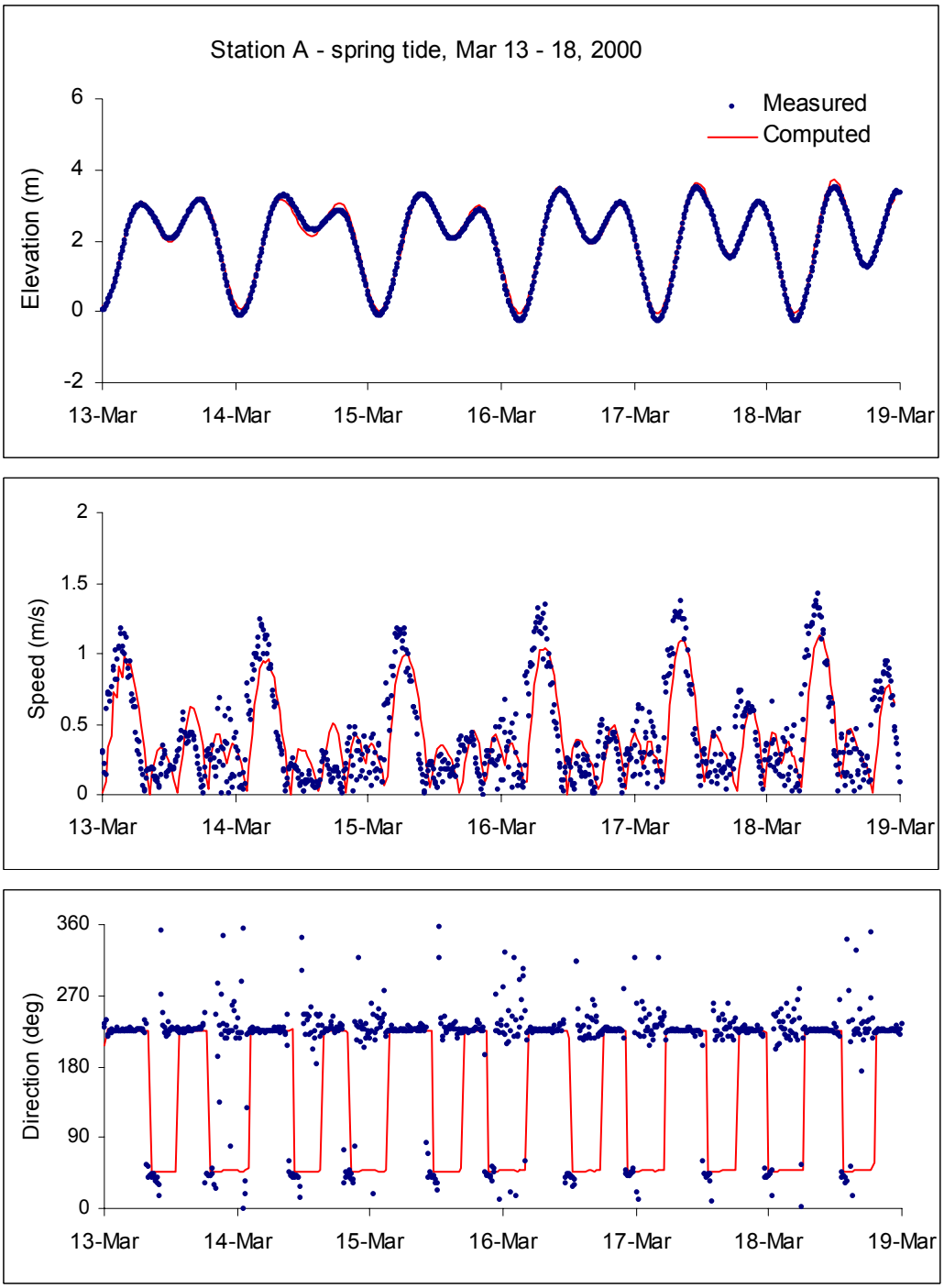

Figure 5-5. Comparison of field data and computed data for spring tide at Station A

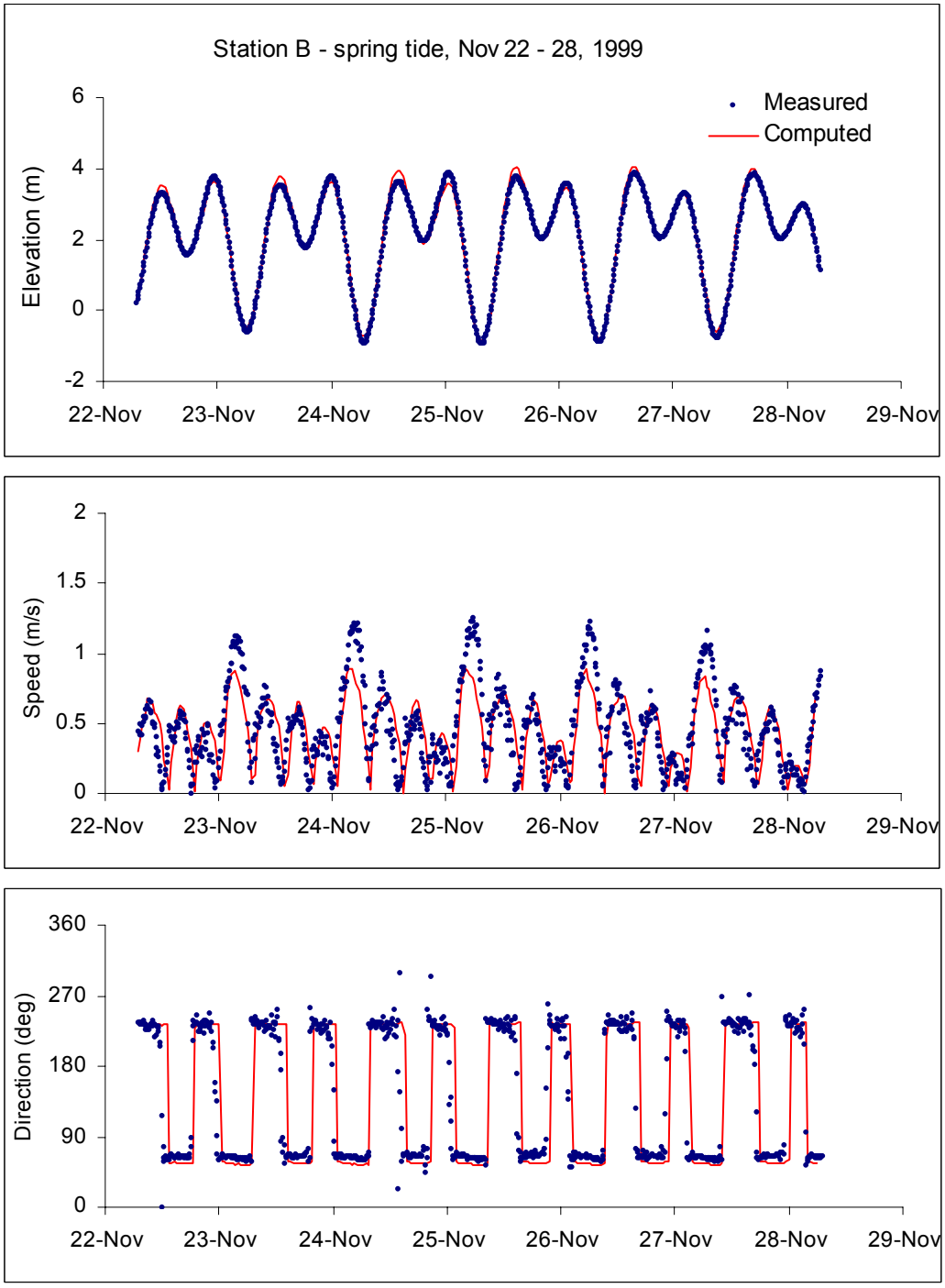

Figure 5-6. Comparison of field data and computed data for spring tide at Station B

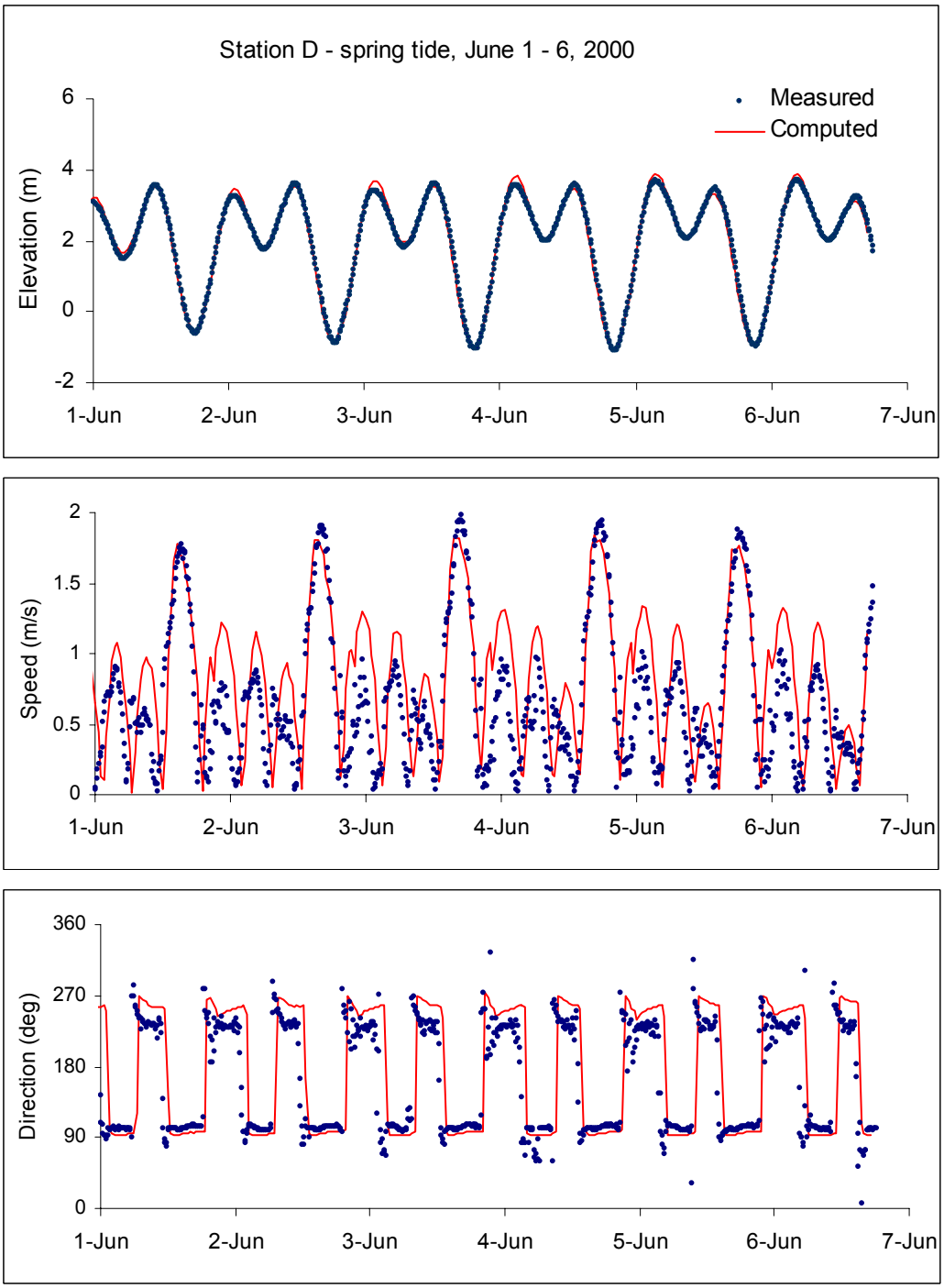

Figure 5-7. Comparison of field data and computed data for spring tide at Station D

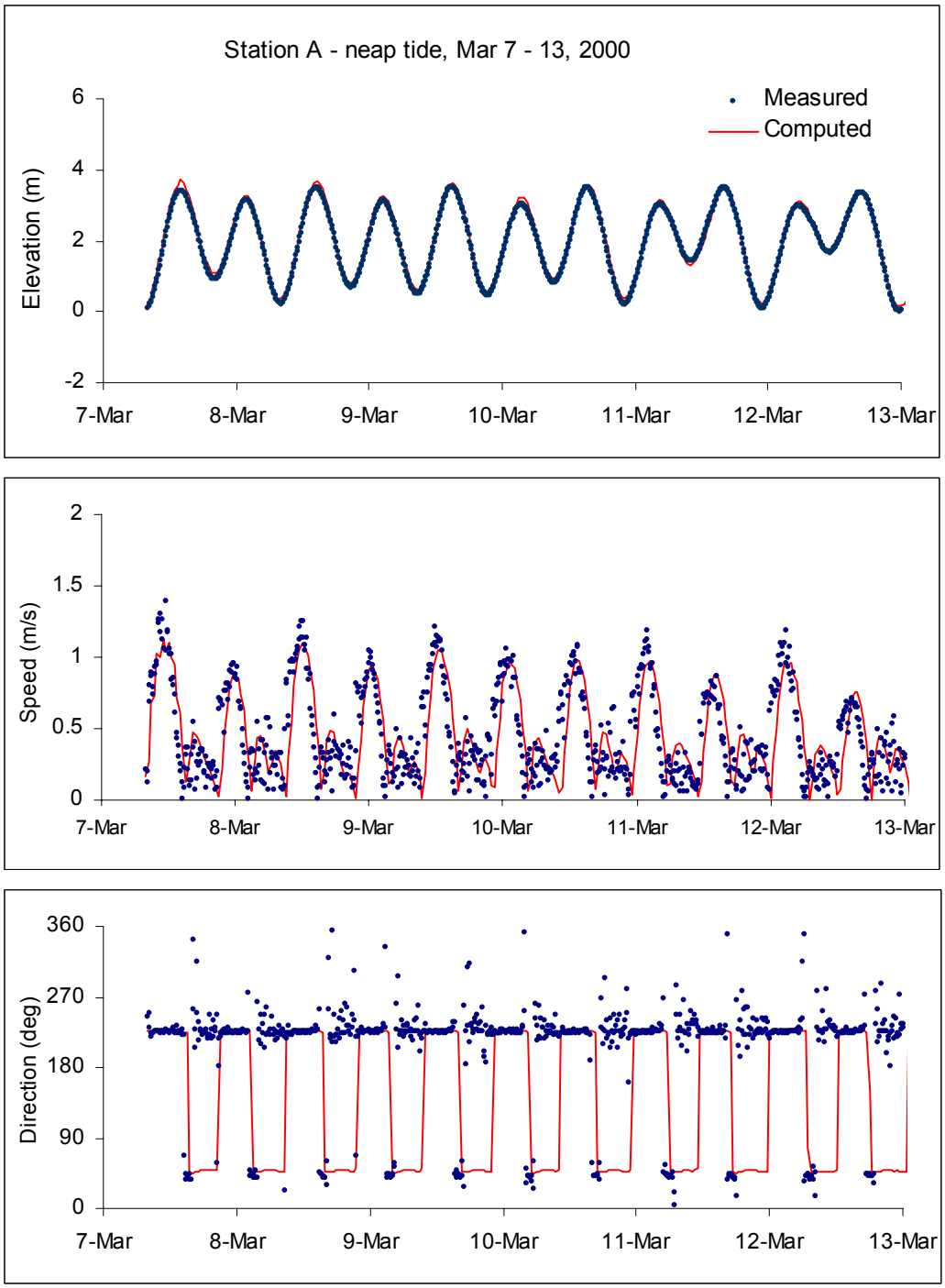

Figure 5-8. Comparison of field data and computed data for neap tide at Station A

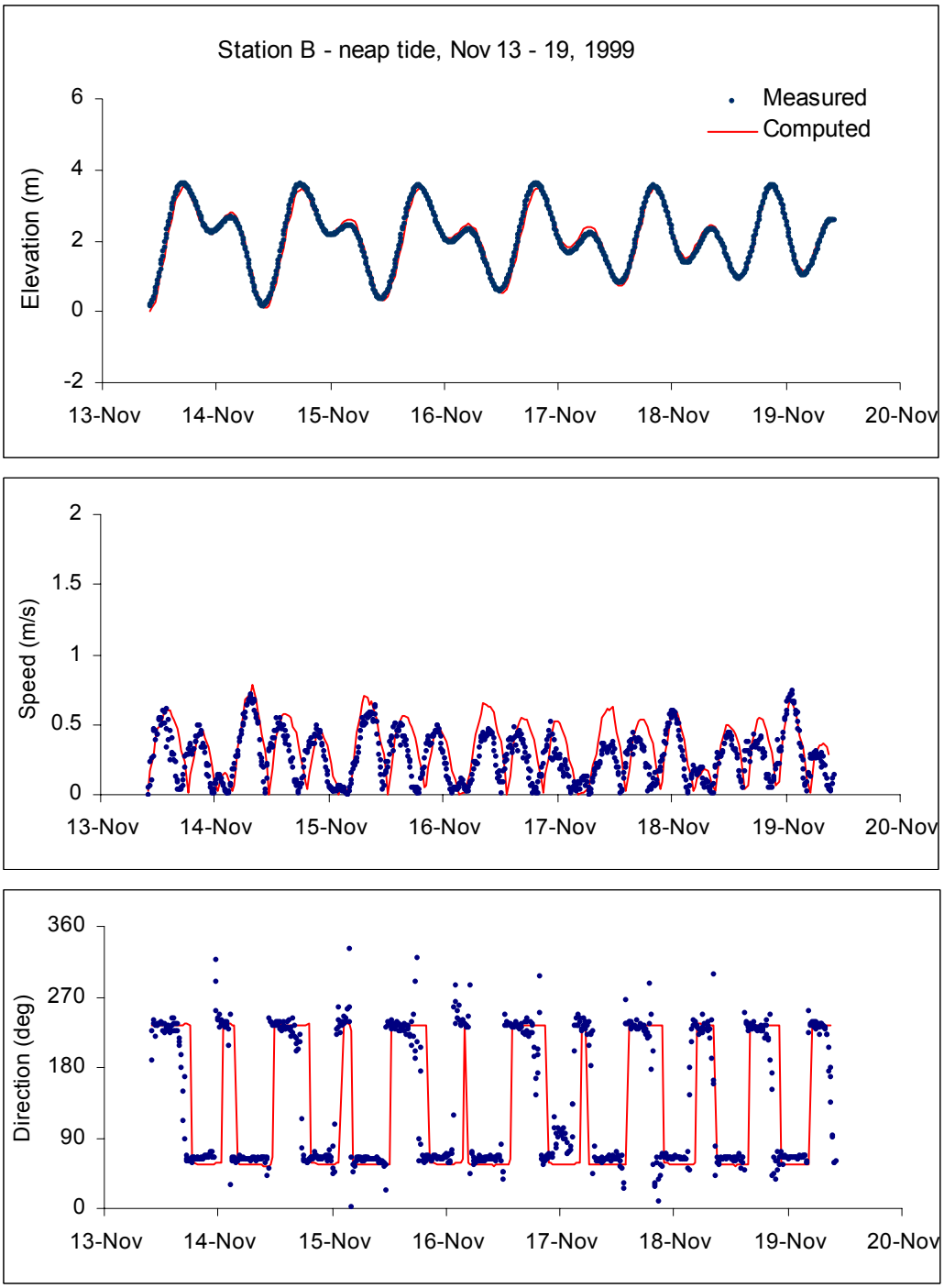

Figure 5-9. Comparison of field data and computed data for neap tide at Station B

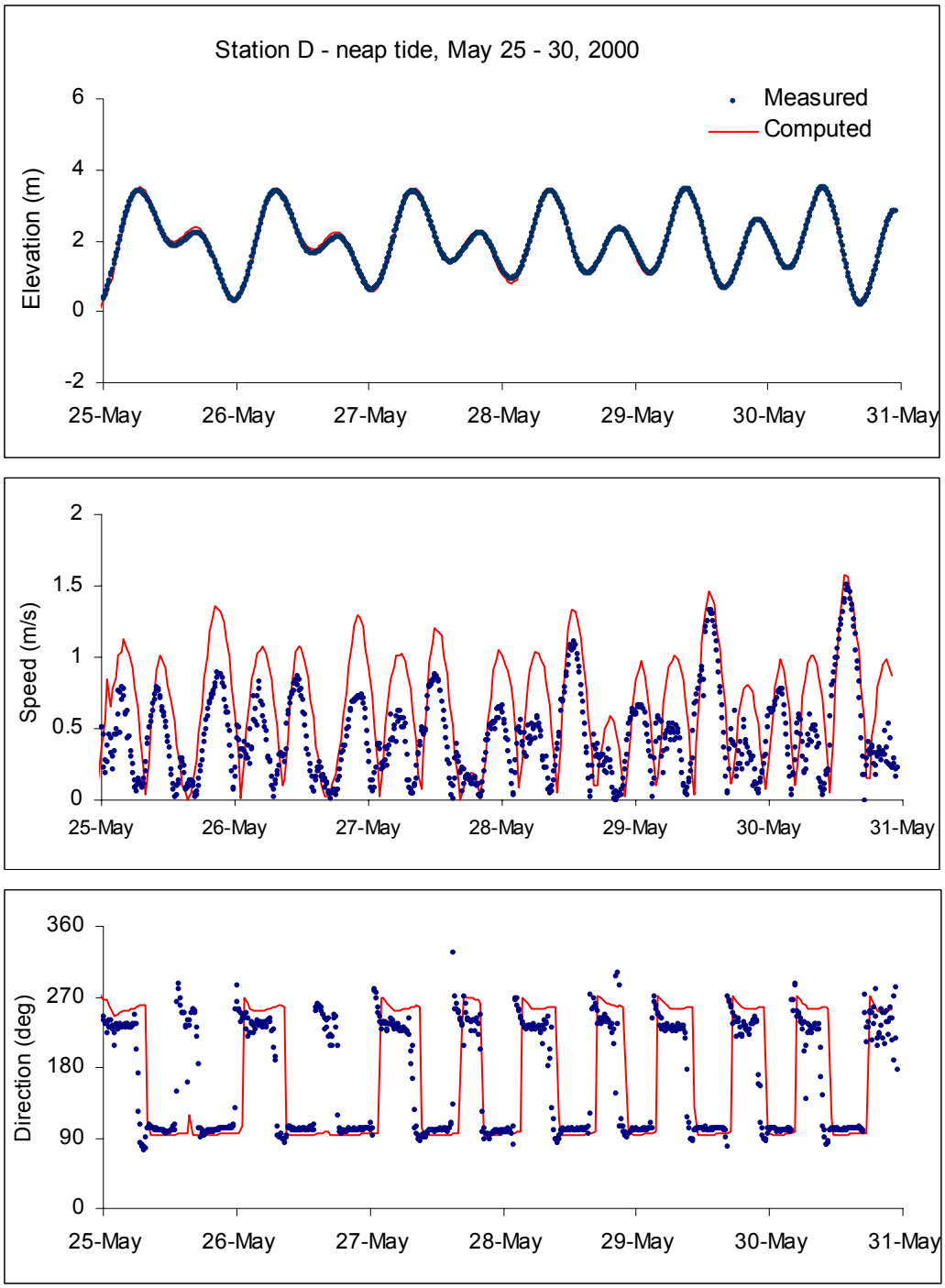

Figure 5-10. Comparison of field data and computed data for neap tide at Station D

5.3 Wind Wave Modeling

Although the wind waves in Rich Passage are not large by comparison to other coastal sites in the Pacific Northwest, they are a significant forcing mechanism for beach morphology in many areas of Rich Passage. This is because they occur for a significant number of hours throughout the year and, because of the orientation of Rich Passage, can have a substantial angle to the shore at breaking.

In order to study the effects of wind waves and to determine their relative importance in comparison to other forcing mechanisms, such as POFF wakes, a wind wave modeling approach has been formulated and applied on a preliminary level. The first stage of the approach is the hindcasting of waves outside of Rich Passage from measured wind records. The sources for the wind data are described in Section 3.6. The second stage is to model the propagation and transformation of these waves from outside Rich Passage to their eventual breaking on the shore.

Both stages of this proposed wave modeling approach are described in this section along with an illustration of the approach that uses waves measured in Sinclair Inlet in February 2005.

5.3.1 Wave Hindcasting

Two wave hindcasting methods were used to predict the wave heights at the IT1 measurement site: the broadly-applied JONSWOP technique (SPM, 1984), and the SEBJ technique (Dupuis et al., 1996), which is designed for small, quick reacting, swell-free bodies of water (reservoirs, lakes).

In both the JONSWOP and SEBJ techniques, individual wind speeds and directions are combined with fetch lengths to hindcast wind wave conditions at a specific point. Both methodologies use similar approaches for data preparation. The two methods will be only briefly described in the following paragraphs.

There are several adjustments required for raw wind speeds collected over land before they can be used as estimations of surface winds for wave prediction. Certain adjustments, such as anemometer elevation and duration-averaging, were not required, since the raw data was in the correct form. Other adjustments were assumed as follows:

- air-sea temperature differences was negligible, R_T =1.0;
- inland wind station factor was assumed to be R_L = 1.1.

The wind measured wind speed, U , is converted to an applied wind stress, U_A, using:

$$U_A = 0.71\, R_T R_L U^{1.23}$$

5.3.1.1 Fetch Delineation

The fetch is the distance over which the wind stress is applied to the body of water. Considerable care and judgment must be used in selecting appropriate fetch lengths in areas subject to strong orographic effects, such as Sinclair Inlet and Rich Passage. The presence of large hills can cause a funneling of the wind along valleys and narrow bodies of water. This orographic effect increases the speed of winds blowing along their axis. However, this phenomenon is highly site-specific and little research is available in the literature to quantify this affect. For the present study, an "average" fetch distance between 200° and 240° was used for all wind directions from the southwest. This distance was 3.5 km for the data collected in Sinclair Inlet (instrument location IT1) used in this section (see section 3.6).

An important aspect of any hindcast is to determine whether, for a given set of conditions, the resulting case is fetch limited or duration limited. In the case of Sinclair inlet, the fetch distances are so small that the duration limit is in the order of 1 hour for winds over 23 km/h.

5.3.1.2 JONSWOP Hindcast Model

The fetch-limited JONSWOP model is given by the following dimensionless equations:

$$\frac{gH_{mo}}{U_A^2} = 1.6x10^{-3}\left(\frac{gF}{U_A^2}\right)^{1/2}$$

$$\frac{gT_m}{U_A} = 2.857x10^{-1}\left(\frac{gF}{U_A^2}\right)^{1/3}$$

where F is fetch length, H_{m0} is the spectral significant wave height, T_m is the period of the peak of the wave spectrum and t is the minimum duration required to ensure fetch-limited conditions.

5.3.1.3 SEBJ Hindcast Model

The fetch-limited SEBJ model is given by the following dimensionless equations:

$$\frac{gH_{mo}}{U_A^2} = 2.47\times10^{-3}\left(\frac{gF}{U_A^2}\right)^{0.45}$$

$$\frac{gT_m}{U_A} = 5.09\times10^{-1}\left(\frac{gF}{U_A^2}\right)^{0.225}$$

5.3.1.4 Hindcast Model Application

The measurements and predictions were compared using preliminary data collected on the afternoon of 4 February 2005. Wind measurements were obtained from the Bremerton Airport (see Section 3.6). The wind speeds and directions over this period are shown in Table 5-3. The wind speed adjustment factors are described above. A constant uniform fetch distance of 3.5 km was applied.

Table 5-3 Measured winds at Bremerton Airport

Time (PST)	Direction (degrees)	Speed (km/h)
11:55	210	35
12:15	210	46
12:35	200	43
12:55	210	39
13:15	210	33
13:35	200	30
13:55	200	31
14:15	210	24

Wave statistics are usually used to validate wave hindcasting approaches. In order to compare real-time wave measurements with hindcast values, however, a correction is required to account for distance between the wind measurement location and the wave measurement location and for the time lag for the wave growth. In the present application, a time lag of 45 minutes was applied to the times of the hindcast values.

The measured and hindcast wave conditions for 4 February 2005 are shown in Figure 5-11. Both hindcast models match the wave growth and decay, both in the wave height and the wave period. From this one case, it would appear that the JONSWOP model reproduces the measured results better.

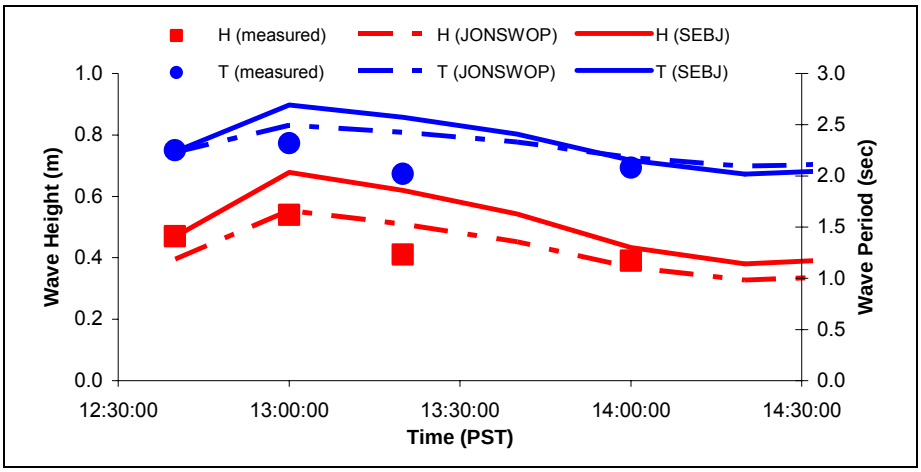

Figure 5-11. Comparison of measured and computed wind wave heights for February 4, 2005

5.3.2 Wave Modeling

As noted above, hindcast wind waves will be used as the input to local wave models to determine the wave conditions along the shores of Rich Passage. There are several wind wave models that can be applied. Two have been selected that offer different advantages. The STWAVE model, developed at the U.S. Army Engineer Research and Development Center (ERDC), is a spectral wave model that can be coupled to the ADCIRC tidal model presently being applied in the study. The STWAVE model is good for large areas, but has only an approximate incorporation of the effects of diffraction, which may be a limitation in the narrow and curving confines of Rich Passage.

Another model that is available and may be applied in the study if required is the CoastL model, a propriety wave model of Pacific International Engineering. This model differs from STWAVE in two main areas. First, it is primarily a wave transformation model. Wave growth within the domain is not included, which should not be a limitation over small domains. Second, CoastL computes wave diffraction, whereas STWAVE approximates it using a diffusion analogy. This is likely to be important in the complicated geometry of Rich Passage.

Both wave models and ADCIRC are generally applied in one of two ways. If a specific time period is to be modeled, then both models can be applied using real-time input data. However, many applications require more general simulations. In these cases, the wave model is applied at selected stages of a representative tide (e.g. average spring tide, average neap tide). A commonly applied technique is to apply the wave model to four stages of the tide: peak flood, high water slack, peak ebb, and low water slack (see Figure 5-12)

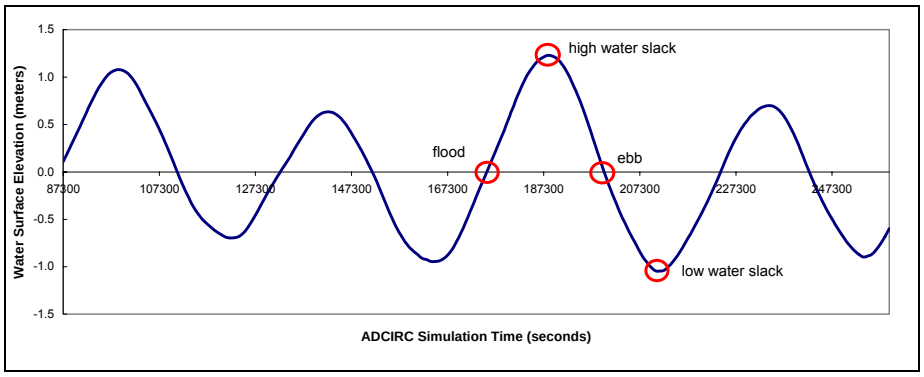

Figure 5-12. Typical four-point application of STWAVE in a tidal cycle

5.3.2.1 STeady-state Spectral WAVE Model (STWAVE)

STWAVE is a steady-state spectral wave model based on the wave action balance equation. It is finite-difference in its formulation and can be used to calculate the spatial distribution of wave heights, wave periods and radiation stresses in shallow water regions. STWAVE considers current- and depth-induced wave refraction and shoaling, depth- and steepness-induced wave breaking, wind-wave growth, and wave-wave interaction and whitecapping. The model also approximates diffraction effects. STWAVE requires the following assumptions:

- mild bottom slope;
- negligible wave reflection;
- spatially homogeneous offshore wave conditions;
- steady-state waves, currents, and winds;
- linear refraction and shoaling;
- depth-uniform current, and;
- negligible bottom friction.

STWAVE was developed at the U.S. Army Engineer Research and Development Center (ERDC) and is widely applied in the coastal engineering community (McKee-Smith et al. 2001).

Flow conditions can be supplied to the STWAVE model from ADCIRC simulations. The two models can be coupled through the Surface Water Modeling System, SMS (Brigham Young University, 2003). SMS provides a Steering Module utility for passing ADCIRC calculated currents to STWAVE and radiation stresses computed by STWAVE to ADCIRC.

5.3.2.2 CoastL Model

The CoastL model (MacDonald, 1998) is composed of a dynamically-coupled refraction-diffraction wave module and a depth-averaged coastal flow module. The wave module uses a wave-period averaged

technique and can be used over areas ranging from tens of meters to tens of kilometers. Approximate non-linear effects are included and either swell or random waves can be simulated in the surf zone. Wave-current interaction with internally generated or externally imposed flow fields is also included. The flow module computes the depth-averaged flows resulting from any combination of wave, wind and tidal forcing. It includes combined wave-current friction and turbulence using a two-equation k-ε closure.

CoastL requires the following assumptions:

- mild bottom slope;
- negligible wave reflection;
- monochromatic wave field;
- steady-state waves, currents;
- no input wind energy over the domain;
- approximate non-linear refraction and shoaling, and;
- depth-uniform current.

Currents from ADCIRC can be used as boundary conditions for the current module.

5.3.2.3 Wave Model Application

Both wave models were applied to the western entrance to Rich Passage to illustrate the type of prediction that is possible using this approach. The conditions illustrated here are the peak conditions measured on 4 February and discussed above. Note that the entrance to Rich Passage is approximately 2.5 km further along fetch from the IT1 site, so a new hindcast was performed. The input wave conditions for the following simulations are H_S=0.68m, T_P=2.87s, θ=245°.

Note that the STWAVE model simulation shown in this section has been performed using a very broad directional spectrum, whereas the CoastL simulation was performed under the assumption of a narrower spectrum. Both models can be applied with directional spectra with varying degrees of spreading.

Figure 5-13 shows the computed wave height patterns and wave directions for the STWAVE simulations. These results may be under-predicting the waves in Rich Passage because of the large amount of energy dissipation between the model boundary and Point White. Figure 5-14 shows the same simulation, but with winds forcing as well. This has the effect of decreasing the dissipation and pushing more energy around Point White.

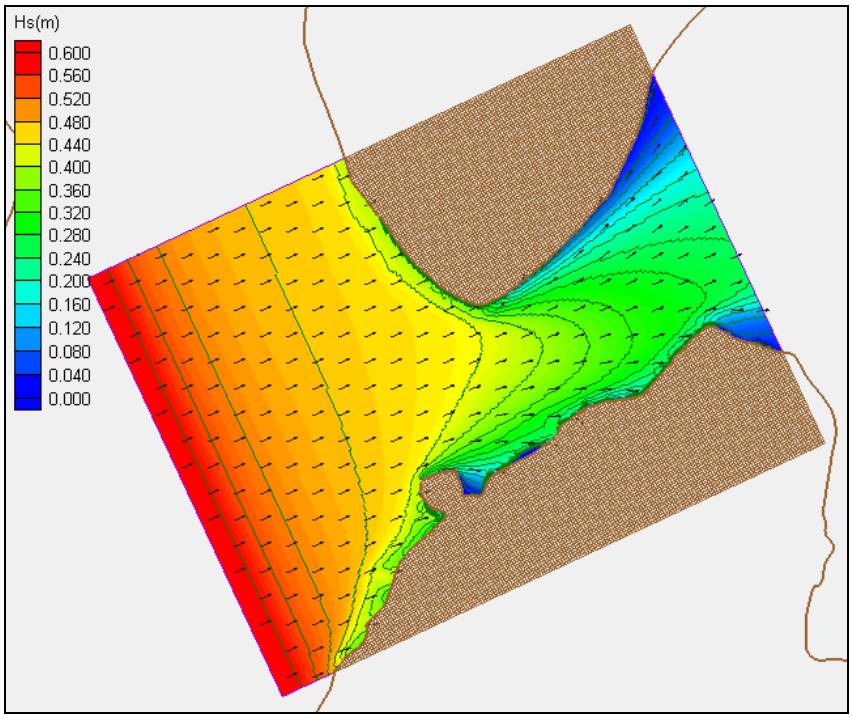

Figure 5-13. Predicted wave heights at the entrance to Rich Passage as predicted by STWAVE (Hs=0.68m, T=2.87s, Dir=245deg)

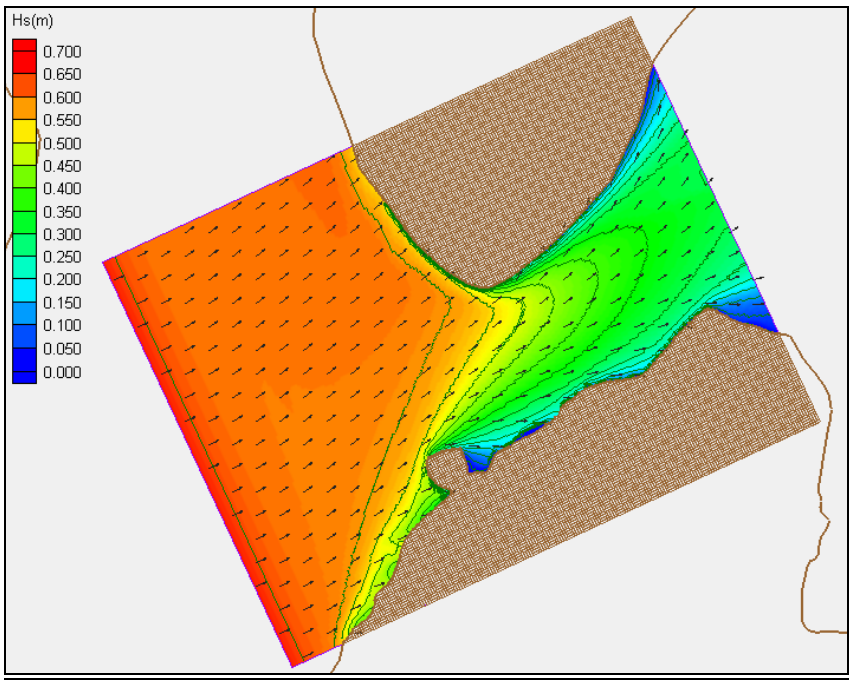

Figure 5-14. Predicted wave heights at the entrance to Rich Passage as predicted by STWAVE (Hs=0.68m, T=2.87s, Dir=245deg, Wind=210deg)

The CoastL model results for a larger area are shown in Figure 5-15. The diffraction of wave energy (in contrast to the diffusion used in the STWAVE model) is illustrated by the focusing of wave energy in the center of the passage. These are very short waves and will not refract until within 50 m of shore, as is illustrated in the detail defined in Figure 5-15 and shown in Figure 5-16.

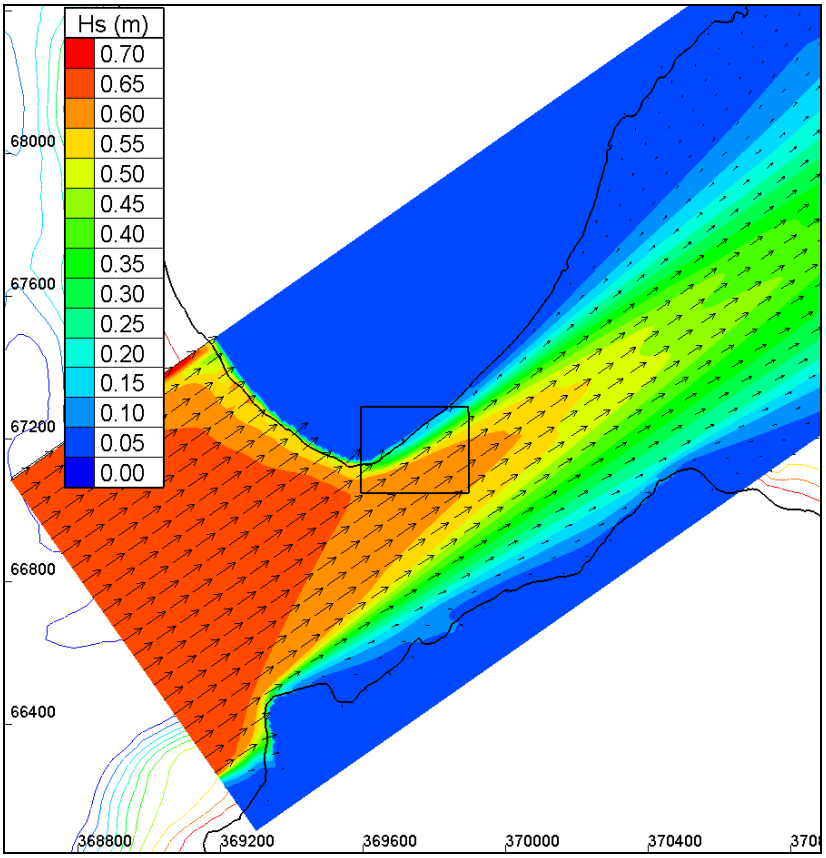

Figure 5-15. Predicted wave heights at the entrance to Rich Passage as predicted by CoastL (Hs=0.68m, T=2.87s, Dir=245deg). Also shows detail for location of Figure 5-6

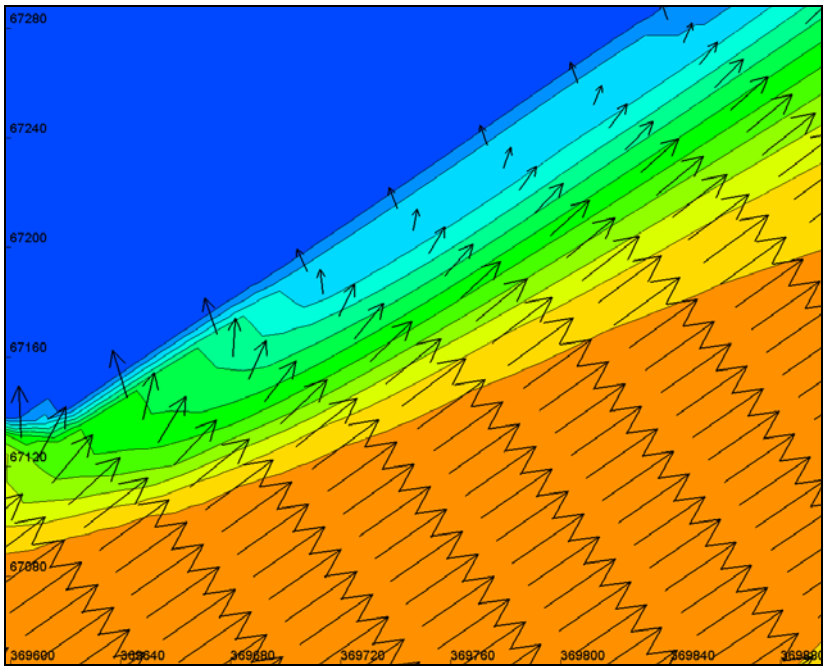

Figure 5-16. Detail of computed wave conditions at the shore near survey site 4 as predicted by CoastL

The results from both models illustrate that larger short waves, such as those used in this example, have a very oblique angle to the shore along this coast. This means that a large proportion of their power can be directed in a longshore direction, which will produce significant littoral transport.

5.4 Wake Generation and Propagation Model

The primary modeling task in this study is the acquisition of a computer model capable of predicting the generation of wakes from high-speed vessels and the transformation of those wakes by currents and bathymetry. This is an especially difficult task for two reasons. First, high-speed vessels often operate in a regime where the wakes they produce cannot exist as free gravity waves. Second, the area over which a solution is required (i.e., the entire length of Rich Passage and part of the neighboring Port Orchard and Sinclair Inlet) is very large. As is outlined in the following sections, no model was found to be available commercially and a new model had to be developed specifically to meet the needs of the current study.

5.4.1 Background

The term *super-critical* is sometimes used to describe high-speed vessels. This refers to the condition that the vessel is moving faster than a wave of the same length can travel in a given depth of water. In other words, the disturbances or wakes produced by such vessels cannot exist as free gravity waves in a classical Kelvin wake pattern.

These vessels may be planing, or not; the super-critical condition is determined by the speed of the vessel and the depth of the water, not on whether the vessel is traveling at sufficient speed to generate enough hydrodynamic lift to raise the vessel partly out of the water.

Displacement vessels produce a monochromatic wake profile, with the wavelength determined from the linkage between the speed of the vessel and the celerity of the wake for the given depth of water.

The differences between super-critical and sub-critical vessel wakes are illustrated in the following three plots. Each figure contains three plots; the upper plot shows the free surface elevation and the wake height determined from a zero-crossing analysis; the middle plot shows the wake period determined from a zero-crossing analysis, and; the lower plot shows the wake energy spectrum in the frequency domain. In Figure 5-17, a high-speed vessel is operating at its super-critical design speed. The wake period shows a smooth, steady decay. The wave energy spectrum shows a series of peaks or energy concentration at a number of frequencies. In Figure 5-18, the same vessel is sailing at a sub-critical speed. Although there are groups in the wave train, the wake period is constant. The wave energy spectrum is monochromatic.

Figure 5-19 shows the results of measurements of a car ferry, a displacement vessel. As with the previous sub-critical results, the wake period is almost constant and, accordingly, the energy is grouped around a single frequency. There is more energy in the low-period part of the spectrum in this case, because of the greater drawdown caused by the acceleration of the flow around the vessel's large hull.

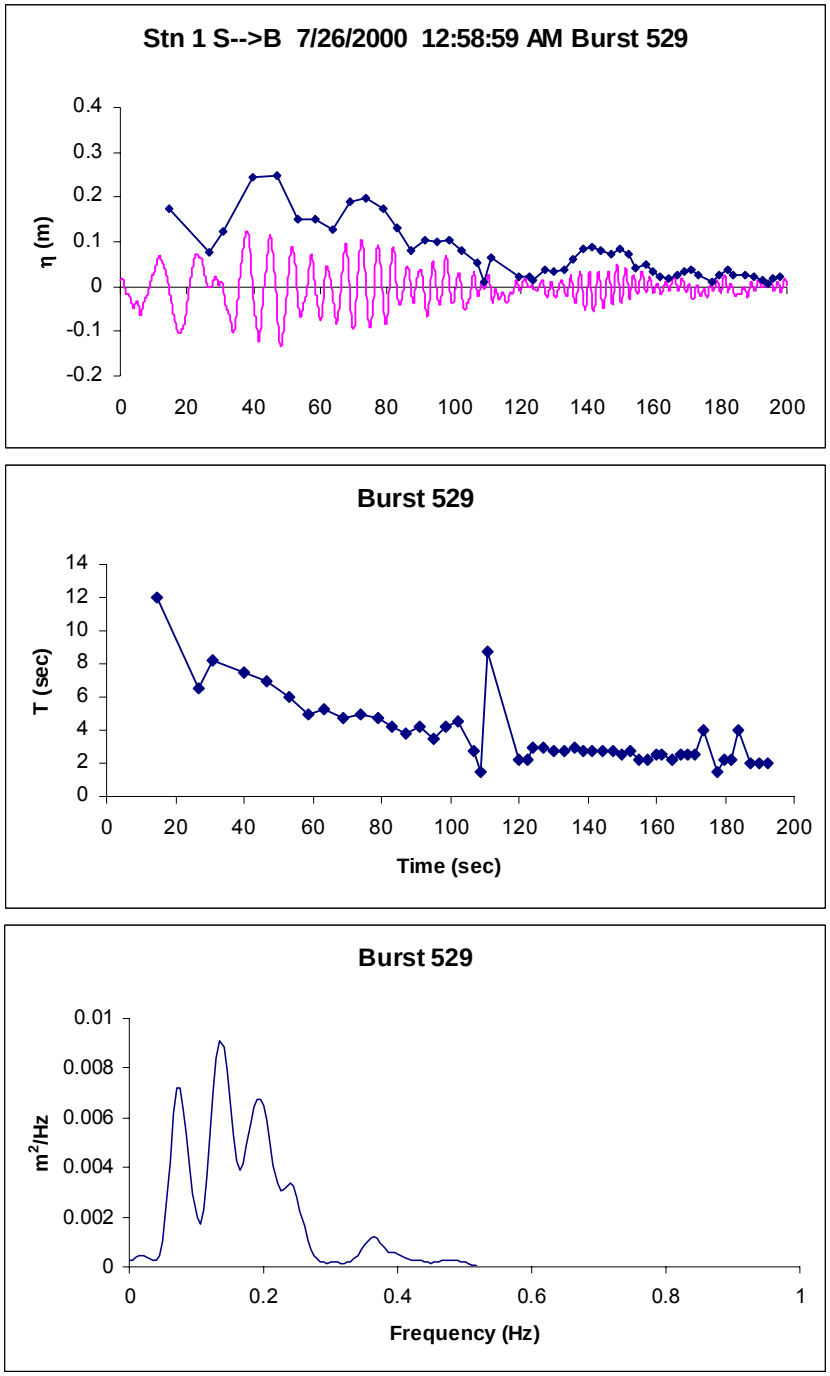

Figure 5-17. Typical results for high-speed vessel at super-critical speed (Top: surface elevation and wake height; Middle: wake period; Bottom: energy spectra)

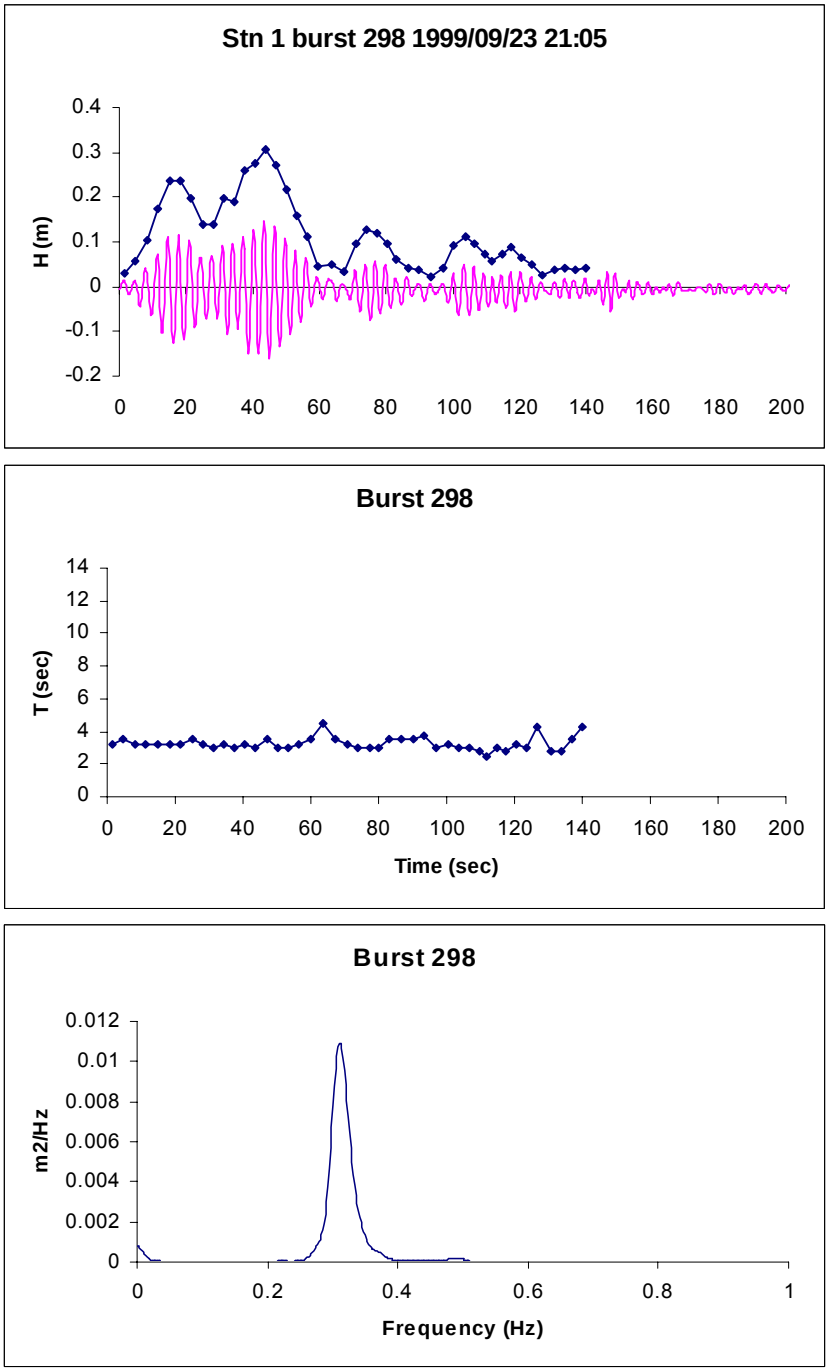

Figure 5-18. Typical results for a high-speed vessel at sub-critical speed (Top: surface elevation and wake height; Middle: wake period; Bottom: energy spectra)

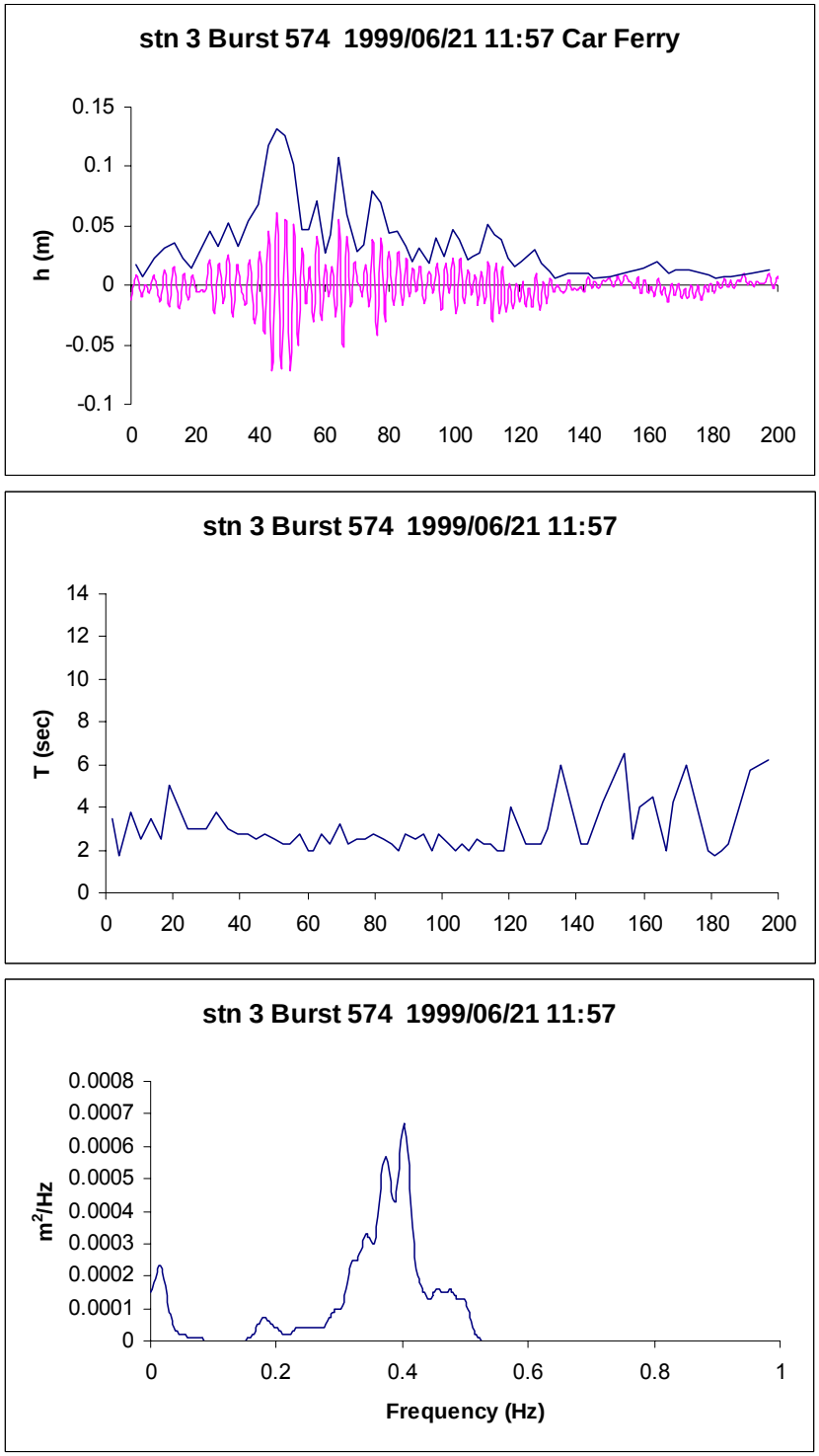

Figure 5-19. Typical results for displacement vessel (Top: surface elevation and wake height; Middle: wake period; Bottom: energy spectra)

Figure 5-20 shows an illustration of the theoretical wake pattern generated by a sub-critical vessel. The wake is composed of two types of waves, diverging wakes that move away from the vessel at an angle of 35.27° and transverse wakes that move in the vessel's direction. Both types of wakes theoretically exist only within a cone set at 19.47° from the vessel. This pattern, first described mathematically by Kelvin (1887), can be derived from simple geometry. The wavelength and speed, or *celerity*, of the wake can be found from simple linear wave theory. As the vessel's speed increases, so does the celerity of the wake. A point will be reached, however, where the vessel is moving faster than its transverse wake and this part of the wake is shed. From this point on (i.e. if the vessel maintains a speed equal to or greater than this speed and the depth remains the same or decreases) the wake pattern will assume a new form.

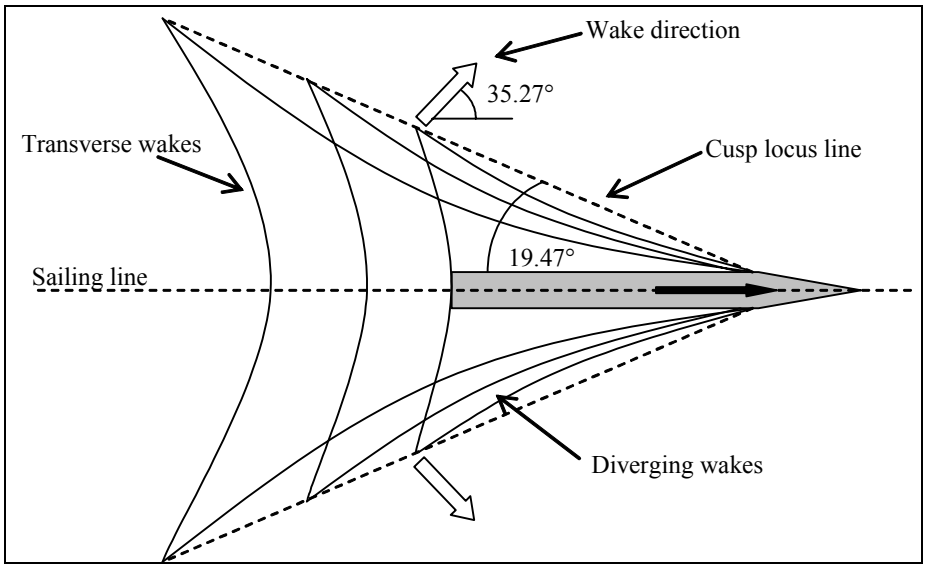

Figure 5-20. Wake pattern generated by a sub-critical vessel

The classical sub-critical and super-critical wake patterns are illustrated in Figure 5-21. The super-critical wake pattern is composed only of diverging wakes.

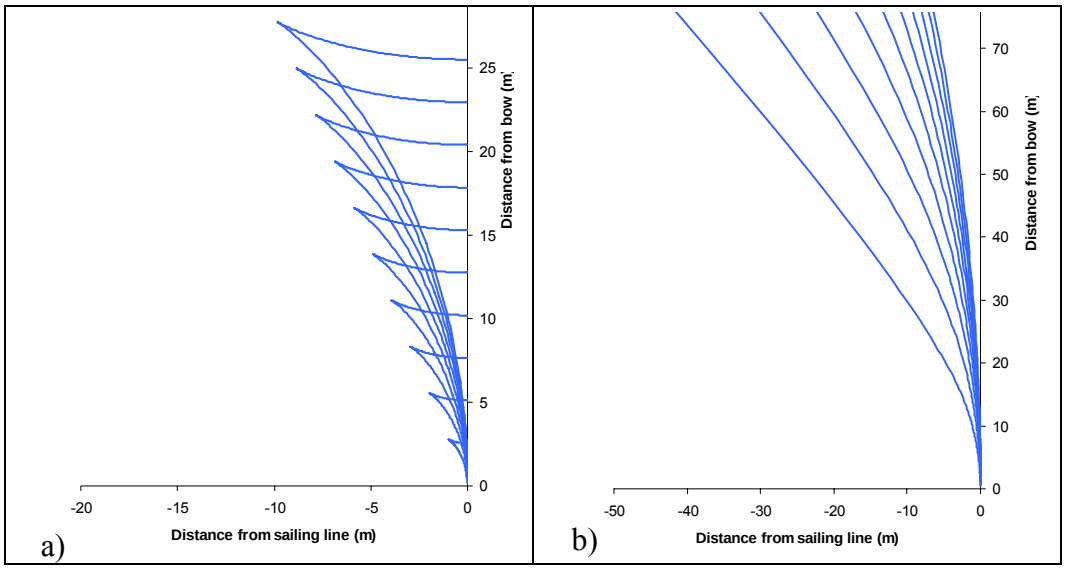

Figure 5-21. Wake pattern produced by: a) sub-critical vessel; b) super-critical vessel

The point at which the wake pattern changes from one form to another is governed by a dimensionless ratio known as the *depth Froude number*, F_d:

$$F_d = \frac{V}{\sqrt{gd}} \qquad \textbf{(1)}$$

where V is the speed of the vessel, d is the depth of water and g is gravitational acceleration. Once the value of F_d exceeds 1, the wake pattern will be super-critical in form. Note that passage through the point $F_d = 1$ can be achieved either by changes in speed or depth.

As will be discussed in detail later in this chapter, a study of the spectral characteristics of a super-critical vessel's wake will show concentrations of energy at certain frequency multiples, or *harmonics*. The frequency of these harmonics is also related to F_d.

The total amount of energy contained in a wake train is somewhat less than the total amount of energy transferred by the vessel to the water, since energy at very high and very low frequencies are not generally considered to be part of the wake. These differences are trivial and will not be considered in the present work. The amount of energy transferred by a vessel to its wake – basically, the size of the wake – is related to a number of factors including its hull shape and displacement. It is also related to another dimensionless ratio known as the *length Froude number*, F_L:

$$F_L = \frac{V}{\sqrt{gL_S}} \qquad \textbf{(2)}$$

where L_S is the length of the vessel. This is a useful quantity in describing the *hump*, the well-known phenomenon in which a vessel's power requirements and wake making capability are maximized at a certain speed. From both a fuel economy standpoint and an erosion minimization standpoint, vessel operation around this point is to be avoided. As mentioned above, the wavelength of the wake produced by a vessel increases with the vessel's speed. At some point, the length of the wake, L, will be twice as long as the vessel:

$$L = 2L_S$$

This is known as the "hump." It is illustrated in Figure 5-22.

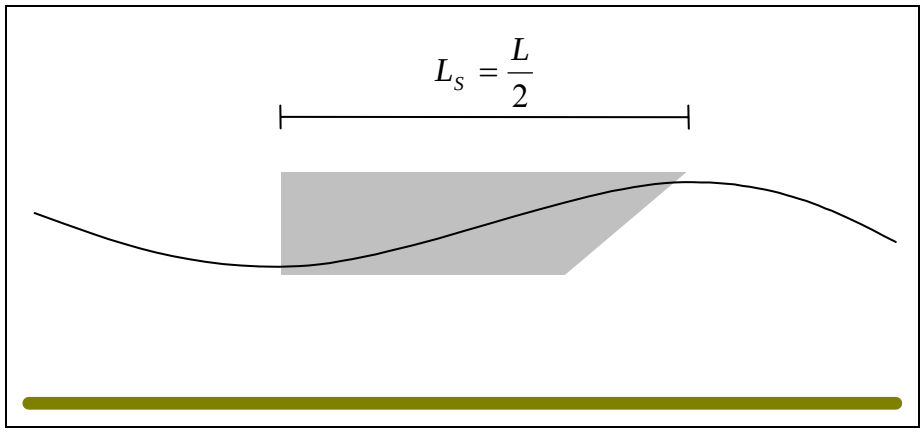

Figure 5-22. Illustration of the *hump*, the speed at which a vessel's wake is twice as long as the vessel itself

The wavelength can be found from:

$$L = \frac{gT^2}{2\pi} \tanh \frac{2\pi d}{L}$$

Substituting for the ship length yields:

$$L_S = \frac{gT^2}{4\pi} \tanh \frac{\pi d}{L_S}$$

The period of the wake, T, can be determined from the speed of the ship and the wavelength of the wake:

$$V = \frac{L}{T} \quad \therefore T = \frac{L}{V} = \frac{2L_S}{V}$$

Substituting this into the equation for the wavelength yields an equation for the speed at the hump:

$$L_S = \frac{g}{4\pi}\left(\frac{2L_S}{V}\right)^2 \tanh\frac{\pi d}{L_S} = \frac{gL_S{}^2}{\pi V^2}\tanh\frac{\pi d}{L_S}$$

$$1 = \frac{gL_S}{\pi V^2}\tanh\frac{\pi d}{L_S}$$

$$\therefore V = \sqrt{\frac{gL_S}{\pi}\tanh\frac{\pi d}{L_S}} \qquad \textbf{(3)}$$

The length Froude Number at the hump speed is thus:

$$F_L = \frac{V}{\sqrt{gL_S}} = \frac{\sqrt{\frac{gL_S}{\pi}\tanh\frac{\pi d}{L_S}}}{\sqrt{gL_S}}$$

$$\therefore F_L = \sqrt{\frac{1}{\pi}\tanh\frac{\pi d}{L_S}}$$

In deep water, the hyperbolic tangent term can be approximated as:

$$\tanh\frac{\pi d}{L_S} \approx 1$$

Therefore, in deep water the two equations become:

$$V = \sqrt{\frac{gL_S}{\pi}}$$

$$F_L = \sqrt{\frac{1}{\pi}}$$

In shallow water, the hyperbolic tangent term can be approximated as:

$$\tanh\frac{\pi d}{L_S} \approx \frac{\pi d}{L_S}$$

Therefore, in shallow water the two equations become:

$$V = \sqrt{gd}$$

$$F_L = \sqrt{\frac{d}{L_S}}$$

For most operations of a high-speed ferry, the speed will be well beyond the hump speed. The hump speed for a 20 m long vessel in Rich Passage (depth is approximately 30 m) is around 15 knots. However, if slow-down zones are imposed, the sailing speed may be near the hump speed and very large wakes may be produced.

5.4.2 Existing Models

A search of the models available to the study found that they fell into one of two groups, depending upon whether the models were limited in applicability because of their theoretical development or because of the computational effort that would be required for their use.

PI Engineering has developed the *Ship-Generated Hydrodynamics* model (*SGH*) to predict the two-dimensional nearshore hydrodynamic flows induced by the passage of large marine vessels and has applied it to numerous problems throughout North America. This model was specifically developed to solve practical problems (i.e., numerous simulations over large areas). The *SGH* model comprises two dynamically-coupled sub-models, one for wakes and one for drawdown currents. This approach is excellent for the study of large marine vessels, classified as displacement hulls, which sail at sub-critical speeds. The drawdown currents generated by high-speed vessels, however, are generally negligible when compared to the wake. As well, the wake of sub-critical vessels is monochromatic and use is made of this in the development of the *SGH* model's governing equations. The resulting phase-averaged equations are not applicable to super-critical vessels.

Sophisticated computational fluid dynamics (CFD) techniques have been developed in conjunction with the naval architecture community (e.g., Raven et al, 1998; Landrini et al., 1999; Henn et al., 2001). These models are not constructed from a ship design standpoint, but are focused on the wake some distance away from the vessel. In contrast to the Danish Hydraulics Institute (DHI) approach, in which the wake is externally imposed as an internal boundary condition, these models have the advantage of generating the wake directly from the solution of the governing equations and the standard kinematic boundary condition imposed at the vessel's hull. These models show great promise from the standpoint of accuracy of the solution in the immediate vicinity of the vessel; however, to reproduce the wake accurately, the hull shape must be very finely resolved. Examples presented generally involve simple analytical hull shapes (e.g., Wigley, 1934) rather than the complicated shapes now used in modern high-speed vessels. These techniques, while providing reasonably accurate predictions of ship wakes, have three additional limitations:

- they are limited to steady-state solutions;
- they are only applicable to areas of constant depth, and;
- they require extremely fine spatial resolution, which results in prohibitive computational requirements. In general, even with very high-powered computers these techniques are limited to within 3 to 5 wavelengths of the vessel (Kofoed-Hansen et al., 1999).

Because of the large area that needs to be modeled and the large number of simulations required, models of this type are not applicable to the present study.

There is another family of methods available for the modeling of ship wakes. Fully non-linear Boussinesq ship wake models (e.g., *Wake2d* from the Canadian Hydraulics Centre) can be used to simulate vessel wake that are not monochromatic This model has been applied to some practical problems (e.g., Davies and Watson, 1999), but it was found that the study areas were generally too large to run such a complex model; 3 minutes of ship passage, in which the wake only propagated one-half of the distance from the sailing line to the shore, required over 24 hours of computer time.

The DHI has also published a Boussinesq-based ship wake model (Kofoed-Hansen and Mikkelsen, 1997); however, the computational effort was found to be huge for large domains, which led DHI to investigate other techniques (Kofoed-Hansen et al, 1999). DHI has modified its Mike 21 Nearshore Spectral Wave (*Mike 21 NSW*) model to permit the modeling of ship wakes over large areas (Kofoed-Hansen et al., 1999). This type of model is formulated from a phase-averaged energy conservation approach. This technique has the advantage of being applicable to very large areas and modeling the transfer of energy between frequencies. This latter capability would seem to be of some advantage in ship wake modeling, since the wake period is known to change as the wake propagates away from the sailing line (Kofoed-Hansen and Mikkelsen, 1997). In practice, however, Kofoed-Hansen et al., (1999) deemed this effect to be negligible and simulated the wake as a monochromatic wave field. A major limitation of the DHI approach is that the NSW model cannot reproduce dispersion, which is the cause of the decay in wake height as the wake travels away from the vessel. The DHI approach requires the specification of a single decay rate that is used to “factor down” the predicted wave heights. The model is also steady-state in form, with the wake input given as a straight line source of energy offshore. It is unclear how the model could be adapted to accommodate more realistic ferry services that include irregular routes and changes in vessel speed.

5.4.3 Proposed Approach

Although the various approaches described in the previous section all have advantages and disadvantages, none is suitable for direct application in the present study. Therefore, a new model was developed that borrowed from the above approaches. Because of the large areas to be modeled and the numerous simulations required, the final approach selected is most similar in theory to that of the *Mike 21 NSW*, although the solution approach and model capabilities differ greatly.

The new model requires the following capabilities:

- Generation of sub- and super-critical wakes
- Variable vessel routing and speed
- Wake transformation, including the effects of:
  - current refraction
  - depth refraction
  - shoaling
  - breaking
  - dispersion
- Efficient solution for large areas and numerous simulations

After careful consideration of the above list, it was decided to develop a kinematic and dynamic wake conservation model using a *Lagrangian* formulation. In this type of model, the solution is cast in terms of individual packets of wave energy transferred from the moving vessel to the flow. The model then tracks the wake energy parcels as they propagate across the domain, as opposed to determining the wake at fixed locations in space and time, which is the case in more traditional *Eulerian* model formulations. Mathematically, the *Lagrangian* approach allows partial differentials to be re-cast as ordinary differentials. The model developed was named the *Lagrangian Super-critical Vessel* model (LSV).

The LSV model is similar to a nearshore wave model in many ways, since away from the vessel, the wakes should behave as free gravity waves. The model allows the prediction of wake height, period and direction spatially as a function of time. There are many advantages to this type of formulation, most notably the ability to simply model a wake with energy across a range of frequencies in a simple and efficient manner. The following sections describe development of the LSV model.

5.4.4 Governing Equations

The LSV model was developed to enable the numerical simulation in two horizontal dimensions of the generation and transformation of a wake field produced by a super-critical vessel in the nearshore environment. The model is based on the conservation of wave energy and the kinematic conservation principle for small amplitude waves. The theory has been extended to include interaction with depth-averaged currents. A series of wave-period and depth-averaging techniques have been used in the derivation of the governing equations. The model is formulated using a Lagrangian framework. The resulting system demands solution of five equations: one for the wake energy, E, two for the x and y wave number vectors, P and Q, and two for the x and y coordinates of the wake energy packet.

5.4.4.1 Wake energy conservation equation

The equation for wake energy is derived from the energy conservation equation for small-amplitude, linear, monochromatic waves in a moving medium (Phillips, 1977):

$$\frac{\partial E}{\partial t} + \frac{\partial}{\partial x_i}\left(E\,U_i + F_i\right) + S_{ij}\,\frac{\partial U_j}{\partial x_i} = D \qquad \textbf{(4)}$$

where E is the total wave energy, F_i is the wave flux vector $\{i = 1,2\}$, S_{ij} is the radiation stress tensor $\{i = 1,2\,;\, j = 1,2\}$, D is the energy dissipation rate, t is time, x_i is the horizontal coordinate vector $\{i = 1,2\}$, and U_i is the depth-average current velocity ($i = 1,2$). The subscripts are the tensor notation for the orthogonal coordinates. Note that the tidal velocities are computed using the ADCIRC model separately.

Noting that the wave flux vector can be expressed as:

$$F_i = c_{g\,i}E$$

Equation **(4)** can be re-written as:

$$\frac{\partial E}{\partial t} + \left(U_i + c_{g\,i}\right)\frac{\partial E}{\partial x_i} + E\,\frac{\partial}{\partial x_i}\left(U_i + c_{g\,i}\right) + S_{ij}\,\frac{\partial U_j}{\partial x_i} = D \qquad \textbf{(5)}$$

A Lagrangian framework requires that the equations be formulated in terms of ordinary differential for the dependent variables. Converting Equation (5) yields:

$$\frac{dE}{dt} + E\,\frac{\partial}{\partial x_i}\left(U_i + c_{g\,i}\right) + S_{ij}\,\frac{\partial U_j}{\partial x_i} = D \qquad \textbf{(6)}$$

This can be written in standard notation as:

$$\begin{aligned}\frac{dE}{dt} &+ E\left(\frac{\partial U}{\partial x} + \frac{\partial V}{\partial y}\right) + E\left(\frac{\partial R_x}{\partial x} + \frac{\partial R_y}{\partial y}\right)\\ &+ S_{xx}\,\frac{\partial U}{\partial x} + S_{xy}\left(\frac{\partial V}{\partial x} + \frac{\partial U}{\partial y}\right) + S_{yy}\,\frac{\partial V}{\partial y} = D\end{aligned} \qquad \textbf{(7)}$$

where:

$$\begin{aligned}R_x &= Pc_g\\ R_y &= Qc_g\end{aligned} \qquad \textbf{(8)}$$

where P and Q are the orthogonal x and y wave number vectors.

Equation (7**)** is solved by numerically integrating over the limits $t_0 \rightarrow t_1$ to obtain the wake energy at time $t + \Delta t$, i.e.:

$$\int_{t_0}^{t_1} \left(\frac{dE}{dt} + E\left(\frac{\partial U}{\partial x} + \frac{\partial V}{\partial y} \right) + E\left(\frac{\partial R_x}{\partial x} + \frac{\partial R_y}{\partial y} \right) + S_{xx}\frac{\partial U}{\partial x} + S_{xy}\left(\frac{\partial V}{\partial x} + \frac{\partial U}{\partial y} \right) + S_{yy}\frac{\partial V}{\partial y} - D \right) dt = 0 \qquad \textbf{(9)}$$

5.3.4.3 Wake number conservation equations

The wave number vectors for the wake field are determined from the *kinematic conservation principle* (Phillips, 1977):

$$\frac{\partial K_i}{\partial t} + \frac{\partial \omega}{\partial x_i} = 0 \qquad \textbf{(10)}$$

where K_i is the wave number vector $\{ i = 1, 2 \}$, ω is the apparent wave frequency. To include the effects of currents, it is assumed that the waves are propagating on a medium moving with velocity U_i. The apparent frequency is then given by the Doppler equation:

$$\omega = \sigma + K_i U_i \qquad \textbf{(11)}$$

where σ is the intrinsic wave frequency. Assuming small amplitude wave theory the intrinsic wave frequency is described by the linear dispersion equation:

$$\sigma^2 = gk \tanh kd \qquad \textbf{(12)}$$

where k is the wave separation factor, d is the depth and g is gravitational acceleration. Equation (10) can be transformed into its final form by applying the condition of zero vorticity of the wave number vectors:

$$\frac{\partial K_i}{\partial x_j} = \frac{\partial K_j}{\partial x_i} \qquad \textbf{(13)}$$

and by noting that the wave group velocity, c_g, can be described by:

$$c_{g\,j} = \frac{c_g}{k} K_j \qquad \textbf{(14)}$$

Substitution of Eqs. (11), (12), (13) and (14) into Eq. (10) yields:

$$\frac{\partial K_i}{\partial t} + \left(\frac{c_g}{k} K_j + U_j \right) \frac{\partial K_j}{\partial x_i} + \frac{\sigma G}{2d} \frac{\partial d}{\partial x_i} + K_j \frac{\partial U_j}{\partial x_i} = 0 \qquad \textbf{(15)}$$

where:

$$G = \frac{2kd}{\sinh 2kd} \qquad \textbf{(16)}$$

This can then be written in Lagrangian form as:

$$\frac{dK_i}{dt} + \frac{\sigma G}{2d}\frac{\partial d}{\partial x_i} + K_j \frac{\partial U_j}{\partial x_i} = 0 \qquad \textbf{(17)}$$

The vector equation, Eq. (17), can be written in the form of two standard Cartesian equations as:

$$\frac{dP}{dt} + \frac{\sigma G}{2d}\frac{\partial d}{\partial x} + P\frac{\partial U}{\partial x} + Q\frac{\partial V}{\partial x} = 0 \qquad \textbf{(18)}$$

$$\frac{dQ}{dt} + \frac{\sigma G}{2d}\frac{\partial d}{\partial y} + P\frac{\partial U}{\partial y} + Q\frac{\partial V}{\partial y} = 0 \qquad \textbf{(19)}$$

where P and Q are the orthogonal x and y wave number vectors formerly represented by K_i $\{i = 1, 2\}$. Equations (18) and (19) are the final form of the wake number vector equations.

Equations (18) and (19) are solved in a similar fashion to the wake energy equation, by integration over the limits $t_0 \rightarrow t_1$:

$$\int_{t_0}^{t_1}\left(\frac{dP}{dt} + \frac{\sigma G}{2d}\frac{\partial d}{\partial x} + P\frac{\partial U}{\partial x} + Q\frac{\partial V}{\partial x}\right)dt = 0 \qquad \textbf{(20)}$$

$$\int_{t_0}^{t_1}\left(\frac{dQ}{dt} + \frac{\sigma G}{2d}\frac{\partial d}{\partial y} + P\frac{\partial U}{\partial y} + Q\frac{\partial V}{\partial y}\right)dt = 0 \qquad \textbf{(21)}$$

5.3.4.4 Characteristics equation

The paths of the wake energy packets are determined from the characteristics equations, which were used (implicitly) in the conversion from partial to ordinary differentials in the above derivations:

$$\frac{dx}{dt} = c_g \frac{P}{k} + U \qquad \textbf{(22)}$$

$$\frac{dy}{dt} = c_g \frac{Q}{k} + V \qquad \textbf{(23)}$$

Equations (22) and (19) are solved numerically in a similar fashion to the wake energy equation by integration over the limits $t_0 \rightarrow t_1$:

$$\int_{t_0}^{t_1}\left[\frac{dx}{dt} - \left(c_g \frac{P}{k} + U\right)\right]dt = 0 \qquad \textbf{(24)}$$

$$\int_{t_0}^{t_1}\left[\frac{dy}{dt}-\left(c_g\frac{Q}{k}+V\right)\right]dt=0 \qquad \textbf{(25)}$$

5.3.5 Initial Kinematic Boundary Conditions

Equations (6), (17), (18), (21), and (22) developed in the previous section form the governing system of the LSV model and can be used to predict wake behavior within the domain of interest (i.e., once the wakes are away from the vessel and prior to breaking). Boundary conditions must be supplied to generate the wakes at the vessel and to control wake heights at the shore through breaking. A major effort in the development of the LSV model was formulating a methodology to determine the initial conditions for super-critical wakes. This includes both the wake pattern and the energy contained at the various frequencies within the wake.

As a vessel moves faster and its wake gets longer, the pattern begins to evolve as shown in Figure 5-23. This phenomenon can be described using the depth Froude number, F_d. The deepwater wake pattern for sub-critical vessels ($F_d << 1$) was first described by Kelvin (1887). As the value of F_d becomes finite and approaches 1, the leading edge of the diverging wake will begin to approach an angle normal to the vessel direction, i.e. the transverse wake direction (see Figure 5-23).

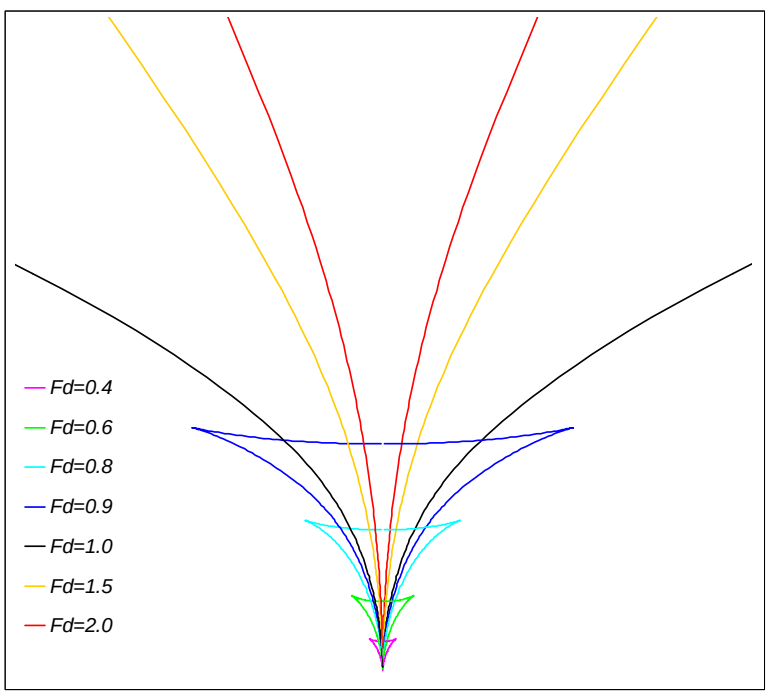

Figure 5-23. Evolution of the wake pattern of a vessel with depth Froude number

An approximate equation to describe this angle as a function of F_d was presented by Weggel and Sorensen (1986):

$$\alpha = 35.27\left[1 - e^{12(F_d - 1)}\right] \quad \textbf{(26)}$$

where α is the diverging wake direction from the sailing line in degrees. The resulting angle only varies rapidly as the F_d approaches unity. As can be seen from Figure 5-23, the angle of the wake also varies rapidly when F_d is greater than unity, although it decreases beyond this point. The situation in this case is more complicated, however, since the frequency of the wake field varies spatially.

A technique for super-critical wake angles has been developed from the approach of Yih and Zhu (1989). Their model is based on three assumptions:

- Phase lines are stationary
- Phase lines are normal to the wave vectors
- Local phase velocity is equal to the component of the velocity of the disturbance normal to the phase line

The three assumptions, cast in equations, form the governing system of equations. The only additional piece of information required is the dispersion equation. By introducing a moving pressure disturbance (the vessel) into the problem, a solution can be obtained for the wake pattern. It should be noted that the solution is equally applicable to sub-critical and super-critical waves.

If the wake is sub-critical, the pattern derived will contain diverging wakes as well as transverse wakes. An example of this is shown in Figure 5-24. If a super-critical wake is modeled, the resulting pattern will only contain diverging wakes. Two illustrations are given in Figures 5-25 and 5-26. Note that as the depth Froude number increase (e.g., an increase in vessel speed for a given depth of water), the wake pattern becomes sleeker.

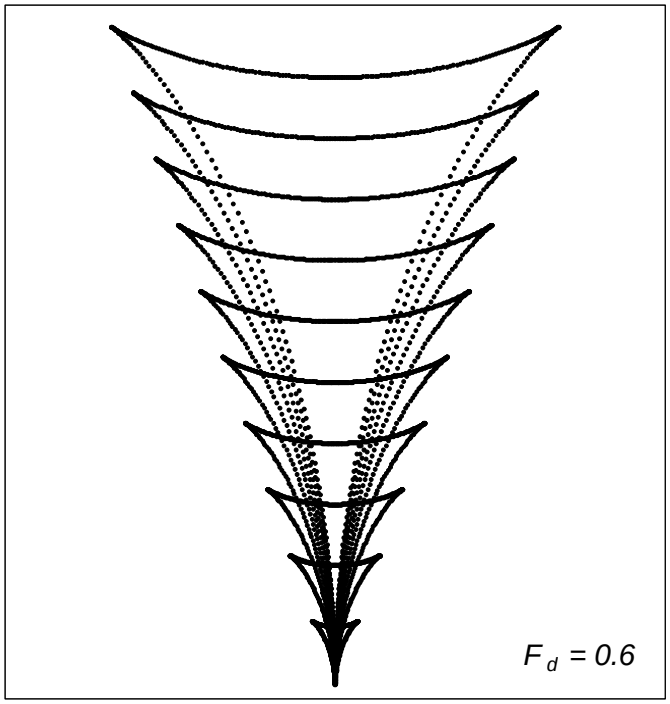

Figure 5-24. Theoretical wake pattern predicted by a sub-critical vessel (F_d =0.6)

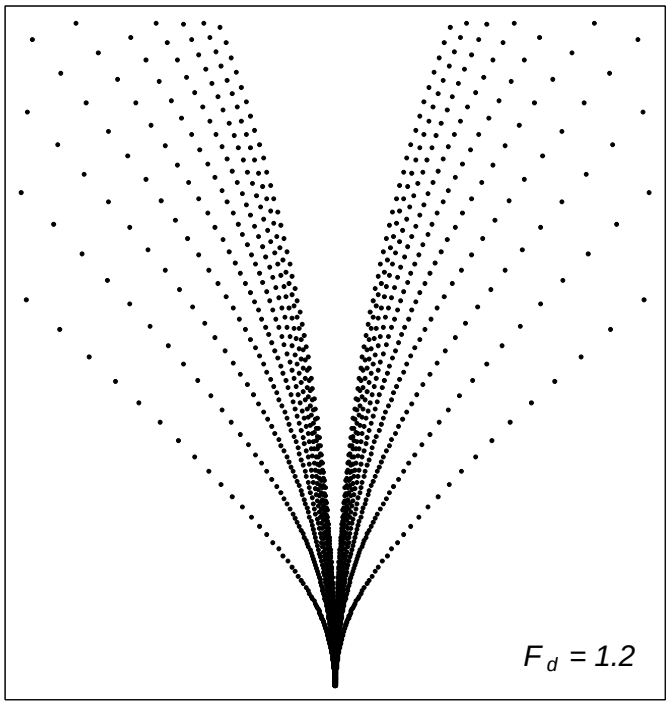

Figure 5-25. Theoretical wake pattern predicted by a super-critical vessel (F_d =1.2)

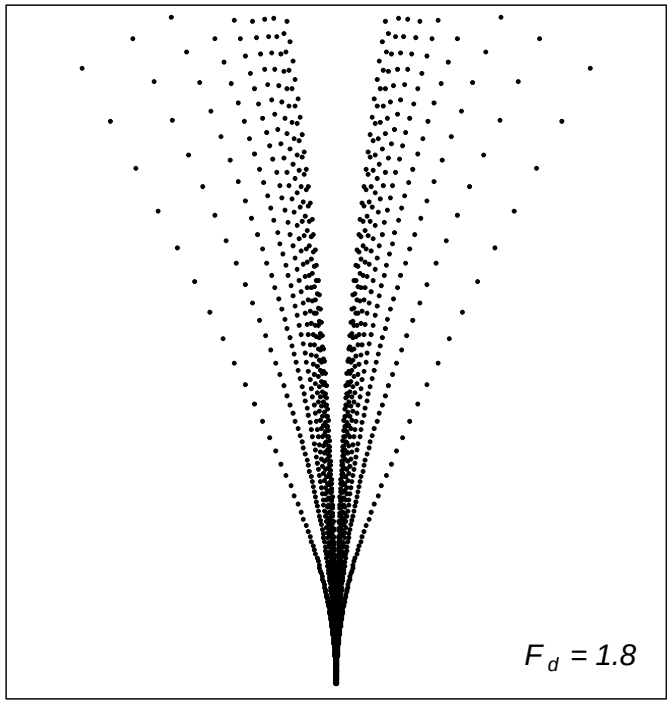

Figure 5-26. Theoretical wake pattern predicted by a super-critical vessel (F_d =1.8)

The wake pattern theory of Yih and Zhu as presented above has two limitations. First, the theory only gives information about the kinematics of the wake field, since the vessel is introduced into the system as an infinitesimal point source without information such as hull shape, etc. The energy (or height) of the wakes must be obtained by other means. This should not be too cumbersome, since ample field data exist to provide this information. Second, the theory is developed with x and y as dependent variables; once a phase and wave number are chosen, the theory will yield the location at which they occur. The theory Could be used directly if it were re-cast with x and y as the independent variables, but this is not a simple exercise, since there are five equations to solve, one of which is transcendental.

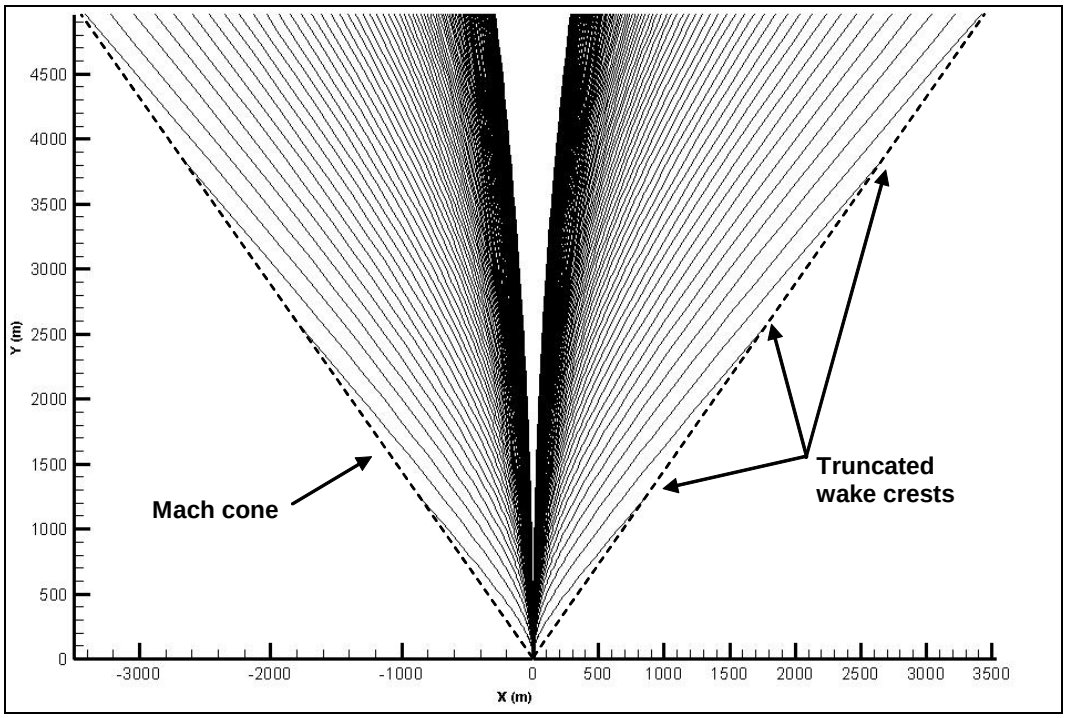

Figure 5-27. Wake crest pattern with Mach cone restriction imposed

A solution was developed to assist in its implementation in the numerical model. At this point, it is important to realize how the wake period and wavelength vary in space. This is illustrated in Figure 5-28. The wake period (and corresponding length) is greatest along the leading edge of the wake and decreases toward the vessel track line.

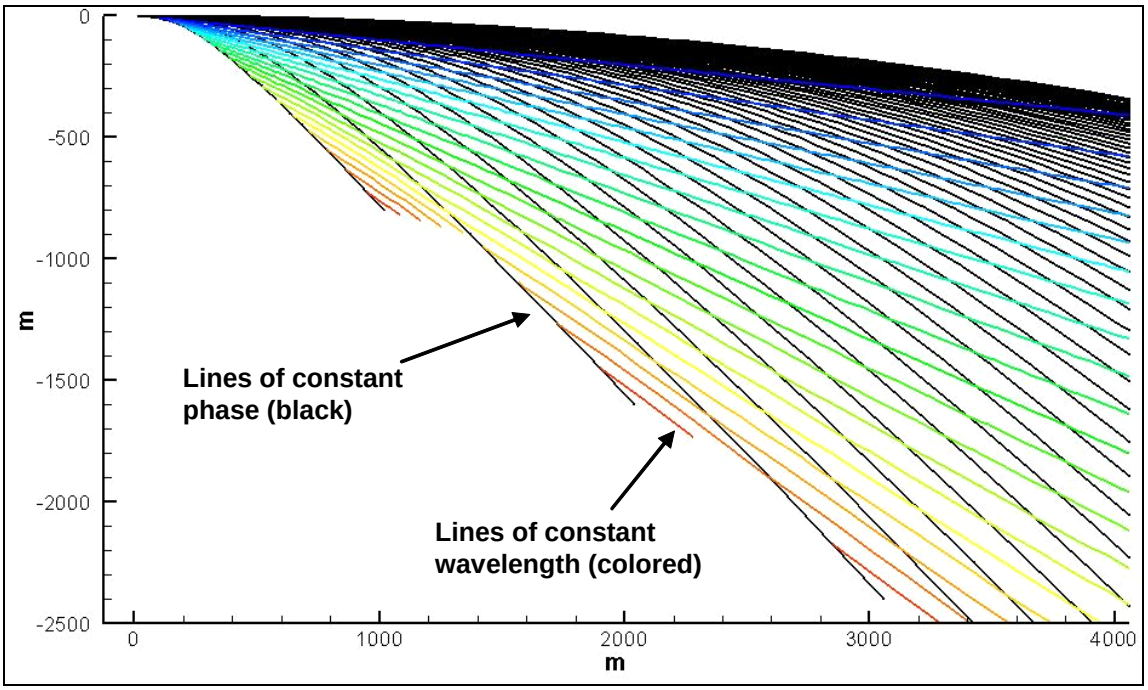

Figure 5-28. Illustration showing phase and wavelength isolines for a typical super-critical wake pattern

5.4.5 Breaking Boundary Conditions

The wake heights are limited in the LSV using the simple breaking criterion:

$$H \leq 0.78d \qquad \textbf{(27)}$$

This method may be replaced at a later date, if warranted.

5.4.6 Initial Dynamic Boundary Conditions

The LSV model requires a description of the energy that is transferred by the vessel to the flow in the wake. As was the case with the wake pattern, this also formed a major component of the development of the LSV model. However, unlike the wake patterns, which relied on a purely theoretical foundation, the energy transfer was based almost exclusively on analysis of measured wake profiles from field trials, since energy transfer is so strongly related to hull shape, vessel trim, etc., and is therefore beyond any theoretical method available at present.

Figure 5-29 shows examples of measured wake energy spectra from trials of the high-speed ferry *Snohomish*. The total wake energy in a test is the integral of the curve. The three tests with similar length Froude number, F_L, values show a similar total wake energy. The one test with a lower value of F_L has higher total wake energy. This is not surprising, since this test was conducted at a length Froude number closer to the hump value.

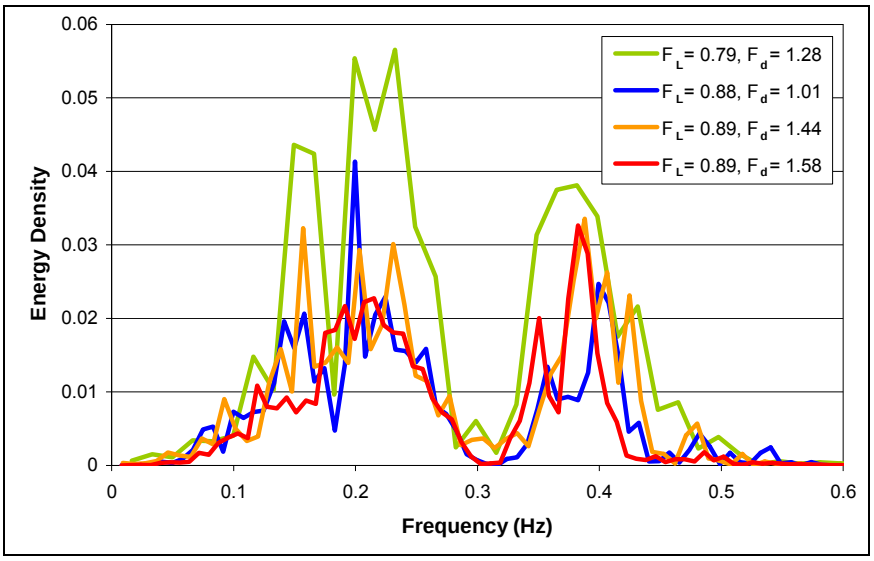

Figure 5-29. Measured wake energy spectra from Snohomish trials

What is surprising is that all four curves in Figure 5-29 show concentrations of energy at the same frequencies. Closer inspection will show that the energy is concentrated around harmonics of a primary frequency of 0.076 Hz (Figure 5-30). This frequency is the theoretical minimum frequency ($f_M = T_M^{-1}$) of the two tests with the higher values of F_d . The theoretical frequency of the test at F_d =1.28 is close, however the technique is inaccurate for values close to 1 (e.g., F_d =1.01).

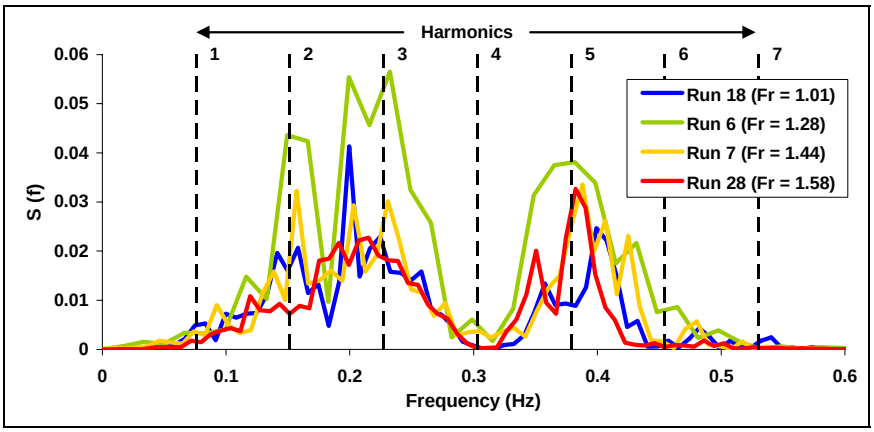

Figure 5-30. Measured wake energy spectra from trials of the *Snohomish* and frequency harmonic frequencies

The following conclusions can be drawn from an inspection of Figure 5-30:

- energy is concentrated around the 2nd, 3rd and 5th harmonics; there is an identifiable absence of energy near the 4th harmonic, and;
- there is little energy leakage below the 1st, or primary, harmonic – perhaps because the 1st harmonic is the limiting minimum frequency

This pattern can be observed in the wake energy spectra from many high-speed vessels. At this point, however, it is unclear whether the harmonics are frequencies that are multiples of the theoretical minimum frequency or some other value related to the vessel.

Regardless of the origin of the primary harmonic frequency, the observation that the energy is concentrated around certain harmonic frequencies (2nd, 3rd and 5th in this example) was used to develop the methodology for input in the LSV model. A vessel's wake energy profile with frequency can be built up from the summation of a series of five independent energy spectra. A Gaussian distribution was selected as the basic shape of these spectra – this distribution is the theoretical solution for energy diffusion with time and/or distance.

The form of the Gaussian distribution is:

$$s(T) = \frac{\varepsilon}{\sqrt{2\pi\sigma^2}} \exp\left[\frac{-1}{2\sigma^2}(T-\mu)^2\right] \qquad \textbf{(28)}$$

where ε is the amplitude of the energy component, σ is the standard deviation of the energy component, μ is the mean period of the energy component. Note that for computational reasons the distribution is constructed in terms of period rather than frequency. The full wake energy spectrum equation (five components) is:

$$S(T) = \sum_{i=1}^{5} \frac{\varepsilon_i}{\sqrt{2\pi\sigma_i^{\,2}}} \exp\left[\frac{-1}{2\sigma_i^{\,2}}(T-\mu_i)^2\right] \qquad \textbf{(29)}$$

An example of the application of Eq. (29) is shown in Figure 5-31. Note that the 4th harmonic is not used (i.e. $\varepsilon_4 = 0$). The distributions appear to be distorted because they are plotted in the frequency domain.

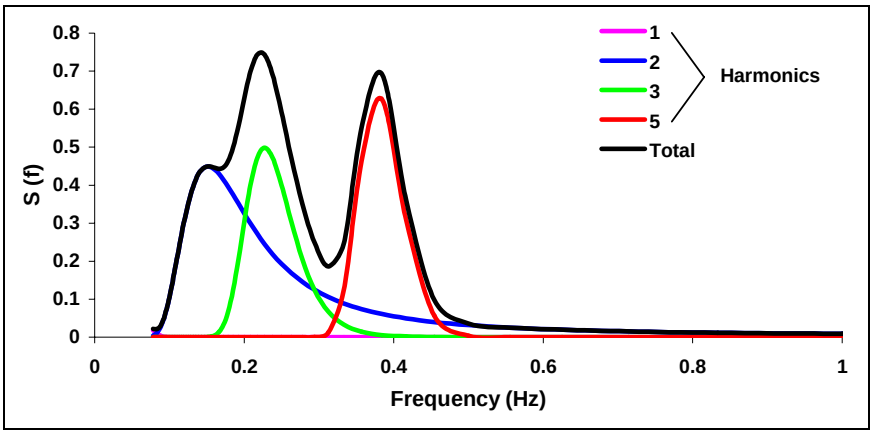

Figure 5-31. Example of a wake spectra composed using a series of Gaussian distributions

The values of coefficients used to simulate a vessel must be obtained by calibration with measured data.

5.4.7 Wake Model Operation

The following sections describe the input and output data required to operate the model, as well as provide illustrations of the form of the model output.

5.4.7.1 Wake model input files

The required input to the wake model is:

- A bathymetry mesh that contains a description of the domain in terms of boundaries and depths
- A route file that contains the (x, y, V) coordinates of the vessel in time
- A vessel file that gives the values of the coefficients for the wake boundary conditions of the vessel
- A trap file that is used to define a region within which wake energy parcel information is collected
- A set of ADCIRC flow files (elevation and currents) for surface elevation and background currents (optional)

5.4.7.2 Wake model output files

The output produced by the wake model is:

- A vessel path file that gives the path of the vessel used by the model
- A wake file that gives the position of the wake energy parcels with time and a set of user-selected attributes

- A trap output file that lists the wake energy parcels collected in the trap
- A breaking file that gives the location and characteristics of each wake energy parcel at breaking.

5.4.7.3 Example wake model output

Since the LSV model is Lagrangian in structure, the model output is based on the individual wake energy parcels. An illustration is shown in Figure 5-32. The wake parcels (here colored according to wake height), have been released at regular intervals at the location that the vessel was at that time. As the vessel progresses, additional parcels are released. The parcels are moving on paths that have an initial orientation dependent upon their frequency. The paths may vary since the parcels propagate according to the bathymetry, currents, etc. that are encountered.

It should be remembered that the parcels represent the total energy (related to wake height) of a certain frequency at a location at specific points in time. They do not represent wake crests and troughs.

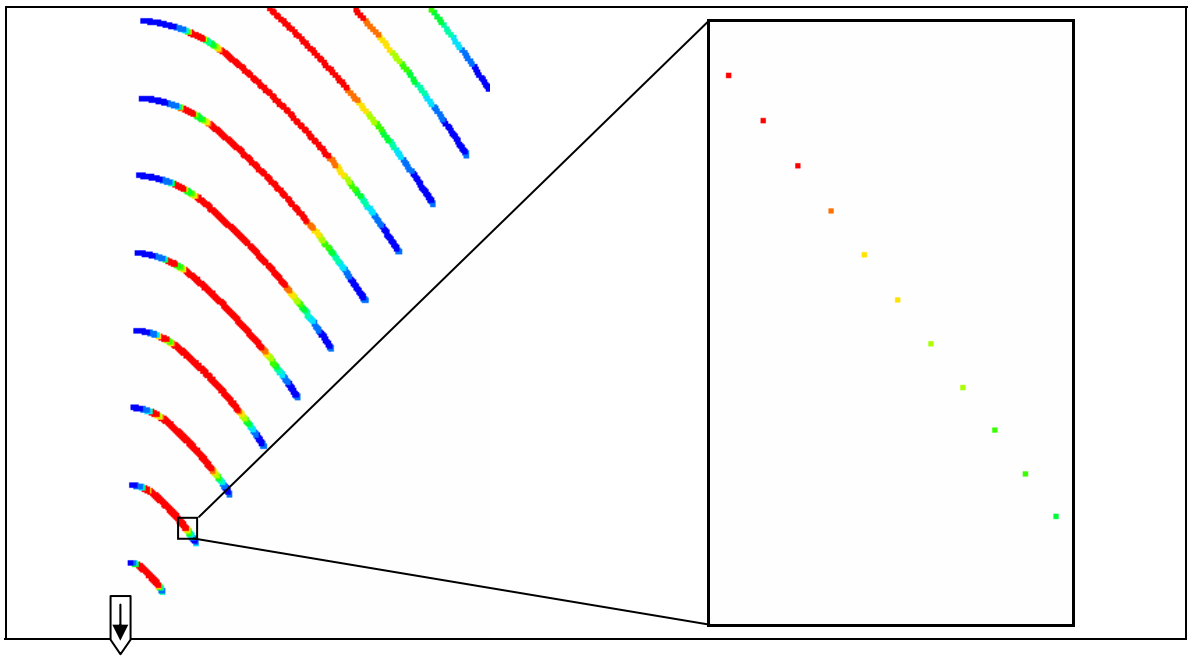

Figure 5-32. Example of wake model parcel output

The example shown in Figure 5-32 is for a case with a very large time between each release. A similar output, but for a much higher frequency of parcel release is shown in Figure 5-33.

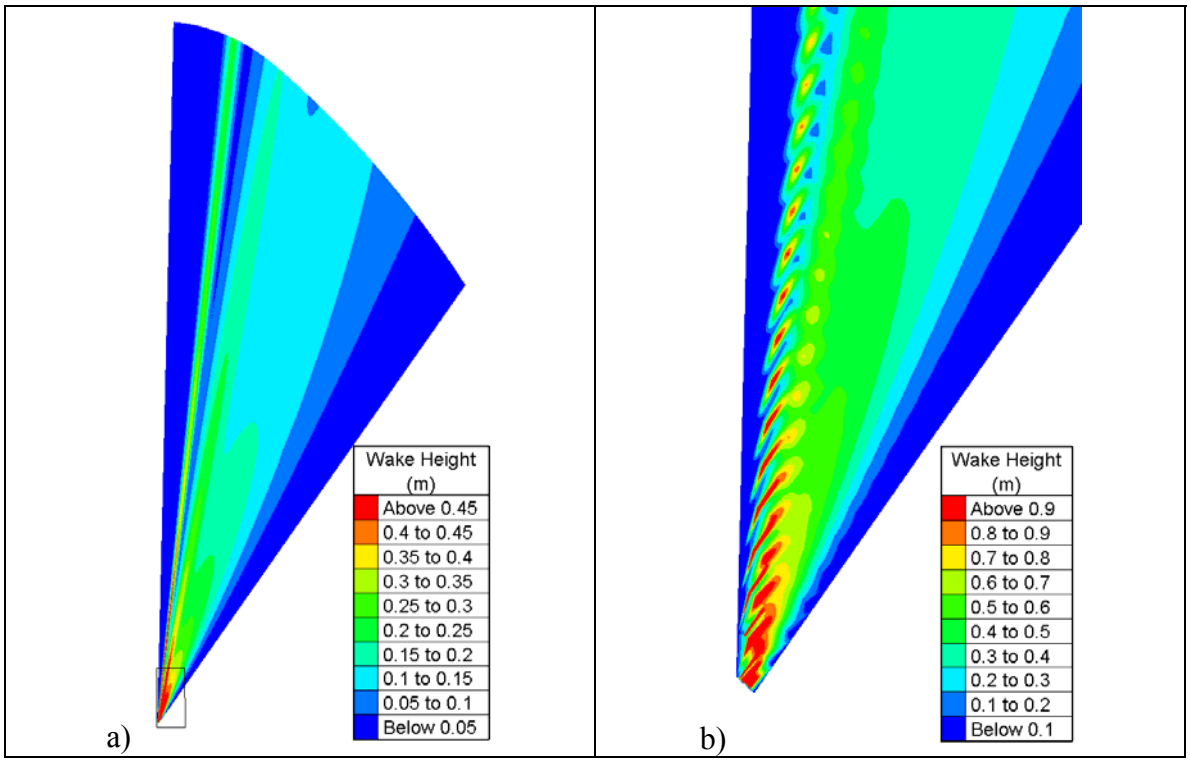

Figure 5-33. LSV model simulation of wake pattern from Chinook: (a) full domain – shows detail window, b) detail around vessel)

5.4.8 Wake Model Validation

The wake model was validated against a number of data sets including deepwater measurements of *Chinook/Snohomish* and *Condor Express* collected and made available to the project by Fox and Associates, and measurements in Rich Passage collected by PI Engineering as described in Section 3.

Validation of the model requires two stages. First, the model must be compared against one or more tests for each vessel in order to determine the coefficients of the wake energy spectrum equation. Second, the calibrated model should be compared to the remaining tests to assess the accuracy of the model.

The results in the following sections will be presented in several forms. These include spatial plots of wake height and period at fixed points in time, and time and frequency series plots of various model output quantities at fixed points in space.

5.4.8.1 Validation with Chinook/Snohomish *deepwater tests*

These tests were conducted by WSF in 2000 and are described in Section 3. WSF and Fox and Associates adjusted these data to a distance of 300 m for their analysis. However, this report only uses the original data, as opposed to the adjusted data for validation.

Four tests were selected for comparison to represent the full range of F_d in the test schedule. These specific tests were chosen because they were long enough to cover the full wake train. The details of tests are shown in Table 5-4.

Table 5-4. *Chinook/Snohomish* Test Cases for LSV Validation

Name	Vessel Speed[2] (knots)	Depth (m)	F_d	F_L
Run_18	35.5	33.3	1.01	0.88
Run_6	31.9	16.8	1.28	0.79
Run_7	35.8	16.8	1.44	0.89
Run_28	36.0	14.0	1.58	0.89

Time series of the results of the four validation tests are shown in Figures 5-34 through 5-37. Each plot shows the surface elevation synthesized from the pressure record and the wake height and period, both determined from a zero up-crossing method. In each case, the wake pattern appears to contain two energy groups, a leading group with wakes that range from 8 sec down to 4 sec, and a trailing group with wakes in the range from 3 sec down to 2 sec. Note also that the wave period decays in a smooth, steady fashion. This is in contrast to the typical wake pattern generated by a sub-critical vessel, such as the car ferry shown earlier in Figure 5-36.

Also shown in Figures 5-24 through 5-37, are the predictions of the *LSV* model for wake height and wake period. In each case, the predicted solution has been synchronized with the measured solution by minimizing the error in the wake period. The predicted wake height time history matches the measured for three of the four tests; only in Test 28, which has the largest depth Froude number, is the correlation not good. It is unclear why this is the case. Figure 5-38 shows the computed value for the same test, but using a different synchronization. This suggests that the error could be associated with the long-period wave energy; while this could be an error in dispersion, it is more likely to be a result of an incorrect initial direction used for this part of the spectrum.

[2] These speeds are the average speeds for a series of runs.

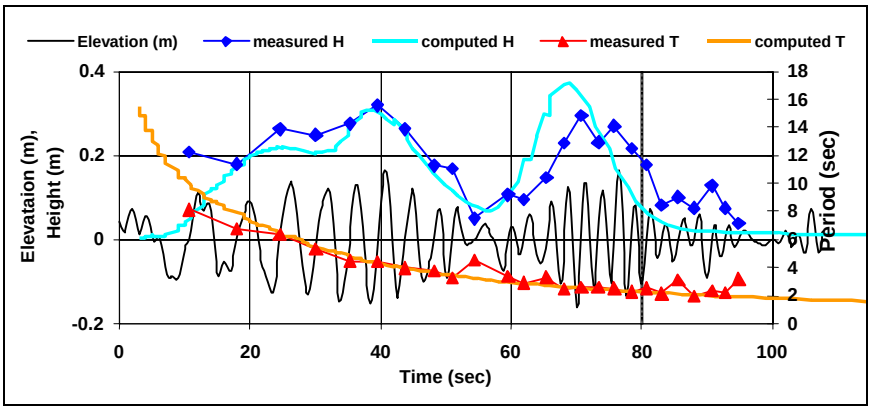

Figure 5-34. ***Snohomish*** **Test 18 (** F_d **=1.01,** F_L **=0.88 – surface elevation, wake height and period computed from field measurements**

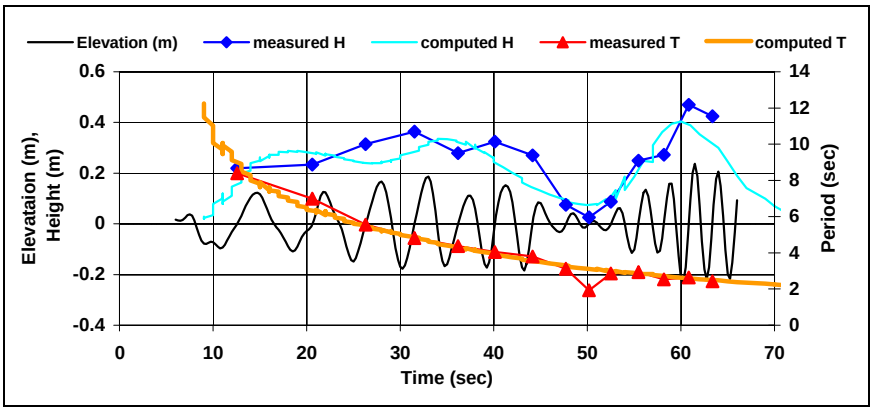

Figure 5-35. ***Snohomish*** **Test 6 (** F_d **=1.28,** F_L **=0.79) – surface elevation, wake height and period computed from field measurements**

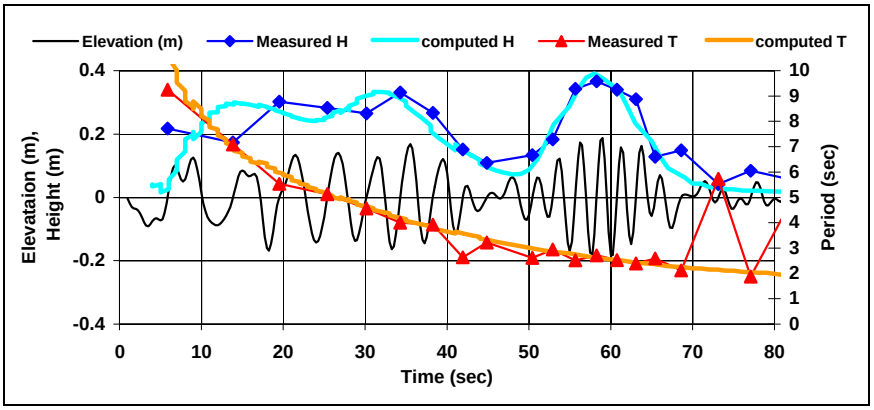

Figure 5-36. ***Snohomish*** **Test 7 (** F_d **=1.44,** F_L **=0.89) – surface elevation, wake height and period computed from field measurements**

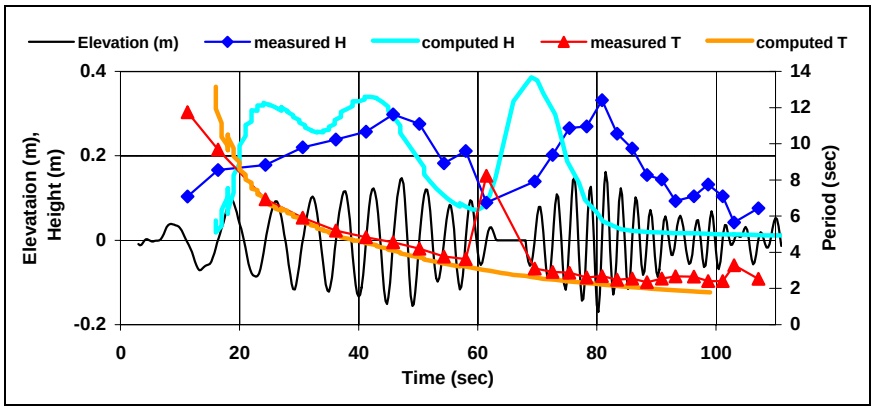

Figure 5-37. *Snohomish* Test 28 (F_d =1.58, F_L =0.89) – surface elevation, wake height and period computed from field measurements – Synchronization 1

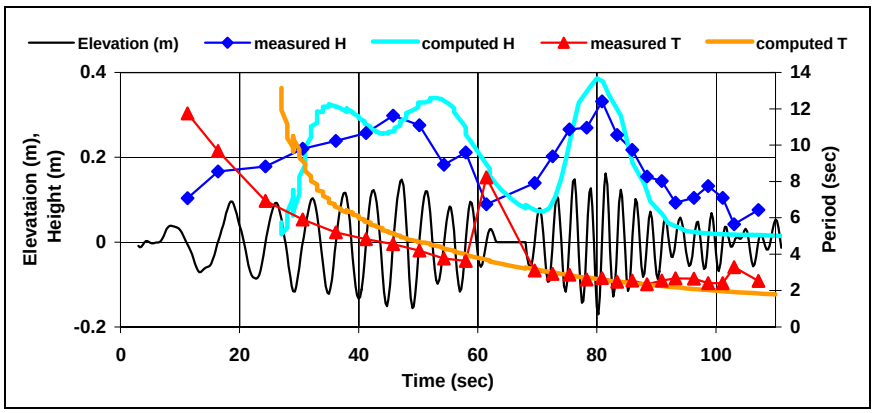

Figure 5-38. *Snohomish* Test 28 (F_d =1.58, F_L =0.89) – surface elevation, wake height and period computed from field measurements – Synchronization 2

The results of the simulations show that the *LSV* model can predict the decay of the wave period observed in measured data. The model can also be calibrated to reproduce the wake height pattern, both in phase and magnitude. There is some suggestion that the leading edge waves for high depth Froude number simulations may be reproduced by the model at too small an angle.

5.4.8.2 Validation with Condor Express *Deepwater Tests*

The LSV model was applied to test results for the fast ferry *Condor Express* in order to calibrate the model for this ship. Unfortunately, the measured results contain a good deal of scatter and it appears that significant wind waves were present at the time of the tests. As well, the results show a much greater dissipation of wave energy over distance (see for example the decay between 79 m and 179 m in a 38 knot simulation shown in Figure 5-39 than is shown in any other measurements or theory. This may suggests that there may be some

problems with the data for this test (i.e. the 90 m offset results). The rate of decay far exceeds any other measured or published values and may be erroneous or may represent some additional process not accounted for in the model simulation (e.g. breaking offshore). The rate of decay between 179 m and 250 m is more in line with expected values.

The decay characteristics of the LSV model for a series of 38 knot runs of the *Condor Express* are shown as the dashed line in Figure 5-40. The model's decay rate is proportional with distance as $x^{-.498}$. This is much greater than the rate $x^{-.333}$ that results from Kelvin theory and associated with sub-critical vessels, but is close to the rate of $x^{-.55}$ used by DHI in their far field modeling of fast ferry wakes (Kofoed-Hansen et al, 1999).

The results for the calibration of the LSV model for the 39 knot and 34 knot tests are shown in Figures 5-41 and 5-42. Although there is substantial scatter in the measured data, the model results follow the general trends of the data.

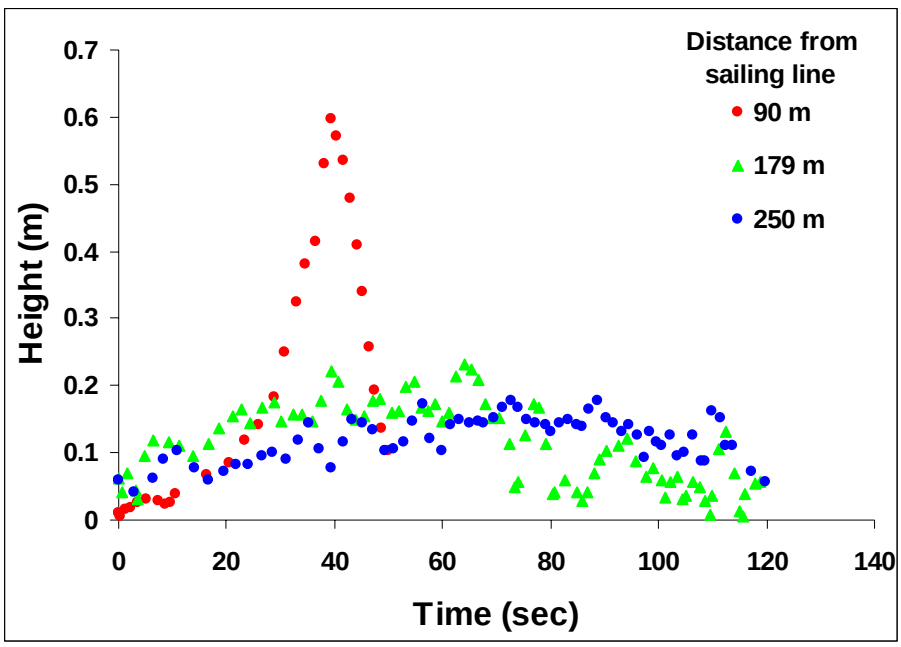

Figure 5-39. Measured wave heights from the Condor Express trials – 39 knot tests (Note: Time axis has been shifted to line up data)

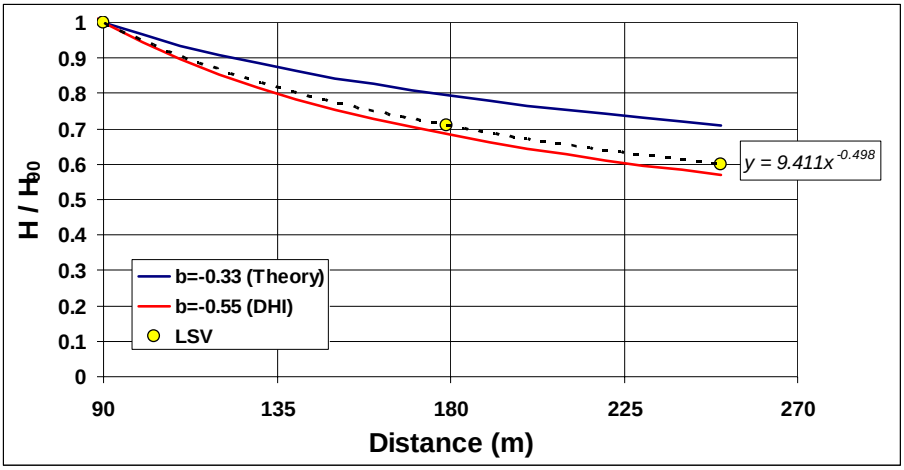

Figure 5-40. Comparison of the decay characteristics of the LSV model with other rates used in the literature

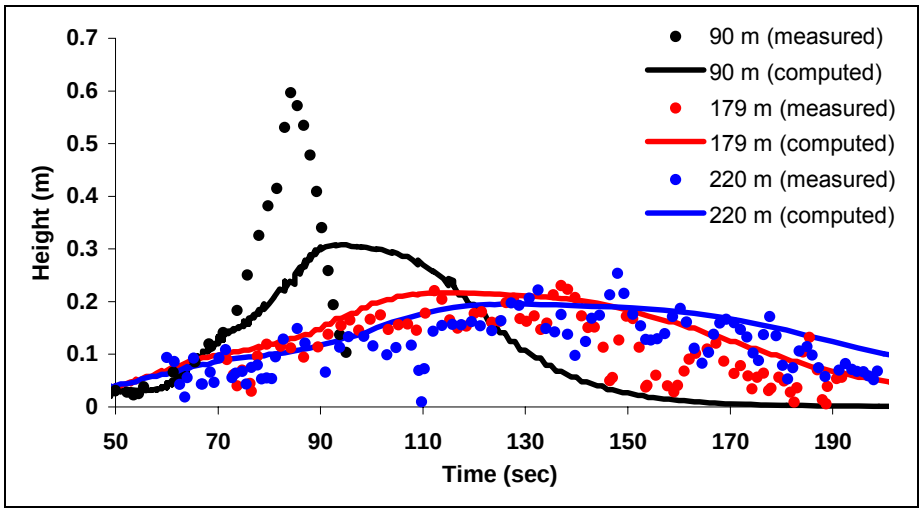

Figure 5-41. Comparison of measured and computed wake heights for *Condor Express* at 39 knots. The measured results for the 90 m offset are dissimilar to any other measurements and may be somewhat suspect. (Note: time axis has been shifted to align start of wake event)

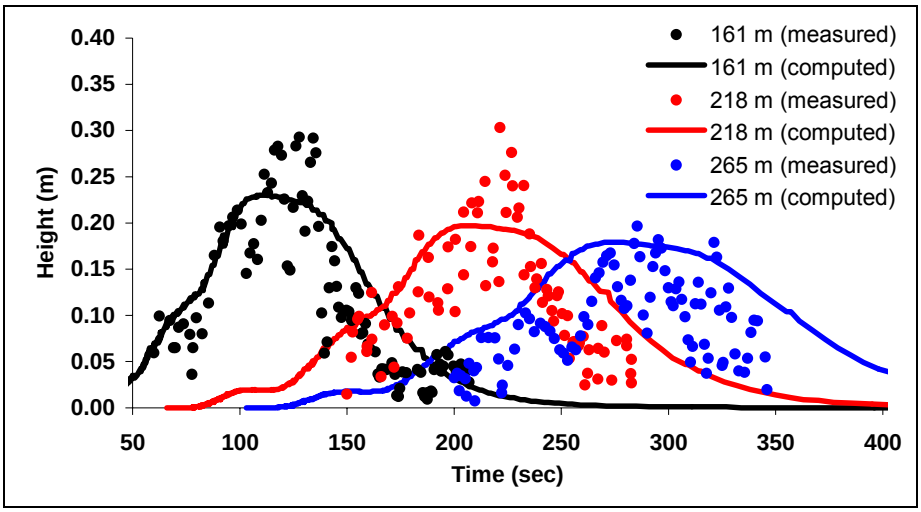

Figure 5-42. Comparison of measured and computed wake heights for *Condor Express* at 34 knots. (Note: time axis has been shifted to align start of wake even

5.4.8.3 Validation with Bravest Deepwater Tests

The LSV model was calibrated for the *Bravest*, a 38-meter aluminum hull, low-wake catamaran designed for a 35 knot operating speed and a capacity of 340 passengers, using data collected by Fox and Associates and provided to Pacific International Engineering. In these tests, the vessel sailed past a moored sensor at a variety of distances. In this section, the measurement results and results computed by LSV for the 31.4 knot are compared. Samples of the wake climate at two locations, 80 m and 180 m, were extracted from the LSV results and are compared to the field measurements in Figures 5-43 and 5-44. The times of the four sets of data were shifted in the plots to align the start of the wake event for easier comparison (Note that the times of the field measurements are meaningless, since these were separate vessel runs).

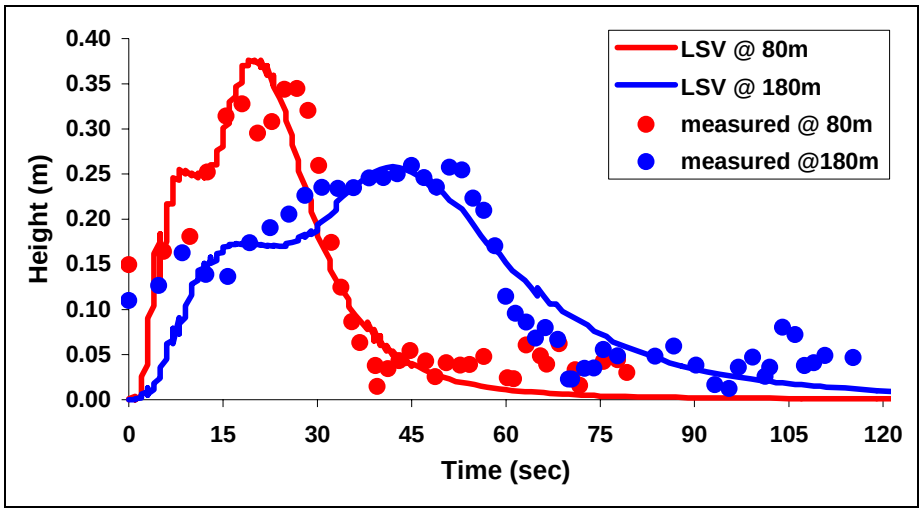

Figure 5-43. Comparison of measured and computed wake height for *Bravest* (Note: time axis has been shifted to align start of wake event)

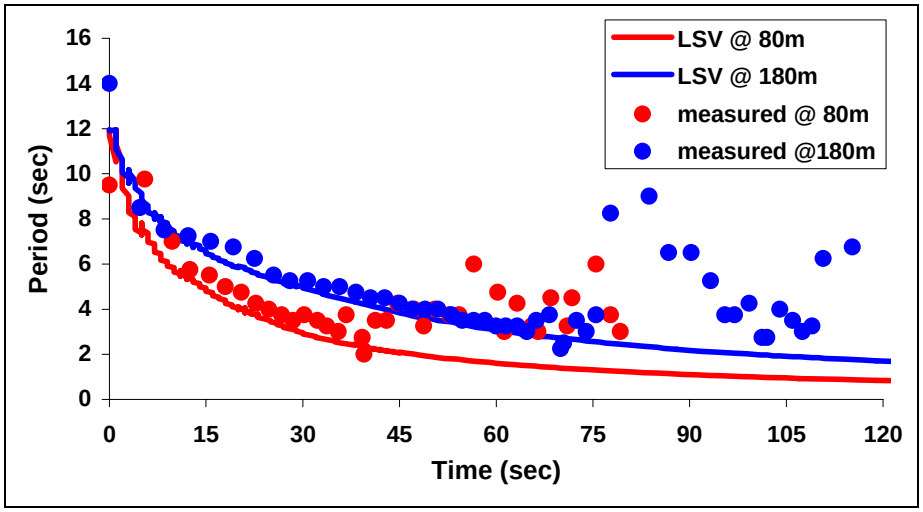

Figure 5-44. Comparison of measured and computed wake period for *Bravest* (Note: time axis has been shifted to align start of wake event)

The LSV model was calibrated to the results at 80 m and shows a good approximation of the wake height time signal, as expected. The wake heights at 180 m are also well matched, which indicates that the spatial decay characteristics of the LSV model are good approximation for super-critical vessels. The wake period characteristics with time are also well reproduced by the model, showing a flattening of the curve with time. This indicates that the temporal dispersion characteristics of super-critical wakes are well represented by the LSV model.

5.4.9 Practical Application in Rich Passage and Surrounding Shorelines

Experience with the LSV model has shown that short-duration, high-density simulations, rather than complete runs of the vessel along the entire route, are the most useful for mapping of wake energy impacting the shore. An illustration of this approach is shown in the three plots in Figure 5-45, which show three points in time after a ferry passage.

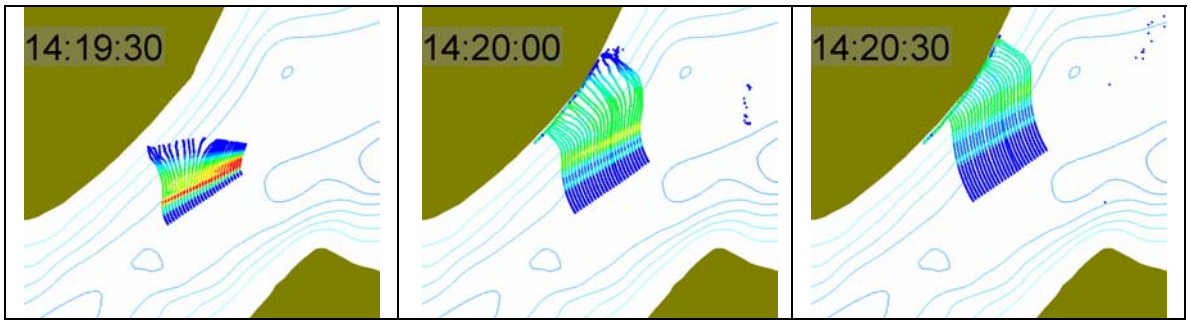

Figure 5-45. Predicted wake height along the Bainbridge Island shore at three times

The application of the LSV model to the shorelines around Rich Passage will be a focus of the project work in the next phase of study.

5.4.10 Additional Developments Required

The LSV model is presently operational and is being used to compute wake impacts on the shores of Rich Passage and the surrounding area. There are several areas in which additional work should be undertaken. These include:

1. Most field data available from Rich Passage are limited to speeds in the 35 knots to 38 knots operational range. Up to this point, all simulations have been performed using vessel wake energy output characteristic of this speed range. Accordingly, the LSV model simulations may only be accurate near these speeds. Because the energy distribution (i.e. the height of the wakes in the pattern) is a function of F_L, data for a vessel at a number of speeds is required to model the full range of wakes. This data is available from the deep water field trials provided by Fox and Associates.
2. There is no variation in the output of wake energy for vessels moving along a curved path because the vessel wake characteristics used in the model are all obtained from the analysis of tests in which the vessel was traveling in a straight line. It is suspected that the wake produced by the vessel will be different on each side and from that of a straight-line transit. Additional calibration test are required to address this issue.

5.5 Wave Impact Assessment Modeling

Impact assessment can take several forms, including absolute and relative assessments. Absolute assessments address all major processes and, in general, the response of the system as a whole is used as the measure. This may result in the construction of a complete deterministic model that predicts the behavior of the system to all processes. In some cases, it is also possible to quantify the effects of each process individually. Relative assessments compare the likely response of the system to the major processes or forcings independently. This type of assessment often focuses on indicators (e.g. sediment transport rate, breaking wave height), rather than on the direct response of the system.

In practice, both relative and absolute assessments are used, with a relative assessment usually undertaken first to identify those processes required for a fuller absolute assessment. As discussed in Sections 2.1 and 2.2, the work in this section is aimed at the determination of thresholds, below which the evolution of the beach is unaffected. While this work will involve the computation of morphological parameters (e.g. wave power, transport rates, erosion/accretion patterns), it is not planned to predict the morphological response of the entire Rich Passage shoreline. This computation of morphological indicators is more achievable than the prediction of the actual morphological response of mixed sand-gravel beaches from just a few waves every few hours over several months.

This section outlines the background to the problem and the approaches used. Work on a number of approaches has been started, including the development of cross-shore profile numerical models and longshore power calculations. This work is being undertaken primarily to identify the most likely avenues for detailed investigation. The work is collected here to assist in setting acceptable wake energy thresholds and to provide source material should detailed modeling become necessary in the future. The most pressing issue, at present, is the need to identify a methodology for beach response so that an assessment of the impacts of various vessels can be quantified.

5.5.1 Relative Impact Assessment - Model Application

The primary tool of the impact assessment will be the LSV model. Its results may be used to provide input to secondary tools (e.g. profile response models) if required. At the present stage, the model's results will be analyzed to determine indicators of potential response. One of the most directly relevant indicators is wake power, P. This quantity is determined from the equation:

$$P = \frac{1}{2} c_g E \sin \alpha_b$$

where α_b is the angle between the wake propagation direction and the local shore normal. This quantity is proportional to longshore littoral transport.

To illustrate the potential applications for this approach, LSV model predictions of longshore wave power at a location near profile monitoring site 3 (Figure 3-5) are shown in Figure 5-46. These preliminary simulations are produced using average speed and route data from numerous GPS position measurements of Chinook class POFFs taken between 1999 and 2002. The simulations are for three POFFs: *M/V Snohomish, M/V Bravest,* and *M/V Condor Express*. Each point in Figure 5-46 represents the power in each individual wake packet at breaking.

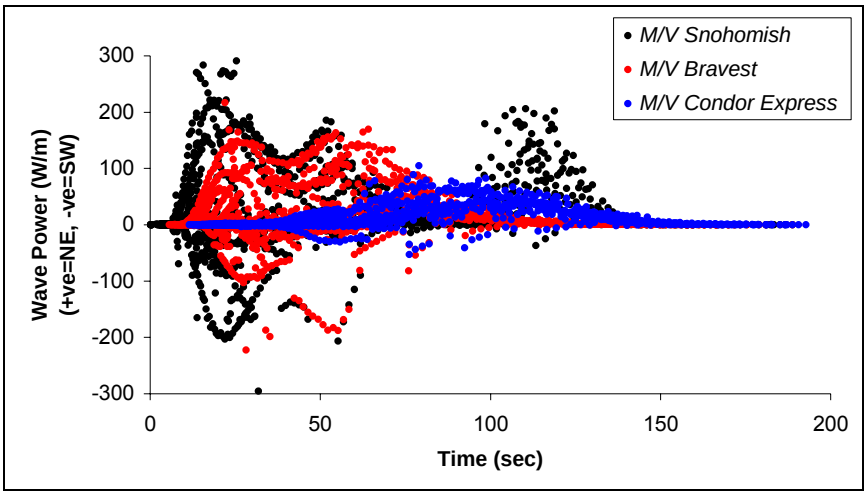

Figure 5-46. Alongshore wave power from the wake of three POFFs (Bremerton to Seattle, high water slack)

The sign of the wave power in Figure 5-46 indicates the direction, with positive indicating a northeastward direction. There is substantial variability in the results; in general, this variability results from the angle between the bearing of the wake at breaking and the strike of the local seabed at that point.

A clearer way to investigate the above results is to examine the cumulative impacts. These are shown in Figure 5-47. It is clear from the results that *Snohomish* produces the largest relative impact at the shore, with *Bravest* somewhat smaller. *Condor Express* produces the least impact.

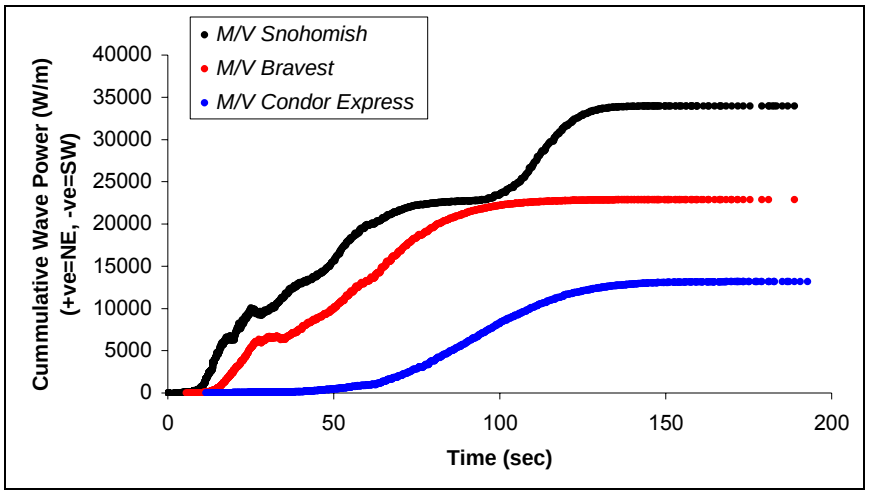

Figure 5-47. Cumulative alongshore wave power from the wake of three POFFs (Bremerton to Seattle, high water slack)

The differences on the return trip (Seattle to Bremerton) are more extreme (see Figure 5-48). *Snohomish* and *Bravest* both show northeastward forcing again, while *Condor Express* produces almost no net impact. This result for *Condor Express* is believed to be caused by wake breaking at the shore with almost a shore-normal angle.

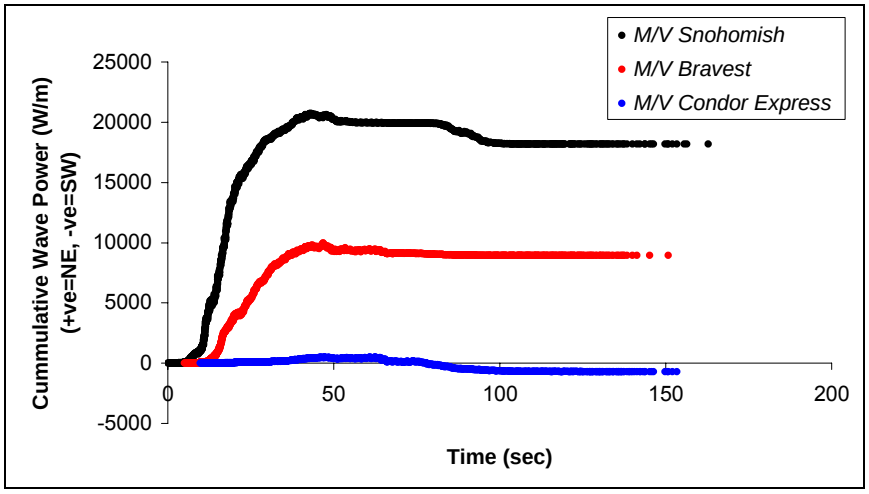

Figure 5-48. Cumulative alongshore wave power from the wake of three POFFs (Seattle to Bremerton, high water slack)

It should be emphasized that the above results are valid for a single route, speed and tidal state (high water slack). Similar runs, but at low water slack, are shown in Figure 5-49 and Figure 5-50. The results of the Bremerton to Seattle simulation (compare Figure 5-49 with Figure 4-47 and Figure 5-50 with Figure 5-48) appear to be fairly independent of tidal state, whereas the Seattle to Bremerton runs are not. At low tide, these latter runs all show a significant southwestward net forcing.

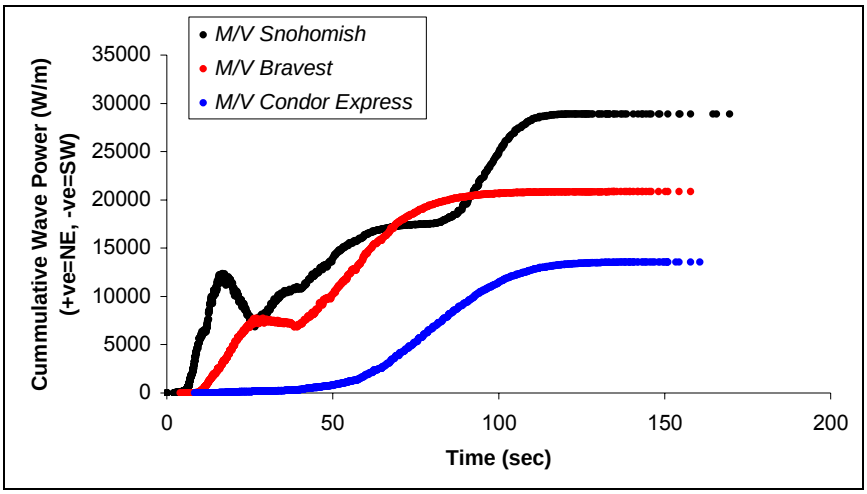

Figure 5-49. Cumulative alongshore wave power from the wake of three POFFs (Bremerton to Seattle, low water slack)

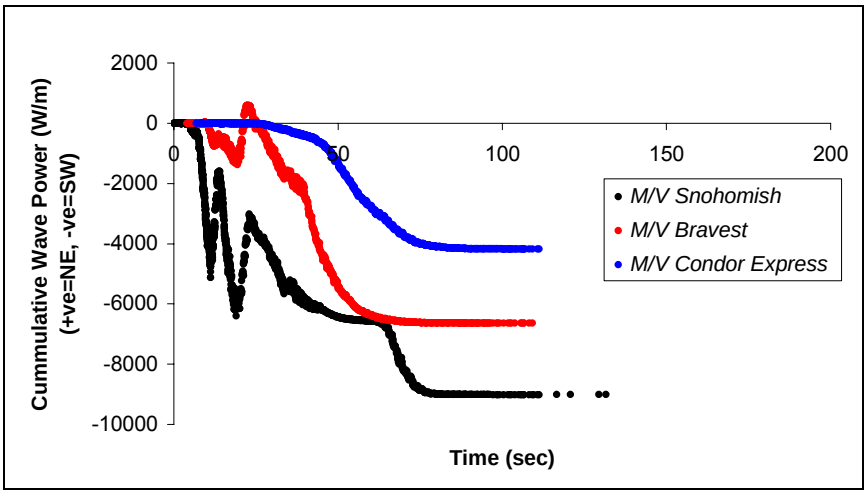

Figure 5-50. Cumulative alongshore wave power from the wake of three POFFs (Seattle to Bremerton, low water slack)

The LSV model is especially useful for producing spatial distributions of wake power. This allows "hot-spots" to be identified and can assist at investigating trends in transport that may be produced by the introduction of POFFs. Figures 5-51 through 5-53 show maps of the port side wake for the *Snohomish*, *Bravest*, and *Condor Express* for the same position along the route and same tidal condition. The maps illustrate the different refraction and shoaling patterns that occur with wakes from each of the three vessels.

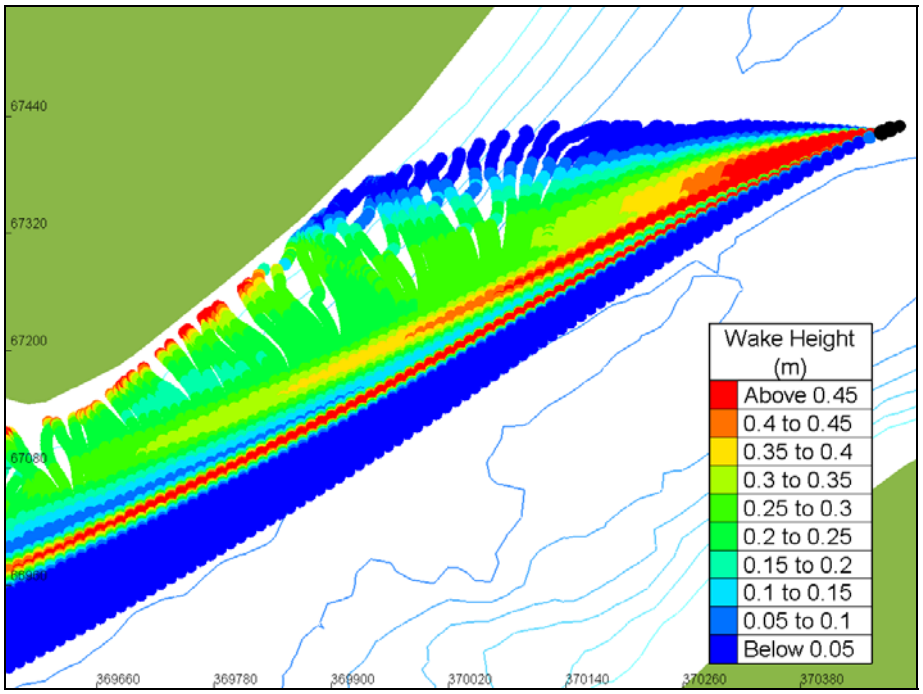

Figure 5-51. Map of port side wake height pattern for *M/V Snohomish* (Bremerton – Seattle, low water slack)

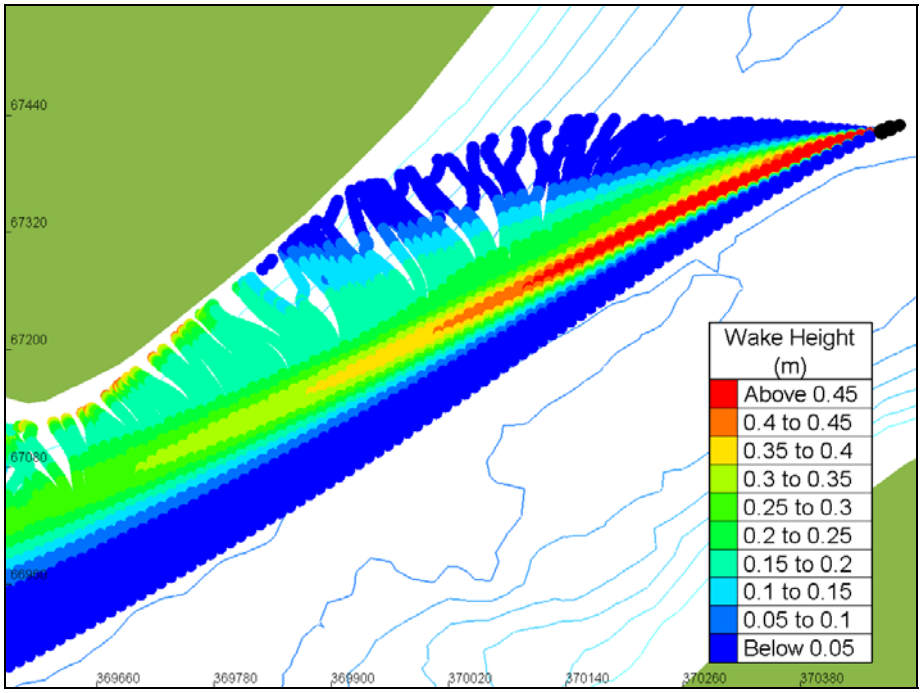

Figure 5-52. Map of port side wake height pattern for *M/V Bravest* (Bremerton – Seattle, low water slack)

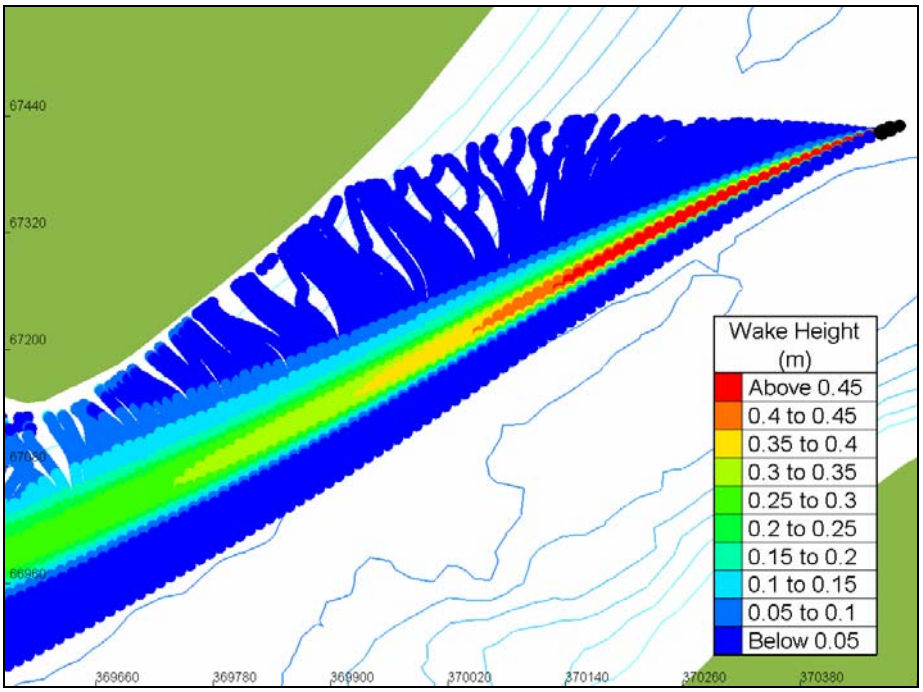

Figure 5-53. Map of port side wake height pattern for *M/V Condor Express* (Bremerton – Seattle, low water slack)

Figure 5-54 through Figure 5-65 show the cumulative wake power at breaking near the shore over a 100 m reach of the shore along Point White. In each plot, the power is shown as a colored circle. The hue of the color indicates direction (blue = wake power directed to the northeast, red = wake power directed to the southwest). The intensity of the color indicates the magnitude of the power. The plots are organized first by vessel, then by route, then by tidal stage. Additional plots showing all LSV results for each vessel, each tidal level, and each direction are provided in Appendix H.

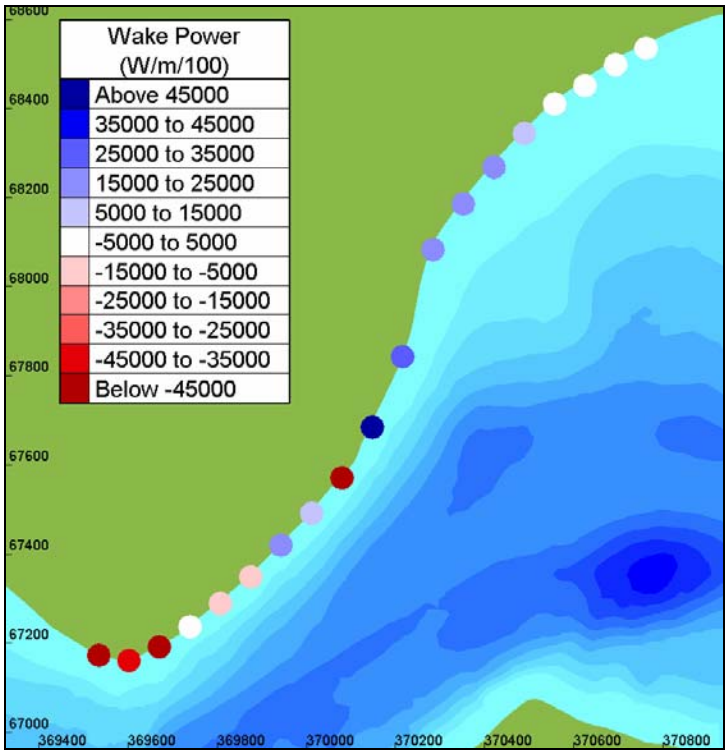

Figure 5-51. Spatial distribution of wake power from *M/V Snohomish* (Seattle-Bremerton, high water slack)

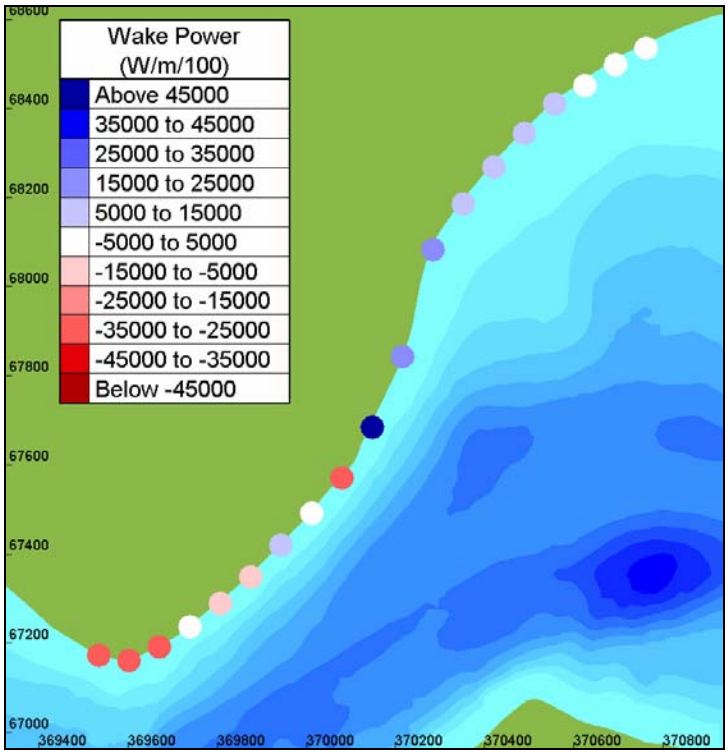

Figure 5-52. Spatial distribution of wake power from *M/V Bravest* (Seattle-Bremerton, high water slack)

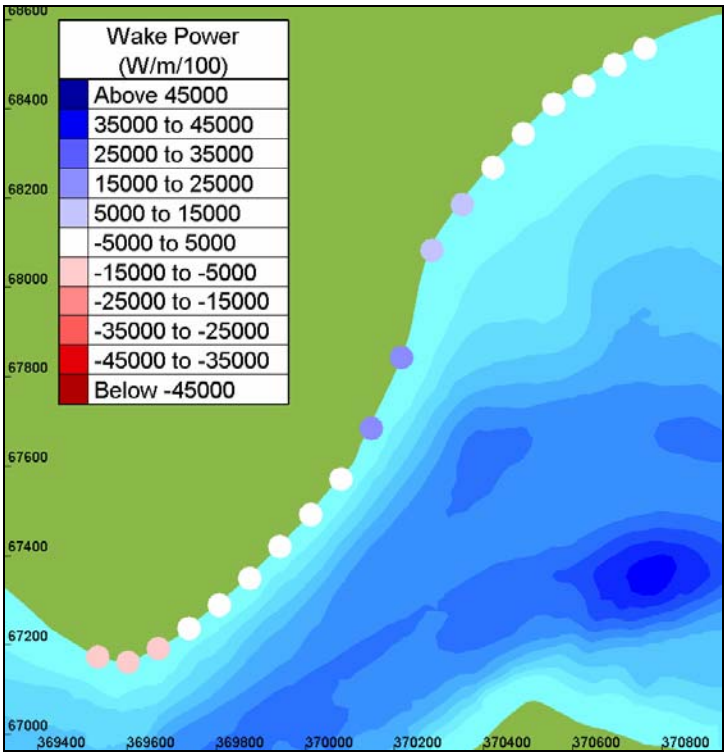

Figure 5-52. Spatial distribution of wake power from *M/V Condor Express* (Seattle-Bremerton, high water slack)

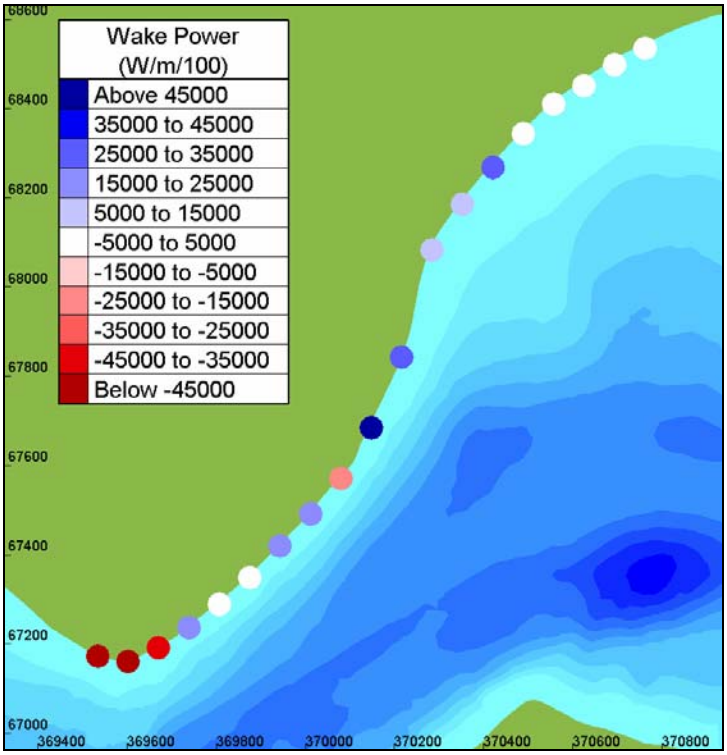

Figure 5-54. Spatial distribution of wake power from *M/V Snohomish* (Bremerton-Seattle, high water slack)

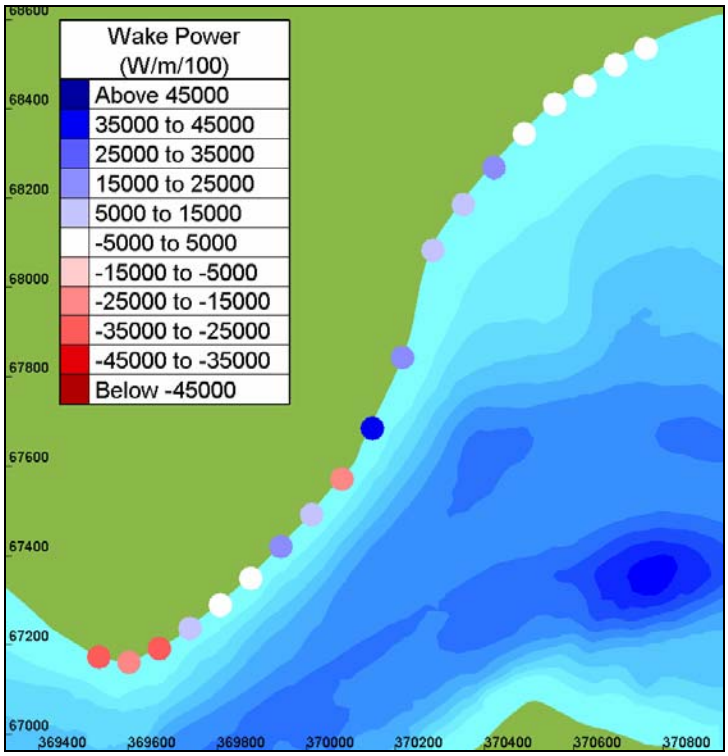

Figure 5-55. Spatial distribution of wake power from *M/V Bravest* (Bremerton-Seattle, high water slack)

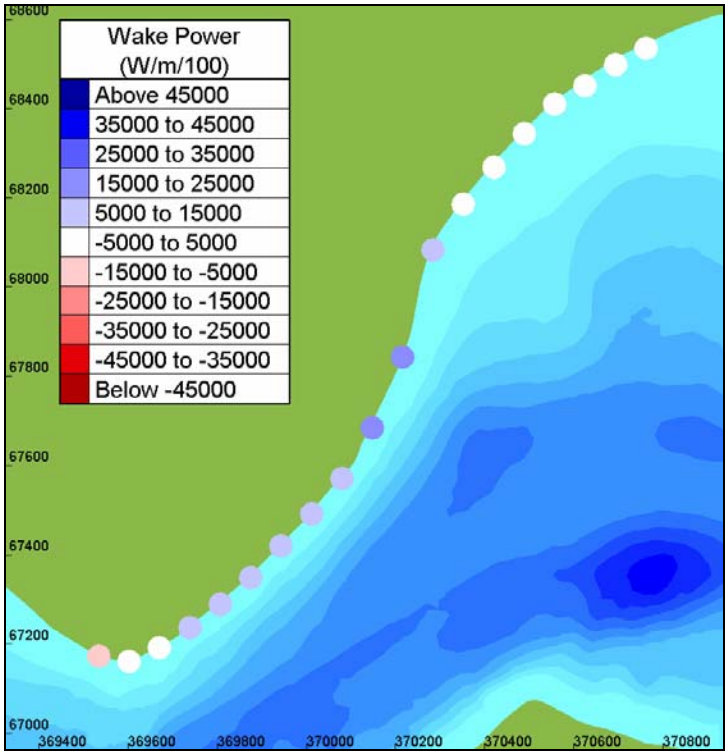

Figure 5-56. Spatial distribution of wake power from *M/V Condor Express* (Bremerton-Seattle, high water slack)

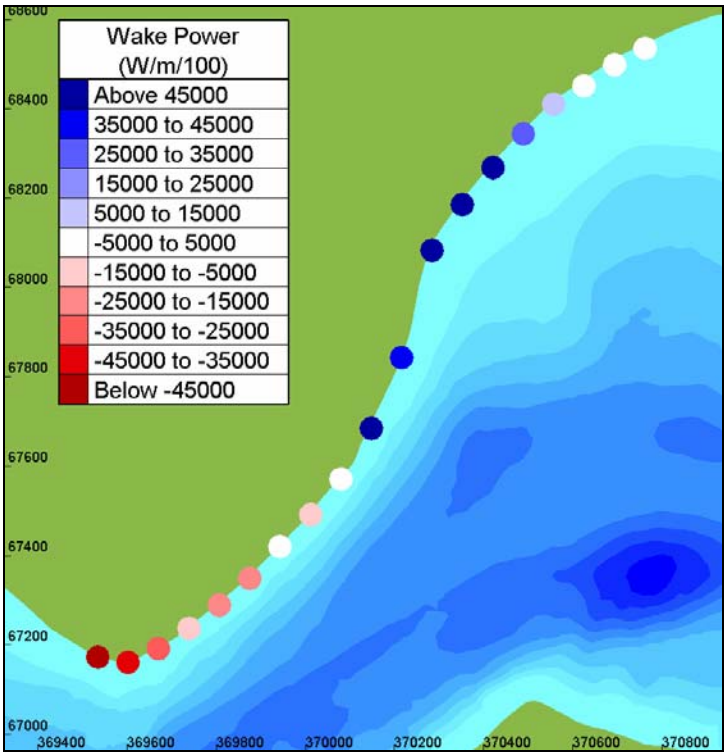

Figure 5-57. Spatial distribution of wake power from *M/V Snohomish* (Seattle-Bremerton, low water slack)

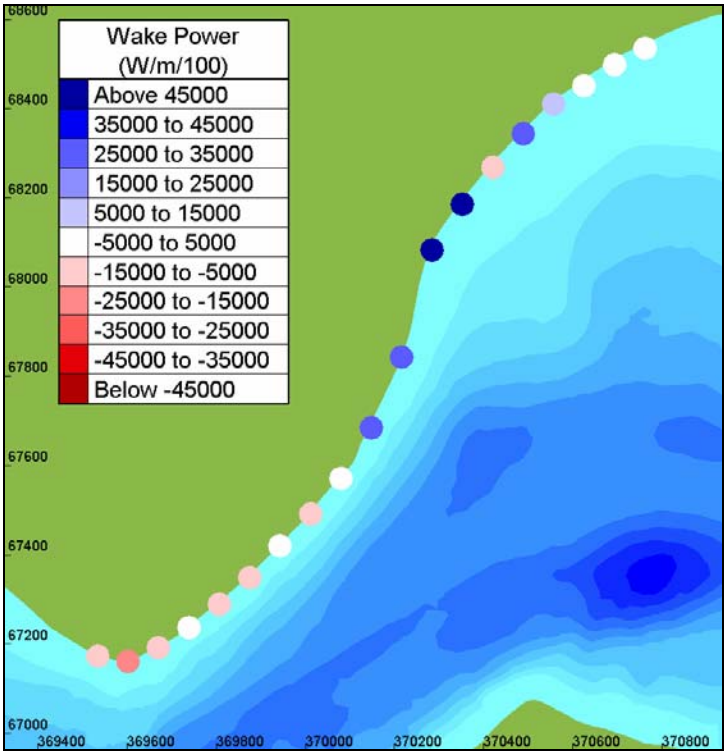

Figure 5-58. Spatial distribution of wake power from *M/V Bravest* (Seattle-Bremerton, low water slack)

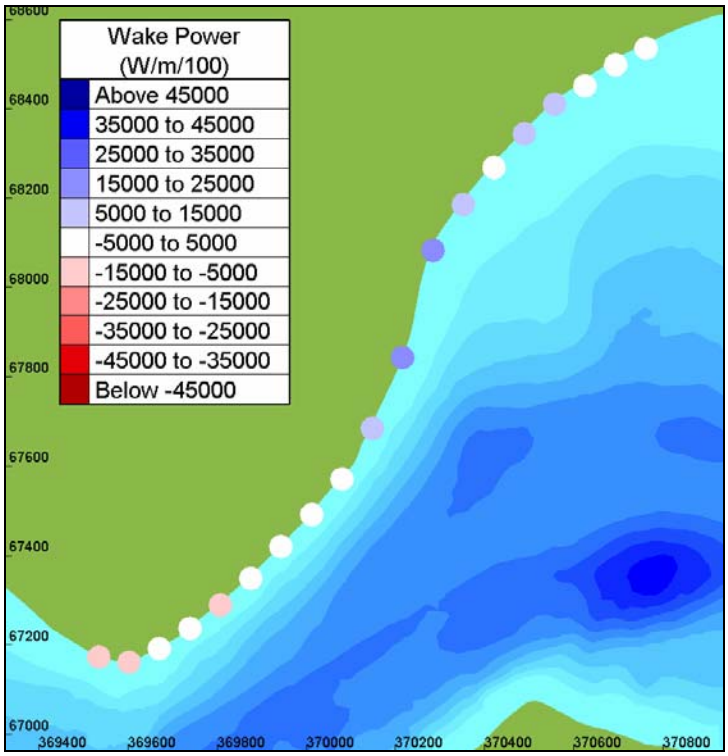

Figure 5-59. Spatial distribution of wake power from *M/V Condor Express* (Seattle-Bremerton, low water slack)

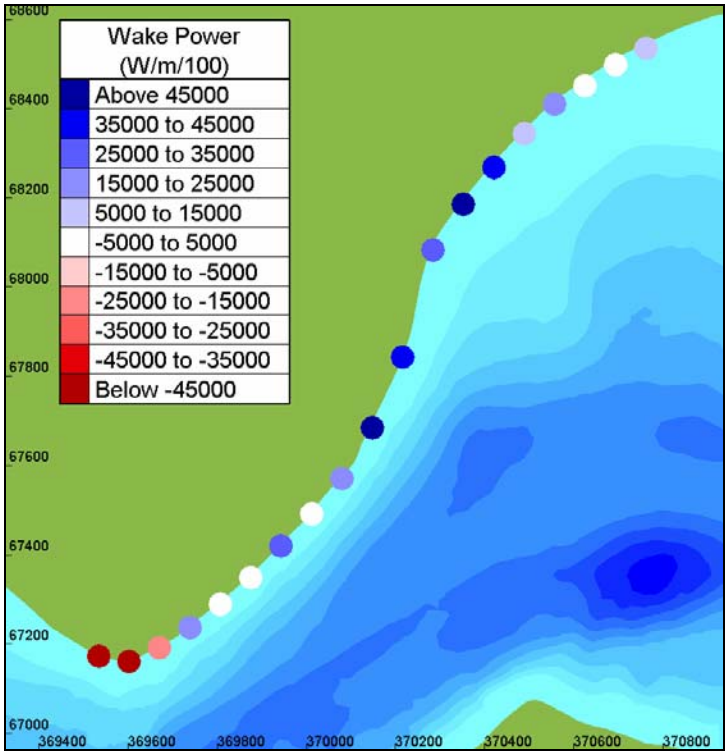

Figure 5-60. Spatial distribution of wake power from *M/V Snohomish* (Bremerton-Seattle, low water slack)

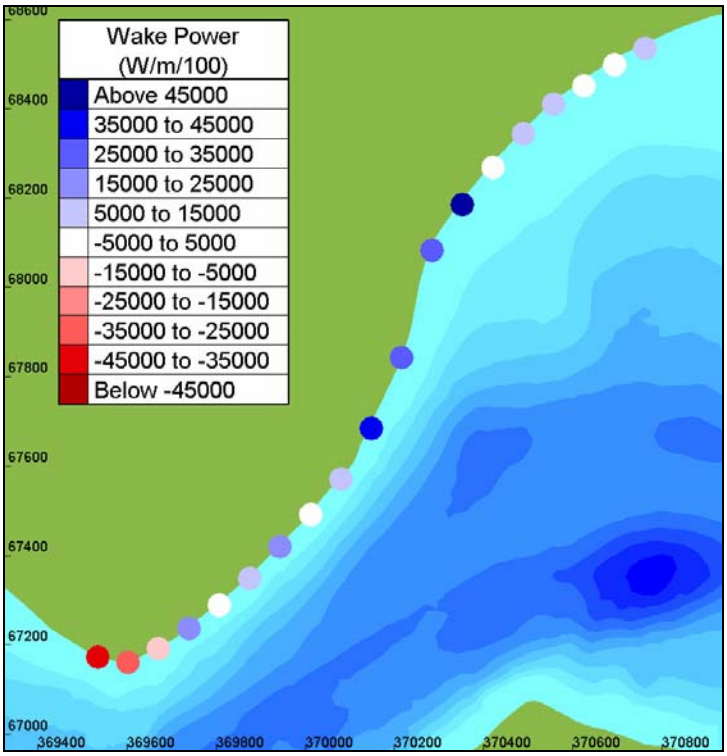

Figure 5-61. Spatial distribution of wake power from *M/V Bravest* (Bremerton-Seattle, low water slack)

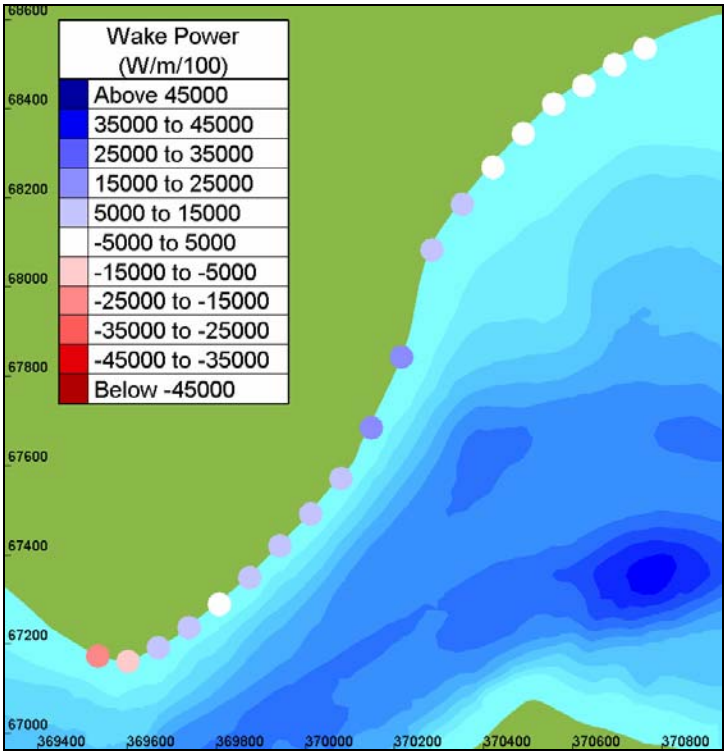

Figure 5-62. Spatial distribution of wake power from *M/V Condor Express* (Bremerton-Seattle, low water slack)

Although these figures are only presented to illustrate the capabilities of the LSV model, there is a large amount of information presented and some conclusions can be drawn. First, as expected from the data presented for the single site near profile monitoring site 3, *M/V Condor Express* generates significantly less wake power at the shore than either *M/V Bravest* or *M/V Snohomish*. Second, wake energy from all vessels has a southwestward bias near the tip of Point White and a northeastward bias along the shore closer to profile monitoring site 5.

Results similar to the above illustrations will be used in the subsequent stages of the study to evaluate alternative low-wake candidate vessels, optimize vessel speeds, routing and, if necessary, to scope out mitigation efforts.

5.5.2 Absolute Impact Assessment - Descriptive Model

As discussed in Section 4, POFF-related changes in beach morphology at monitoring sites at Point White appear to have been caused by both longshore and cross-shore sediment transport. It is not clear which, if either, process dominates. The following paragraphs describe two conceptual models that can be used to describe the morphological response; the first model addresses the problem assuming it is dominated by longshore transport, whereas the second assumes that cross-shore processes dominate.

The progression of the erosional pattern may provide some guidance as to the relative importance of the cross-shore and longshore sediment transport processes. The pattern of erosion described in Section 4 can be explained using the following model:

- The pre-POFF sediment transport system is in equilibrium
  - Beach material (mostly gravel) is in motion across the profile
  - Rate of transport is unknown
  - Net direction of transport is unknown
- The introduction of the fast ferries leads to a significant increase in the rate of transport to the northeast along the eastern shore of Point White
- Since the transport rate increased along the entire shore, there is no change in the profile at any location providing the gravel moving from the south and to that location balances the gravel moving to the north and away from that location
- The gravel entering the system near the tip of Point White (if any) has not changed and, consequently, this area will soon show a deflation in the profile until bedrock is reached
- As the profile is starved of gravel, deflation occurs up-drift of the location

- This process is gradually translated along the shore to the northeast

It was noted that when the POFFs ceased high-speed operations, the profiles gradually re-built to their pre-POFF states. The above model can also be used to explain this re-building of the profiles along the Point White shore if the net pre-POFF sediment transport along this shore is directed to the southwest.

A problem with the purely longshore conceptual model for beach response is that it will only predict a profile with erosion/accretion across the entire beach in the cross-shore direction. It cannot explain downcutting at the bulkhead and accretion lower on the beach (see Figure 4-1).

Another model, based primarily on cross-shore transport, can also be developed to describe the morphological development. Gravel transported by waves in the surf zone may follow a zigzag pattern (van Rijn, 1998); material is transported up and down the foreshore, as well as along it. Under this scenario, there is a tendency for gravel to be deposited in a berm-trough-berm profile, with a berm above the swash zone and another further offshore (e.g. van der Meer, 1988). This profile is not evident in profiles taken along the Point White shore, either before or after the ferry service. In the pre-ferry service case, this may be due to the relatively large tidal range as compared to the incident wave climate. The point of action of the waves is moved up and down the shore. The resulting profile is linear but with a relatively steep slope, since the tendency is for gravel to be transported inshore. During the period of POFF service, the presence of much larger waves causes a rapid transformation towards the classic berm-trough-berm profile. Due to the presence of the bulkheads, however, the shore is too confined in the cross-shore to allow the classic profile to develop. Gravel is pulled offshore from the base of the bulkheads because the waves are sufficiently large at high water, resulting in a truncated trough-berm profile. This is illustrated in Figure 4-1, which shows that downcutting at the bulkhead is accompanied by local accretion offshore.

One problem with a purely cross-shore conceptual model is that is will yield an erosion pattern that is uniform in the alongshore direction. As noted by Bill Reynolds, the development of the erosion pattern is not uniform with time along the shore.

5.5.3 Absolute Impact Assessment - Proposed Approach

As stated at the start of this report, the ultimate aim of the project is to determine whether a POFF systemcan be developed with high-speed vessels that do not have negative impact on the shore. If this were achieved, no beach evolution modeling would be necessary. If one is

necessary, then a beach evolution model based on the following outline would be developed.

In order to produce a conceptual model that can describe both the development of the beach profile in the cross-shore, especially the downcutting at the bulkheads – the major cause for concern – and the temporal/spatial lags in the erosion patterns, a three-dimensional conceptual model must be utilized. In this model, the beach responds primarily in a cross-shore mode (local or small-scale response), with the supply governed by longshore transport (regional or large-scale response).

The combined model would be formulated in the following manner:

- The shore in question would be divided into a finite number of cells
- The cross-shore profile in each cell along the shore would be predicted at each time step using a pre-determined volume of sediment.
    - The profile would respond to wave and tide forcing according to an established predictive equation (e.g. van Hijum, 1977; Powell, 1990)
    - Wind waves as well as vessel waves would be considered
- Each cell would be subject to longshore transport
    - The rate would be computed using an existing bulk predictor approach (e.g., CERC)
    - Sediment divergence would be computed using predictions at each of the two lateral boundaries
- Each profile would have a volumetric storage capacity for sediment
    - This could be determined from the maximum beach slope possible at the bulkhead
    - If storage in the cell was below capacity, sediment would be retained in that cell
    - If storage in the cell was at capacity, sediment would be passed on to the next down-drift cell

The model should be able to respond to the absence of large waves to permit the beach to re-build. This may necessitate a feeding rate of sediment. Work will be necessary in the next stage of the study to determine whether the above model is required.

6.0 Wake and Wake Impact Studies with a Foil-assisted Catamaran

Section 3.7 summarized wake trial data collected from several candidate vessels and identified that a foil-assisted catamaran was one of three hull forms considered worthy of further consideration in the study including. The analysis of existing trial data collected by *Fox and Associates* indicated that the foil-assisted catamaran *Condor Express* built by All American Marine, Inc of Bellingham, WA and designed by Technikraft Inc., NZ had lower wash characteristics than any vessel with capacity of 149 passengers and had significant potential as a candidate POFF vessel for use in Rich Passage. Towards the end of the first year of study, *Spirit*, a sister ship to the *Condor Express*, was constructed by All American Marine (Figure 6-1). Although *Spirit* was designed as a whale watch tour vessel for use in Alaska, and the design was not optimized for wake wash, the availability of the foil-assisted vessel provide a unique opportunity to conduct in-situ research tests with a state-of-the-art candidate hull to tests its wake generation characteristics and to develop data on potential shoreline impacts from wakes.

A series of research tests were planned with *Spirit* to provide data for direct validation of the numerical wake and shoreline response models. The models and *Spirit* trial data will enable a detailed assessment of potential shore impacts and provide data and tools to evaluate possible shore protection solutions for areas where impacts cannot be minimized. In the first year of Study, the research vessel was acquired for charter, mobilized, and outfitted with onboard instrumentation for research testing, oceanographic instrumentation was prepared and deployed for measurement of the wakes, and a preliminary intensive trial was executed in Port Orchard reach. The research testing with *Spirit* and the analysis an application of data will continue in the second year of study to examine shoreline impacts in Rich Passage.

Intensive research testing of the vessel and detailed wake measurements were conducted on a portion of the Seattle to Bremerton route (Port Orchard Bay) on February 4 and 5, 2005(Figure 6-2). The purpose of the intensive testing was to provide detailed measurements of wake patterns for calibration and verification of the wake prediction models being developed as part of the study. The intensive tests focused on gathering vessel operating and wake data. During the intensive trials, the experimental vessel was operated through a range of speeds between 15 and 35 knots and at a range of distances between 1000 and 3000 ft from shore in Port Orchard Bay. The measurements for the intensive trials included:

- Deployment of a 4-point cross-shore instrument array at Port Orchard Bay (Figures 6-3 and 6-4). The sensors deployed included 2 non-directional wave gauges and 2 velocity and pressure sensing gauges located within 1000 ft of the shoreline and a capacitance wire gauge at the shoreline. The sensors measured time series of wave heights, wave orbital velocities, wave directions, and wave period at a range of distances from the sailing line and for a range of vessel speeds.

- Vertical aerial photography was acquired of wakes to determine planview shape of the wakes at a range of speeds above 30 knots (an example is shown in Figure 6-5).
- On-board measurements were also acquired from the research vessel. The wake produced by a high speed vessel is strongly influenced by a number of factors, including its speed, hull shape, and depth of water. The hull shape is particularly important, and its influence is difficult to assess, since the draft and trim varies with speed. Instruments were installed on *Spirit* to record the dynamic motion of the vessel (heave, pitch, roll) (Figure 6-6) as well as its vertical and horizontal position in time. The data from these instruments will be used to determine the trim of the vessel and lift created by the vessel's foil and the vessel's speed and position in the next phase of Study. Example time series from the on-board instruments is shown in Figure 6-7. The pitch data exhibit the variation in vessel trim as the boat accelerated from 15 knots to over 30 knots in this example.
- One non-directional wave gauge was re-deployed in Port Orchard Bay at the location of the outer station for the intensive trials. Further trials were conducted throughout February in Port Orchard Bay at speeds above 25 knots to test the effects of interceptors on vessel performance and wake generation.
- The *Spirit* is designed to carry up to 149 passengers and the weight of these passengers would have a significant affect on the displacement and performance of the vessel. During the field trials, water tanks have been installed on the vessel to provide extra ballast up to 20000 pounds to represent the passengers' weight. A full or partial load of passengers is being simulated by adjusting the water levels in these tanks (Figure 6-8).
- Unprocessed wave and vessel data collected during the intensive tests with Spirit are provided on a CD with this report. Analysis of the data is planned for a later phase of the Study.

Research tests and wake measurements also began on the Seattle to Bremerton route through Rich Passage following the first set of intensive trials on February 7. These trials will help quantify wake impacts to shorelines and to understand wake behavior near the shoreline. The data will be processed and analysed as part of the next phase of study. In the Rich Passage trials, the vessel follows the actual Seattle-Bremerton ferry route from the Bremerton ferry terminal through Port Orchard Reach and Rich Passage to a point east of Orchard Point on Puget Sound. The Spirit made between 4 and 8 return trips on this route each day to allow data on wake and shore conditions along the route to be gathered during a wide range of weather and tide conditions. Measurements of wake heights at the shore are being taken at a number of points in Rich Passage throughout the field trials. The analysis of the measurements will help to identify local areas of high and low wake energy and provide data for verification of the numerical wake propagation models.

Figure 6-1. The research test vessel *M/V Spirit* in Rich Passage

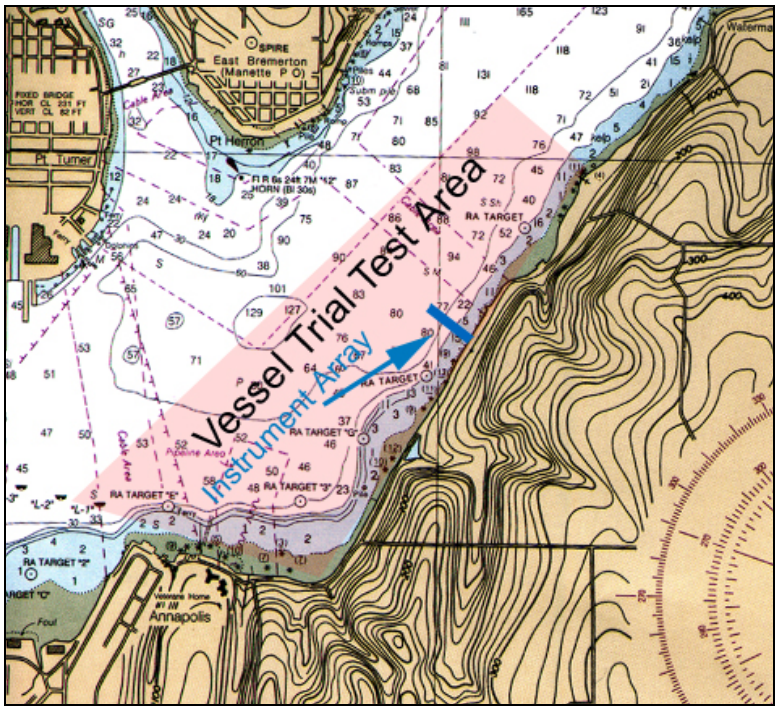

Figure 6-2. Location of the 5-point instrument array for intensive trials of *M/V Spirit* in Port Orchard Reach

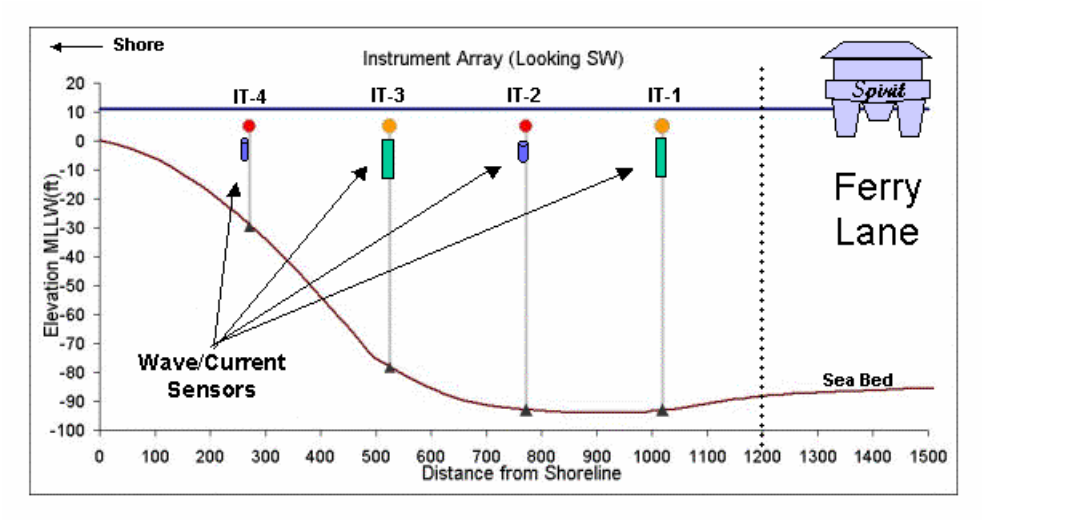

Figure 6-3. Cross-shore profile seaward of mllw showing the location of the 4 stations in the instrument array

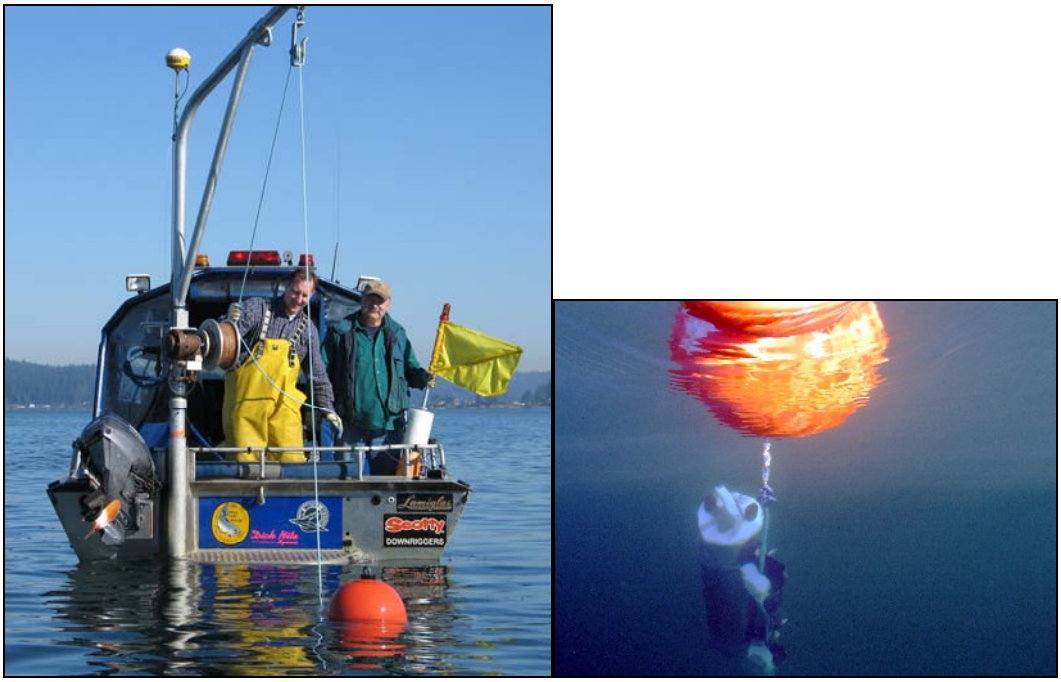

Figure 6-4. Deployment of a wave gauge on a taut-line mooring at the instrument array in Port Orchard Reach

Figure 6-5. Aerial photograph of Spirit Wake (30-35 knots) at the instrument array

Figure 6-6. Dynamic motion sensor installed on M/V Spirit. The sensor signal was multi-plexed with signals from Real-Time Kinematic GPS, and compass

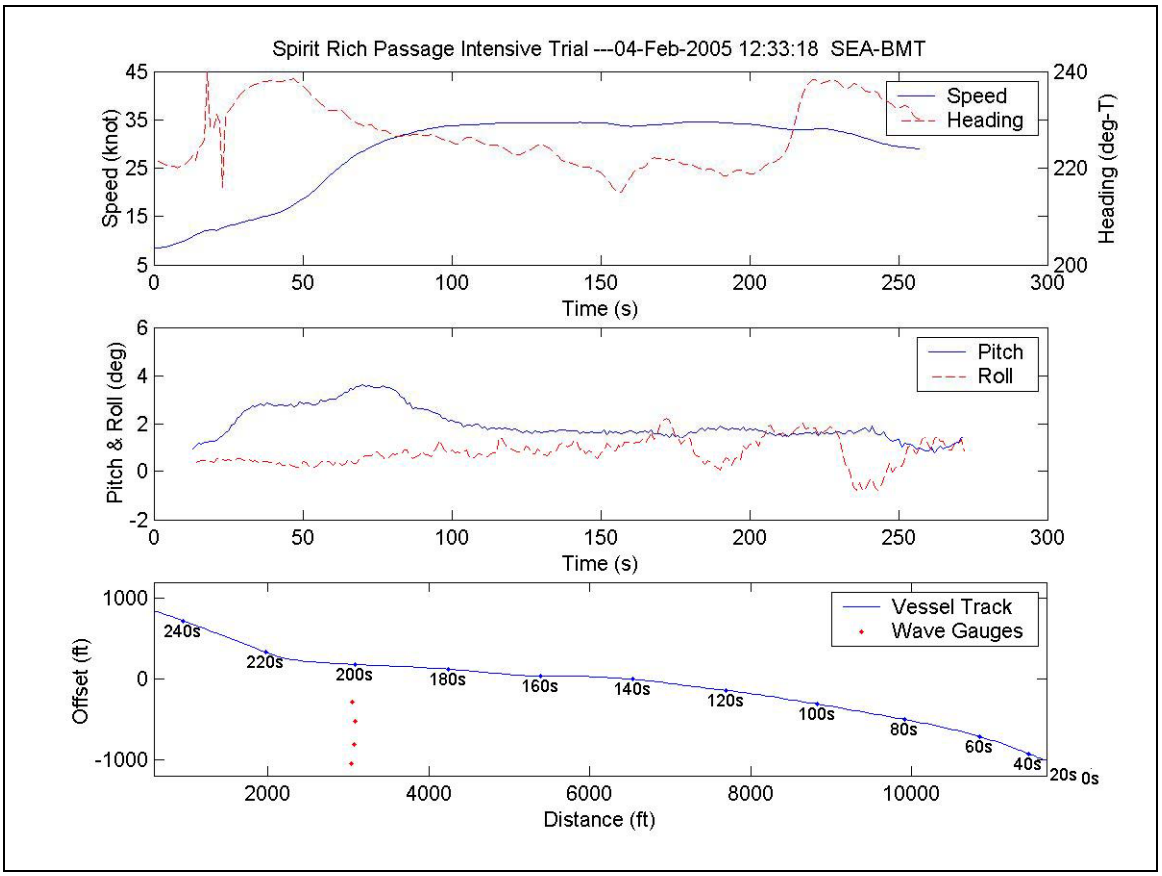

Figure 6-7. Time series of vessel speed and heading (top panel), vessel pitch and roll (middle panel), and vessel track relative to instrument position (lower panel) through time during an intensive trial run on February 4, 2005

Figure 6-8. Water tanks used for ballast on board the research test vessel *M/V Spirit*

7.0 Summary and Recommendations

Despite considerable interest over the past two decades in providing an efficient passenger–only fast ferry (POFF) service on central Puget Sound between the cities of Seattle and Bremerton, a major difficulty arises owing to the need for waterborne traffic between the cities to pass through Rich Passage, a narrow body of water separating the south end of Bainbridge Island from the mainland portion of Kitsap Peninsula at Port Orchard. In the past, Rich Passage property owners have filed complaints that eventually lead to a lawsuit in which the property owners alleged that bulkhead damage, beach erosion, and biological degradation were caused by wakes from Washington State Ferries high-speed ferries. In October 2001, the State Attorney General reached a settlement with Rich Passage property owners concerning damage to property associated with POFF operation through Rich Passage and agreed to maintain speeds of passenger ferries at less than 16 knots through Rich Passage.

The Rich Passage Passenger Only Fast Ferry Study is designed to investigate the feasibility of restoring POFF service between Seattle and Bremerton. The Study was initiated in June 2004 and is funded under a federal grant program administered by the Federal Transportation Administration (FTA), designed to support research and investigations of emerging transportation systems. This report documents the first phase of the Rich Passage Passenger Only Fast Ferry Study conducted between June 2004 and February 2005.

It is anticipated that a successful POFF operation will contribute to sustainable growth in the region by:

- Improving commuter mobility
  - Reducing average travel time to approximately 30 to 35 minutes for Bremerton - Seattle commuters
  - Offering more sailings/day to increase commuter flexibility
- Minimizing negative impacts to the environment
  - avoiding significant impact to existing habitat and wildlife
  - avoiding or mitigating impacts to shorelines or property along the route
- Offering a cost-competitive alternative to conventional car ferry service

The Study aims to provide the data, tools, analysis, and outreach necessary to preclude legal action against a POFF operation that might follow from recommendations or findings of the study. This will require careful balancing of tradeoffs between a vessel-based solution and shoreline effects mitigation.

The study is a multi-disciplinary effort with specific tasks including outreach to waterfront property owners and the general public, numerical model development and application, physical and biological monitoring and data analysis, coastal engineering, and research testing of a state-of-the-art foil-assisted catamaran. Outreach efforts include meetings and communication with property owners and the general public, posting of information on a project website, and distribution of a series of newsletters.

A critical step in the study process is to accurately assess potential shore and marine impacts associated with POFF watercraft that may be chosen to operate in Rich

Passage. The general approach to the evaluation of impacts associated with alternative POFF operations is an iterative process involving the collection and analysis of data and the development and application of numerical models for predicting wakes, wind waves, tidal processes, and shoreline response. Data from previous studies provide a benchmark against which to compare potential alternatives in terms of relative impacts. Wake trial data and in-situ measurements from previous POFF operations are also used to develop and verify a wake propagation predictive model. The wake propagation model is coupled with a tidal circulation model and wind-wave model to predict nearshore waves, currents, and sediment transport conditions for base case and POFF operation alternatives. Impacts are assessed on the basis of physical and biological criteria and metrics for a set of representative indicator sites. Relationships generated for indicator sites will ultimately be applied to generate data for system-wide impact assessments. The POFF operation is either optimized by improvements to vessel design, operating speed, or routing. In cases where potential impacts following optimization may be unavoidable, development and analysis of mitigation alternatives will be required.

Data required for the study include information on waterfront properties, shoreline protection schemes, shore types, sediment characteristics, bathymetry and topography, tidal currents and water levels, and wave and wake climates in Rich Passage. Wake data from trials of various POFF vessels were acquired for development of the wake prediction models.

The first generation of models was developed from a review of relevant existing data on shorelines and their response to wakes, waves and tidal processes in Rich Passage, and available wake trial data from a range of low-wake vessels that could provide a POFF design. New physical and biological monitoring data were collected from the Rich Passage environment in the first phase of study to provide a baseline for the current studies and a comparison against conditions during previous POFF operations.

A review of previous work and discussions with long time residents in the study area reveals that in addition to impacts caused by POFF, there is evidence that sand beach areas have undergone considerable seasonal and long term cyclic fluctuations prior to and since the introduction of POFF in the mid 1980s. Also relevant is the fact that since the 1950s, the majority of the shoreline in the study area has become bordered by some form of shore protection structure. Structures built prior to the mid-1980s were built to protect properties from beach and bluff erosion that would have been occurring as a result of coastal processes prior to the introduction of POFF. It is also notable that a number of factors related to the design of a large number of the bulkheads and seawalls present in the study area may have lead to an exacerbation of the erosion that occurred during previous POFF operations over the last decade.

These factors include:

- Reduction, or in most cases, total elimination of the primary source of sediment supply to the upper foreshore
- Construction of the bulkhead or structure seaward of Mean Higher High Water (MHHW)

- Presence of a vertical impermeable face which enhances wave reflection with the potential to increase scour of sediment from in front of the structure and to intercept alongshore transport of sediment
- Absence of adequate toe protection to prevent erosion of the structure foundation, loss of back fill material from behind the structure and potential failure or collapses of the structure.

The irregular planform shape of the Rich Passage shoreline results in compartmentalization of the coast into several discrete littoral cells ranging from a few tens of meters in length up to a kilometer or more. Beaches in the Rich Passage study area are typically either pocket (embayed) beaches composed of varying mixtures of shell hash, silt, and sand, overlying bedrock, or open beaches composed of varying mixtures of shell hash, sand, gravel and cobble overlying bedrock. Pocket beaches or embayed beaches, such as those found in Lynwood Bay, Clam Bay, and adjacent to Waterman Point, Middle Point, and around Point Glover, feature a relatively steep foreshore transitioning to a low tide terrace or bedrock platform. The more exposed open beaches, such as those extending along Enetai Beach, Watermans, and Point White, may lack a low tide terrace in which case the steep foreshore transitions more directly to deep water.

The Rich Passage sediment distribution is also relatively complex. The beach may consist of a hard bottom, a sand beach, a gravel beach, a mixed sand and gravel beach, a cobble "lag" layer overlying and "armoring" a sand layer, or some combination of these. The Study has added data to characterize the sediment distribution of beaches in the Study area. Samples of beach armor layer were acquired photographically and sub surface samples were acquired by coring. The results of analysis are presented as appendices to this report.

Change in the form of erosion was detected on Point White, Bainbridge Island beaches within one month of the POFF speed increase during previous POFF operations in May 2000. Gravel was eroded from the upper beach and transported down the profile as well as alongshore. Erosion progressed alongshore to the northeast along Point White. Removal of gravel exposed the underlying sand layer with depth varying from 6 inches to 2 feet. The magnitude of the material loss at the base of bulkheads varied from approximately 6 inches to over 3 feet. After the POFF ferry speed was reduced from 32 to 14 knots through Rich Passage in October 2001, the Bainbridge Island beaches returned to their approximate original slope and sediment composition within six months to one year.

The response of the beaches in the study area to POFF operation is a result of many factors that include the following:

- the differences between POFF wakes and non-POFF wakes
- differences between wind waves and wakes
- beaches composed of mixed sediments
- high water level variations
- low relative ambient wave height to water depth ratio

Several factors have been noted to influence the unique behavioral response of mixed beaches, these include:

- Hydraulic conductivity
- Reflection and long waves
- Threshold of motion and entrainment processes
- Interactions with Coastal Structures
- Tidal range
- Proximity to deep water

The response of the beaches in Rich Passage does not follow the high-energy gravel-cobble dominated beach model; rather, it is more consistent with the response expected for a low-energy mixed beach (e.g., Quick and Dyksterhuis, 1994; Nordstrom and Jackson, 1993). Larger waves caused by POFFs result in erosion and removal of coarse and fine sediment particles from the upper beach; the smaller waves at slower POFF speeds result in accretion of gravel on the upper beach. Rich Passage is also very complex in planform. The different wave angles at the shoreline, and different longshore transport rates and directions are likely significant factors affecting shoreline changes.

The physical and biological response to wake, wave and current processes is strongly influenced by variations in water levels. Water level variations in the study area are mainly controlled by astronomical tides. However, other factors that may affect water level in the study area besides astronomical forcing include storm surges, seasonal effects of water temperatures, El Niño, and climate change. Analysis conducted aspart of this Study has shown that sea-levels fluctuations of up to 0.4 m in the central Puget Sound are correlated with the occurrence of El Niño and La Niña cycles. In general, higher water levels make beach properties along the Rich Passage shorelines more vulnerable to wave and wake actions because more wave energy is able to reach backshore beach areas, directly act on bulkheads and seawalls, and waves may overtop bulkheads and seawalls during high water levels.

Wake time series and associated vessel speeds and positions from *Chinook*, *Snohomish*, *Tyee*, and several WSF car ferries were extracted from water surface elevation time series from in-situ nearshore measurements collected by PI Engineering. Wake time series measurements from trials of a number of candidate vessels were obtained from Fox and Associates. These vessel trial data include: *M/V Chinook/Snohomish, M/V Bravest, M/V St. Nicholas, M/V Tyee, M/V Condor Express,* and *M/V Red Jet 4*.

Comparison of the maximum wake height and maximum energy density of several of the vessels that have been measured by Fox and Associates reveals that a number of conventional displacement catamarans as well as the foil-assisted catamaran, *Condor Express*, achieved normalized wake heights and energy densities that were lower than the *Chinook* trial results at speeds of 25 knots or higher. Additional review of compiled wake wash data published in the scientific and engineering literature as part of this study identified three candidate hull forms considered worthy of further

consideration in this study: air cavity hull catamaran, air-lubricated hull catamaran, and foil-assisted catamaran.

Wake trial time series from full-scale measurements of the air cavity and air-lubricated type hulls are not publicly or readily available at the time of this report. *Condor Express* provides an example of the potential for a foil-assisted catamaran to produce low wake heights and energy density.

Effects of vessel wake and run-up on the biological community in the intertidal and shallow subtidal zone (from MHHW to MLLW) were last investigated in 2001 (WSDOT, 2001). The 2001 studies included surveys of intertidal habitat, benthic infauna, and aquatic vegetation (kelp, macro-algae, and eelgrass). As part of the Study, a biological survey of monitoring sites within Rich Passage was conducted in January, 2005 prior to the start of trials of a high-speed candidate vessel. The purpose of this survey was to obtain winter baseline information on the existing biological community and nearshore habitat in Rich Passage for comparison with data to be collected during and after the vessel trials.

Several different numerical models are required to investigate the impacts of fast ferry wakes relative to other mechanisms on the shorelines of Rich Passage. These include:

- a tidal model to predict the water levels and currents;
- a wind wave prediction model to predict the growth, propagation, and transformation of wind generated waves;
- a wake generation and propagation model to predict the wake produced by different vessels and its transformation from the vessel to the shore, and;
- a shore response model to predict the response of the shore over time.

Tidal circulation modeling is essential for studies in the Rich Passage area because of the large tidal range and strong tidal currents. The propagation and transformation of a wake is dependent upon the movement of the water in which it is traveling. As well, the wake patterns and wake heights produced by a vessel vary with the depth of water in which the vessel is sailing. At the shore, the part of the beach profile exposed to wake action is controlled by the tidal elevation at the time. The ADCIRC model was selected to model tidal currents and water level changes. The model was validated with field measurements collected by Pacific International Engineering. Results show that the ADCIRC model of Rich Passage is sufficiently accurate to be used as a platform for modeling wake and wave transformations in the study area.

The Rich Passage study area is a fetch-limited environment. Significant wind wave growth can occur along fetches to the southwest (Port Orchard reach and Sinclair Inlet) and the southeast (Rich Passage and Puget Sound). Wind wave prediction modeling is required to predict the growth and decay of waves in response to wind records in these areas. Preliminary comparison of wind wave measurements with wave growth equations has been conducted as part of this Study in Sinclair inlet. The wind waves provided input to the CoastL combined wave and current model to predict the transformation of the wind waves by currents and bathymetry to provide preliminary estimates of nearshore wave heights, periods, and directions. Further

modeling and analysis is needed in the next phase of study to develop a nearshore wind wave climate for the study area for comparison with the vessel wake climate.

The primary modeling task in this study involved the development of a computer model capable of predicting the generation of wakes from high-speed vessels and the transformation of those wakes by currents and bathymetry. This is an especially difficult task for two reasons. First, high-speed vessels often operate in a regime where the wakes they produce cannot exist as free gravity waves. Second, the area over which a solution is required (i.e., the entire length of Rich Passage and part of the neighboring Port Orchard and Sinclair Inlet) is very large.

A review of the various existing approaches for high speed wake prediction revealed a number of advantages and disadvantages, and none was found to be suitable for direct application in the present study. Therefore, a new model was developed that borrowed from a variety of approaches.

As a precursor to modeling, the differences between super-critical and sub-critical vessel wakes were analyzed and illustrated with field measurements as part of the Study. The wake generated by a high speed vessel operating at super-critical speed exhibits a continuous smooth, steady decay in wake period; the wave energy spectrum shows a series of peaks or energy concentration at certain frequency multiples, or *harmonics*. The frequency of these harmonics is also related to the depth Froude number, F_d. In contrast, the same vessel sailing at a sub-critical speed generates a wake train in which the wake period is constant; the wave energy spectrum is monochromatic.

A kinematic and dynamic wake conservation model using a *Lagrangian* formulation was developed as part of the Study. In the Lagrangian Super-critical Vessel (LSV) model, the solution is cast in terms of individual packets of wave energy transferred from the moving vessel to the flow. The model then tracks the wake energy parcels as they propagate across the domain. The model allows the prediction of wake height, period and direction spatially as a function of time. There are many advantages to this type of formulation, most notably the ability to simply model a wake with energy across a range of frequencies in a simple and efficient manner.

The new model has the following capabilities:

- Generation of sub- and super-critical wakes
- Variable vessel routing and speed
- Wake transformation, including the effects of:
  - current refraction
  - depth refraction
  - shoaling
  - breaking
  - dispersion
- Efficient solution for large areas and numerous simulations

The LSV model requires a description of the wake pattern and the energy that is transferred by the vessel to the flow in the wake. The formulation of the wake pattern for the model relies on a purely theoretical foundation, whereas, the energy transfer is based almost exclusively on spectral and time domain analysis of measured wake profiles from field trials, because energy transfer is so strongly related to hull shape, vessel trim, etc., and is therefore beyond any theoretical method available at present.

The wake model was validated against a number of data sets including deepwater measurements of *Chinook/Snohomish* and *Condor Express* collected and made available to the project by Fox and Associates, and measurements in Rich Passage collected by PI Engineering during previous studies.

The results of the simulations show that the *LSV* model can predict the decay of the wave period observed in measured data. The model can also be calibrated to reproduce the wake height pattern, both in phase and magnitude. There is some suggestion that the leading edge waves for high depth Froude number simulations may be reproduced by the model at too small an angle.

Work on a number of approaches for application of the LSV model to POFF impact assessment, including the development of cross-shore profile numerical models and longshore power calculations have been started in the first year of study.

Research testing was initiated with the foil-assisted catamaran *M/V Spirit* built by All American Marine, Inc of Bellingham, WA and designed by Technikraft Inc., NZ to test a candidate low-wake vessel both in terms of wake characteristics and potential shoreline impacts. The trials and research testing will provide valuable data for direct validation of the numerical wake and shoreline response models. The models and data will enable a detailed assessment of potential shore impacts and provide a tool to evaluate possible shore protection solutions for areas where impacts cannot be minimized. In the first year of Study, the research vessel was acquired, mobilized, and outfitted for the trials, instrumentation was prepared and deployed for measurement of the wakes and a preliminary intensive trial was executed in Port Orchard reach. The vessel trials will continue in the second year of study and will be used to examine shoreline impacts in Rich Passage.

7.1 Recommendations

Later phases of study should involve:

- in-situ and model testing of low-wake candidate hulls;
- wake monitoring and additional physical and biological monitoring to gather data for model development and verification;
- analysis and interpretation of wake data , research vessel performance data, and shoreline impact data and application to model enhancement;
- application and enhancement of the predictive models to evaluate alternative POFF plans including potential candidate low-wake vessels, vessel operating speeds and vessel routings, and vessel testing against various shoreline configurations and compositions, at various tide and current levels to assess shoreline impacts;

- development and evaluation of alternative conceptual plans for addressing any unavoidable effects on shorelines;
- an economic analysis to assess existing and new rider demand, vessel operating costs for the POFF service and to evaluate potential cost recovery plans and alternatives;
- a system wide water level and wave overtopping analysis is needed to assess the location and extent of vulnerable bulkheads and seawalls in the study area, and;
- compilation of a project GIS to integrate various geospatial data and provide a decision support tool to guide future analysis.

A more comprehensive analysis of wind wave climate at representative locations in the study area is required to determine the relative importance of wind waves to other forcing mechanisms in causing beach changes. Wave modeling is needed to predict and hindcast wind wave conditions for offshore locations in Rich Passage. Combined wave and current modeling is needed to transform the offshore waves to the nearshore areas so that the comparisons can be made between wind wave parameters and vessel-generated wake parameters.

The LSV model became operational in the first phase of the Study, it will be applied in later phases to compute wake impacts on the shores of Rich Passage and the Study area. The areas of model development and application in which additional work should be undertaken include:

1. LSV modeling should encompass a full range of potential wakes for any given vessel. Up to this point, all LSV simulations have been performed using vessel wake energy output characteristic of the 35 knots to 38 knots operational range. Accordingly, the LSV model simulations may only be accurate near these speeds. Because the energy distribution (i.e. the height of the wakes in the pattern) is a function of F_L, data for a vessel at a number of speeds is required to model the full range of wakes. Data is available from the deep water field trials provided by Fox and Associates and from the field measurements obtained by PI Engineering. There is no variation in the output of wake energy for vessels moving along a curved path because the vessel wake characteristics used in the model are all obtained from the analysis of tests in which the vessel was traveling in a straight line. It is suspected that the wake produced by the vessel will be different on each side and from that of a straight-line transit. Additional calibration test are required to address this issue.

8.0 References

Best, P. N. 2004. Bainbridge Island Nearshore Structure Inventory. In T. W. Droscher and D.A. Fraser (eds). Proceedings of the 2003 Georgia Basin/Puget Sound Research Conference. Puget Sound Action Team: Olympia, WA.

Bradbury, A. P. and McCabe, M. (2003). *Morphodynamic Response of Shingle and Mixed Sand/Shingle Beaches in Large Scale Tests – Preliminary Observations*, Hydrolab II, Budapest, 22-23 May 2003, pp. 9-1 to 9-11.

Brigham Young University (2002): *SMS 8.0 User's Manual*. Environmental Modeling Research Laboratory, Brigham Young University. 216 pp.

Coates, T. T. and Lowe, J. P. 1993. Three-dimensional response of open and groyned shingle beaches. HR Wallingford Report SR 288.

Crapper, G. D. 1984. Introduction to Water Waves. Ellis Horwood Limited.

Damgaard, J. S. and Soulsby, R. L. (1996). *Longshore Bed-Load Transport*, Proc. Inter. Conf. Coastal Engineering, ASCE, pp. 3614-3627.

Davies, M. H. and Watson, D. A.W. (1999): *Modélization du transport sédimentaire dans l'estuaire du Saint-Laurent*. Rapport technique HYD-TR-026, Canadian Hydraulics Centre, Ottawa.

de San Roman-Blanco, B. L. and Holmes, P. (2002). *Further Insight on Behaviour of Mixed Sand and Gravel Beaches – Large Scale Experiments on Profile Development*, Proc. 28th Inter. Conf. Coastal Engineering, ASCE, pp. 2651-2663.

Downing, J. (1983). The coast of Puget Sound: Its processes and development. Seattle, University of Washington Press.

Dupuis, P., Tournier, J-P. and Caron, O. (1996): Wave climate of large reservoirs and a revised wave hindcast formula. *Proc. Inter. Conf. Coastal Engrg*., pp. 1233-1246.

Everts, C. H. 1973. Particle overpassing on flat, granular boundaries. Journal of Waterways Ports Ocean & Harbor Division, 99 (W4), pp. 425-438.

Everts, C. H., Eldon, C.D. and Moore, J. (2002). *Performance of Cobble Berms in Southern California*, Shore & Beach, Vol. 70, No. 4, pp. 5-14.

Fenton, J. D. and Abbott, J. E. 1977. Initial movement of grains on a streambed: the effect of relative protrusion. Proceedings of the Royal Society of London, A 352, pp. 523-531.

Fox and Associates, 2002. M/V Condor Express wake wash measurement trials, 2/22/2002. Trial Report conducted for All American Marine, Inc.

Fox and Associates, 2005. pers comm. Verbal communication and e-mail correspondence Fox/Osborne; Stumbo Osborne concerning Red Jet 4.

Fox, K. 2000. Letter to Michael Bennett, Mosquito Fleet Whale Watching Charters, 1724 West Marine View Drive, Everett, WA 98201, Subj: ST. NICHOLAS Wake Wash Test Results, (April 18, 2000).

Fox, K. Stumbo, S. C., and Elliot, L. 2000. Wake wash measurement trials M/V St Nicholas. Trial Report conducted for Allan Marine, Inc. April 2000.

Friedrich, E. 1999. Taking back the beach. The SUN Newspaper, Bremerton, WA, October 14, 1999, http://www.thesunlink.com/news/99october/daily/1014a1c.html.

Harris, R. G. (1954). The surface winds over Puget Sound and the Strait of Juan de Fuca and their oceanographic effects. School of Oceanography. Seattle, WA, University of Washington: 101.

Hartman Associates, Inc., 1990. Impacts of the passenger-only fast-ferry wake – Rich Passage to Bremerton, report prepared for Washington State Ferry. Prepared in Association with Science Applications International Corporation, Merit Systems, Inc. and Dalton, Olmstead, Parametrix, and Fgluevand, Inc.

Havelock, T. H. 1908. The Propagation of Groups of Waves in Dispersive Media, with Application to Waves on Water Produced by a Traveling Disturbance. Proceedings of the Royal Society of London, Series A, 81, 398-430.

Henn, R., Sharma, S.D. and Jiang, T. (2001): Influence of canal topography on ship waves in shallow water. *16th Int. Workshop on Water Waves and Floating Bodies*. R.I.N.A.

Holmes, P., Baldock, T. E, Chan, T. C. and Neshaei, M. A. L. (1996). *Beach Evolution under Random Waves*, Proc. 25th Inter. Conf. Coastal Engineering, ASCE, pp. 3006-3019.

Isla, F. I. (1993). *Overpassing and Armouring Phenomena on Gravel Beaches*, Marine Geology, (110), pp. 369-376.

Jacobsen, E. E. and M. L. Schwarts (1981). "The use of geomorphic indicators to determine the direction of net shore-drift." Shore and Beach **49**(4): 38-42.

Kelvin, W. T. 1887. *On Ship Waves*. Proceedings of the Institute of Mechanical Engineers, 409-433.

Keuler, R. F. (1988). Map showing coastal erosion, sediment supply, and longshore transport in the Port Townsend 30- by 60-minute quadrangle. Puget Sound Region, Washington. US Geological Survey.

Kitsap Ferry Company, 2005. pers comm. Verbal communication Donkert/Osborne; concerning *M/V Spirit of Adventure.*

Kofoed-Hansen, H. and Mikkelsen, A. C. (1997): *Wake wash from fast ferries in Denmark*. Proc. 4th Inter. Conf. on Fast Sea Transportation, Sydney, Australia, pp 471-478.

Kofoed-Hansen, H., Jensen, T., Kirkegaard, J. and Fuchs, J. (1999): *Prediction of wake wash from high-speed craft in coastal areas*. Proc. Conf. Hydrodynamics of High Speed Craft. pp. 24-25.

Komar, P. D. (1998b). *The Pacific Northwest coast: Living with the shores of Oregon and Washington.* Duke University Press, Durham, South Carolina.

Komar, P. D. and Li, Z. 1986. Pivoting analysis of the selective entrainment of sediments by shape and size with application to gravel threshold. Sedimentology, 33: 425-436.

Landrini, M., Colagrossi, A. and Tulin, M.P. (1999): Breaking bow and stern waves: Numerical simulations. *15th Int. Workshop on Water Waves and Floating Bodies*. R.I.N.A.

Lavelle, J. W., H. O. Mofjeld, et al. (1988). A multiply-connected channel model of tides and tidal currents in Puget Sound, Washington and a comparison with updated observations. Seattle, WA, Pacific Marine Environmental Laboratory: 103.

Luettich, R. A., J. J. Westerink, and N.W. Scheffner, 1992, ADCIRC: an advanced three-dimensional circulation model for shelves, coasts and estuaries. Report 1: theory and methodology of ADCIRC-2DDI and ADCIRC-3DL. Dredging Research Program Technical Report DRP-92-6, U.S. Army Engineers Waterways Experiment Station, Vicksburg, MS, 137p.

MacDonald, N.J. (1998). "*Numerical modelling of non-linear wave-induced nearshore circulation*" Ph.D. dissertation, Department of Civil Engineering, University of Liverpool, U.K., 566 pp.

Mason, T. and Coates, T. T. (2001). *Sediment Transport Processes on Mixed Beaches: A Review for Shoreline Management*, Journal of Coastal Research, 17(3), pp. 645-657.

Mason, T., Voulgaris, G., Simmonds, D. J., and Collins, M. B. 1997. Hydrodynamics and sediment transport on composite (mixed sand/shingle) beaches: a comparison. Coastal Dynamics '97. American Society of Civil Engineers. pp. 48-57.

McKee Smith, J., Sherlock, A. R.. Resio, D. T., 2001. *STWAVE: Steady-State and Spectral Wave Model User's Manual for STWAVE, Version 3.0*, ERDC/CHL SR-01-1. Washington, DC: US Army Corps of Engineers.

Miller, K. A. (1997). Sediment Dynamics on Wemyss Beach, South Fife, unpublished M.Phil. thesis, Department of Geology, University of St. Andrews.

Miller, M. C. (2003). Bainbridge Island Nearshore Assessment, Summary of Best Available Science, Chapter 3, Nearshore Physicial Processes. Battelle, Pacific Northwest Laboratory. http://www.ci.bainbridge-isl.wa.us/nearshore.asp

Mofjeld, H. O. and L. H. Larsen (1984). Tides and tidal currents of the inland waters of western Washington. Seattle, Washington, Pacific Marine Environmental Laboratory: 51.

Naden, P., 1987. An erosion criterion for gravel-bed rivers. Earth Surface Processes and Landforms, 12: 83-93.

Nordstrom, K. F. (1992). Estuarine beaches: An introduction to the physical and human factos affecting use and management of beaches in estuaries, lagoons, bays, and fjords. London, Elsvier Applied Science.

Nordstrom, K. F. and Jackson, N. L. (1993). Distribution of surface pebbles with changes in wave energy on a sandy estuarine beach. Journal of Sedimentary Petrology. 63: 1152-1159.

Pacific International Engineering, PLLC. (1999). Rich Passage Shoreline Erosion. Technical Report for WSF, June 16, 1999.

Pacific International Engineering, PLLC. (2002a). Rich Passage Shoreline Vessel Wake Data Analysis. Technical Memorandum for RPWAST, February 18, 2002. .

Pacific International Engineering, PLLC. (2002b). Rich Passage Shoreline Categories. Technical Memorandum for RPWAST, February 18, 2002.

Pacific International Engineering, PLLC. (2003). Tyee wakes and operational speed analysis, Rich Passage, Waterman Point to Bremerton, Technical Report for WSF.

Pacific International Engineering, PLLC (2003). Rich Passage Shoreline Vessel Wake Data Analysis, Technical Memorandum, January 22, 2003.

Pacific International Engineering, PLLC (2004). Trip Report: Preliminary site assessment (June 3, 2004). Y-8977 Waver Energy Evaluation of Passenger Only Fast Ferries in Rich Passage.

Petrov, V. A. (1989). *The Differentiation of Material on Gravel Beaches*, Oceanology, (29) pp. 208-212.

Phillips, O. M. (1977): *Dynamics of the Upper Ocean*. Cambridge University Press, 2nd Ed., Cambridge, 336 pp

Powell, K. A. (1988). *The Dynamic Response of Shingle Beaches to Random Waves*, Proc. 21st Inter. Conf. Coastal Engineering, ASCE, pp. 1763-1773.

Powell, K. A. (1990). "Predicting Short Term Profile Response for Shingle Beaches", Hydraulics Research, Wallingford, Report SR 219.

Quick, M. C. and Dyksterhuis, P. (1994). *Cross-shore Transport for Beaches of Mixed Sand and Gravel*, International Symposium: Waves-Physical and Numerical Modeling (Canadian Society of Civil Engineers), pp. 1443-1452.

Raven, H. C. (1998): Inviscid calculations of ship wave making --- capabilities, limitations and prospects, *Proc. 22nd Symposium on Naval Hydrodynamics*, Washington DC, U.S.A.

Reynolds, W. J. 2004. personal communication, field notes from site visit, June 2004.

Rich Passage Wave Action Study Team, 2001. Rich Passage Wave Action Study, Monitoring Program Summary Report, Prepared for Washington State Ferries, August 2001.

Rich Passage Wave Action Study Team, 2002. Operation of the Passenger-only fast ferry service between Seattle and Bremerton, Technical Memorandum prepared by the Rich Passage Wave Action Study Team, Prepared for Washington State Ferries, February 2002.

Schwartz, M. L., R. S. Wallace, et al. (1989). Net shore-drift in Puget Sound Engineering Geology in Washington, Volume II. Olympia, WA. Washington Division of Geology and Earth Resources Bulletin 78: 1137-1145.

Shipman, H. (1996). "Puget Sound Beach Replenishment", Proceedings of the Coastal Society, 15th Annual Conference, July 14-17, 1996, Seattle, Washington, pp. 448-454.

Shipman, H. (1997). "Gravel Beach Nourishment in Puget Sound", Annual Meeting of the Shore and Beach Preservation Association-abstracts, Long Island, NY.

Shipman, H. (2001). Coastal landsliding on Puget Sound: a review of landsliding occurring between 1996 and 1999. Olympia, Shorelands and Environmental Assistance Program, Washington Depart of Ecology: 87.

Smith, Thomas M., and Reynolds, R. W., (2003). Extended Reconstruction of Global Sea Surface Temperatures Based on COADS Data (1854-1997). *J. Climate,* **16 (10),** 1495-1510.

Sorensen, R. M. 1997. Prediction of vessel-generated waves with reference to vessels common to the Upper Mississippi River System. Interim report for the Upper Mississippi Rover-Illinois Waterway System Navigation Study, US Army Corps of Engineers, ENV rept. 4, 50p.

Stoker, J. J. 1957. Water Waves. Interscience Publishers, NY. p. 567.

Stumbo, S. C. 1998. Chief Naval Architect, WSF, March 25, 1998, letter to Jack Davis, New York Fast Ferry Services, Inc., 311 East Boston Post Road, Mamaroneck, NY 10543, Subj: M/V BRAVEST Wake Wash Test Results

Stumbo, S. C. pers. comm., September 15, 2004 – e-mail correspondence and phone conversation: Stumbo/Osborne.

Stumbo, S. C., Fox, K., and Elliott, L. 1999. Hull form considerations in the design of low wake wash catamarans. Proceedings of the SNAME International FAST '99 Conference, Seattle, WA, August 1999.

Stumbo, S. C., Fox, K., and Elliott, L. 2000. An assessment of wake wash reduction of fast ferries at supercritical Froude numbers and at optimized trim.

Stumbo, S. C., Fox, K., Dvorak, F., and Elliott, L. 1998. The prediction, measurement and analysis of wake wash from marine vessels. Marine Technology, Society of Naval Architects and Marine Engineers, Proceedings of Canadian Institute of Marine Engineers High Speed Vessel Conference, June 1998.

US Army Corps of Engineers (1984). Shore Protection Manual, Waterways Experiment Station, Vicksburg, Mississippi.

US Army Corps of Engineers (1986). "Shore Protection Manual", Waterways Experiment Station, Vicksburg, Mississippi.

US Army Corps of Engineers (2001). Coastal Engineering Manual - EM1110-2-1100 (Part II).

van der Meer, J. W. 1988. Rock slopes and gravel beaches under wave attack. Delft Hydraulics Publications, No. 396.

Van Hijum, E. (1977): *Equilibrium profiles and longshore transport of coarse material under wave attack.* Delft Hydraulics Laboratory, Publication No. 147.

Van Hijum, E. 1976. Equilibrium profiles and longshore transport of coarse material under regular and irregular wave attack. Delft Hydraulics Laboratory, Publication no. 274, Netherlands.

van Rijn, L.C. (1998): Principles of Coastal Morphology. Aqua Publications., Amsterdam, NL.

van Wellen, E., Chadwick, A. J. and Mason, T. (2000). *A Review and Assessment of Longshore Sediment Transport Equations for Coarse-Grained Beaches*, Coastal Engineering, Vol. 40(3), pp. 243-275.

Verhey, H. J. and Bogaerts, M. P. 1989. Ship waves and the stability of armour layers protecting slopes. Proceedings of the 9th International Harbor Congress, Antwerp, Belgium.

Walker, J. R., Everts, C. H., Schmelig, S. and Demirel, V. (1991). *Observations of a Tidal Inlet on a Shingle Beach*, Proc. Coastal Sediments '91, ASCE, pp. 975-989.

Wallace, R. S. (1988). "Quantification of net shore-drift in Puget Sound and the Strait of Juan de Fuca, Washington." Journal of Coastal Research **4**(3): 395-403.

Washington State Department of Ecology (Ecology). (2000b). Digital Oblique Aerial Photographs. Washington State Department of Ecology, Shoreline and Environmental Assistance Program: Olympia, WA.

Washington State Department of Natural Resources (WDNR). 2000. Ortho-rectified aerial photographs.

Washington State Department of Natural Resources (WDNR). 2001. The Washington State Shore Zone Inventory. Washington State Department of Natural Resources, Nearshore Habitat Program: Olympia, WA.

Weggel, J.R. and Sorensen, R.L. (1986): *Ship wave prediction for port and channel design*. Proc. Ports'86 Conf. Oakland, CA. ASCE, pp. 797-814.

Wigley, W.C.S. 1934. *A comparison of experiment and calculated wave profiles and wave resistance of a form having parabolic waterlines*. Proceedings of the Royal Society, A 144.

WSDOT, 2005. Washington State Ferries, Winter 2005 Schedule Seattle/Bremerton. http://www.wsdot.wa.gov/ferries/schedules/current/index.cfm?route=sea-br.

Yih, C-S and Zhu, S. (1989): *Patterns of ship waves*. Quart. Appl. Math. Vol. XLVII, No. 1. pp. 17-33.

Youngmann, C. (1977-1980). Coastal zone atlas of Washington. Olympia, WA, State of Washington, Dept. of Ecology.